

SPECTROSCOPY AT MICROWAVE AND RADIO FREQUENCIES

A thesis presented by

Kenneth W. Moore

in part fulfilment of the requirements for the degree of

Doctor of Philosophy at the

University of Glasgow.

April 1968

Supervisor: Dr. A.L. Porte

ProQuest Number: 11011862

All rights reserved

INFORMATION TO ALL USERS

The quality of this reproduction is dependent upon the quality of the copy submitted.

In the unlikely event that the author did not send a complete manuscript and there are missing pages, these will be noted. Also, if material had to be removed, a note will indicate the deletion.



ProQuest 11011862

Published by ProQuest LLC (2018). Copyright of the Dissertation is held by the Author.

All rights reserved.

This work is protected against unauthorized copying under Title 17, United States Code
Microform Edition © ProQuest LLC.

ProQuest LLC.
789 East Eisenhower Parkway
P.O. Box 1346
Ann Arbor, MI 48106 – 1346

SUMMARY

Part A introduces the origin of proton chemical shifts and coupling constants, and discusses the significance of these quantities for studies of conformation and configuration in organic molecules. The general theories of chemical shifts and coupling constants are then applied to pyranosides and in particular to the high resolution proton magnetic resonance spectra of saturated deuteriochloroform solutions of the four compounds:

A: methyl 2-acetoxymercuri-2-deoxy- β -D-glucopyranoside triacetate

B: methyl 2-chloromercuri-2-deoxy- β -D-glucopyranoside triacetate

C: methyl 2-chloromercuri-2-deoxy- α -D-mannopyranoside triacetate

D: methyl 2-chloromercuri-2-deoxy- α -D-galactopyranoside triacetate.

Compounds containing pyranoside rings exist usually in one of the two possible chair conformations, designated by Reeves as C1 and 1C: other things being equal, the C1 conformation is preferred for most D-hexoses and their derivatives.

The spectra of the four compounds have been analysed, fully for the ring proton absorptions, using programs written for the DEUCE and KDF 9 computers in Glasgow University. The chemical shifts and coupling constants resulting from the analyses are given.

Interpretation of these chemical shifts and coupling constants has confirmed that the compounds do have the structures and configurations described by A, B, C and D above. This is

especially important for compound C, about whose configuration there has been some controversy.

The ring proton coupling constants in particular show that compounds A, B, and C in saturated deuterochloroform solution have essentially C1 chair forms, with some distortion, and that compound D exists as a very distorted C1 chair conformer, almost in a half-boat conformation: some of these conclusions are supported by X-ray analyses.

Apart from the analysis of the ring proton absorption peaks, the methoxy proton chemical shifts agree well with previous findings concerning this substituent, and the acetoxy proton chemical shifts are not inconsistent with the results of other workers.

No spin-spin coupling between mercury isotopes and the protons H(1), H(2) or H(3) has been explicitly observed.

The peaks in the spectrum of compound D are broadened slightly relative to the peaks in the spectra of the other compounds. This may be because of kinetic effects involving the presence in low concentration of another conformer in the solution, or to unresolved couplings, perhaps long-range proton-proton couplings.

In Part B, nuclear quadrupole resonance (NQR) spectroscopy is introduced, and quadrupole resonance is treated theoretically, with special reference to the ^{14}N nucleus. A description

is given of the two main types of instrument used to detect NQR: the marginal oscillator and the super-regenerative oscillator. Modulation is discussed.

Two complete spectrometer systems for detection of ^{14}N NQR have been designed and constructed, and details of these systems are given. The first system uses a marginal oscillator; the second uses a super-regenerative oscillator which is externally quenched.

In Part C, the factors which contribute to the electric field gradient tensor and so to the NQR frequencies in an isolated molecule are analysed. Methods of finding various molecular and atomic parameters which are needed for estimating the contributions of these factors are reviewed and discussed, and a few possible extensions or modifications of some of these methods are suggested. Mathematical techniques for evaluating the integrals which come out of these methods are also briefly reviewed. Intermolecular effects on the electric field gradient tensor are discussed briefly.

The results are then given of the application to some simple molecules of the methods described and suggested earlier, with some further discussion of points of important detail. These results seem to be promising enough to justify a proper, more detailed, study of the possibilities of semi-empirical calculations of NQR frequencies.

ACKNOWLEDGEMENTS

This thesis owes much to many helpful discussions with staff and research students in and outside of the Chemistry Department of the University of Glasgow, and to their advice and help. They are so many that they cannot all be named individually, but I should like to thank in particular: Dr. A.L. Porte, for suggesting most of the research described, and for his continuing enthusiasm and encouragement; Prof. J.M. Robertson, for a demonstratorship at the end of the research period; Dr. J.C.P. Schwarz of the University of Edinburgh for supplying the compounds studied in Part A; Mr. M. Riggins and Mr. A. Harvey of the Chemistry Department workshops, who made invaluable contributions to the construction of the spectrometers; and Mr. J. Hardy, for his guidance and assistance in electronics.

Finally, I want of course to express my thanks to the Science Research Council for the award of a Research Studentship, during the tenure of which most of the work described was done.

CONTENTS

General Introduction	1
PART A	3
Chapter 1. General theory of nuclear magnetic resonance	4
1.1 Energy levels	4
1.2 Detection of energy levels	5
1.3 The production of spectra	6
1.4 Nuclear magnetic resonance spectrometers .	10
Chapter 2. Nuclear magnetic resonance and carbohydrate structure	12
2.1 Introduction: the pyranoside ring . . .	12
2.2 The origin of the chemical shift . . .	16
2.3 Chemical shift and stereochemistry. . .	23
2.4 The origin of spin-spin coupling . . .	26
2.5 Spin-spin coupling and stereochemistry . .	32
Chapter 3. Nuclear magnetic resonance of some mercury (II) sugar derivatives	39
3.1 Experimental details.	39
3.2 Standardisation and calibration of spectra .	41
3.3 Analysis of the spectra	43
3.4 The initial set of parameters.	44
3.5 Calculation of spectra	44
3.6 Refinement of parameters.	47
3.7 Results	49

Chapter 4. Interpretation of results	58
4.1 Chemical preliminaries	58
4.2 Effects due to the mercury atom	62
4.3 Ring proton chemical shifts	64
4.4 Substituent chemical shifts	66
4.5 Analysis of the ring proton coupling constants	67
4.6 Other effects.	76
Appendix A1. References for part A	78
Appendix A2. Summary of part A	83
PART B	85
Chapter 1. General theory of nuclear quadrupole	
resonance	86
1.1 Introduction	86
1.2 The interaction of a nucleus with an electric	
field	87
1.3 The quadrupolar energy levels for ^{14}N	93
Chapter 2. Instrumentation in nuclear quadrupole	
resonance spectroscopy.	97
2.1 Introduction	97
2.2 The continuous wave oscillator	99
2.3 The super-regenerative oscillator.	100
2.4 Modulation	108
Chapter 3. The design and construction of two	
spectrometer systems for ^{14}N NQR.	116
3.1 Preliminaries.	116

3.2 The main spectrometer system.	116
3.3 The sample coil assembly: low-temperature work	122
3.4 The oscillator-preamplifier unit	125
3.5 The modulation and bias unit.	133
3.6 The phase-shift unit	137
3.7 The narrow-band amplifier	142
3.8 The square-wave generator	147
3.9 The phase-sensitive detector.	150
3.10 Auxiliary units	151
3.11 Operation of the spectrometer	155
3.12 Testing spectrometer performance.	156
3.13 The super-regenerative oscillator	157
3.14 Auxiliary equipment	163
3.15 Conclusions	166
Appendix B1. References for Part B	169
Appendix B2. Summary of part B	171
PART C	172
Chapter 1. Intramolecular contributions to the field	
gradient	173
1.1 Introduction	173
1.2 Intramolecular contributions: introduction .	174
1.3 Application to nitrogen-containing compounds	179
1.4 Simplification of the more general equation.	185
1.5 The "atomic" coefficients	188
1.6 The "molecular" coefficients.	195

1.7 Choice of explicit atomic orbitals . . .	215
1.8 Evaluation of the integrals . . .	237
Chapter 2. Intermolecular effects and temperature	
dependence	248
2.1 Introduction	248
2.2 Direct intermolecular effects . . .	250
2.3 Indirect intermolecular effects . . .	253
2.4 Intermolecular bonding	260
2.5 Temperature dependence: introduction . .	264
2.6 The direct temperature dependence. . .	267
Chapter 3. Trial calculations of field-gradient tensors 271	
3.1 Introduction	271
3.2 The molecular calculations	272
3.3 Discussion and conclusions	277
Appendix C1. Observed NQR of ^{14}N	281
Appendix C2. References for part C	293
Appendix C3. Summary of part C	307

FOREWORD

This thesis gives an account of experimental and theoretical work in the two related fields of Nuclear Magnetic Resonance Spectroscopy (NMR) and Nuclear Quadrupole Resonance Spectroscopy (NQR). It is divided into three parts, A, B and C: part A is concerned with NMR and parts B and C with NQR.

Part A demonstrates a correlation of experimentally observed data (spectral line frequencies and intensities) with other observed or theoretical quantities. Part B describes the main part of the experimental work, the design and construction of a Nuclear Quadrupole Resonance Spectrometer intended for the detection of pure NQR signals arising from ^{14}N . Part C is a contribution to the interpretation of reported NQR spectral parameters, and their correlation with other molecular and crystal properties.

Each of the parts is divided into chapters and again into sections: apart from the following General Introduction they are self-contained.

GENERAL INTRODUCTION

All nuclei have associated with them a total spin quantum number I , which can take integral or half-integral positive values. When $I=0$, the electromagnetic behaviour of the nucleus is that of a point charge, and is of little or no interest in nuclear spectroscopy. When $I \geq \frac{1}{2}$, the nucleus has magnetic dipolar properties, so that its energy is quantised in a magnetic field: NMR spectroscopy is concerned essentially with observations of transitions between the allowed energy levels of such a nucleus. The most fruitful NMR studies have involved the nucleus ^1H , for which $I=\frac{1}{2}$, and part A deals with an investigation in proton magnetic resonance.

When $I \geq 1$, the nucleus has, in addition to its magnetic properties, an electric quadrupole moment. In some cases, electric moments of higher order (octupole, hexadecapole) exist, but they are generally small enough to be unimportant for chemical purposes. The question of higher moments is taken up again briefly in part B. For the nucleus ^{14}N , $I=1$, and parts B and C deal, experimentally and theoretically respectively, with the NQR of that nucleus.

The magnetic and electric moments interact not only with externally applied magnetic and electrical fields, but also with internal fields which are due mainly to the electrons (and also the nuclei) of the molecule and of the crystal in

which the nuclei are situated. Since chemistry is so largely the study of the behaviour of electrons in atoms, molecules and crystals, it is the study of those internal fields through their interaction with certain nuclei which gives NMR and NQR their chemical interest and importance.

PART A.

NUCLEAR MAGNETIC RESONANCE SPECTROSCOPY

1.1 Energy levels

Most nucleons, and certainly protons and neutrons, possess a property which is most naturally identified with angular momentum. A nucleus is a system of nucleons coupled together, so that any one state of the nucleus has a resultant angular momentum (which may of course be equal to zero). In nuclear spectroscopy of the types which are discussed in this thesis, only the ground state of the nucleus is of considerable importance. Thus many nuclei in their ground states have a total magnetic moment $\underline{\mu}$ and a total angular momentum \underline{J} . These two vectors can be taken to be parallel, so that we can write

$$\underline{\mu} = \gamma \underline{J} \qquad 1.1.1$$

with γ a scalar, defined by equation 1.1.1, called the magnetogyric ratio. The quantity γ depends on the nuclear state, but it is to be expected that it will be a constant for the ground state of a nucleus.

In quantum theory, $\underline{\mu}$ and \underline{J} are treated as parallel vector operators: two vector operators are considered parallel if the ratio of their matrix elements of the same eigenfunction, in any arbitrary direction, is a constant (compare with the Wigner-Eckart theorem). It is usual to define a dimensionless vector operator \underline{I} such that

$$\underline{J} = \hbar \underline{I} \quad 1.1.2$$

\underline{I}^2 has eigenvalues $I(I+1)$, where I is the spin quantum number which is referred to in the General Introduction.

In a static magnetic field \underline{H} , a nucleus in whose ground state I is not equal to zero will interact with the field. The Hamiltonian for its interaction energy has the form:

$$\mathcal{H} = -\underline{\mu} \cdot \underline{H} \quad 1.1.3$$

If we suppose the field to have magnitude H , directed along the z -axis, then, using equations 1.1.1, 1.1.2 and 1.1.3,

$$\mathcal{H} = -\gamma \hbar H I_z \quad 1.1.4$$

where I_z is the z -component of \underline{I} . The eigenvalues of this Hamiltonian are multiples of the eigenvalues of I_z , whose eigenvalues are conventionally denoted by m , where m may take any of the $2I+1$ values $I, I-1, \dots, -I$. So the allowed energies, E_m , of the nucleus are:

$$E_m = -\gamma \hbar H m \quad m = I, I-1, \dots, -I \quad 1.1.5$$

Thus the ground state of a nucleus ($I \neq 0$) is split by a magnetic field into $2I+1$ substates, and NMR spectroscopy depends on the detection of transitions between these substates, which are equally spaced and which differ in energy by $\gamma \hbar H$.

1.2 Detection of energy levels

The presence of the energy levels E_m given by equation 1.1.5 can be detected by an interaction which will cause transitions between the levels, and observation of the resulting

absorption of energy. The most commonly used coupling between levels is an alternating magnetic field applied perpendicular to the static field, say in the x-direction. If the amplitude of the alternating field is H_x , and its angular frequency ω , then H_x gives rise to a perturbing term \mathcal{H}' in the Hamiltonian;

$$\mathcal{H}' = -\gamma \hbar H_x I_x \cos \omega t \quad 1.2.1$$

The operator I_x has matrix elements between the states m and m' which are zero unless $m' = m \pm 1$, provided that the perturbation \mathcal{H}' is small compared to \mathcal{H} . It follows that in such a case allowed transitions are between levels adjacent in energy. A transition involves energy ΔE where from equation 1.1.5

$$\Delta E = \gamma \hbar H. \quad 1.2.2$$

Further, the conservation of energy requires that

$$\Delta E = \hbar \omega, \quad 1.2.3$$

and combination of equations 1.2.2 and 1.2.3 gives

$$\omega = \gamma H. \quad 1.2.4$$

For a proton, μ (and therefore γ) is small, but an applied field H of about 14,000 oersteds brings the resonance frequency as given by equation 1.2.4 to around 60 Mc/s, which is conveniently handled by existing radiofrequency techniques.

1.3 The production of spectra

If equation 1.2.4 were true for all nuclei without modification, nuclear magnetic resonance would be of no chemical interest: all nuclei of one type would resonate at the same frequency

for a particular applied field, and the resonance would serve only as a measure of γ . However, spectra (corresponding to absorption at different frequencies) are produced in NMR because each nucleus in a sample is subjected to a magnetic field which is different from the externally applied field by amounts which depend on the physical and chemical environment of the nucleus. The modifications to the external field depend especially upon the electrons of the molecule in which the nucleus is situated: hence, as pointed out in the General Introduction, the chemical interest of NMR.

The form of the spectrum obtained depends first on the physical state of the sample. In solids, the magnetic field at a nucleus is affected mainly by surrounding nuclear magnetic dipoles, and the spectrum obtained is referred to as broad-line: this type of NMR spectrum is not discussed in this thesis. In liquids, rapid molecular tumbling causes these direct nuclear magnetic dipole-dipole interactions to time-average to zero, and the line width is now largely determined by the homogeneity of the applied field (but also by kinetic and other effects in some solutions). The spectra arising from the resonance absorption of nuclei in liquids in an applied magnetic field of high homogeneity are referred to as high-resolution NMR spectra.

But as foreshadowed above, even in liquids the magnetic field seen by the resonant nucleus is not in general equal to

the external applied magnetic field. Two important and quite distinct mechanisms operate to produce this inequality: the chemical shift effect and spin-spin coupling.

It is found experimentally that the same nuclide in different molecular surroundings gives rise to different absorption peaks. It is found further that this splitting, the "chemical shift", is proportional to the fixed RF frequency of the spectrometer oscillator, as described in section 1.4 below. If the effect is attributed to the fact that a nucleus experiences a magnetic field ΔH in addition to the external applied field H_0 , we may write for the field H at the nucleus:

$$H = H_0 + \Delta H \quad 1.3.1$$

Since $\Delta H \ll H_0$, we may define a constant σ by:

$$\Delta H = -\sigma H_0 \quad 1.3.2$$

The quantity σ is independent of H_0 and is characteristic of a particular nuclide in a particular chemical environment. It is often called the "screening constant" for that environment. Equations 1.3.1 and 1.3.2 together with equation 1.2.4 give:

$$\omega = \gamma H_0 (1 - \sigma) \quad 1.3.3$$

and this shift $-\gamma H_0 \sigma$ in frequency from that of the bare nucleus is called the "chemical shift".

NMR experiments effectively measure the different values of σ associated with different molecular surroundings and so supply information about these surroundings.

The resonance lines due to different chemical shifts are, in many compounds, themselves found to possess a fine structure. This further splitting is due to an apparent coupling of nuclei among themselves, the so-called indirect, or spin-spin, coupling; the effect is transmitted through the electrons of the molecule.

In a very simplified picture, the effect of one nucleus A (total spin quantum number I) on a nearby nucleus B is to change the field experienced by nucleus B to one of $2I+1$ possible values, corresponding to the $2I+1$ possible orientations of nucleus A in the magnetic field. In a large assembly of nuclei, each of the $2I+1$ orientations will be seen by some of the B nuclei, so that the absorption due to the B nuclei will be split into $2I+1$ peaks.

For the particularly simple case of the proton, $I = \frac{1}{2}$, so that a set of n equivalent protons will split the absorption of a neighbouring proton into $n+1$ peaks. Furthermore, these $n+1$ peaks have intensities proportional to the statistical probability of the corresponding total I_z of the assembly of n protons. In other words, the $n+1$ peaks will have intensities, in this approximation, proportional to the coefficients of the expansion of $(x+y)^n$.

In many NMR spectra, it is roughly true that the peaks of the fine structure due to spin-spin interaction of A with B are equally separated, and this separation is a good starting-point

value for a determination of the so-called coupling constant, J_{AB} , between A and B.

A more rigorous discussion of the chemical shift and especially of spin-spin coupling is given in the following chapters. But an application of the simple ideas outlined in this chapter gives rise to a "first-order" calculated spectrum which is almost always the first stage in the analysis of complicated NMR spectra such as those described later in chapter 3. Inadequate therefore as the present treatment is for anything more than a naive analysis of NMR spectra, it cannot be ignored.

1.4 Nuclear magnetic resonance spectrometers

In a practical NMR spectrometer, the sample of the compound under study is placed in a strong external magnetic field, and a fixed-frequency oscillating field is applied at right angles to the static field. (It is easier electronically to vary the applied field than to vary the radio-frequency). The variation of the external magnetic field is accomplished by means of a pair of sweep coils, mounted so that the field which they generate is superimposed parallel to the static field. This small sweep field is varied slowly and linearly, and protons in different chemical environments (in particular experiencing different values of σ and/or J) come into resonance when the field, H , which they see satisfies the practical form of equation 1.2.4:

$$\nu_0 = \frac{\gamma H}{2\pi} \qquad 1.4.1$$

where ν_0 is the fixed oscillator frequency. When the transition takes place, a signal is observed and recorded, so that a trace having the usual appearance of a spectrum can be obtained. The sample tube is spun by means of a small air-turbine. This effectively averages out inequalities in the field and so increases the homogeneity of the applied magnetic field and resolution. Further experimental details are given in chapter 3.

2.1 Introduction: the pyranoside ring

The chapter following this one gives the details of an NMR investigation into the structure of some substituted aldohexoses. These compounds are rather special examples of the substituted pyranoside ring. To supply a background to the experiment of chapter 3 and the interpretation of chapter 4, and to give a context to the discussion of NMR and carbohydrate structure in this chapter, a very brief account of the stereochemistry of pyranosides is given.

If we assume (it is a considerable assumption) that all the carbon atoms in a cyclohexane ring system are sp^3 hybridised, then a number of conformations of the ring are possible. The insertion of a hetero-atom, oxygen in the case of the pyranoside ring system, doubles the number of conceivable conformations: the pyranoside ring may exist in eight different limiting conformations, two chair forms and six boat forms. These structures, interaccessible by a rotation operation about carbon-carbon or carbon-oxygen bonds, are referred to as conformers. Reeves⁶⁹ has suggested a notation for these conformers which has come into general use: in this notation, the two chair forms are designated C1 and 1C (see figure 2.1, page 13) and the six boat conformations as B1, B2, B3, 1B, 2B, and 3B.

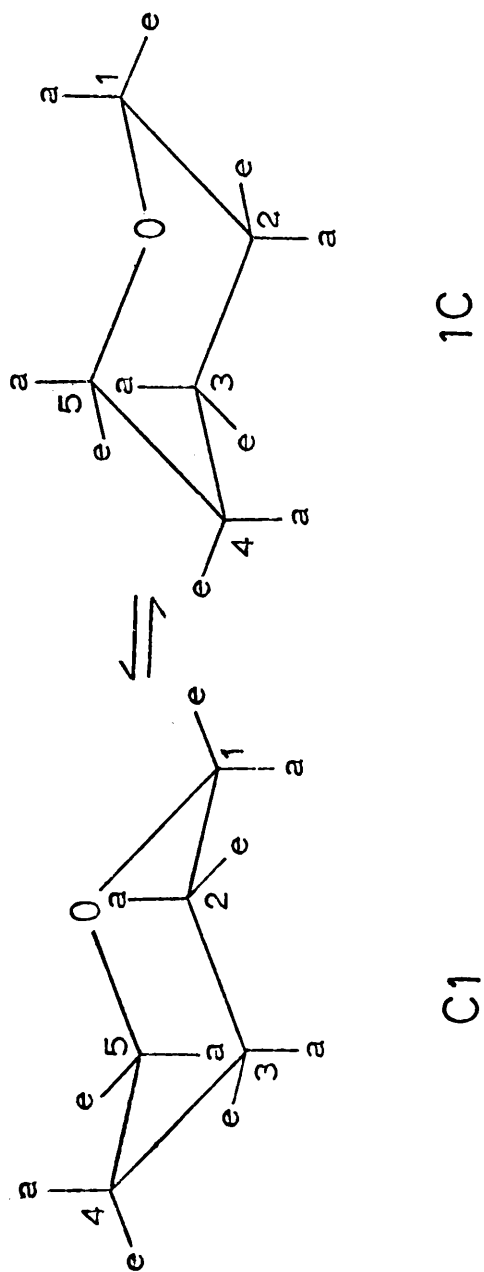


Figure 2.1. The conformers C1 and 1C.

The existence of boat forms is precluded except in special cases (such as methyl 2,6-anhydro- α -D-altropyranoside, which can exist only in form B2)⁷³. The general argument against the boat forms is that in them many groups on adjacent carbon atoms are in an eclipsed arrangement (they fall one behind the other when the molecule is viewed along the relevant carbon-carbon bond), and this eclipsed arrangement is higher in energy and so conformationally less stable, because of non-bonded interactions between the substituent groups, than the non-eclipsed arrangement which exists in the chair conformations.

The pyranosides, then, are capable of existing in either of the two conformations C1 or 1C (figure 2.1). It can be seen from figure 2.1 that in both conformers, there are two types of substituent position. If a very rough plane of the pyranoside ring is imagined, then there are substituents roughly perpendicular to this plane, indicated by 'a' in the figure (the so-called axial substituents) and also substituents more or less in the plane of the ring, indicated by 'e' in the figure and referred to as equatorial substituents. The changes from C1 to 1C or 1C to C1 make all the previously axial substituents equatorial and vice-versa. Since the conformers are in equilibrium, a decision on which one is preferred involves an estimate of their relative stabilities. Reeves⁶⁸ has assigned numerical values to certain of the more common possible

interactions. In particular, it is considered that axial interactions, involving especially the CH_2OH group on C(5), which is axial in the $1C$ conformer, with axial substituents on the 1 and 3 positions, confer high instability on this conformer. In general, then, that most pyranoside rings in D-hexoses, in most circumstances, have the preferred conformation $C1$ ^{8,14,30,40}. This has frequently been confirmed experimentally, especially by the NMR analyses mentioned later in this chapter^{45,46,47,52,67}.

Nevertheless, these non-bonded repulsions, which lead one to preclude boat forms from most conformational analyses, and which lead one to choose $C1$ as the dominant conformer in preference to $1C$ ³², can also lead to considerable distortions of the "perfect" chair forms of figure 2.1. The influence of non-bonded interactions of the type outlined here becomes particularly compelling when the substituent groups are large, and the compounds examined in the next chapter are examples of the distorting effects of large substituent groups.

In conclusion, it may be useful to gather together here the definitions of some common expressions used in conformational analysis⁵⁵. Suppose two adjacent carbon atoms C(1) and C(2) which are directly σ -bonded, with a substituent A on C(1) and a substituent B on C(2). If we look along the C(1)-C(2) bond (as in the Newman convention), then the angle of projection between the C(1)-A bond and the C(2)-B bond is called the dihedral angle

between the bonds. When this angle is zero, A and B are eclipsed; when it is about 60° they are skew (or syn); when it is about 180° they are staggered (or anti).

2.2 The origin of the chemical shift

It is worth pointing out first that H_{app} , the magnetic field in the air-gap of the spectrometer magnet, is not equal to the "external applied field" H_o of section 1.3. H_{app} is modified by the liquid in the sample tube, and is given by:

$$H_o = H_{app}(1 - \alpha\kappa) \quad 2.2.1$$

where κ is the volume diamagnetic susceptibility of the medium in the sample tube, and α is a constant which depends (among other things) on the shape of the sample. Values of α were found to range from 2.3 to 3.0 for a variety of binary mixtures in cylindrical sample tubes oriented transversely to the field¹⁰. The effect is important mainly for comparisons involving liquids of different κ . The significance of equation 2.2.1 in the standardisation of NMR spectra is taken up in chapter 3. We turn now to a more detailed treatment of the origin of the σ of equations 1.3.2 and 1.3.3.

We imagine a molecule, containing the nucleus whose nuclear magnetic interactions are under consideration, and with a fixed nuclear configuration, in a uniform magnetic field H_o . This magnetic field will act on the electrons and on the nuclei of the molecule, so changing the energy of the electron-nucleus

interactions, in a manner to be examined shortly. However, the change can be described, as in equation 1.3.2, in terms of an additional field $\Delta \underline{H}$, which in general is not parallel to \underline{H}_0 at any nucleus. Thus a better form of equation 1.3.2 is:

$$\Delta \underline{H} = -\underline{g} \underline{H}_0 \quad 2.2.2$$

where \underline{g} is a second-rank tensor whose elements depend upon the environment of the nucleus: only if \underline{H} is along one of the principal axes of \underline{g} will $\Delta \underline{H}$ be parallel to \underline{H}_0 . But in practice NMR is carried out in conditions where molecular rotation is rapid, and the chemical shift is determined by an average component of $\Delta \underline{H}$ along \underline{H}_0 over many rotations. In this way the tensor \underline{g} can be replaced by the scalar σ :

$$\sigma = 1/3 (\sigma_{11} + \sigma_{22} + \sigma_{33}) \quad 2.2.3$$

in the usual notation for tensors. This σ is the experimental σ of equation 1.3.2, and this quantity is one which a theory of chemical shifts should try to predict.

The first general theory of chemical shifts was given by Ramsey⁶⁴, and a rather different approach emphasising the physical origin of the shift is given by Slichter⁷⁵; the present discussion is simply a short summary of the theory not based especially on either account.

Chemical shifts are the result of the simultaneous interaction of the resonant nucleus, the electrons of the molecule,

and the field \underline{H}_0 . The magnetic influences of the nuclear magnetic dipole and \underline{H}_0 can be represented by (vector) potentials \underline{A}_{Kj} and \underline{A}_{Oj} respectively:

$$\underline{A}_{Kj} = r_j^{-3}(\underline{\mu} \times \underline{r}_j) \quad 2.2.4$$

$$\underline{A}_{Oj} = \frac{1}{2}\underline{H}_0 \times (\underline{r}_j - \underline{R}) \quad 2.2.5$$

where the subscript j refers to the value at the j th electron at position \underline{r}_j , $\underline{\mu}$ is as before the nuclear magnetic moment (equation 1.1.1), and \underline{R} is a convenient unspecified origin relative to the nucleus. The choice of \underline{R} involves a choice of gauge as in standard electromagnetic theory: it can be shown that \underline{R} is the point about which electronic angular momentum is measured. The most obvious choice is $\underline{R} = 0$, corresponding to the measurement of angular momentum about the nucleus, since electronic wave functions are classified as linear combinations of s , p etc. functions. But if the electron orbit is multicentred, the best choice of gauge is not always so obvious. It is easily seen that the vector potentials of equations 2.2.4 and 2.2.5 satisfy the definition of vector potential:

$$\underline{\nabla}_j \times \underline{A}_{Oj} = \underline{H}_0 \quad 2.2.6$$

$$\underline{\nabla}_j \times \underline{A}_{Kj} = \underline{H}_K \quad 2.2.7$$

The Hamiltonian for the N electrons, including the effect of the two fields, is:

$$\mathcal{H} = \sum_j \frac{1}{2m} \left(\frac{\hbar}{i} \underline{\nabla}_j + \frac{e}{c} \underline{A}_{Oj} + \frac{e}{c} \underline{A}_{Kj} \right)^2 + V \quad 2.2.8$$

where e is the electronic charge and m the electronic mass, c is the velocity of light and V represents all potential energy, including that of possible external electric fields. Now since $\underline{\mu}$, the nuclear magnetic moment of equation 2.2.4, is small in comparison to electronic moments, terms in A_{Kj}^2 in equation 2.2.8 can be ignored, and terms linear in A_{Kj} can be regarded as perturbations on the remainder of the complete Hamiltonian \mathcal{H} . This perturbation Hamiltonian \mathcal{H}' is given by:

$$\mathcal{H}' = \sum_j \frac{e}{2mc} \left[\left(\frac{\hbar}{i} \nabla_j + \frac{e}{c} \underline{A}_{0j} \right) \underline{A}_{Kj} + \underline{A}_{Kj} \left(\frac{\hbar}{i} \nabla_j + \frac{e}{c} \underline{A}_{0j} \right) \right] \quad 2.2.9$$

Using equation 2.2.5 for \underline{A}_{Kj} , equation 2.2.9 gives a first-order perturbation energy E' on Ψ , the wave equation for all N electrons in the presence of \underline{H}_0 but in the absence of the nuclear interaction, of:

$$E' = \underline{\mu} \cdot \sum_j \int \underline{r}_j^{-3} (\underline{r}_j \times \underline{J}_{0j}) d\tau_j \quad 2.2.10$$

where

$$\underline{J}_{0j} = \int \left[\frac{\hbar e}{2mci} (\Psi^* \nabla_j \Psi - \Psi \nabla_j \Psi^*) - \frac{e^2}{mc^2} \underline{A}_{0j} \Psi^* \Psi \right] d\tau'_j \quad 2.2.11$$

$d\tau'_j$ representing integration over all the electrons except j^{th} .

Equation 2.2.10 has the form of an interaction of the nuclear magnetic moment $\underline{\mu}$ with a current density \underline{J}_{0j} (a function of the \underline{r}_j only), and \underline{J}_{0j} can therefore be interpreted as a current density due to both \underline{H}_0 and \underline{H}_K (the first of the terms in the square brackets in equation 2.2.11 is the current density when $\underline{H}_0 = 0$).

With this physical interpretation, ΔH of equation 2.2.2 can be written:

$$\Delta H = \sum_j \int r_j^{-3} (\underline{r}_j \times \underline{J}_{oj}) d\tau_j \quad 2.2.12$$

To evaluate ΔH and thence σ , it is necessary to know the Ψ of equation 2.2.11. Ψ can be considered to be the resulting perturbed function when Ψ_0 (the total electronic function in the absence of H_0) is perturbed by H_0 , i.e. the applied field is now regarded as a perturbation on the electronic wave function. By supposing H_0 to be small, this new perturbing Hamiltonian, $\mathcal{H}_{\text{pert}}$, connected with A_0 , is found, by arguments exactly like those given for \mathcal{H} , to be:

$$\mathcal{H}_{\text{pert}} = \frac{e}{2mc} \sum_j \left(\frac{\hbar}{i} \nabla_j \cdot \underline{A}_{oj} + \underline{A}_{oj} \cdot \frac{\hbar}{i} \nabla_j \right) \quad 2.2.13$$

and the corresponding perturbed wave functions Ψ from first-order perturbation theory are:

$$\Psi = \Psi_0 + \sum_n \frac{(n | \mathcal{H}_{\text{pert}} | 0)}{E_0 - E_n} \Psi_n \quad 2.2.14$$

where E_0 and E_n are the eigenvalues for the ground state and nth excited state wave functions Ψ_0 and Ψ_n respectively in the absence of H_0 .

For simplicity, we can take $H_0 = kH$ (i.e. along the z-axis), and calculate only σ_{zz} (equation 2.2.3) by evaluation of ΔH of equation 2.2.12 using equation 2.2.14 for Ψ in the expression for \underline{J}_{oj} , with $\underline{R} = 0$ (equation 2.2.5) in the expression for \underline{A}_{oj} . This gives:

$$\sigma_{zz} = \frac{e^2}{2mc^2} \left(\left| \sum_j \frac{x_j^2 + y_j^2}{r_j^2} \right| 0 \right) - \left(\frac{e\hbar}{2mc} \right)^2 \sum_n \left\{ (E_n - E_0)^{-1} \left[\left(0 \left| \sum_j L_{zj} \right| n \right) \left(n \left| \sum_i 2L_{zi}/r_i^3 \right| 0 \right) + \left(0 \left| \sum_j 2L_{zj}/r_j^3 \right| n \right) \left(n \left| \sum_i L_{zi} \right| 0 \right) \right] \right\} \quad 2.2.15$$

where L_{zj} is the z-component of the dimensionless operator \underline{L}_j :

$$\underline{L}_j = -i\mathbf{r}_j \times \nabla_j \quad 2.2.16$$

The expressions for σ_{yy} and σ_{xx} are similarly derived. Equation 2.2.15 is a form of Ramsey's formula. The first term is similar to the Lamb formula for atoms. It makes a positive contribution to σ , and so can be interpreted as arising from a "diamagnetic" current in the molecule. In the same way the second term, making a negative contribution to σ , can be associated with a paramagnetic current. Physically it corresponds to a hindrance of the diamagnetic effect due to the fact that the molecule is not in general axially symmetric about the z-axis (otherwise the second term vanishes).

Evaluation of equation 2.2.15 presents real difficulties. A knowledge of the functions $|0\rangle$, the ground state function of equation 2.2.14, is not easy to get for molecules of any interesting complexity, and reasonable functions $|n\rangle$ for excited states are even harder to obtain. Even if, as in a frequent approximation, all the electronic excitation energies $E_n - E_0$ are replaced by an average value Δ , so that the sum over excited states can be carried out using the quantum-mechanical

sum rule and an expression for σ involving only Δ and ground states derived, equation 2.2.15 is not practical for molecules of any size. Apart from the remaining difficulty of estimating $|0\rangle$, the two terms, the diamagnetic and the paramagnetic, both become large, so that σ is the very small difference between two very large quantities, in slightly bigger molecules. What is needed is a means of considering the screening as due to local contributions.

Saika and Slichter⁷⁴ suggested such a method, which was elaborated by Pople⁶¹. The screening is divided into four separate contributions:

1. The diamagnetic currents for the atom
2. The paramagnetic currents for that atom
3. The contributions from other atoms (including bonds)
4. The contribution from interatomic currents.

Effect 4 is important mainly when electrons are free to migrate within a largely delocalised molecular orbital, as in a conjugated or aromatic molecule: it is an unimportant effect for carbohydrates, and we need not consider it in what follows. The electron population in the vicinity of a proton is much lower than for any other nucleus, so that for a proton effect 3 is relatively considerably more important than for other nuclei. Also, since effect 2 corresponds to a mixing, as an effect of the applied field, of suitable excited states with the ground state (compare

equation 2.2.15 second term), and since these excited states lie for the hydrogen atom at high energies, we would expect effect 2 to be unimportant too. It is effect 3 which is important in deciding steric effects on the chemical shift of hydrogen in carbohydrates, and it is these effects which will be described.

2.3 Chemical shift and stereochemistry

As pointed out in section 2.1, there is an equilibrium between the conformers of a carbohydrate, with one of the conformers usually "preferred". If the inversion is slow (if the inversion barrier is high), the pyranoside ring may be taken, at least to begin with, to exist in one conformation³, and this is the practical justification for the following discussion.

The most important direct shielding in carbohydrates comes from the ring-oxygen atom, which is the cause of the typical low-field shift of the anomeric hydrogen atom (see the results of chapters 3 and 4). But it is found that chemically identical substituent groups, and the ring protons themselves, have different chemical shifts depending on whether they are equatorial or axial^{4,6,52}. This is accounted for by effect 3 above, arising especially from distant carbon-carbon or carbon-oxygen single bonds. If the circulations from other atoms or bonds are spherically symmetric, the isotropic field produced by these circulations would average to zero in experimental situations (in liquids). But a carbon-carbon single bond, for example, shows

diamagnetic anisotropy: its transverse diamagnetic susceptibility χ_T is greater than χ_L , its longitudinal diamagnetic susceptibility¹¹. We can define the anisotropy, $\Delta\chi$, by:

$$\Delta\chi = \chi_T - \chi_L \quad 2.3.1$$

Pople⁶¹ and McConnell⁵⁴ have given an expression for the axially symmetric case by use of the approximation of replacing the circulations by magnetic dipoles at the electrical centre of gravity G of the bond. The expression is:

$$\Delta\sigma = (1/3r^3)(1 - 3\cos^2\vartheta)(\Delta\chi) \quad 2.3.2$$

where r is the distance between G and the proton, and ϑ the angle between the vector r and the axis of symmetry of the bond. Note that the factor $(1 - 3\cos^2\vartheta)$ changes sign at $\vartheta = 55^\circ 44'$, so that the effect of equation 2.3.2 may be a shielding or a deshielding one. Substituents on C(1) of a pyranoside ring (figure 2.1), whether axial or equatorial, are symmetrically oriented to the C(1)-C(2) and the C(1)-O bonds, but all the other ring bonds are differently oriented to axial or equatorial substituents on C(1): the effect of the C(2)-C(3) and O-C(5) bonds is of course greatest. Calculations on this basis, using equation 2.3.2, gave Jackman³⁶ results for protons in the cyclohexane ring which are in astonishingly close agreement with the experimental results of Lomieux⁴⁶. Calculations of the same sort for the ring protons of carbohydrates have been made by Lenz and Hoeschen⁵² and by Hall²⁷. Lenz and Hoeschen, using a value for $\Delta\chi$ for the C-O

bond of $+10.8 \times 10^{-30} \text{ cm}^3/\text{molecule}$ (this value they calculated) and for the C-C bond the previously calculated¹¹ value of $5.5 \times 10^{-30} \text{ cm}^3/\text{molecule}$, obtained a very close correlation with observed chemical shifts of the ring protons of β -D-glucopyranose and β -D-mannopyranose. Hall²⁷ has had some success in developing a more general relationship between ring proton chemical shifts and conformation at C(2).

The most extensively studied substituent chemical shift in carbohydrates is that of the acetoxy (CH_3COO) group protons. The first such study was the important paper of Lomieux et al.⁴⁶. They found that the protons of an axial acetoxy group absorb at lower applied field than those of an equatorial group, and subsequent work^{21,29,34,47,70} has substantiated this and led to an acceptance of acetoxy proton chemical shifts as fairly diagnostic of conformation. But deformation of the pyranoside ring, or the presence of other bulky substituents²⁸, can change these chemical shifts, as indeed can solvent effects (not unexpectedly)^{7,26}.

The analysis of the NMR spectrum of protons directly bonded to the pyranoside ring is useful for carbohydrate conformational studies in that the axial-equatorial shift for carbohydrates is similar to that for the exhaustively investigated cyclohexane derivatives. Lenz and Heeschen⁵² have established this, and have explained ring proton shifts in glucose and in mannose

by calculations similar to those of Jackman³⁶ described above.

Methoxy group proton chemical shifts have also been investigated by Lemieux et al.⁴⁶, who showed that the equatorial chemical shifts are often lower than the axial (the reverse of the behaviour of acetoxy protons), but that this is not nearly so useful in establishing conformation as the acetoxy proton chemical shift trend. Other work^{5,7} has confirmed this, and shown in fact that the methoxyl resonance indicates conformation only if C(2) has a hydroxyl substituent, a condition which the compounds of chapter 3 fall far short of fulfilling.

Other substituents have been studied²⁶, but only the three types of chemical shift described have any relevance to the compounds of the present investigation. The relationship of the work described in this section to that described in chapter 3 is touched on where appropriate in chapter 4.

2.4 The origin of spin-spin coupling

The general theory of spin-spin coupling is algebraically complicated, and it is outlined here only very briefly. Spin-spin coupling, first observed separately by Gutowsky and McCall²⁴ and by Hahn and Maxwell²⁵, was first fully explained in the paper by Ramsey and Purcell⁶⁶, and developed further by Ramsey⁶⁵.

The complete Hamiltonian for electron motion in the field of nuclei with magnetic dipole moments can be written as the sum of six Hamiltonians:

$$\mathcal{H} - V = \sum_{n=1}^6 \mathcal{H}_n \quad 2.4.1$$

where:

$$\begin{aligned} \mathcal{H}_1 &= \sum_j \frac{1}{2m} \left(\frac{\hbar}{i} \nabla_j + \frac{e}{c} \sum_K \gamma_K \underline{I}_K \times \underline{r}_{jK} / r_{jK} \right)^2 \\ \mathcal{H}_2 &= 2\beta\hbar \sum_j \sum_K \gamma_K \left[3(\underline{S}_j \cdot \underline{r}_{jK})(\underline{I}_K \cdot \underline{r}_{jK}) r_{jK}^{-5} \right. \\ &\quad \left. - (\underline{S}_{jK} \cdot \underline{I}_K) r_{jK}^{-3} \right] \end{aligned} \quad 2.4.2$$

$$\mathcal{H}_3 = (8\beta\hbar)/3 \sum_j \sum_K \gamma_K \delta(\underline{r}_{jK}) \underline{S}_j \cdot \underline{I}_K \quad 2.4.4$$

\mathcal{H}_4 , \mathcal{H}_5 and \mathcal{H}_6 are the electron spin-spin, orbital-orbital and spin-orbital interaction parts of the Hamiltonian: like V , the electrostatic potential energy, they do not involve the nuclear spin vectors \underline{I}_K , and so play no part in what follows. The sums are over the j electrons, mass m , charge e , and electron spin vectors \underline{S}_j at positions \underline{r}_j , and the K nuclei, with magnetogyric ratios γ_K at positions \underline{r}_K . Also, the Bohr magneton

$$\beta = e\hbar/2mc \quad 2.4.5$$

and
$$\underline{r}_{jK} = \underline{r}_j - \underline{r}_K \quad 2.4.6$$

The Dirac δ function $\delta(\underline{r}_{jK})$ selects a value when $\underline{r}_{jK} = 0$ in any integration over the co-ordinates of the j th electron.

The energy of interaction of the two nuclei due to their interaction with the electrons can be found by taking those parts of \mathcal{H} involving \underline{I}_K as a perturbation in second order (first-order matrix elements for a ground state with total orbital angular

momentum zero are equal to zero) on the other parts of \mathcal{H} .

The cross terms in \mathcal{H}_1 and \mathcal{H}_2 and in \mathcal{H}_1 and \mathcal{H}_3 vanish. Cross terms in \mathcal{H}_2 and \mathcal{H}_3 , although not zero, have been shown by Ramsey⁶⁵ to average to zero in conditions of frequent collisions. Thus the contribution to the total coupling constant $J_{KK'}$ between two nuclei (section 1.3) from the three Hamiltonians \mathcal{H}_1 , \mathcal{H}_2 and \mathcal{H}_3 can be treated separately, which we shall now do in reverse order, since \mathcal{H}_3 has proved⁶⁵ to make the greatest contribution to $J_{KK'}$ (see below) and is best dealt with first.

\mathcal{H}_3 can be interpreted as the correction necessary to \mathcal{H}_2 , which assumes simple magnetic dipolar behaviour for the nuclei and the electrons, when the nuclei and electrons are so nearly in "contact" that the point-dipole approximation is no longer a good one, and the magnetic dipole volume distributions, particularly in the nucleus, need to be considered. Electrons in the s-state, whose wave function is not zero at the nucleus, are in "contact" with the nucleus in this sense. \mathcal{H}_3 is like the term introduced by Fermi²⁰ to account for hyperfine structure in atomic spectra. Also, the Dirac δ function of \mathcal{H}_3 depends upon the electronic properties at the nucleus, and thus \mathcal{H}_3 is often referred to as the (Fermi) contact term. The second-order perturbation from \mathcal{H}_3 is given by:

$$E_{\text{pert}(3)} = - \sum_{n \neq 0} (E_n - E_0)^{-1} \langle 0 | \mathcal{H}_3 | n \rangle \langle n | \mathcal{H}_3 | 0 \rangle \quad 2.4.7$$

with symbols as in section 2.2. Substitution of equation 2.4.4 in equation 2.4.7 and selection of the terms linear in $\underline{I}_K \underline{I}_{K'}$, gives eventually for the contribution $E_{\text{pert}(3)}$ of \mathcal{H}_3 to E_{pert} a term of the form:

$$E_{\text{pert}(3)} = U_{\alpha\beta} \underline{I}_{K\alpha} \cdot \underline{I}_{K'\beta} \quad 2.4.8$$

where $U_{\alpha\beta}$ is a second rank tensor, with molecular-fixed axes. In conditions for experimentally observed coupling it can be replaced by its rotational average, which is a scalar, and if we make the usual conversion of energy to units of cycles/second, then:

$$E_{\text{pert}(3)} = h J_{KK'}(3) \underline{I}_K \cdot \underline{I}_{K'} \quad 2.4.9$$

This leads, with the approximation of using an average electronic excitation energy Δ for the $E_n - E_0$, as in section 2.2, to an expression for $J_{KK'}(3)$:

$$J_{KK'}(3) = - (128h\beta^2/27) \gamma_K \gamma_{K'} \Delta^{-1} \langle 0 | \sum_i \sum_j \delta(\underline{r}_{iK}) \delta(\underline{r}_{jK'}) \underline{S}_i \cdot \underline{S}_j | 0 \rangle \quad 2.4.10$$

\mathcal{H}_2 represents the dipole-dipole interactions between nuclear and electronic magnetic moments. A procedure identical to that outlined for \mathcal{H}_3 gives a contribution $J_{KK'}(2)$ to $J_{KK'}$ from \mathcal{H}_2 of:

$$J_{KK'}(2) = -(2h\beta^2/3\pi^2) \gamma_K \gamma_{K'} \Delta^{-1} \left\{ 0 \left| \left[3(\underline{s}_j \cdot \underline{r}_{jK}) \underline{r}_{jK} \underline{r}_{jK}^{-5} - \underline{s}_j \underline{r}_{jK}^{-3} \right. \right. \right. \\ \left. \left. \left. + 3(\underline{s}_{iK'} \cdot \underline{r}_{iK'}) \underline{r}_{iK'} \underline{r}_{iK'}^{-5} - \underline{s}_{iK'} \underline{r}_{iK'}^{-3} \right] \right| 0 \right\} \\ 2.4.11$$

\mathcal{H}_1 describes the kinetic energies of the electrons and their classical interaction as charged particles moving relative to the nuclear magnetic field. The contribution $J_{KK'}(1)$ of \mathcal{H}_1 to $J_{KK'}$ is due to the influence of the nuclear magnetic moments on the orbital electronic currents (compare section 2.2). This can be thought of as the setting up of induced electronic currents in the molecule by the nucleus K, with the production in turn by these currents of a secondary magnetic field at nucleus K'. This obvious mechanism was in essence the first proposed^{65,66} to account for spin-spin coupling, but it fails by an order of magnitude to explain the observed values of spin-spin coupling constants. Expansion of the \mathcal{H}_1 of equation 2.4.2 reveals two terms in the Hamiltonian which are linear in $\underline{I}_K \cdot \underline{I}_{K'}$. These terms, by methods broadly similar to those for \mathcal{H}_2 and \mathcal{H}_3 , (actually one of the terms is already of second-order in \underline{I} , and its first-order matrix element may be used), give contributions $J_{KK'}(1a)$ and $J_{KK'}(1b)$ to $J_{KK'}$:

$$J_{KK'}(1a) = (e^2 h / 6\pi^2 m c^2) \gamma_K \gamma_{K'} (0 \left| \sum_j \underline{r}_{jK} \cdot \underline{r}_{jK'} \underline{r}_{jK}^{-3} \underline{r}_{jK'}^{-3} \right| 0) \\ 2.4.12$$

and

$$J_{KK'}(1b) = -(2h\beta^2/3\pi^2)\gamma_K\gamma_{K'}\Delta^{-1}(0) \sum_i \sum_j r_{iK}^{-3} r_{jK'}^{-3} (\underline{r}_{iK} \times \underline{\nabla}_i) \cdot (\underline{r}_{jK'} \times \underline{\nabla}_j) |0\rangle \quad 2.4.13$$

As has been said, it turns out that $J_{KK'}(3)$ is a more important term for proton-proton coupling than $J_{KK'}(1a)$, $J_{KK'}(1b)$ or $J_{KK'}(2)$. For example, Ramsey⁶⁵ has made estimates of the magnitudes of the contributions of $J_{KK'}(1)$ and $J_{KK'}(2)$ in the hydrogen molecule. His values are $J_{KK'}(1) < 0.5$ c/s, and $J_{KK'}(2) \approx 3$ c/s, which compare with an estimate for $J_{KK'}(3)$ of about 40 c/s. This importance of $J_{KK'}(3)$ for protons is mainly because the electrons around a proton are generally well described by an s-type atomic orbital, while $J_{KK'}(1b)$ and $J_{KK'}(2)$ depend on atomic orbitals of p, d, f ... types. $J_{KK'}(1a)$ in addition is always quite small. It is reasonable to expect therefore that many of the observations on spin-spin coupling could be explained by appeal to equation 2.4.10. That involves first a knowledge of (or an estimate of) Δ , and second a specification of the ground state total electronic wave function $|0\rangle$ of equation 2.4.10. The second requirement has been tackled by use of both molecular-orbital (MO) theory and valence-bond (VB) theory: the problem is the same, of course, as in the evaluation of (section 2.2).

A MO treatment neglecting configuration interaction was first given in full by McConnell⁵³. His treatment predicted

on this basis that $J_{HH'} > 0$ (for any two protons H and H'), contrary to some experimental evidence², particularly as regards geminal coupling constants.

Pople and Bothner-By⁶² have given a more recent MO treatment, especially for coupling constants between geminal hydrogen atoms, which gives satisfactory interpretations of physical data, and accounts well for relative signs of coupling constants.

However, it appears that the VB approach given by Karplus et al.³⁹ and developed most importantly by Karplus³⁸ gives the best and most significant results for our purpose: the application of NMR to conformation studies in carbohydrates.

2.5 Spin-spin coupling and stereochemistry

Karplus³⁸ has shown that for a $^1\Sigma$ molecule whose ground state wave function ψ_0 is given by the equation

$$\psi_0 = \sum_j c_j \psi_j \quad 2.5.1$$

where the ψ_j are nonionic canonical VB structures and the c_j their weighting coefficients, if it is assumed that the one-electron orbitals are orthogonal and that the contributions to the electron density at one nucleus from electrons in orbitals centred on another nucleus are negligible, then equation 2.4.10 yields after a certain amount of manipulation:

$$J_{KK'}(3) = (128h\beta^2/27) \gamma_K \gamma_{K'} (4\Delta)^{-1} \phi_K(0) \phi_{K'}(0) \\ \times \sum_{j,k} c_j c_k (1/2^n - i_{jk}) [1 + 2^r j_k (P_{KK'})] \quad 2.5.2$$

The notation is as for equation 2.4.10, with the additions that $\varphi_K(0)$ and $\varphi_{K'}(0)$ are the electron densities at nuclei K and K' respectively, and the sum is taken over pairs j,k of a total of n canonical structures: i_{jk} is the number of islands, and $f_{jk}(P_{KK'})$ the exchange factor involved for nuclei K and K', in the superposition diagram for structures j and k.

The main problem in the evaluation of equation 2.5.2, the finding of reasonably accurate values for the c_j , is reduced by the consideration of only a small number of canonical structures (five for ethane). An account of the methods used for evaluation of the integrals involved in finding the c_j is of interest only in general VB theory and is not given here. $J_{KK'}(3)$ is calculated for ethane (and by extension ethane-like systems) assuming sp^3 hybridisation and using the calculated values of c_j along with various standard results of VB theory. The computed values were found to depend on φ (which is now a dihedral angle between two vicinal carbon-hydrogen bonds - see section 2.1 - and not the φ of equation 2.5.2). Karplus found that the values could be approximately fitted to φ by an equation of the form:

$$J = J_0 \cos^2 \varphi + K \quad 2.5.3$$

where we now drop subscripts: J refers to the coupling constant between two protons bonded to two adjacent carbon atoms which are both sp^3 hybridised, φ is the dihedral angle and J_0 and K are parameters whose values were found to be:

$$\left. \begin{aligned} J_0 &= 8.5, \quad 0^\circ \leq \varphi \leq 90^\circ \\ &= 9.5, \quad 90^\circ \leq \varphi \leq 180^\circ \\ K &= -0.28 \end{aligned} \right\} 2.5.4$$

all in c/s. There is evidence that these values are dependent, however, on the other carbon atom substituents.

This angular dependence of coupling constants had previously been observed in carbohydrate derivatives by Lemieux et al.⁴⁶. The Karplus relationship was applied by Lemieux⁴³, without any allowance for substituent effects^{42,82} (see below).

The first of a number of important empirical and semi-empirical modifications to equations 2.5.3-4 was made by Lenz and Heeschen⁵², who assumed that φ was subject to a harmonic oscillation of $\pm 15^\circ$, giving rise to a time-averaging correction. They found a modified form of the Karplus equation, using the observed spin-spin coupling in 2-deoxy-D-arabino-hexopyranose (probably not a suitable model compound for carbohydrates in general), which took the form:

$$J = F(J_0 \cos^2 \varphi - 0.28) \quad 2.5.5$$

with $F = 1.09 \pm 0.05$, compared to effectively $F = 1$ in equations 2.5.3-4. J_0 is the same as in equation 2.5.4.

A very similarly based modification, but perhaps more reliable²⁶, is due to Abraham et al.¹, who found modified values J'_0 of J_0 as follows:

$$\left. \begin{aligned} J'_0 &= 9.3, \quad 0^\circ \leq \varphi \leq 90^\circ \\ &= 10.4, \quad 90^\circ \leq \varphi \leq 180^\circ \end{aligned} \right\} 2.5.6$$

Abraham et al. used a better model compound, and attempted to justify the choice of $\varphi = 120^\circ$ for the relevant dihedral angle.

Lemieux et al.⁴⁶ have suggested a different way of modifying the original Karplus parameters. It is found experimentally that the unmodified Karplus equation gives values of J which are too low for a given φ , especially for $\varphi > 90^\circ$: note that equations 2.5.5 and 2.5.6 both have the effect of increasing the value of J for a given φ . From an analysis of the spectrum of 1,3-dioxolane, and a value for the appropriate dihedral angles based not on assumption but on the values which gave the best fit to the shape of the curve of equation 2.5.3, they suggested that the curve of equation 2.5.3 should be subject to an upward displacement of 2.2 c/s. This value removed the discrepancy between the value from the unmodified Karplus equation of the coupling constant for the best-fit dihedral angle and the observed coupling constant. This amounts to a modification of the parameters of equation 2.5.4 to give new values J''_0 and K''_0 :

$$\left. \begin{aligned} J''_0 &= 8.5, \quad 0^\circ \leq \varphi \leq 90^\circ \\ &= 9.5, \quad 90^\circ \leq \varphi \leq 180^\circ \\ K''_0 &= 1.92 \end{aligned} \right\} 2.5.7$$

Equations 2.5.4, 2.5.5, 2.5.6 and 2.5.7 give the four most important possible sets of parameters for evaluation of dihedral

angles in carbohydrates, and it is not clear which of at least the three modifications is best: all have given physically sensible results, and some criticisms can be made of all of them (see chapter 4). Karplus has commented on these empirical adjustments of his original equation³⁷; he concludes that alleged accuracies of one or two degrees in φ are meaningless. This question is taken up again in chapter 4.

The foregoing modifications to Karplus's relationship are all based essentially on making an allowance for a substituent effect. More fundamental, although still empirical, attempts at making such an allowance have been presented by Williamson⁸², Laszlo and Schleyer⁴² and extensively by Williamson et al.⁸³. It has been found^{42,82,83} that an observed vicinal coupling constant J_{obs} between two protons is affected by the electronegativity E_R of a substituent on one of the carbon atoms which carries one of the protons involved in the coupling. The experimental data can be well fitted by:

$$J_{\text{obs}} = J^0 - \alpha E_R \quad 2.5.8$$

where J^0 and α are empirical constants (almost always positive) which depend on the system. The electronegativity E_R is defined by¹²

$$E_R = 0.0114\delta + 1.78 \quad 2.5.9$$

where δ is the chemical shift in c/s at 60 Mc/s between the methyl and methylene protons of a series of monosubstituted

ethanes $\text{CH}_3\text{CH}_2\text{X}$; equation 2.5.9 is then the electronegativity of X.

The values of the parameters of equation 2.5.8 for various systems are given by Laszlo and Schleyer⁴². For the $\text{CH}_3\text{CH}_2\text{X}$ system they are²² $J^0 = 8.4$, $\alpha = 0.40$. No reliable values have been reported for six-membered saturated ring systems.

All spin-spin coupling so far discussed has been vicinal, that is between protons on the fragment $=\text{CH}-\text{CH}=$. But there are of course other types of coupling: geminal, between protons on the same carbon atom (frequently not observed in straightforward NMR experiments because the two protons are often magnetically equivalent) and coupling between protons more distant than vicinal, the so-called long-range couplings.

Many long-range spin-spin couplings have been observed⁷⁶, but the most important for our purposes is coupling through four σ bonds. Like the vicinal (three-bond) coupling described above, this type of spin-spin coupling shows strong steric dependence. Most though not all⁶⁰ of the observed long-range couplings appear to involve four coplanar σ bonds of zig-zag conformation (in the form of a W), so that this type of interaction can be concisely referred to as W-coupling.

It has been suggested by Meinwald and Lewis⁵⁸ that the interaction does not involve the two centre bonds of the W structure at all, but is due to direct interaction between the

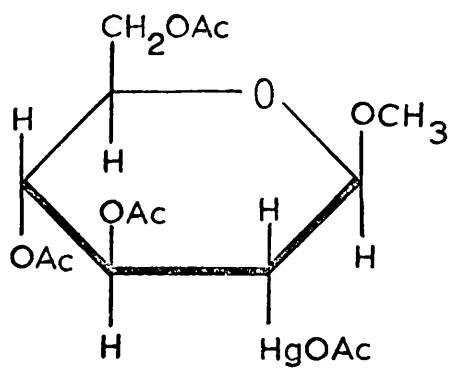
small orbitals of the carbon atoms to which the coupling protons are bonded. The size of the coupling constant in such situations is, apart from a few exceptional cases, not more than about 2 c/s, and is often closer to 1 c/s.

3.1 Experimental details

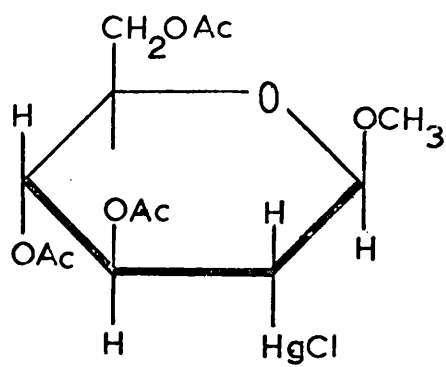
The four compounds whose NMR spectra were observed and analysed are, with the letters used to refer to them in this and the following chapter:

- A: methyl 2-acetoxymercuri-2-deoxy- β -D-glucopyranoside triacetate,
- B: methyl 2-chloromercuri-2-deoxy- β -D-glucopyranoside triacetate,
- C: methyl 2-chloromercuri-2-deoxy- α -D-mannopyranoside triacetate,
- D: methyl 2-chloromercuri-2-deoxy- α -D-galactopyranoside triacetate.

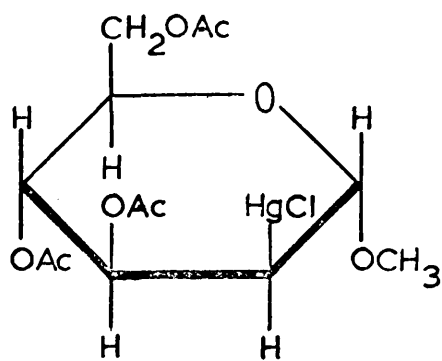
The configurations of these compounds, which are assumed at this stage to clarify the following exposition, are shown in figure 3.1 (page 40). The compounds were all examined in saturated deuterochloroform solution; solubilities are in the range 80 - 100 mg/ml. Proton magnetic resonance spectra were recorded at an applied fixed radiofrequency of 60 Mc/s using an A.E.I. RS2 spectrometer. For each compound, two series of spectra were run. In series 1, a number of scans, both upfield and downfield, were run of the range of chemical shifts from $\tau = 2$ to $\tau = 10$ (see section 3.2 below for an explanation of these Tiers's τ values). The second series was run only over the range of absorptions of the compound, under conditions of the highest attainable resolution with that spectrometer. Four to six series 1 spectra



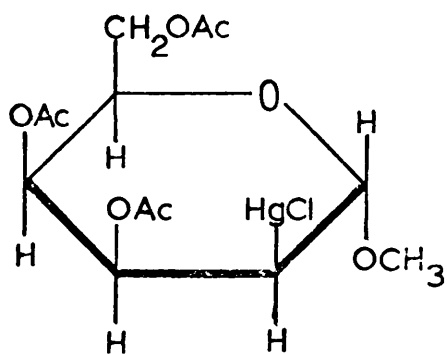
A



B



C



D

Figure 3.1. Assumed Haworth formulae for compounds A to D.

were run for each compound, and a large number of series 2, both upfield- and downfield-swept (eight each for compounds A, B and D, and twelve for compound C). Differences in the peak positions for upfield or downfield sweeps were not significant at the sweep rates used. The analysis described in sections 3.3 - 3.6 was performed on average peak positions for the series 2 spectra. Typical traces obtained for compounds A, B, C and D swept upfield (field increasing from left to right) are shown at the bottoms of figures 3.2, 3.3, 3.4, and 3.5 respectively.

3.2 Standardisation and calibration of spectra

Shielding constants, as defined by equations 1.3.1, 1.3.2 and 1.4.1, and discussed in the previous chapter, are more commonly expressed in terms of the chemical shift of a resonance position from that of a reference substance. This shift is proportional to the magnitude of the applied field, and it is useful to define a dimensionless quantity δ_H , independent of H_{app} ;

$$\delta_H = (H'_{app} - H'_{app(r)})/H'_{app(r)} \quad 3.2.1$$

where H'_{app} is the field, at a given transmitter frequency (compare equation 1.4.1) at which the protons in the sample substance come into resonance, and $H'_{app(r)}$ is the corresponding field for the protons of the reference substance.

The resonance field will in general show a concentration dependence, since (equation 2.2.1) a solute will generally have an (unknown) volume diamagnetic susceptibility different from

the value for the solvent. However, if the reference substance is in solution with the sample (and if certain other conditions are met)¹⁰ then δ_H of equation 3.2.1 will be independent of concentration, since H_{app} and $H_{app}(r)$ will be similarly affected. To avoid irregularities, both solvent and reference should have low molecular anisotropy. In these investigations the solvent was deuteriochloroform and the internal reference substance tetramethylsilane (TMS), now almost universally adopted for non-aqueous solutions. Apart from its low anisotropy, TMS is useful because it gives a single sharp peak at higher field than most organic proton absorption fields. It is also volatile, so that the sample substance can be recovered easily.

The spectra were calibrated using an audio side-band technique. If an audio-frequency ν_A is superimposed on the fixed oscillator radiofrequency ν_0 , it produces sidebands at frequencies $\nu_0 \pm \nu_A$. From equations 1.4.1 and 1.3.3, TMS absorbs at the field H' due to ν_0 , given by

$$H' = 2\pi\nu_0/\gamma(1 - \sigma) = k_T\nu_0 \quad 3.2.2$$

and also at fields H'_A due to $\nu_0 \pm \nu_A$, given by:

$$H'_A = 2(\nu_0 \pm \nu_A)/\gamma(1 - \sigma) = k_T(\nu_0 \pm \nu_A) \quad 3.2.3$$

Use of equations 3.2.2 and 3.2.3 in 3.2.1 gives the separation δ for these two peaks as:

$$\delta = \pm \nu_A/\nu_0 \quad 3.2.4$$

It is usual to express δ in parts per million (p.p.m.). Thus,

for $\nu_0 = 60$ Mc/s, and a ν_A of 480 c/s, $\delta = 8$ p.p.m.: peaks 8 p.p.m. away from the TMS peak are observed (in practice only that sideband downfield of the TMS peak), and by this means the spectrum is calibrated. δ_H is similarly expressed in p.p.m. As is usual, chemical shifts are expressed on Tiers's τ scale⁷⁷:

$$\tau = 10 - \delta_H \quad 3.2.5$$

where δ_H is in p.p.m. as defined by equation 3.2.1 and evaluated by use of the calibration from equation 3.2.4.

Equation 3.2.4 indicates why it is possible to express any separation in terms of frequency units at constant field, even though the spectrum was obtained with constant frequency at variable field. In what follows, the usual convention is adopted of expressing chemical shifts in τ units, but coupling constants in c/s.

3.3 Analysis of the spectra

In the observed spectra in figures 3.2c, 3.3c, 3.4c and 3.5c, certain assignments can be made very easily: the intense transitions due to the acetoxy and methoxy protons are picked out readily enough. But the absorptions due to the remaining protons, to the ring and methylene protons, form a complex set of bands which need a more subtle method of analysis. The procedure adopted to analyse the spectra is as follows:

1. An initial set of parameters, chemical shifts for every proton and spin-spin coupling constants between every pair of protons,

is postulated.

2. The theoretical spectrum for this set of parameters is calculated.
3. By comparison of the calculated spectrum with the observed spectrum, alterations to the set of parameters of step 1 can be made so as to reduce the discrepancies between the two spectra: this is referred to as refinement of the parameters.
4. This new set of parameters can then be used again as the parameters for step 2.

We now deal with the details of each step.

3.4 The initial set of parameters

It is not necessary for the first set of parameters to be very accurate. Examination of the spectra, and the application of the simple "first-order" considerations outlined in section 1.3, help in the initial assignments. Chemical considerations, and experience of the typical chemical shifts of protons in carbohydrates (see for example sections 2.2 and 2.3), also play a considerable part. However, good initial values merely reduce the labour of finding the final best parameters: in principle at least, the initial choice does not affect the final values.

3.5 Calculation of spectra

The mathematics of the calculation of an NMR spectrum is well established, and has been described via both wave-mechanical⁶³ and group-theoretical descriptions⁸⁴. Both the positions of

the absorption lines (transition energies) and transition intensities need to be calculated.

A complete set of basic spin eigenfunctions ψ_i , which are normalised and antisymmetrised products of the wave functions for each proton, are chosen. The possible eigenfunctions for a single proton can be represented by α and β , corresponding to an I_z of $+\frac{1}{2}$ and $-\frac{1}{2}$ respectively. Stationary state wave functions for the system are expressible as a linear combination of the ψ_i :

$$\psi = \sum_i c_i \psi_i \quad 3.5.1$$

The values of the c_i are chosen so that the system has minimum energy. A suitable form for the energy is:

$$E = \frac{\int \psi^* \mathcal{H} \psi d\tau}{\int \psi^* \psi d\tau} \quad 3.5.2$$

where E is the eigenvalue of the operator

$$\mathcal{H} = \mathcal{H}^0 + \mathcal{H}' \quad 3.5.3$$

operating on ψ . \mathcal{H}^0 is given for n protons by an extension of equation 1.1.4 (in energy rather than frequency units):

$$\mathcal{H}^0 = \sum_{j=1}^n \gamma_j H_{I_z j} / 2\pi \quad 3.5.4$$

and \mathcal{H}' has the form explained in section 2.4 (compare equation 2.4.9):

$$\mathcal{H}' = \sum_{i < j} J_{ij} \mathbf{I}_i \cdot \mathbf{I}_j \quad 3.5.5$$

Following the usual variational procedure, use of equations 3.5.1, 3.5.3, 3.5.4 and 3.5.5 in equation 3.5.2, and differentiation

of E with respect to the c_i yields a set of secular equations. For non-trivial solutions of these equations, the secular determinant must be zero. After use is made of the normalisation and orthogonality of the basic functions, the secular matrix has diagonal elements of the form $H_{ii} - E$, and off-diagonal elements of the form H_{ij} , where the H_{ij} are the matrix elements of the Hamiltonian of equation 3.5.3 between functions i and j (i may equal j). These matrix elements vanish between functions of different total z -component of spin F_z , and the matrix can often be further reduced by considerations of symmetry and selectivity of operators. Diagonalisation of the submatrices leads to a set of values E for the possible energies of the system, and knowledge of E gives the values of the c_i for each ψ , so determining the total wave functions.

The energies E can be used to determine the energies of those transitions not forbidden by the usual selection rule that the change in F_z should be ± 1 . The eigenfunctions ψ are then used to calculate transition intensities.

First-order theory gives the intensity $I_{m \rightarrow n}$ of the transition between two states of total functions ψ_m and ψ_n to be approximately:

$$I_{m \rightarrow n} \propto \left(\int \psi_m^* \mathcal{H}' \psi_n d\tau \right)^2 \quad 3.5.6$$

where \mathcal{H}' is the perturbing Hamiltonian (not that of equation 3.5.5). It has the same form as equation 1.2.1:

$$\mathcal{H}' = -\gamma H_x I_x \cos \omega t \quad 3.5.7$$

The matrix elements of equation 3.5.6 can be evaluated by use of equation 3.5.7 and expansion, using the previously calculated total wave functions Ψ , to give the intensities of the transitions on an arbitrary scale.

The calculations described in this section were performed using program RW1, written by Wallace,⁸⁰ on the DEUCE computer, and program IVA, an amended and augmented program written by Morton-Blake for the KDF 9 computer and based on a program translated by Kaptein from a Fortran program. Both computers used were in the computing department of the University of Glasgow.

3.6 Refinement of parameters

Two methods were adopted in the refinement of parameters. In the first, and simpler, the calculated spectrum was drawn up by hand and compared with the observed spectrum, drawn up to the same frequency and intensity scale. The notation commonly used in the analysis of proton magnetic resonance spectra is to designate one magnetically equivalent set⁵⁷ of n protons by A_n (n of course may = 1), and a second set of m magnetically distinct protons strongly coupled to the set A by B_m . ("Strongly coupled" means that the chemical shift between the A set and the B set is not very much greater than the spin-spin coupling between them.) A further set of protons strongly coupled to A and B is designated by C , and so on. Similarly, sets of protons

not strongly coupled to the A, B, C ... protons are designated by the letters X, Y Now compilations are available^{63,81} of the typical spectra for common types (AB_2 , ABX_2 etc.). An examination of the way in which a change in one parameter affects the published spectrum for the correctly chosen type, and a comparison of the discrepancies between the calculated and observed spectra, give an indication of how to change that parameter so as to reduce these discrepancies.

The types of system chosen for each compound are given in the keys to figures 3.2 to 3.5.

The second method is more mathematical. It is based on an analysis of the change in a transition energy due to simultaneous changes in all the parameters, and so depends upon the setting-up of a matrix (the T matrix) of partial differential coefficients of all the transition energies with respect to all of the $\frac{1}{2}n(n+1)$ parameters which determine the spectrum of n protons. The T matrix is formulated from the sets of coefficients of the ψ_j of step 1, section 3.3, which are obtainable from the program which calculates eigenfunctions as part of the calculation of spectra as described in section 3.5. A program to perform these calculations, written by Wallace⁸⁰, was used, on the DEUCE computer. This program reduces the total discrepancies of observed and calculated transition energies, and in a number (say ten) of cycles may reduce it considerably for a

given set of assignments. The program includes a facility whereby it is not necessary at first to assign all the theoretical transition energies of non-zero intensity. However, as refinement proceeds, additional assignments can be made and some assignments may need to be changed, so that it is necessary after every two or three computer refinement cycles to revert to the first method of informed guesswork about how the parameters should be changed.

The results of Table 3.1 are the outcome of a number of refinement cycles varying between twelve and thirty-five for each compound. After each cycle, the new parameters were used in step 2, as described in section 3.3 above.

3.7 Results

Table 3.1 gives the sets of values, chemical shifts and coupling constants, which emerged from the final cycle of refinement for each compound. These sets of parameters were used to calculate the line spectra of figures 3.2b, 3.3b, 3.4b and 3.5b. The estimated accuracies of the parameters are indicated in the footnotes to the table.

Figure 3.2 refers to compound A, figure 3.3 to compound B, 3.4 to compound C and 3.5 to compound D. Part c of each figure shows a typical series 2 spectrum of the corresponding compound (see section 3.1), and it should be emphasised that the calculated spectrum of part b of each figure is intended to give the best

fit to the average of all the series 2 spectra run for the compound, and that the intensities in parts b are proportional to the heights of the lines, whereas the comparable intensities of parts c are of course proportional to the areas under the peaks. Parts a of each figure are intended to indicate how the calculated spectra b arise from the absorption positions of the protons.

Table 3.1. Proton chemical shifts^a and coupling constants^b
for solutions of compounds A, B, C and D in CDCl₃

Compound:	A	B	C	D
<u>Chemical Shifts^a</u>				
H(1)	5.33	5.23	4.89	4.95
H(2)	7.40	7.38	6.69	7.17
H(3)	4.78	4.72	4.15	4.28
H(4)	5.05	4.99	5.01	4.71
H(5)	6.29	6.13	5.96	5.75
H(A) ^f	5.68	5.60	5.76	5.93
H(B) ^f	5.88	5.78	5.76	5.93
-OCH ₃	6.49	6.39	6.61	6.68
-CO ₂ CH ₃	$\begin{cases} 7.92 \\ 7.96 \end{cases}$	7.82	$\begin{cases} 7.89 \\ 7.94 \end{cases}$	$\begin{cases} 7.75 \\ 7.98 \end{cases}$
<u>Coupling Constants^b</u>				
J ₁₂	10.0 ₁	9.7 ₈	1.5 ₀	-0 ^c
J ₂₃	10.9 ₃	11.2 ₆	5.3 ₅	5.1 ₆
J ₃₄	8.9 ₀	9.4 ₉	9.0 ₅	3.0 ₉
J ₄₅	9.0 ₀	7.3 ₈	9.3 ₅	-0 ^c
J _{5A} ^f	5.8 ₀	4.6 ₁	~8 ^d	7.0
J _{5B} ^f	3.2 ₃	2.7 ₈	~8 ^d	7.0
J _{AB} ^g	11.9	12.5	- ^e	- ^e

(Notes on following page)

Notes to table 3.1

- a Chemical shifts are in τ units and are given to the nearest 0.01 τ unit.
- b Coupling constants are in units of c/s., and unless otherwise indicated (see c, d and e) are accurate to within ± 0.2 c/s.
 J_{XY} indicates the coupling constant between protons H(X) and H(Y): these latter symbols are used in this table only, to represent the chemical shifts of the corresponding protons.
- c Less than $|0.3|$ c/s.
- d These coupling constants can be altered by relatively large amounts without appreciably affecting the calculated spectrum.
- e Not available from the spectrum.
- f Protons A and B are the methylene (C(6)) protons
- g J_{AB} is almost certainly negative, but changing its sign has little or no effect on the calculated spectra.

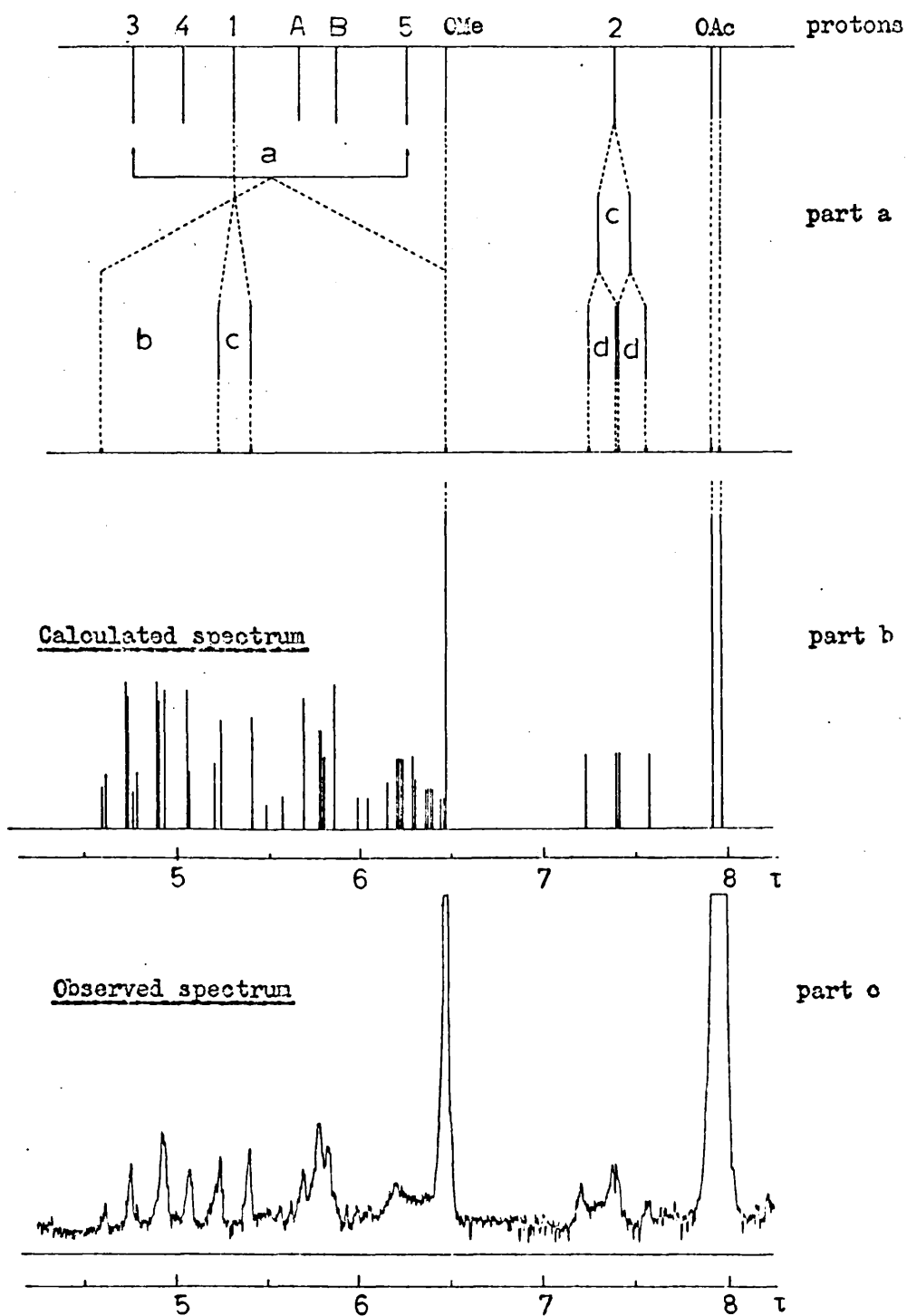


Figure 3.2. Observed and calculated spectra for compound A

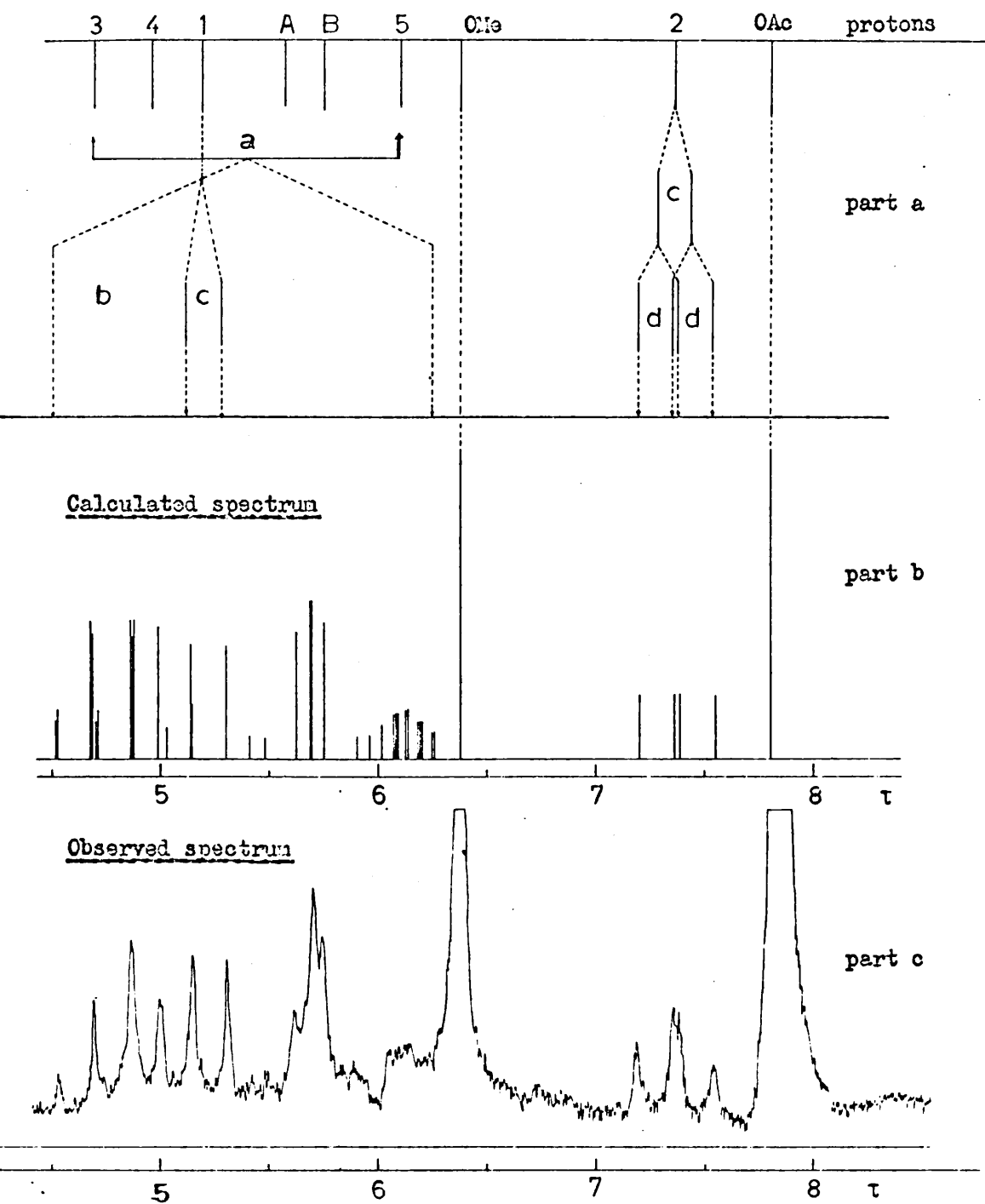


Figure 3.3. Observed and calculated spectra for compound B.

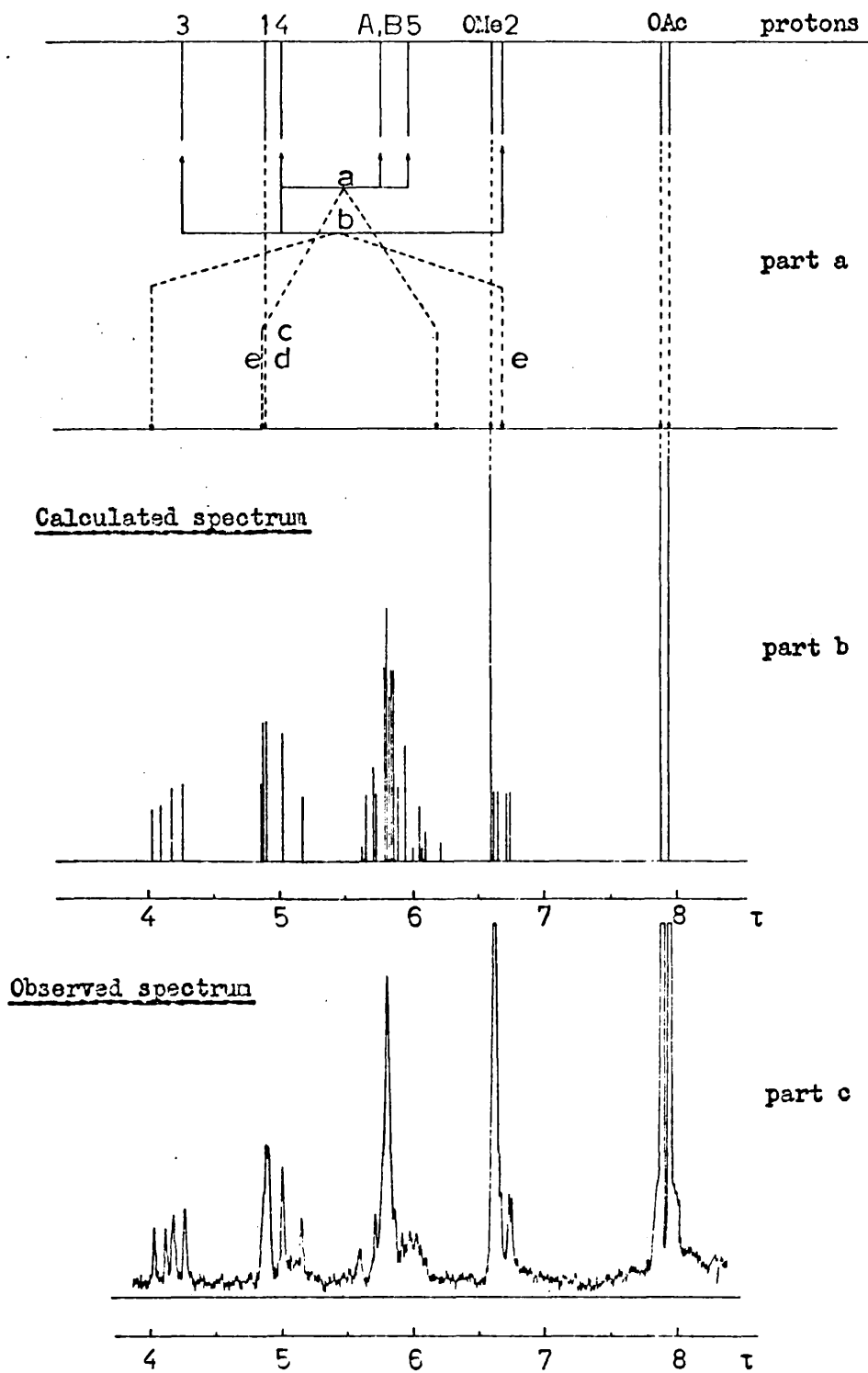


Figure 3.4. Observed and calculated spectra for compound C.

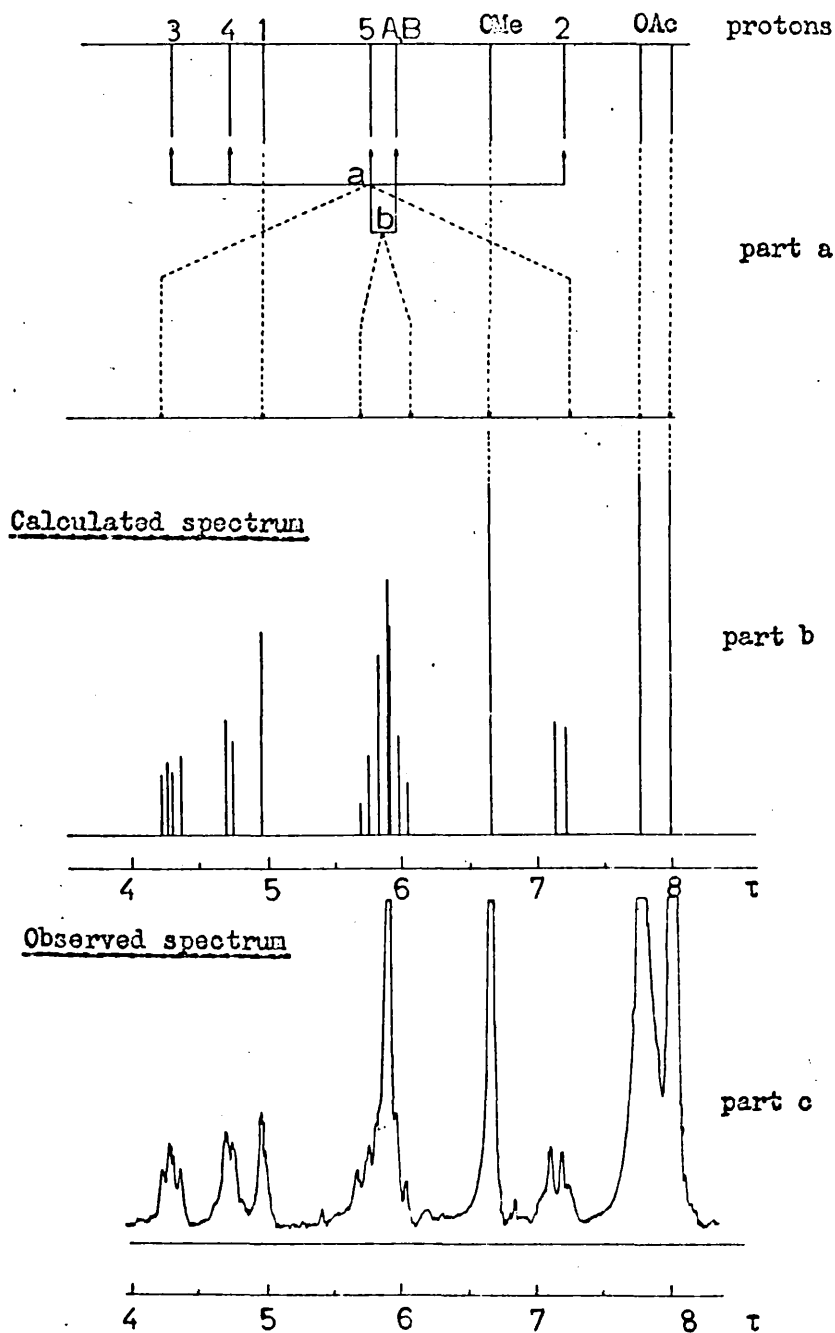


Figure 3.5. Observed and calculated spectra for compound D.

Key to figures 3.2, 3.3, 3.4 and 3.5

In all figures, part a shows the origins of the spectra.

Figure 3.2 Compound A

- a H(A)H(B)H(3)H(4)H(5) calculated as a 5-spin (ABCDE) system.
- b H(3) couples with H(2): $J_{23} = 10.9_3$ c/s.
- c $J_{12} = 10.0_1$ c/s.
- d $J_{23} = 10.9_3$ c/s.

Figure 3.3 Compound B

- a H(A)H(B)H(3)H(4)H(5) calculated as a 5-spin (ABCDE) system.
- b H(3) couples with H(2): $J_{23} = 11.2_6$ c/s.
- c $J_{12} = 9.7_8$ c/s.
- d $J_{23} = 11.2_6$ c/s.

Figure 3.4 Compound C

- a H(4)H(5)H(A)H(B) calculated as a 4-spin (ABCD) system.
- b H(2)H(3)H(4) calculated as a 3-spin (ABC) system.
- c H(4) couples with H(5): $J_{45} = 9.3_5$ c/s.
- d H(4) couples with H(3): $J_{34} = 9.0_5$ c/s.
- e H(1) couples with H(2): $J_{12} = 1.5_0$ c/s.

Figure 3.5 Compound D

- a H(2)H(3)H(4) calculated as a 3-spin (ABC) system.
- b H(5)H(A)H(B) calculated as a 3-spin (AB₂) system.

4.1 Chemical preliminaries

The methoxymercuration of tri-O-acetyl-D-glucal (compound E, figure 4.1, page 59) with mercuric acetate in methanol, followed by reaction with sodium chloride, gives approximately equal amounts of compounds B and C. If the reaction with sodium chloride is omitted, compound A can be isolated; this is converted to compound B with sodium chloride and must have the same stereochemistry.^{35,56} Compound D (figure 4.2, page 60) is prepared by methoxymercuration of tri-O-acetyl-D-galactal and reaction with sodium chloride.

The configuration at C(1) can be examined by reduction of the compounds with potassium borohydride to the corresponding 2-deoxyglycosides, and this reduction has also been used³⁵ to establish that, as expected, the methoxyl group becomes attached to C(1) in the methoxymercuration. Such reductions yield the 2-deoxy- β -D-glycosides from compounds A and B, and the 2-deoxy- α -D-glycosides from compounds C and D. This appears to prove that compound C in particular is an α -mannose derivative. However, there is some disagreement on this point, since compound C can be interconverted⁷¹ with a compound P (also obtainable by methoxymercuration of D-glucal; see figure 4.1) to which Manolopoulos et al.⁵⁶ have assigned the β -manno configuration. They present two pieces of evidence. First, they find that

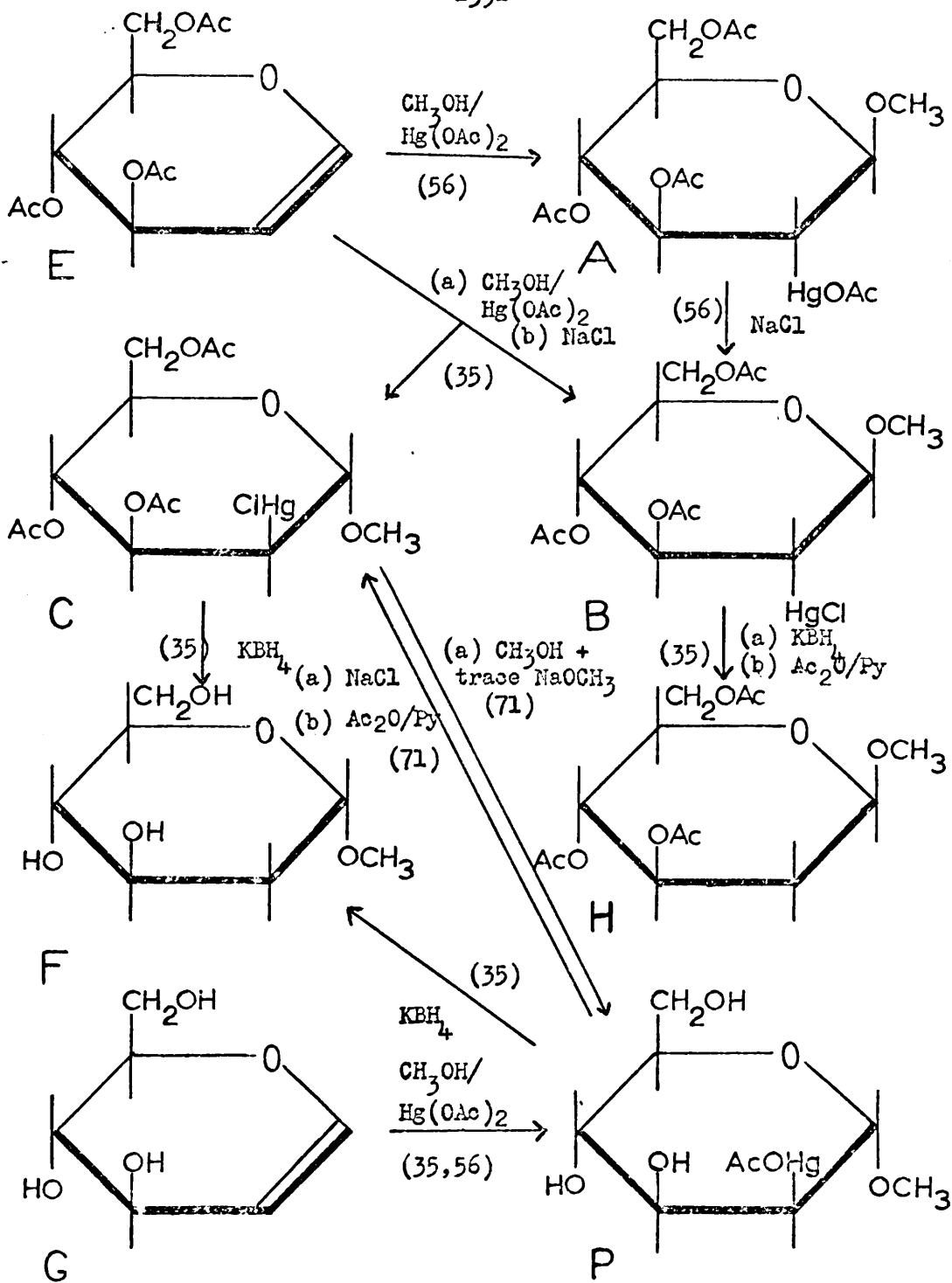


Figure 4.1 Summary of the chemistry: compounds A, B and C.

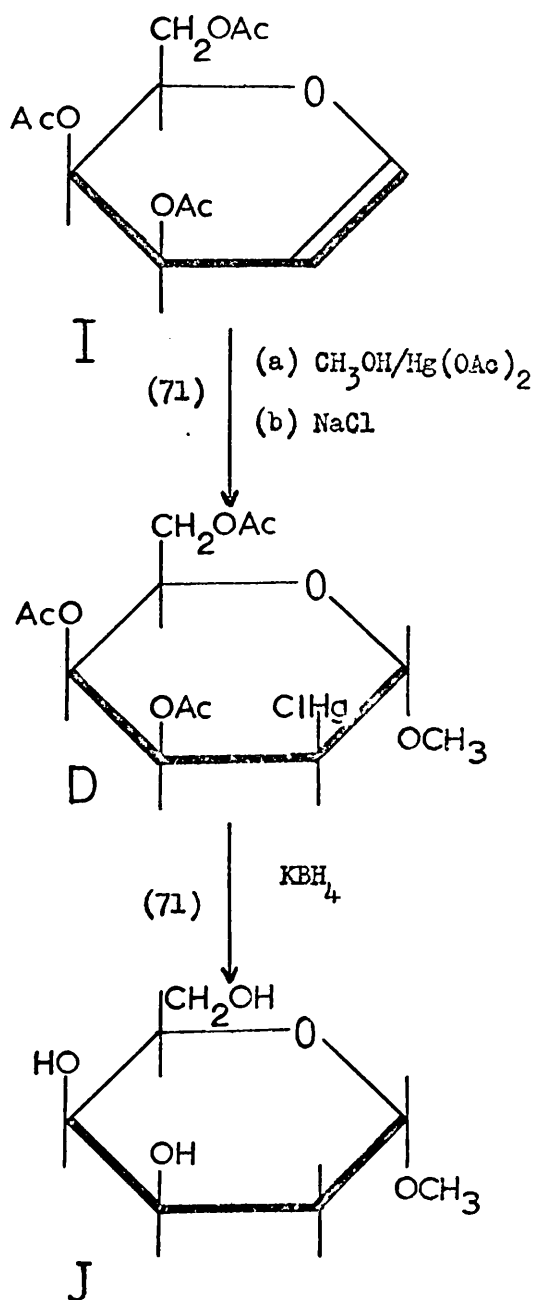


Figure 4.2 Summary of the chemistry: compound D.

Key to figures 4.1 and 4.2

Compounds A, B, C and D are the same as those in the text. The full systematic names of the other compounds are given below, on the assumption that the attributed structures given in this thesis are correct.

A: methyl 2-acetoxymercuri-2-deoxy- β -D-glucopyranoside triacetate

B: methyl 2-chloromercuri-2-deoxy- β -D-glucopyranoside triacetate
(structure established by X-ray analysis)¹⁷

C: methyl 2-chloromercuri-2-deoxy- α -D-mannopyranoside triacetate

D: methyl 2-chloromercuri-2-deoxy- α -D-talopyranoside triacetate
(structure supported by partial X-ray analysis)⁶

E: tri-O-acetyl D-glucal.

F: methyl 2-deoxy- α -D-glucopyranoside (confirms configuration at C(1))

G: D-glucal

H: methyl 2-deoxy- β -D-glucopyranoside triacetate

I: D-galactal

J: methyl 2-deoxy- α -D-galactopyranoside (confirms configuration at C(1)).

P: methyl 2-acetoxymercuri-2-deoxy- α -D-mannopyranoside (given the β -manno structure in (56))

Figures in brackets refer to references.

compound P with $\text{Br}_2/\text{CH}_3\text{OH}$ gives methyl 2-bromo-2-deoxy- β -D-glucopyranoside. This is explained by Riddell and Schwarz⁷¹ as involving deoxymercuration to D-glucal followed by methoxybromination: such a reaction has since been reported⁴⁴. Their second piece of evidence is based on the rate of deoxymercuration with sodium iodide of compound P. The argument is that the time elapsing before the appearance of the first precipitate of mercuric iodide is a measure of the ease of deoxymercuration (this is in any case doubtful) and this leads them to claim a 1,2-cis structure for compound P and thence for compound C. But Riddell and Schwarz⁷¹ were unable to repeat these observations, and indeed have found that 0.1 M mercuric iodide is completely soluble in 0.4M ethanolic sodium iodide. Thus the allegation that compound C has a β -manno structure would appear to be mistakenly based. However, it is of interest to examine the NMR evidence on this point, which is done where appropriate in the following sections.

The configuration at C(2) also needs to be established. Although electrophilic additions such as methoxymercuration generally occur by trans-addition⁷⁹, it may involve cis-addition^{78,79}. As will be seen below, the NMR evidence is that trans-addition occurs in these compounds.

4.2 Effects due to the mercury atom

It is clear that the presence of mercury in the compounds studied constitutes the most striking difference between these

compounds and the subjects of previous investigations. Mercury is a fairly large atom (Van der Waals radius 1.5 Å) and the size of the groups in which it is found in these compounds must be considerably greater. It is metallic, and the Hg-C bond shows many unusual features for a metal-carbon bond, including a very low bond energy⁷². Both from a very simplified picture of the shielding effect of mercury on a proton bonded to the same carbon atom¹⁸, and more importantly from a large number of experimental results^{31,59} it is to be expected that the proton on the mercury-bearing carbon atom will be well shielded and will absorb at higher applied field. In all the compounds studied, H(2) does indeed absorb at highest applied field, being displaced upfield by about 2.5 p.p.m. This observation helps confirm that the mercury atom is in fact substituted in position 2 of the pyranoside ring.

The more common isotopes of mercury, ²⁰²Hg and ²⁰⁰Hg, have I = 0, but ¹⁹⁹Hg (natural abundance 16.86%) and ²⁰¹Hg (natural abundance 13.24%) have I = 1/2 and 3/2 respectively. Couplings of the protons in the fragment ¹⁹⁹Hg - CH - CH - have been observed: in almost all cases the coupling of the mercury atom with the β proton has been greater than that with the α proton, being of the order of 200 to 300 c/s. The range of β-proton couplings is greater than the range of α-proton couplings. Except perhaps in compound D (see section 4.5) no Hg-H couplings have been

observed: in all cases the spectra of the compounds were scanned on well upfield of the TMS peak (not shown in the observed spectra of figures 3.2 to 3.5) and in no case was the high field wing of the H(1), H(2), or H(3) absorption, due to coupling with mercury, convincingly seen. This is almost certainly because of the low solubilities of the compounds, taken together with the rather low natural abundances of the magnetically active isotopes of mercury, and the already (sometimes considerably) split peaks due to H(1), H(2) and H(3). In addition, quadrupole relaxation effects in the case of ^{201}Hg may have broadened the spin-spin splitting satellite peaks beyond detection (see section 4.6). Other effects possibly associated with the mercury atom are brought up in sections 4.3 and 4.5.

4.3 Ring proton chemical shifts

It will be shown in section 4.5 especially that the compounds A, B, C and D do have the configurations of figure 3.1 and do take up (more or less distorted) C1 chair conformations in deuteriochloroform solution. If for the moment the distortions are ignored and the compounds are imagined in the "perfect" chair conformations of section 2.1, then the various ring protons can be assigned to axial or equatorial orientations. Then it is easily seen that H(3) is axial in all the compounds, while H(1), H(2) and H(4) are either axial or equatorial in different compounds. An inspection of Table 3.1 shows that H(1), H(2) and H(4) absorb at lower

applied field when they are equatorial than when they are axial. This is in accordance with the findings of Lemieux et al.⁴⁶, so that the chemical shift of ring protons, although not in general reliable (section 2.5) appears to reflect conformation and seems not to be affected by mercury substitution in the compounds examined.

The point of especial interest in this connection is the configuration at C(1) in compound C. The coupling constants (see section 4.5) show that compound C is a manno derivative rather than a gluco derivative, and that fixes the configuration at C(2). But the configuration at C(1) is not available from the coupling constant J_{12} ^{44,49,50}. However, since the anomeric proton H(1) in particular absorbs downfield in compound C compared with compounds A and B (A and B must have similar conformation - section 4.1 - and compound B has been shown to have a β -gluco structure in the solid phase by X-ray analysis¹⁷) and is similar to compound D (which, a partial X-ray analysis indicates, has an α -manno structure at C(1) and C(2) in the crystal⁶), this is evidence in favour of the α -anomer for compound C.

In addition, H(5) absorbs downfield in compound C as compared to compounds A and B, which is compatible with the reported^{49,50} deshielding of H(5) in carbohydrate derivatives by an axial oxygen function on C(1): this also supports the α -anomeric structure for compound C.

An interesting observation is that H(3) in these compounds absorbs at lower applied field when it is trans to the mercury atom than when it is cis. If the effect is general, and no other information appears to be available on whether or not it is general, it may be due either to through-space shielding associated with diamagnetic anisotropies in the mercury function (the cis-proton, being nearer to the mercury function, is more shielded than is the trans-proton) or to effects transmitted through the molecule itself. It would be premature, however, to embark on an explanation of an effect observed only in these four compounds.

4.4 Substituent chemical shifts

In all of the compounds A, B, C and D, the main purposes of the study were to arrive at some conformational and configurational information on the pyranoside rings, particularly by an analysis of that part of the NMR spectrum arising from the ring protons: this analysis gives information mainly through the ring-proton coupling constants. The experimental conditions necessary to study the weak ring-proton absorptions resulted in very intense absorption peaks from the protons of the substituent methoxy and acetoxy groups (see observed spectra). No attempt was made to study the substituent groups proton resonance in any detail, and in the case of the acetoxy groups, only an estimate was generally made of the centre of gravity of the relatively very intense peaks. Nevertheless, the observed chemical shifts can

be compared at least qualitatively with previous values for the chemical shifts of such substituent group protons in carbohydrate rings.^{5,7,28,29,34,46,70} (see section 2.3). It is very likely that in those compounds (A, C and D) in which two acetoxy proton resonance peaks were easily seen, the resonances corresponded to the two different chemical positions of the $\text{CH}_3\text{COO-}$ group rather than to the axial-equatorial difference referred to in section 2.3: only in compound D are there both axial and equatorial acetoxy substituents. The chemical shifts observed are similar to those previously found for this type of compound.

In compounds A and B, if the conformations are taken as in section 4.3 to be undistorted C_1 , the methoxy substituents are equatorial, whereas in compounds C and D they are axial. Table 3.1 shows that the methoxy group protons of compounds A and B have lower τ values than the corresponding protons of compounds C and D. This observation is further support for the α -anomeric, rather than the β -anomeric, structure for compound C: the NMR evidence (this section and section 4.3) is consistent on this point. In accordance then with the findings described in section 4.3, axial methoxy protons absorb at higher applied field than do equatorial methoxy protons, in the compounds A to D as in most other carbohydrate derivatives.

4.5 Analysis of the ring proton coupling constants

Subject to the comments below and of section 4.6, an application

of the equation of Karplus and modifications of it (section 2.5) leads to the conclusion that the compounds A to D have more or less distorted C1 chair conformations. As a starting point for the interpretation of the ring proton coupling constants, figure 4.3 (page 69) shows the four compounds in this conformation.

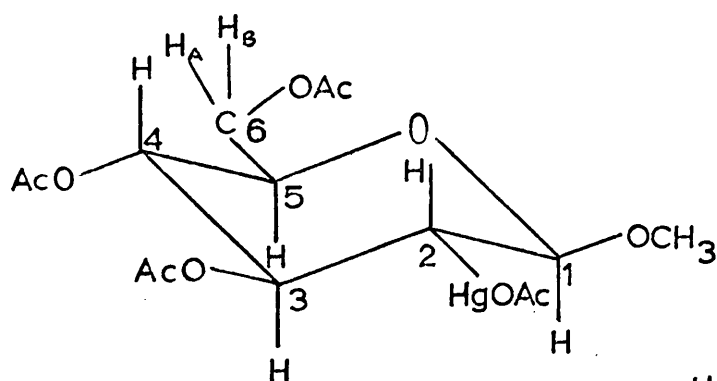
In compounds A and B, different chemical shifts for H(A) and H(B), and different coupling constants J_{5A} and J_{5B} are found. This indicates that there is hindrance to free rotation about the C(5)-C(6) bond in these compounds; and no doubt there is some restriction to the same rotation in compounds C and D also. However, the chemical shifts between H(5), H(A) and H(B) are very small, so that the uncertainty in evaluating J_{5A} , J_{5B} and J_{AB} from the observed spectra is large, and any attempt to deduce any more information about the preferred conformations of the $-\text{CH}.\text{CH}_2\text{OCOCH}_3$ fragments than the fact that preferred conformations exist, could hardly be justified.

However, all the other coupling constants are believed to be reliable to ± 0.2 c/s. It is therefore reasonable and of interest to attempt to get more detailed information from these on the ring conformations. The equations of section 2.5 all have the form:

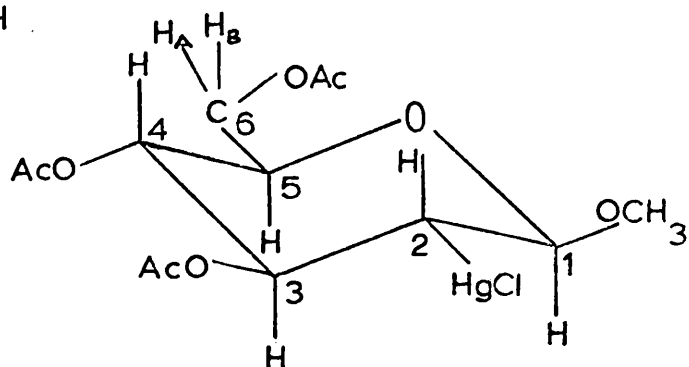
$$J = J_0 \cos^2 \varphi + K \quad 4.4.1$$

so that we can solve for φ using:

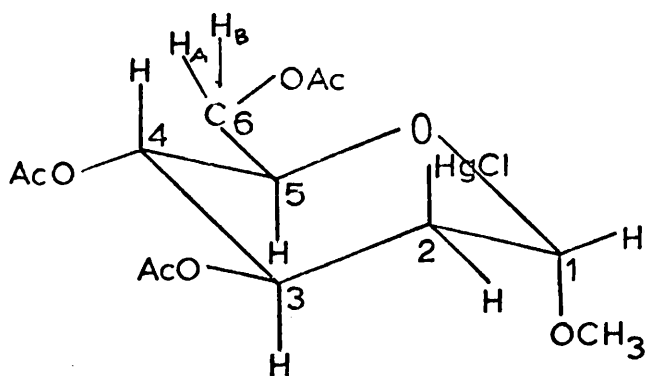
$$\cos^2 \varphi = (J - K)/J_0 \quad 4.4.2$$



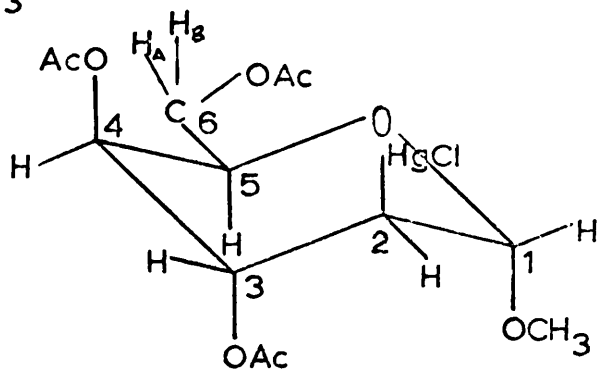
A



B



C



D

Figure 4.3. Compounds A to D in perfect C1 conformation.

Now the left-hand side of equation 4.4.2 has the limits $0 \leq \cos^2 \varphi \leq 1$ which in turn leads to limits for J, the observed value of the coupling constant, of $K \leq J \leq J_0 + K$ ($J_0 > 0$). This means that any of the forms of the Karplus equation has a solution only within these limits on J. In fact none of the modifications is adequate to account for the whole range of the coupling constants observed in these spectra. It is more usual for the observed coupling constant to exceed the upper limit $J_0 + K$, leading to $\cos^2 \varphi > 1$, but in the modified form of Lemieux et al⁵¹, in addition the smaller values of J lead to $\cos^2 \varphi < 0$. In these cases, when J has exceeded the upper limit for the equation, $\cos^2 \varphi = 1$ has been taken, and when J has fallen below the lower limit, $\cos^2 \varphi = 0$ has been assumed.

Within these limitations, Table 4.1 shows the results of the application of the unmodified Karplus³⁸ equation (column headed K), the Lenz-Heeschen equation (column headed H): in this column the range of values of the dihedral angle arises from the uncertainty of the value of F in equation 2.5.5, the Abraham equation (column headed A) and the Lemieux equation (column headed L). In the table, the angles have been quoted to the nearest degree purely for the purpose of comparison between the different methods, and not of course because it is imagined that the results are accurate to within one degree. All the equations are quadratic in $\cos \varphi$ and give two (unsymmetrical about 90°)

Table 4.1. Interpretations of ring proton coupling constants

Compound	Dihedral Angle	K	H	A	L	E
A	H(1)H(2)	*180°	168°-*180°	174°	157°	180°
	H(2)H(3)	*180°	*180°	*180°	167°	180°
	H(3)H(4)	170°	157°-165°	160°	149°	180°
	H(4)H(5)	171°	158°-166°	161°	150°	180°
B	H(1)H(2)	*180°	165°-*180°	170°	155°	180°
	H(2)H(3)	*180°	*180°	*180°	173°	180°
	H(3)H(4)	*180°	162°-174°	166°	153°	180°
	H(4)H(5)	154°	147°-152°	149°	139°	180°
C	H(1)H(2)	63° <u>or</u> 116°	63°-64° <u>or</u> 114°-115°	64° <u>or</u> 114°	**90°	60°
	H(2)H(3)	35°	37°-40°	39°	51°	60°
	H(3)H(4)	172°	158°-169°	161°	150°	180°
	H(4)H(5)	*180°	161°-171°	164°	152°	180°
	H(1)H(2)	80° <u>or</u> 100°	80° <u>or</u> 100°	80° <u>or</u> 100°	**90° 52°	60° 60°
D	H(2)H(3)	37°	38°-41°	40°	52°	60°
	H(3)H(4)	51°	52°-54°	53°	68°	60°

(continued on page 72)

Table 4.1. Interpretations of ring proton coupling constants

(continued)

Compound	Dihedral Angle	K	H	A	L	E
D	H(4)H(5)	80° <u>or</u> 100°	80° <u>or</u> 100°	80° <u>or</u> 100°	**90°	60°

Notes:

* The value of J gave $\cos^2 \varphi > 1$.

** The value of J gave $\cos^2 \varphi < 0$.

solutions for φ . However construction of models and quite simple geometrical considerations generally enable one to distinguish that set of solutions, consisting of a choice of one from each pair of solutions, which is mutually consistent. Occasionally such a choice cannot be made (for example when the solutions are close together) and this is indicated in the table. The last column (headed E) of the table gives the values "expected" for the dihedral angles on the basis of a six-membered ring with all angles the tetrahedral angle in an undistorted C1 chair conformation.

In the table above, no allowance has been made for the effect of substituent electronegativity (section 2.5). The electronegativity for mercury given by Gordy and Thomas²³ (a modified Pauling scale) is 1.9. The electronegativity on the Cavanaugh and Dailey¹² scale needs a suitable model compound for its determination (section 2.5), and a monosubstituted ethane does not exist: the closest is mercury diethyl, $\text{Hg}(\text{CH}_2\text{CH}_3)_2$, for which two discordant values^{15,19} for the chemical shift between the methyl and methylene protons are reported of 22.5 and 16.4 c/s (after correction to 60 Mc/s). However, if we take $\delta = 20$ c/s in equation 2.5.9, we get for E_R a value of 2.0, which is at least reasonable. As has been said in section 2.5, values of the parameters J° and α of equation 2.5.8 are not available for six-membered ring systems, and quoted values of the parameters^{42,82,83} depend so markedly on the system studied, with no easily discernible

trend, and further the electronegativity correction is so dependent on the configuration of the carbon atoms bearing the protons between which coupling is measured⁹, that it is almost certainly better to make no correction at all than to make one which would be based on guesswork. Despite this, it is probably safe to say that E_R for mercury is lower than E_R for hydrogen, and certainly lower than E_R for oxygen (Gordy and Thomas²³ give electronegativities of 2.1 and 3.5 for hydrogen and oxygen respectively). Although no parameter values for equation 2.5.8 are available, it is likely that the form of the equation still holds good, with J^0 and α both positive. In that case, J_{obs} will be higher because of mercury substitution. In compound C, for example, J_{12} is similar in magnitude to values found for other α -mannopyranosides^{13,33,44,50}, but J_{23} is somewhat larger than the value of around 3 c/s commonly found^{13,33,44}; but it is in agreement with the value found in compound D. It is also noteworthy that $J_{2,3}$ in the methyl 2-deoxyglucopyranosides is around 5.0 c/s. A higher value of J_{obs} leads in turn to a higher value of $\cos^2 \varphi$ in equation 4.4.2, and to values of φ closer to 0° ($\varphi < 90^\circ$) or to 180° ($\varphi > 90^\circ$). This can be borne in mind in interpreting the values of φ for the dihedral angles H(1)H(2) and H(2)H(3).

It must also be remembered that the C-O-C angle is in fact less than the tetrahedral angle of $109^\circ 28'$, and that this will have the effect of reducing by small and varying amounts the

angles in column E of table 4.1.

Inspection of that table then shows that the significant deviations from the "expected" values in compounds A, B and C concern the dihedral angles $H(\widehat{3})H(4)$ and $H(\widehat{4})H(5)$, both of which are reduced. This can be accounted for by supposing that in these compounds C(4) moves down towards the mean plane defined by the atoms C(2), C(3), C(5) and O. An X-ray analysis¹⁷ of compound B indicates no significant deviations from this picture.

As regards compound D, it is worth pointing out first that a comparison of the $H(3)H(4)$ entries of Table 4.1 with each other show that compound D is indeed a talose derivative, and not a galactose derivative (which could have resulted had the methoxy-mercuration proceeded by cis-addition). In this compound, the distortion appears to be of a different kind from that described for the other three compounds, perhaps essentially because only in compound D is 2,4 diaxial repulsion between the $-HgCl$ and the $-OCOCH_3$ residues possible. The significant distortions in this compound can be rationalised by supposing that C(2) moves down towards the mean plane containing the atoms C(3), C(4), O and C(1), and that the $-CH_2OCOCH_3$ fragment on C(5) is repelled away from the axial $-OCOCH_3$ residue on C(4), with some tilting back of the C(4)-O or of the Hg-C bond, or of both. The overall conformational picture in compound D is then of a half-boat conformer. It is interesting that a partial X-ray analysis⁶

of compound D, done after the NMR work was completed, has indicated that the Hg to O(4) distance is greater than would be expected in the absence of distortion. The distortions in the solid suggested to explain the X-ray findings are exactly like those proposed here to account for the NMR spectrum in solution.

4.6 Other effects

The absorption peaks in the spectrum of compound D appear to be broader than those in the other spectra, and measurements, by comparison with the absorption peak of TMS in the complete spectrum show that the peaks due to H(1), H(2), H(3) and H(4) at least are indeed broader (based on the full line width at half-height) by a factor of about 1.6. This is not a very large broadening, and explanations of this observation based on the spectrum in one set of conditions must be speculative.

Broadening of the absorptions may be due to Hg-H coupling differences in two conformers (say the C1 and the 1C chair conformers) being a case of incomplete collapse of the H(1), H(2) and H(3) absorption peaks, or to kinetic broadening effects. Also, quadrupolar relaxation of ^{201}Hg may lead to broadening of the H(2) absorption peak. But these mechanisms would apply equally to compounds A, B and C.

Compound D, in an undistorted C1 conformation, is the only one in which two protons (H(2) and H(4)) are in the W conformation which normally appears to be necessary for long-range spin-spin

coupling across four σ bonds. But the magnitude of this coupling falls off sharply as the W is distorted (section 2.5), and compound D is considerably distorted, so that any coupling would be small, and in fact it is not explicitly observed, but it may be that the absorption peaks from H(2) and H(4) are broadened because of an unresolved small splitting of this type.

A final possibility is that another conformation of compound D, probably the LC conformer, is present in CDCl_3 solution, although in such small concentration that its NMR spectrum is not separately observed. In these circumstances, broadening of the absorption lines of the protons of compound D could occur either as a result of lifetime broadening from a slow exchange rate, or as a result of incomplete exchange narrowing from an only moderately fast exchange rate. Further spectra of compound D, run at a number of different temperatures, would be needed to decide between these possibilities.

1. R.J. Abraham, L.D. Hall, L. Hough and K.A. McLauchlan, Chem. and Ind., 1962, 213; J. Chem. Soc., 1962, 3699.
2. S. Alexander, J. Chem. Phys., 1958, 28, 338.
3. J.E. Anderson, Quart. Rev., 1965, 19, 426.
4. E.R. Andrew, "Nuclear Magnetic Resonance", Cambridge University Press, Cambridge, 1956.
5. F.A.L. Anet, R.A.B. Bannard and L.D. Hall, Canad. J. Chem., 1963, 41, 2331.
6. J. Bain and M.M. Harding, J. Chem. Soc., 1965, 4025.
7. S.A. Barker, J. Homer, M.C. Keith and L.F. Thomas, J. Chem. Soc., 1963, 1538.
8. D.H.R. Barton, J. Chem. Soc., 1953, 1027.
9. H. Booth, Tetrahedron Letters, 1965, 24, 411.
10. A.A. Bothner-By and R.E. Glick, J. Chem. Phys., 1957, 26, 1647; 1957, 26, 1651.
11. A.A. Bothner-By and C. Naar-Colin, Ann. New York Acad. Sci., 1958, 70, 833.
12. R.J. Cavanaugh and B.P. Dailey, J. Chem. Phys., 1961, 34, 1099.
13. B. Coxon, Tetrahedron, 1965, 21, 3481.
14. W.G. Dauben and K.S. Pitzer, "Steric Effects in Organic Chemistry", chapter 1, John Wiley & Sons, Inc., New York, 1956.
15. R.E. Dessey, T.J. Flautt, H.H. Jaffé and G.F. Reynolds, J. Chem. Phys., 1959, 30, 1422.

16. W.C. Dickinson, Phys. Rev., 1951, 81, 717.
17. H.W.W. Ehrlich, J. Chem. Soc., 1962, 509.
18. J.W. Emsley, J. Feeney and L.H. Sutcliffe, "High Resolution Nuclear Magnetic Resonance Spectroscopy", Pergamon Press, Oxford, 1966.
19. D.F. Evans and J.P. Maher, J. Chem. Soc., 1962, 5127.
20. E. Fermi, Z. Physik, 1930, 60, 320.
21. S. Furberg and P. Pedersen, Acta Chem. Scand., 1963, 17, 1160.
22. R.E. Glick and A.A. Bothner-By, J. Chem. Phys., 1956, 25, 362.
23. W. Gordy and W.J.O. Thomas, J. Chem. Phys., 1956, 24, 139.
24. H.S. Gutowsky and D.W. McCall, Phys. Rev., 1951, 82, 748.
25. E.L. Hahn and D.E. Maxwell, Phys. Rev., 1951, 84, 1246.
26. L.D. Hall, Adv. Carbohydrate Chem., 1964, 19, 51.
27. L.D. Hall, Tetrahedron Letters, 1964, 23, 1457.
28. L.D. Hall and L. Hough, Proc. Chem. Soc., 1962, 382.
29. L.D. Hall, L. Hough, K.A. McLauchlan and K.G.R. Pachler, Chem. and Ind., 1962, 1465.
30. O. Hassel, Quart. Rev., 1953, 7, 221.
31. J.V. Hatton, W.G. Schneider and W. Siebrand, J. Chem. Phys., 1963, 39, 1330.
32. D. Horton and W.N. Turner, Chem. Communications, 1965, 113.
33. D. Horton and W.N. Turner, J. Org. Chem., 1965, 42, 3387.
34. L. Hough and S.H. Shute, Chem. and Ind., 1962, 1827.
35. G.R. Inglis, J.C.P. Schwarz and L. McLaren, J. Chem. Soc., 1962, 1014.

36. L.M. Jackman, "Applications of Nuclear Magnetic Resonance Spectroscopy in Organic Chemistry", Pergamon Press, London, 1959.
37. M. Karplus, J. Amer. Chem. Soc., 1963, 85, 2871.
38. M. Karplus, J. Chem. Phys., 1959, 30, 6; 1959, 30, 11.
39. M. Karplus, D.H. Anderson, T.C. Farrar and H.S. Gutowsky, J. Chem. Phys., 1957, 27, 597.
40. W. Klyne, "Progress in Stereochemistry, I", chapter 2, Butterworth & Co. Ltd., London, 1954.
41. W. Lamb, Phys. Rev., 1941, 60, 817.
42. P. Laszlo and P von R. Schleyer, J. Amer. Chem. Soc., 1963, 85, 2709.
43. R.U. Lemieux, Canad. J. Chem., 1961, 39, 116.
44. R.U. Lemieux and B. Fraser-Reid., Canad J. Chem., 1966, 44, 249.
45. R.U. Lemieux, R.K. Kullnig, H.J. Bernstein and W.G. Schneider, J. Amer. Chem. Soc., 1957, 79, 1005.
46. R.U. Lemieux, R.K. Kullnig, H.J. Bernstein and W.G. Schneider, J. Amer. Chem. Soc., 1958, 80, 6098.
47. R.U. Lemieux, R.K. Kullnig and R.T. Moir, J. Amer. Chem. Soc., 1958, 80, 2237.
48. R.U. Lemieux and A.R. Morgan, Canad. J. Chem., 1965, 43, 2199.
49. R.U. Lemieux and J.D. Stevens, Canad. J. Chem., 1965, 43, 2059.
50. R.U. Lemieux and J.D. Stevens, Canad. J. Chem., 1966, 44, 249.

51. R.U. Lemieux, J.D. Stevens and R.R. Fraser, *Canad. J. Chem.*, 1962, 40, 1955.
52. R.W. Lenz and J.P. Heeschen, *J. Polymer Sci.*, 1961, 51, 247.
53. H.M. McConnell, *J. Chem. Phys.*, 1956, 24, 460.
54. H.M. McConnell, *J. Chem. Phys.*, 1957, 27, 226.
55. e.g. J. McKenna, "Conformational Analysis of Organic Compounds", Royal Institute of Chemistry Lecture Series 1966, No. 1.
56. P.T. Manolopoulos, M. Mednick and N.N. Lichtin, *J. Amer. Chem. Soc.*, 1962, 84, 2203.
57. M.L. Martin and G.J. Martin, *Bull. Soc. chim. France*, 1966, 2117.
58. J. Meinwald and A. Lewis, *J. Amer. Chem. Soc.*, 1961, 83, 2769.
59. D. Moy, E. Emerson and J.P. Oliver, *Inorg. Chem.*, 1963, 2, 1261.
60. e.g. Y. Osawa and M. Neuman, *J. Amer. Chem. Soc.* 1963, 85, 2856.
61. J.A. Pople, *Proc. Roy. Soc.*, 1957, A239, 541; 1957, A239, 550.
62. J.A. Pople and A.A. Bothner-By, *J. Chem. Phys.*, 1965, 42, 1339.
63. J.A. Pople, W.G. Schneider and H.J. Bernstein, "High-Resolution Nuclear Magnetic Resonance", McGraw-Hill, New York, 1959.
64. N.F. Ramsey, *Phys. Rev.*, 1950, 78, 699; 1952, 86, 243.
65. N.F. Ramsey, *Phys. Rev.*, 1953, 91, 303.
66. N.F. Ramsey and E.M. Purcell, *Phys. Rev.*, 1952, 85, 143.
67. R.A. Raphael in E.H. Rodd (ed.), "The Chemistry of Carbon Compounds", 2A, 132, Elsevier Publishing Company, Amsterdam, 1953.
68. R.E. Reeves, *Adv. Carbohydrate Chem.*, 1951, 6, 124.

69. R.E. Reeves, J. Amer. Chem. Soc., 1950, 72, 1499.
70. A.C. Richardson and K.A. McLauchlan, J. Chem. Soc., 1962, 2499.
71. W. Riddell and J.C.P. Schwarz, unpublished work.
72. E.G. Rochow, D.T. Hund and R.N. Lewis, "The Chemistry of
Organometallic Compounds", John Wiley, New York, 1957.
73. D.A. Rosenfeld, N.K. Richtmeyer and C.S. Hudson, J. Amer.
Chem. Soc., 1948, 70, 2201.
74. A. Saika and C.P. Slichter, J. Chem. Phys., 1954, 22, 26.
75. C.P. Slichter, "Principles of Magnetic Resonance", Harper and Row,
New York, 1963.
76. S. Sternhell, Rev. Pure Appl. Chem. (Australia), 1964, 14, 15.
77. G.V.D. Tiers, J. Phys Chem., 1958, 62, 1151.
78. T.G. Traylor, J. Amer. Chem. Soc., 1964, 86, 244.
79. T.G. Traylor and A.W. Baker, J. Amer. Chem. Soc., 1963, 85,
2746.
80. R. Wallace, Ph.D. Thesis, Glasgow, 1964.
81. K.B. Wiberg and B.J. Nist, "The Interpretation of NMR Spectra",
W.A. Benjamin, New York, 1962.
82. K.L. Williamson, J. Amer. Chem. Soc., 1963, 85, 516.
83. K.L. Williamson, C.A. Lanford and C.P. Nicholson, J. Amer.
Chem. Soc., 1964, 86, 762.
84. E.B. Wilson, J. Chem. Phys., 1957, 27, 60.

Part A introduces the origin of proton chemical shifts and coupling constants, and discusses the significance of these quantities for studies of conformation and configuration in organic molecules.

The general theories of chemical shifts and coupling constants are then applied to pyranosides and in particular to the high resolution proton magnetic resonance spectra of saturated deuterio-chloroform solutions of the four compounds:

A: methyl 2-acetoxymercuri-2-deoxy- β -D-glucopyranoside triacetate

B: methyl 2-chloromercuri-2-deoxy- β -D-glucopyranoside triacetate

C: methyl 2-chloromercuri-2-deoxy- α -D-mannopyranoside triacetate

D: methyl 2-chloromercuri-2-deoxy- α -D-talopyranoside triacetate.

Compounds containing pyranoside rings exist usually in one of the two possible chair conformations, designated by Reeves as C1 and 1C: other things being equal, the C1 conformation is preferred for most D-hexoses and their derivatives.

The spectra of the four compounds have been analysed, fully for the ring proton absorptions, using programs written for the DEUCE and KDF 9 computers in Glasgow University. The chemical shifts and coupling constants resulting from the analyses are given in table 3.1 (page 51).

Interpretation of these chemical shifts and coupling constants has confirmed that the compounds do have the structures and configurations described by A, B, C and D above. This is

especially important for compound C, about whose configuration there has been some controversy.

The ring proton coupling constants in particular show that compounds A, B, and C in saturated deuterochloroform solution have essentially C1 chair forms, with some distortion, and that compound D exists as a very distorted C1 chair conformer, almost in a half-boat conformation: some of these conclusions are supported by X-ray analyses.

Apart from the analysis of the ring proton absorption peaks, the methoxy proton chemical shifts agree well with previous findings concerning this substituent, and the acetoxy proton chemical shifts are not inconsistent with the results of other workers.

No spin-spin coupling between mercury isotopes and the protons H(1), H(2) or H(3) has been explicitly observed.

The peaks in the spectrum of compound D are broadened slightly relative to the peaks in the spectra of the other compounds. This may be because of kinetic effects involving the presence in low concentration of another conformer in the solution, or to unresolved couplings, perhaps long-range proton-proton couplings.

PART B.

NUCLEAR QUADRUPOLE RESONANCE SPECTROSCOPY OF ^{14}N

1.1 Introduction

NMR and NQR both rest on the fact that a nuclear state can be split into a number of substates. In NMR, the major cause of this splitting into substates is the interaction of the nuclear magnetic dipole with an externally applied magnetic field. In NQR, on the other hand, the splitting is caused by the interaction of the nuclear electric quadrupole moment with the gradient of an electric field which originates within the sample itself. The chief sources of the electric field at the resonant quadrupolar nucleus are the electrons of the molecule of which the nucleus is a part, although other effects make smaller but still important contributions to the electric field. The splitting of nuclear levels due to nuclear quadrupole interactions with this internally produced field is therefore sensitive especially to the electronic environment of the nucleus. Suitable nuclei can be used effectively as observers of electron distribution in the molecule, and of the charge distribution in the crystal, in which nuclei of the resonant type are situated. NQR is concerned only with solids, and it will be seen (Part C) that crystal and typical solid-state effects are important in interpreting NQR findings.

The general theory of NQR interactions is now dealt with,

to give an indication of the results and information to be gained from such a method of investigation.

1.2 The interaction of a nucleus with an electric field

Because the expectation values of angular momentum obey the same equations of motion quantum mechanically and classically, it is justified to derive a classical expression involving angular momentum, and then to substitute quantum mechanical operators. A discussion of the limitations of this procedure is given in many textbooks of quantum mechanics.^{1, 11, 23, 24}

The interaction energy E of a charge distribution of density ρ with a potential V due to external sources is:

$$E = \int_{\text{all space}} \rho(\underline{r}) V(\underline{r}) d\tau \quad 1.2.1$$

where \underline{r} is the position vector from an arbitrary origin. $V(\underline{r})$ can now be expanded in a number of (equivalent) ways, one of which is a Taylor series expansion about the origin:

$$\begin{aligned} V(\underline{r}) = V(0) + \sum_{\alpha} \alpha \left(\frac{\partial V}{\partial \alpha} \right)_{r=0} + \frac{1}{2!} \sum_{\alpha, \beta} \alpha \beta \left(\frac{\partial^2 V}{\partial \alpha \partial \beta} \right)_{r=0} \\ + \frac{1}{3!} \sum_{\alpha, \beta, \gamma} \alpha \beta \gamma \left(\frac{\partial^3 V}{\partial \alpha \partial \beta \partial \gamma} \right)_{r=0} + \dots \end{aligned} \quad 1.2.2$$

so that

$$E = V(0) \int \rho d\tau + \sum_{\alpha} V_{\alpha} \int \alpha \rho d\tau + (1/2!) \sum_{\alpha, \beta} V_{\alpha\beta} \int \alpha \beta \rho d\tau + \dots \quad 1.2.3$$

where the integrations are over all space, $\alpha, \beta, \gamma, \dots$ are generalised co-ordinates which can for example take the equivalences x, y , or z in a Cartesian co-ordinate system, the notation

$()_{r=0}$ is used for the value of the function in parentheses

when $r = 0$, and we define:

$$V_{\alpha} = \left(\frac{\partial V}{\partial \alpha} \right)_{r=0}$$

$$V_{\alpha\beta} = \left(\frac{\partial^2 V}{\partial \alpha \partial \beta} \right)_{r=0} \quad \text{etc. for } \alpha, \beta, \gamma \dots$$

The first term of equation 1.2.3 is the "monopole" interaction. It is the contribution to the total energy from a point charge, equal in magnitude to the total nuclear charge, interacting with the potential at the origin. The second term is a dipole interaction term: it is zero if the nucleus has defined parity (in any case the position of the nucleus in equilibrium in an electric field is such that V_{α} tends to zero). The third term is the quadrupolar interaction term, and the n th term of equation 1.2.3 is the (2^{n-1}) -pole term. For n odd, the term is usually non-zero, but for $n = 1$, the interaction is independent of nuclear orientation, and need only be considered in optical spectra; for $n \geq 5$, observations are difficult because the term is small (for $n = 5$ it is about 1 c/s), and furthermore the term is always zero for $I < n - 2$.

So a quadrupolar energy E_Q (which will later be associated with a Hamiltonian \mathcal{H}_Q) can be written as:

$$E_Q = \frac{1}{2} \sum_{\alpha\beta} V_{\alpha\beta} \int \alpha\beta \rho dt \quad 1.2.4$$

A simplification ensues if one defines

$$Q_{\alpha\beta} = \int (3\alpha\beta - \delta_{\alpha\beta} r^2) \rho dt \quad 1.2.5$$

where $\delta_{\alpha\beta} = 1$ if $\alpha = \beta$, and is zero otherwise: this definition has recently been criticised³. Then

$$\int \alpha\beta\rho d\tau = (1/3)(Q_{\alpha\beta} + \int \delta_{\alpha\beta} r^2 \rho d\tau) \quad 1.2.6$$

Substitution in equation 1.2.4 using equation 1.2.6 gives:

$$E_Q = (1/6) \sum_{\alpha,\beta} (V_{\alpha\beta} Q_{\alpha\beta} + V_{\alpha\beta} \delta_{\alpha\beta} \int r^2 \rho d\tau) \quad 1.2.7$$

If V is a potential field satisfying the Poisson equation, then

$$\sum_{\alpha} V_{\alpha\alpha} = -4\pi\rho_k \quad 1.2.8$$

where ρ_k is the electronic probability charge density at the nucleus. The quantity ρ_k is of course independent of the orientation of the nucleus relative to the tensor $V_{\alpha\beta}$, and the quadrupolar interaction energy E_Q can be written in the form

$$E_Q = (1/6) \sum_{\alpha,\beta} V_{\alpha\beta} Q_{\alpha\beta} + K \quad 1.2.9$$

where K is given by:

$$K = -(2\pi\rho_k/3) \int r^2 \rho d\tau \quad 1.2.10$$

K is different for different nuclear isomers or isotopes. It is however clearly independent of nuclear orientation, and cannot therefore affect a transition energy, although of course it does affect absolute values of energy levels. Thus, any constant (orientation-independent) value of K may be assumed without affecting the finally derived transition energies. Very considerable algebraic complexity is avoided if K is taken to be zero, and this is usually done. $K = 0$ is equivalent to assuming a Laplacian electronic potential field. Thus equation 1.2.8 may be simplified to:

$$\sum_{\alpha} V_{\alpha\alpha} = 0 \quad 1.2.11$$

without serious loss of generality.

The first term of equation 1.2.9 can be regarded then as the product of two rank two symmetric tensors, $V_{\alpha\beta}$ and $Q_{\alpha\beta}$. If x , y and z are now reserved to denote the principal axes of the tensor $V_{\alpha\beta}$, then if the potential field has a symmetry such that

$$V_{xx} = V_{yy} = V_{zz} \quad 1.2.12$$

as for example in suitable cubic or in spherical symmetry, then equation 1.2.12 and equation 1.2.8 together with equation 1.2.9 show that $E_Q = 0$: no quadrupole transitions can be observed.

The next stage is to find the quantum mechanical operators. For the nuclear tensor $Q_{\alpha\beta}$ an operator can be got by substituting $\bar{\rho}$, the operator for ρ . The operator $\bar{\rho}$ is given by:

$$\bar{\rho} = e \sum_{\substack{\text{protons} \\ k}} \delta(\underline{r} - \underline{r}_k) \quad 1.2.13$$

and is substituted in equation 1.2.5. The summation over protons only is justified so long as protons are held to be the only source of electric charge density in the nucleus. Putting equation 1.2.13 into equation 1.2.5 gives for the operator $\bar{Q}_{\alpha\beta}$:

$$\begin{aligned} \bar{Q}_{\alpha\beta} &= e \sum_{\substack{\text{protons} \\ k}} \int (3\alpha\beta - \delta_{\alpha\beta} r^2) \delta(\underline{r} - \underline{r}_k) d\tau \\ &= e \sum_{\substack{\text{protons} \\ k}} (3\alpha_k \beta_k - \delta_{\alpha\beta} r_k^2) \end{aligned} \quad 1.2.14$$

where $\delta_{\alpha\beta}$ is an abbreviation of $\delta_{\alpha_k \beta_k}$, and α_k etc. are the

co-ordinates of the k th proton.

Now it is a result readily derived from the generalised Wigner-Eckart theorem, subject to important limitations on the nature of $F\{p\}$, $\{p\}$ and $\{q\}$ below, that:

$$(JM_J\lambda|F\{p\}|J'M_J'\lambda') = (JM_J\lambda|F\{q\}|J'M_J'\lambda').C(J,\lambda,J',\lambda') \quad 1.2.15$$

where the ket $|JM_J\lambda\rangle$ for example is associated with J , a total angular momentum quantum number, M_J , a quantum number for the component of J in one co-ordinate, and λ , the set of other quantum numbers required to define sufficiently the eigenstate, of the nucleus in this case. The notation $\{p\}$ is used for the set of variables derived from a vector-type operator \underline{p} , e.g. $p, p_x, p_y, p_z, p^2, p^+, p^-$ etc. C is a function of $J, \lambda, J',$ and λ' only: specifically it is not a function of M_J or M_J' .

It can be shown that the limitations mentioned above are obeyed when $p \equiv r_k$ and $q \equiv I$. Thus $F\{q\}$ of equation 1.2.15 for the present case in which $J = I, M_J = m, F\{p\} = \bar{Q}_{\alpha\beta}$ as given by equation 1.2.14, can be obtained. These substitutions yield:

$$(Im\lambda|e \sum_k^{\text{protons}} (3\alpha_k\beta_k - \delta_{\alpha\beta}r_k^2)|I'm'\lambda') \\ = C.(Im\lambda|(3/2)[I_\alpha I_\beta + I_\beta I_\alpha] - \delta_{\alpha\beta}I^2|I'm'\lambda') \quad 1.2.16$$

The right-hand side of equation 1.2.16 gives a very general expression for the matrix elements of $\bar{Q}_{\alpha\beta}$, but NQR spectroscopy is concerned with only one nucleus in its nuclear ground state, i.e. with a case in which $I = I'$ and $\lambda = \lambda'$. This gives:

$$\begin{aligned}
 (I_m \lambda | e \sum_k^{\text{protons}} (3\alpha_k \beta_k - \delta_{\alpha\beta} r_k^2) | I_m' \lambda) \\
 = C. (I_m \lambda | (3/2) [I_\alpha I_\beta + I_\beta I_\alpha] - \delta_{\alpha\beta} I^2 | I_m' \lambda) \quad 1.2.17
 \end{aligned}$$

C is obtained by evaluating that matrix element for which $\alpha = \beta = z$,

and $m = m' = I$:

$$\begin{aligned}
 (II \lambda | e \sum_k^{\text{protons}} (3z_k^2 - r_k^2) | II \lambda) &= C. (II \lambda | 3I_z^2 - I^2 | II \lambda) \\
 &= C. I(2I - 1) \quad 1.2.18
 \end{aligned}$$

The quadrupole moment, eQ , of a nucleus is now defined by^{2,12}:

$$eQ = (II \lambda | e \sum_k^{\text{protons}} (3z_k^2 - r_k^2) | II \lambda) \quad 1.2.19$$

so that, from equation 1.2.18:

$$C = eQ/I(2I - 1) \quad 1.2.20$$

Putting the values of equations 1.2.17 and 1.2.20 in equation

1.2.9 yields:

$$\mathcal{H}_Q = \frac{eQ}{6I(2I - 1)} \sum_{\alpha, \beta} V_{\alpha\beta} \left(\frac{3}{2} [I_\alpha I_\beta + I_\beta I_\alpha] - \delta_{\alpha\beta} I^2 \right) \quad 1.2.21$$

The nuclear charge distribution tensor $Q_{\alpha\beta}$ has, then, been replaced by a single parameter Q : this is justified by the classical statement that the nuclear charge distribution has axial symmetry, or by the fact that the nucleus in one state has a fixed angular momentum associated with it. As pointed out above, the potential tensor $V_{\alpha\beta}$ can be contracted by rotation to its principal axes, when all off-diagonal components ($\alpha \neq \beta$) are zero. A further simplification ensues since the potential tensor $V_{\alpha\beta}$ is traceless by assumption (equation 1.2.11). When these

modifications are made, equation 1.2.21 becomes:

$$\mathcal{H}_Q = \frac{eQ}{4I(2I-1)} \left[V_{zz} (3I_z^2 - I^2) + (V_{xx} - V_{yy})(I_x^2 - I_y^2) \right] \quad 1.2.22$$

Finally, the conventional substitutions

$$\begin{aligned} V_{zz} &= q \\ \frac{V_{xx} - V_{yy}}{V_{zz}} &= \eta \end{aligned} \quad 1.2.23$$

are made. The axes are chosen so that $|V_{xx}| \leq |V_{yy}| \leq |V_{zz}|$, to give the standard form of the quadrupolar interaction Hamiltonian \mathcal{H}_Q :

$$\mathcal{H}_Q = \frac{eQq}{4I(2I-1)} \left[(3I_z^2 - I^2) + \eta(I_x^2 - I_y^2) \right] \quad 1.2.24$$

1.3 The quadrupolar energy levels for \mathcal{U}_N

It is often useful to apply a steady external field to the sample in NQR, in which case \mathcal{H}_Q of equation 1.2.24 must have added to it a magnetic interaction Hamiltonian. If, however, the magnetic interaction is zero or otherwise negligible, the interaction is called "pure quadrupole resonance". But the transitions between the energy levels which are derived below are induced by coupling between the nuclear magnetic dipole and an applied alternating magnetic field, with a non-vanishing component perpendicular to the z-axis. For convenience two cases can be distinguished, $\eta = 0$ and $\eta \neq 0$.

If $\eta = 0$, I_z commutes with \mathcal{H}_Q and the eigenfunctions of I_z , say ψ_m , are also eigenfunctions of \mathcal{H}_Q . The matrix elements $(m | \mathcal{H}_Q | m)$ are given by

$$(m | \mathcal{H}_Q | m) = \frac{eQq}{4I(2I-1)} [3m^2 - I(I+1)] \quad 1.3.1$$

Equation 1.3.1 has been obtained from equation 1.2.24 by putting $\eta = 0$.

The nucleus of greatest interest for this and the following part is ^{14}N , for which $I = 1$, and it is as well to derive formulae for this particular case, as the general case would be pointlessly complicated. Then for ^{14}N , equation 1.3.1 becomes:

$$\begin{aligned} E_1 &= (1 | \mathcal{H}_Q | 1) = (-1 | \mathcal{H}_Q | -1) = eQq/4 \\ E_0 &= (0 | \mathcal{H}_Q | 0) = -eQq/2 \end{aligned} \quad 1.3.2$$

Equation 1.3.2 shows explicitly that the levels $m = +1$ and $m = -1$ are degenerate, as implied by the fact that only m^2 is involved in equation 1.3.1. This double degeneracy for $m \neq 1$ is an example of a Kramers degeneracy. In general it is lifted by a magnetic field.

Thus, when $\eta = 0$ for ^{14}N , there is only one transition whose energy in frequency units is given by:

$$\nu_0 = 3eQq/4h \quad 1.3.3$$

The quantity eQq/h is called the quadrupole coupling constant. It is usually expressed in Mc/s, and it is often written simply as eQq , with Planck's constant, inconsistently, omitted.

If $\eta \neq 0$, I_z and \mathcal{H}_Q do not commute. Linear combinations

of the ψ_m are needed to describe the three levels, but when $I = 1$ standard diagonalisation procedures, with the usual normalisation and orthogonalisation conditions, give a simple set of wave functions:

$$\begin{aligned}\psi_A &= \frac{1}{\sqrt{2}}(\psi_{+1} + \psi_{-1}) \\ \psi_B &= \frac{1}{\sqrt{2}}(\psi_{+1} - \psi_{-1}) \\ \psi_C &= \psi_0\end{aligned}\tag{1.3.4}$$

The corresponding energy eigenvalues are: (eQq is now in frequency units)

$$\begin{aligned}E_A &= (1 + \eta) \frac{eQq}{4} \\ E_B &= (1 - \eta) \frac{eQq}{4} \\ E_C &= -eQq/2\end{aligned}\tag{1.3.5}$$

These three energy levels lead to three transition frequencies:

$$\begin{aligned}v_1 &= (3 + \eta) \frac{eQq}{4} \\ v_2 &= (3 - \eta) \frac{eQq}{4} \\ v_3 &= \frac{eQq}{2} \eta\end{aligned}\tag{1.3.6}$$

In terms of v_1 and v_2 , eQq and η are given by:

$$eQq = \frac{2}{3} (v_1 + v_2)\tag{1.3.7a}$$

$$\eta = 3 \frac{v_1 - v_2}{v_1 + v_2}\tag{1.3.7b}$$

and also

$$v_3 = (v_1 - v_2)\tag{1.3.7c}$$

Thus a ^{14}N nucleus in one environment will in theory display three resonance lines, but v_3 is at so low a frequency that

most workers (there are a few exceptions^{4,13}) have considered it to be unobservable: in any case its position supplies no information not available from the positions of ν_1 and ν_2 . Equations 1.3.7a and 1.3.7b show that eQq and η can be determined for ^{14}N by the observation of the two high-frequency lines in the pure quadrupole resonance spectrum if it is known that $\eta \neq 0$. However, two lines may correspond to two different values of q and $\eta = 0$, that is to two different molecular or crystal-lattice sites for the ^{14}N nucleus. This apparent ambiguity can usually be resolved experimentally (by an examination of the effect of the application of a small external magnetic field) or from a knowledge of what is chemically and physically reasonable.

2.1 Introduction

A short account of very general experimental considerations is given by some reviewers, mostly with reference to the detection of halogen resonances, e.g. Das and Hahn⁶.

As mentioned at the beginning of section 1.3, transitions are induced between the energy levels given by equation 1.3.5 by applying an external alternating magnetic field of amplitude H_1 whose component in the xy plane is not zero. Some values of H_1 are more suitable than others. If

$$\gamma^2 H_1^2 T_1 T_2 \gg 1 \quad 2.1.1$$

where γ is the magnetogyric ratio of the nucleus, T_1 is a spin-lattice and T_2 a spin-spin relaxation time, then the nuclear resonance is saturated.¹⁹ For line shape measurements, indeed, H_1 should be such that

$$\gamma^2 H_1^2 T_1 T_2 \ll 1 \quad 2.1.2$$

although if it is too small then the signal is undetectable.

In practical NQR spectrometers, the sample is subjected to the alternating field H_1 by placing it inside a coil which is part of a radio-frequency (RF) oscillator. In NMR spectroscopy, the sample can be subjected to a fixed RF, and the magnetic field varied so that different nuclei come into resonance at that

frequency. In NQR spectroscopy, the frequency of the transition is determined by the sample, and it is necessary to vary the frequency of the RF oscillator. How this is done in practice without sacrificing too much oscillator stability, coherence and uniformity, and without introducing too much noise, is described in chapter 3.

Those resonances which have been reported for ^{14}N are in the range 0 - 10 Mc/s. This range of frequencies is considerable, and it has to be attained by using a number of RF sample coils, each of which resonates with the variable capacitor in the oscillator over a part of the total range. Since an oscillator which can operate over a large frequency range is needed, some limitation on oscillator sensitivity must be made. Nevertheless, NQR signals are extremely weak, and high sensitivity is necessary. A compromise has to be made between these two conflicting requirements, and at present this is done by means of one of two types of oscillator:

1. Continuous-wave (marginal) oscillators
2. Super-regenerative oscillators.

The practical details of the construction of two spectrometer systems intended for the study of ^{14}N NQR absorption, one using a marginal and the other a super-regenerative oscillator, are given in chapter 3. A brief description will now be given of the operation principles of these two types of oscillator:

the basis of their operation is the basis of operation of the whole NQR spectrometer.

2.2 The continuous wave oscillator

Oscillators of this type were first developed for nuclear spectroscopy by Pound and Knight²⁰ and by Roberts²¹. In them, the sample is placed inside a coil (an inductance) which is tuned up to, through, and past the resonance frequency by means of some type of variable capacitor. By using the inductive-capacitive circuit as an oscillating element with electronic feedback, the voltage level of the oscillation becomes a function of frequency because of nuclear absorption around the resonance frequency: the level of oscillation falls as the frequency of the oscillator becomes equal to the NQR frequency of the sample.

The positive feedback (regeneration) is arranged so that it is just sufficient to maintain oscillations. In this situation, the valve characteristic curve is such that the oscillation level changes most on going through a nuclear quadrupole resonance: the oscillator is at its most sensitive. Also, at higher RF levels the nature of the oscillator valve characteristics gives rise to noise components of a wider range of frequencies, and greater noise is produced. Thirdly, the RF level in the oscillator is kept low to avoid the conditions described above which might cause saturation of the nuclear quadrupole absorptions. The way of detecting the change in oscillation level is described in

section 2.4 below.

2.3 The super-regenerative oscillator³⁰

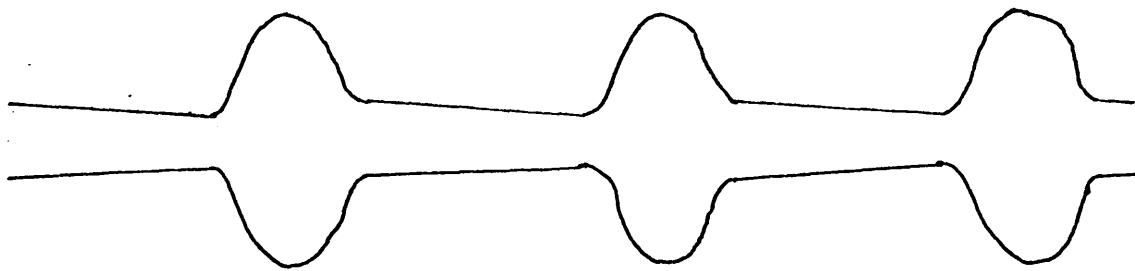
The essential feature of a super-regenerative oscillator is that it delivers short bursts of RF power to the sample, in contrast to the continuous oscillation of a marginal oscillator. The frequency of these bursts is called the "quench frequency" and the phenomenon itself is called "quenching". Quenching of an oscillator, leading to super-regenerative behaviour, may be accomplished in one of two important ways, corresponding to the so-called self-quenching and the externally quenched oscillator. In the self-quenching oscillator, the valve, being in the oscillating circuit, runs grid current. This leads to a build-up of negative charge on the grid which eventually stops the valve conducting and quenches the RF oscillations. The negative charge on the grid is allowed to leak away only slowly through a sufficiently large resistive-capacitive network between the grid and cathode: this is why the charge builds up while the circuit is oscillating. When the oscillations stop, the negative charge leaks away to the point where the valve can once more conduct, and the whole cycle begins again. A more complete account of the changes in the self-quenching cycle is given by Wallace²⁷.

A more versatile, although more complicated, instrument is the externally quenched oscillator. In this type, the RF

oscillations are allowed or suppressed by applying a varying voltage, either directly or indirectly, to the second (control) grid of a pentode or to the grid of a triode. Thus the oscillator quenches at the same frequency as this externally applied frequency, which is therefore the quench frequency. This means that the quench frequency can be varied directly by varying the frequency of the quench oscillator, which supplies the quench waveform (sinusoidal or square-wave), whereas the quench frequency in a self-quenching oscillator depends mainly on the RC value of the circuit on the oscillator valve grid.

Figure 2.1 (page 102) shows a number of different RF waveforms at a super-regenerative oscillator valve anode. If the RF envelope appears as in figure 2.1a, the RF oscillations are being quenched before they can reach their limiting amplitude. This amplitude depends on the non-linear characteristics of the oscillator. Such a situation is called the "linear mode", since the oscillator output voltage is proportional to the input voltage across the tank circuit. The adjustment of an oscillator to this mode is very critical, and very dependent on other operating conditions. Circuits are available to maintain this adjustment automatically, but for NQR detection it is unnecessary to keep the oscillator in the linear mode.

If the RF envelope has the appearance of figure 2.1b, the oscillations reach their limiting amplitude before quenching.



a: linear mode

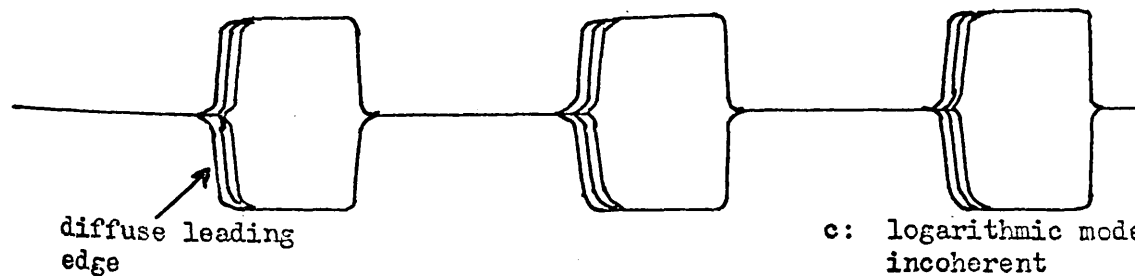
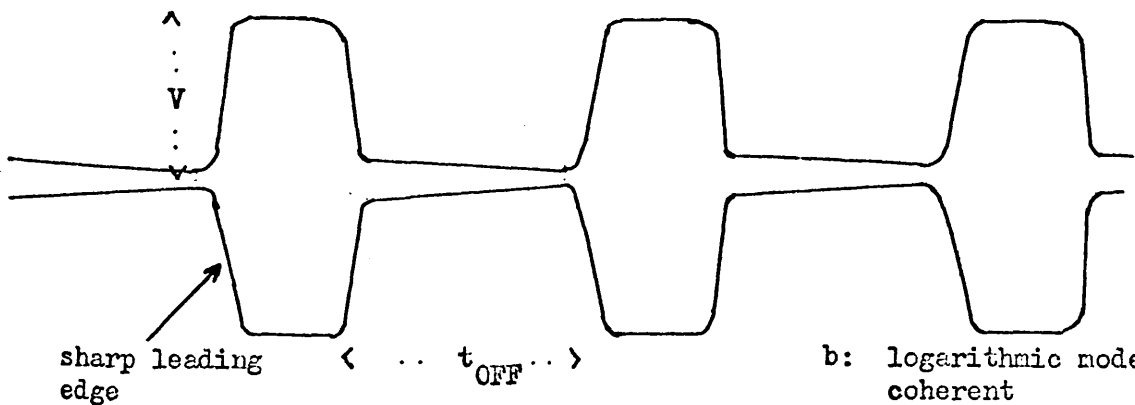


Figure 2.1. Oscillation envelopes of super-regenerative oscillator.

In this mode, the relationship between input and output is logarithmic, and the mode is called the "logarithmic mode". However, for small input signals, which are the rule in NQR, the relationship is very nearly linear, and this has been verified experimentally. The adjustment of an oscillator in the logarithmic mode is less critical than the adjustment for the linear mode, but it is still very frequency-dependent: around 3 Mc/s oscillator frequency, re-adjustment is necessary about every 200 Kc/s change in RF.

The RF waveforms in figures 2.1b and 2.1c both correspond to a super-regenerative oscillator in the logarithmic mode. The important difference between them is that figure 2.1b corresponds to a coherent state, figure 2.1c to an incoherent one. When the quench waveform goes sufficiently positive, the oscillator valve can conduct again and RF oscillations build up. If the oscillations from the previous RF pulse have decayed below the oscillator noise level, the build-up is from the random noise voltages in the tank circuit, and the phase relationship between pulses of RF oscillation is also random. The oscillator is in an incoherent state, and its RF waveform is as in figure 2.1c, with the leading edge of each pulse appearing diffuse on the oscilloscope screen. If on the other hand the RF oscillations have not decayed to below the noise level, the build-up is from these residual RF oscillations, and it starts sooner. The

oscillator is in a coherent state, and the bursts of oscillation are in phase. The appearance of the RF envelope is as indicated in figure 2.1b, and the leading edges appear sharp.

In the coherent state, the power spectrum consists of a number of sharp narrow bands at frequencies ν_n given by

$$\nu_n = \nu_R + n\nu_Q \quad 2.3.1$$

where ν_R is the unquenched oscillator frequency, ν_Q is the quench frequency, and n is an integer. The most intense band is at $\nu_0 = \nu_R$, and the intensity falls off symmetrically on either side of this central frequency. In the completely incoherent state the oscillator power distribution is a broad band with its maximum at ν_R . The coherent and incoherent states represent two extremes, and any intermediate condition is also possible. In such an intermediate state, the power distribution has maxima at the frequencies given by equation 2.3.1, but the power level falls away relatively slowly on either side of these maxima, and may not reach zero at frequencies between those given by equation 2.3.1. In this intermediate state power spectrum, the most intense maximum is again at $\nu_0 = \nu_R$.

The degree of coherence can affect the oscillator sensitivity in two important ways. First, the oscillator gain increases as coherence decreases. Although the signal-to-noise ratio is very little affected, the gain of many oscillators is so low in the highly coherent state as compared to a less coherent one

that the oscillator coherence must be reduced to a certain extent so as to get a reasonably high output voltage for the next stage of the spectrometer. Second, as explained above, the width of the lines in the power spectrum increases with decreasing oscillator coherence, so that as the coherence decreases, the effectiveness of the oscillator in exciting nuclear resonance increases, until the width of these lines is equal to the resonance linewidth. After this point, decreasing coherence and increasing oscillator linewidth cause the effectiveness to fall off rapidly. At the optimum coherence, all the nuclei in the sample are excited, and the signal intensity obtainable is increased: compare the marginal oscillator, whose linewidth is always much less than the NQR linewidth.

It can be shown²⁵ that the output voltage V_1 developed by a super-regenerative oscillator at the central frequency is given by:

$$V_1 \div k \cdot \frac{2C}{G_1} \cdot 4\pi V Q \eta \sqrt{1 - \nu t_{OFF}} \exp(G_0 t_{OFF}/2C) \cdot \chi'' \quad 2.3.2$$

where V and t_{OFF} are indicated on figure 2.1b, k is a constant for a particular instrument, C is the total capacitance in the tank circuit (C of course varies as the frequency is swept), G_0 is the circuit conductance during the off-period, G_1 is the effective negative conductance across the tank circuit, ν is the quench frequency and χ'' is the real part of the sample susceptibility. Q is the quality factor and η the filling factor of the tank circuit. The equation is quoted since it summarises many of the factors affecting the gain of the usual super-

-regenerative oscillator. Thus, the gain depends on the operating frequency (i.e. on C) and, in the simpler type of external quenching in which ν and t_{OFF} cannot be separately controlled, very much on the quench frequency.

The choice of ν and t_{OFF} does not depend only on the values which give the greatest V_1 , as indicated by equation 2.3.2. Two other things need to be separately considered. First and more obviously, ν and t_{OFF} (and perhaps RF amplitude too) need to be selected to give the optimum coherence. The second consideration concerns the mechanism of detection of the nuclear resonance by this type of oscillator. While, and just after, the sample experiences the burst of RF, two effects may occur. First, the nuclei may absorb energy, leading to an increase in the time constant for build-up, and to a decrease in the time constant for decay, of the RF oscillations: both of these reduce the integrated pulse energy. Second, if t_{OFF} is not much longer than the spin-spin relaxation time T_2 (typical values of T_2 for ^{14}N , as measured by NMR techniques¹⁶, are given in the range 4.5 to 34 milliseconds), then any coherent nuclear precession resulting from the previous burst of RF causes a signal voltage from which the oscillations build up in the next 'on' period: this tends to increase the integrated pulse energy. Now Dean⁷ has argued that it is the second effect that is more important in

detecting NQR signals in super-regenerative oscillators (the assumption that this is true was indeed made in the derivation of equation 2.3.2), so that t_{OFF} should not be chosen to be much greater than T_2 .

Generally some of the sidebands of the centre frequency, and often several of them, are of sufficient intensity to excite a quadrupole resonance as the oscillator centre frequency is swept. This causes the characteristic complex output of the super-regenerative oscillator. This output is often confusing for a number of reasons. It is usually difficult to tell if several different quadrupole resonance frequencies are present because of different values of q , non-zero η , or both, in the notation of chapter 1. Line-shape measurements cannot usually be attempted. Measurement of the actual absorption frequency has to rely on picking out the most intense line, and often this choice is uncertain: the usual method has been to vary the quench frequency, and to select that line whose position changes least with variation of the central frequency. However these disadvantages can be overcome by systems of sideband suppression, by modulating the quench frequency, and of automatic frequency calibration, as described by Tong²⁵.

The super-regenerative oscillator has a number of intrinsic advantages over the marginal continuous oscillator. The latter must be kept in conditions of high sensitivity at low oscillation levels over quite long periods, while nevertheless maintaining

maximum selectivity, minimum noise and a very large amplification in the rest of the spectrometer: a fairly difficult experimental task. The former, however, essentially passes through its condition of maximum sensitivity once every quench cycle, which reduces the need for stable very critical adjustment or such frequent readjustment. Moreover, the oscillation bursts at resonance are initiated by the nuclear signal rather than by noise as they are away from the resonance condition. This accounts for the experimentally observed fact that the super-regenerative oscillator gives fairly large signal-to-noise ratios.

Both types of oscillator, then, give a change in energy (RF level) due to the absorption of energy by the nuclei at resonance. The means of detecting this change will now be considered.

2.4 Modulation

Changes in the RF level at the sample coil are detected by modulating the RF with a suitable audio-frequency (AF). This can be done in two main ways: externally (Zeeman modulation, which results in amplitude modulation at resonance) and internally to the oscillator (frequency modulation).

In the Zeeman modulation method, the sample is placed between a pair of Helmholtz coils through which the modulating audio-frequency (usually a square-wave which falls to DC zero at one extreme of the wave) is passed. The sample consequently experiences

a magnetic field which is switched on and off at the frequency of the modulating signal. When the field is off, the nuclei absorb energy from the oscillating circuit, and the RF level drops. When the field is on, the transition energies are altered (without for the moment considering details) so that the frequency of the oscillator no longer satisfies the resonance condition and the RF level returns to its value away from resonance. Thus at resonance an additional AF, plus many harmonics of it, is superimposed on the RF of the oscillator. This AF can then be detected and displayed by the methods described in chapter 3.

Zeeman modulation has been the most frequently used to detect ^{14}N resonances. This is interesting because the NQR spectroscopy of nitrogen-containing compounds is probably the least well-suited to the Zeeman method.

A magnetic field of magnitude H alters the positions of the observable transitions as given by equations 1.3.6 in the absence of H . Ignoring the low-frequency transition, which can be found theoretically for this case by methods like those of section 1.3, the altered transition frequencies are:

$$\begin{aligned} \nu_1' &= (3 + \eta)K + \frac{D^2 \cos^2 \vartheta}{2\eta K} + \frac{2D^2 \sin^2 \vartheta \cos^2 \varphi}{(3 - \eta)K} + \frac{D^2 \sin^2 \vartheta \sin^2 \varphi}{(3 + \eta)K} \\ \nu_2' &= (3 - \eta)K - \frac{D^2 \cos^2 \vartheta}{2\eta K} + \frac{2D^2 \sin^2 \vartheta \sin^2 \varphi}{(3 + \eta)K} + \frac{D^2 \sin^2 \vartheta \cos^2 \varphi}{(3 - \eta)K} \end{aligned} \quad 2.4.1$$

The equations 2.4.1 are the expressions derived by Kruger¹⁵, and have been evaluated here for the case of interest to us, $I = 1$.

In these equations

$$K = eQq/4 \quad 2.4.2$$

with eQq , as in equations 1.3.6, in frequency units, and

$$D = \gamma H/2\pi \quad 2.4.3$$

where γ is the magnetogyric ratio of the nucleus, and ϑ and φ are respectively the azimuthal angle and the angular displacement in the xy plane of the direction of the magnetic field vector \underline{H} relative to the co-ordinate system defined by the principal axes of the potential field gradient tensor: other symbols have the same meaning as in equations 1.3.6. The important point about equations 2.4.1 for our purpose is that the Zeeman modulation method depends on the effectiveness of the magnetic field \underline{H} in shifting the transition frequencies away from the oscillator frequency, and that equation 2.4.1 shows that as η increases, H must also be increased to produce the same shift. Thus as η rises, the effectiveness of Zeeman modulation in the detection of NQR signals is lessened.^{5,13,17} Higher values of η have been detected (up to 32%) by using Zeeman modulation with a stronger modulating magnetic field (50 oersted^{14,17}). However, these stronger magnetic fields for modulation are less easily regulated electronically. Since nitrogen nuclei are often found in situations where η is high, the use of Zeeman modulation no doubt accounts for some of the numerous reported failures to observe NQR in ¹⁴N-containing samples which should have a high coupling constant.

In this situation, the other type of modulation, frequency modulation, is preferable.

In frequency modulation, the radio-frequency of the oscillator is varied at an audio-frequency. This is nowadays achieved by applying a waveform, generally sinusoidal, at the audio-frequency to a voltage-variable capacitor incorporated in the tank circuit². This then results in a fluctuation of the oscillator RF at the modulation frequency applied to the voltage-variable capacitor, and also in amplitude modulation of the RF level. The depth of this frequency modulation depends on the characteristics of the RF circuit and of the voltage-variable capacitor. Two possibilities present themselves within the method of frequency modulation: the depth of modulation may be less than the line width (rather loosely interpreted) of the NQR signal, or it may be greater than the NQR signal line width.

Figure 2.2 (page 112) shows how the audio-modulation of the oscillator RF arises when the frequency modulation swing is less than the line width of the NQR signal. A typical resonance line shape is shown in figure 2.2a. This curve represents the magnitude of the decrease E_p in the RF level as the RF oscillator is tuned slowly through a resonance frequency. In figure 2.2a, suppose that the RF oscillator is tuned up to the frequency ν_1 and at the same time is sinusoidally frequency modulated at audio-frequency with amplitude $\Delta\nu/2$ (i.e. the modulation

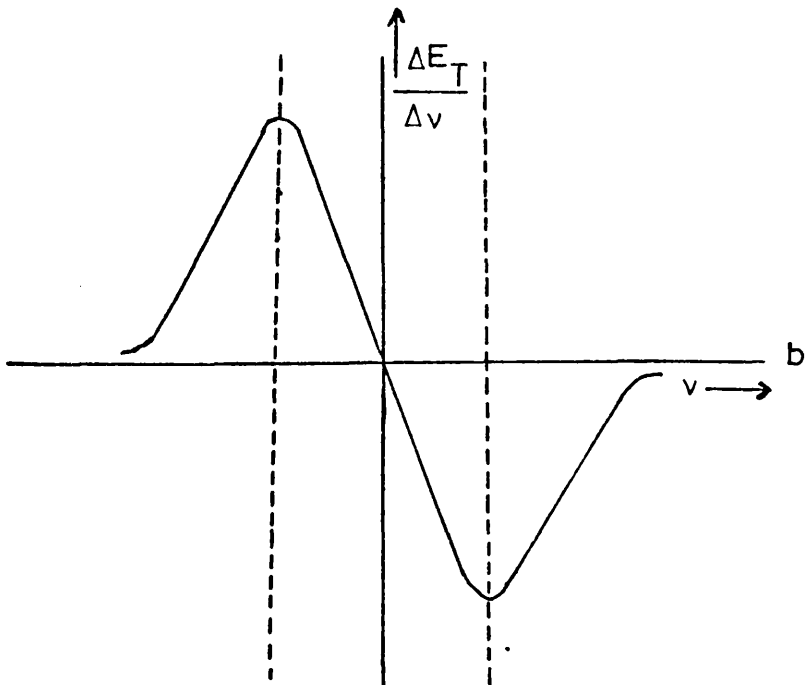
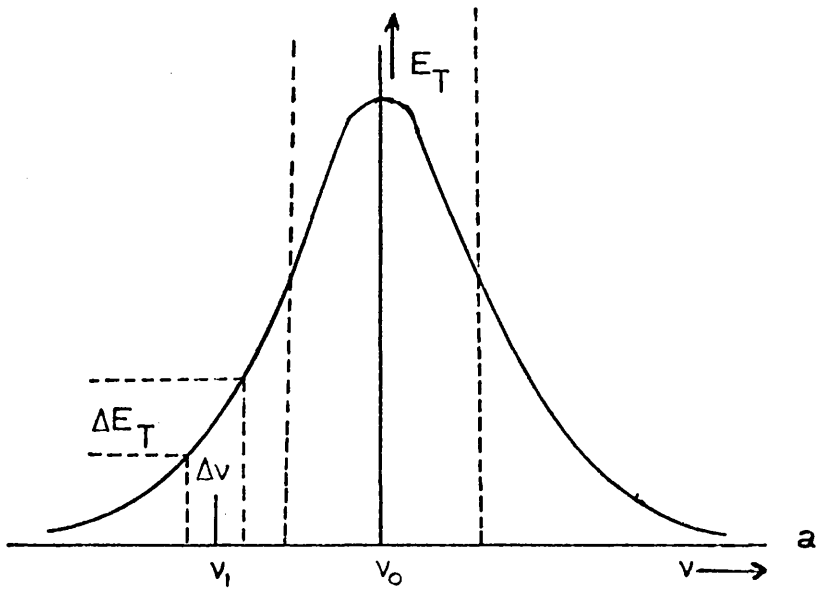
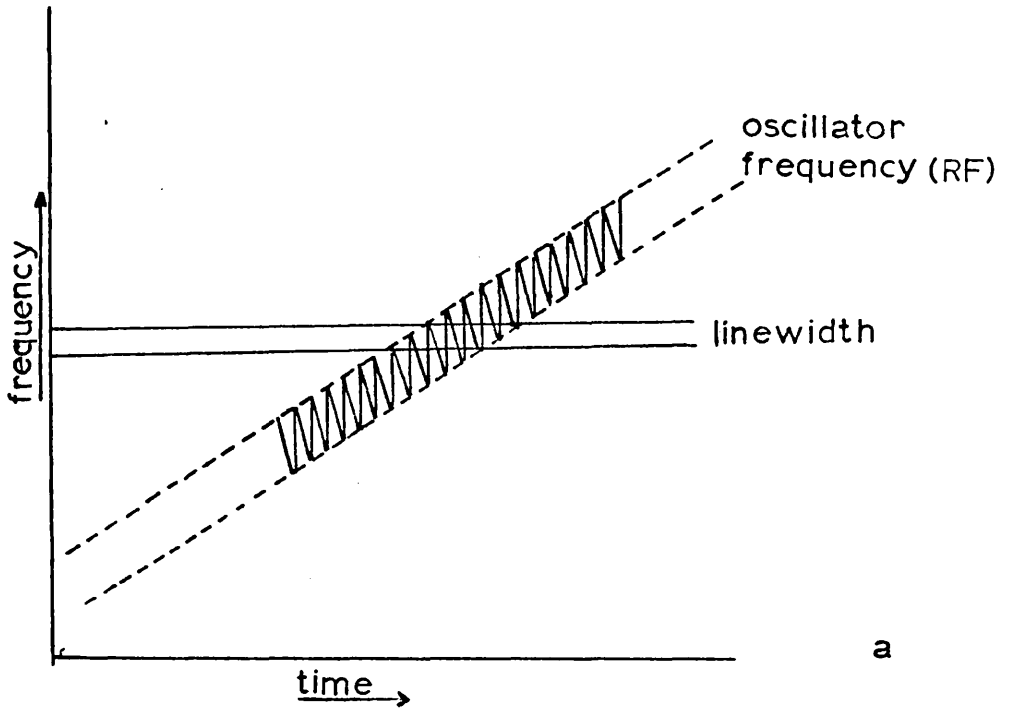


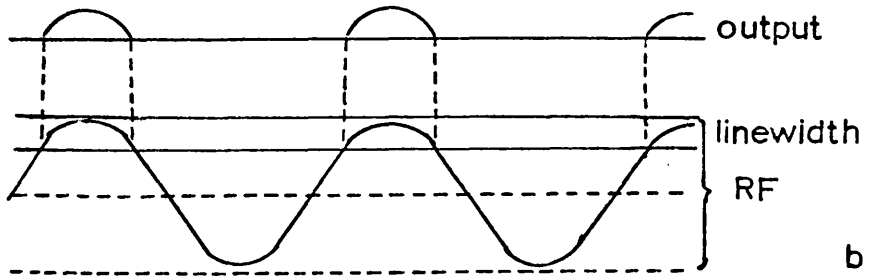
Figure 2.2. Origin of signal: modulation less than linewidth.

total swing is $\Delta\nu$ as indicated in figure 2.2a). The amplitude of the RF in the oscillating circuit would vary at the same audio-frequency with amplitude $\Delta E_T/2$. This amplitude modulation of the RF is detected, amplified and finally displayed by the methods described in the following chapter. The amplitude $\Delta E_T/2$ obviously depends on the gradient of the absorption curve at ν_1 . Thus, as the frequency of the oscillator is varied, say in the direction indicated in figure 2.2a, the output $\Delta E_T/2$ varies as the derivative of the absorption curve, as shown in figure 2.2b.

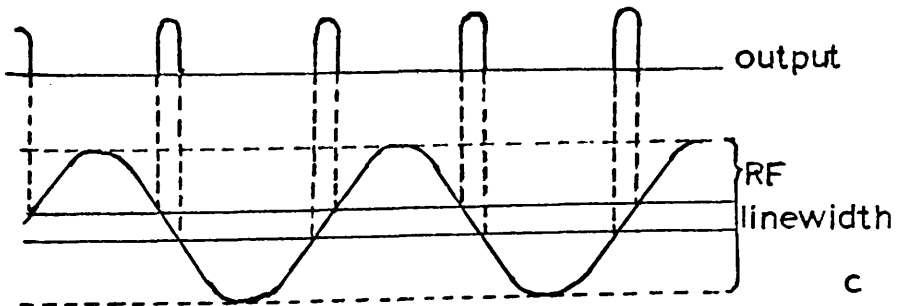
Figure 2.3 (page 114) illustrates how the change in RF level is detected when the depth of frequency modulation is greater than the line width of the NQR absorption signal. Here the line width is represented by the two horizontal lines in figure 2.3a, corresponding perhaps to the width between the two vertical dashed lines of figure 2.2a, and the variation of the oscillator frequency with time is represented: both the linear sweep variation and the approximately sinusoidal frequency modulation are shown. As the oscillator frequency nears the NQR absorption frequency, the frequency of the oscillator satisfies the absorption condition at one extreme of the frequency modulation cycle, and a signal is generated in the form of a series of pulses at the same frequency as that of the frequency modulation: this is represented in figure 2.3b. As the centre frequency of the oscillator reaches



a



b



c

Figure 2.3. Origin of signal: modulation greater than linewidth.

the NQR absorption frequency, the frequency of the oscillator sweeps back and forth through the resonance signal, as shown in figure 2.3c. For each cycle, the resonance condition is satisfied twice, and the signal produced is a series of pulses at twice the modulation frequency (i.e. at the first harmonic of the modulation frequency). When this system of modulation is used, it is the second signal described, at the first harmonic of the modulation frequency, which is detected, amplified and displayed, since it is this signal which has the longer duration on sweeping through a resonance line.

The choice of modulation frequency is arbitrary, although in a super-regenerative oscillator it should be much smaller than the quench frequency. In practice, it should also be chosen so as to avoid as far as possible interference from outside sources, especially 50 c/s mains pickup.

3.1 Preliminaries

Two spectrometer systems for the detection of ^{14}N nuclear quadrupole resonances have been built, one system using a marginal oscillator and the other a super-regenerative oscillator. Sections 3.2 to 3.12 give the constructional details of the marginal oscillator system, and the rest of this chapter gives similar details for the super-regenerative oscillator system.

3.2 The main spectrometer system

The main spectrometer system incorporates a marginal continuous wave oscillator of the type described in section 2.2. Internal frequency modulation is employed. The amplitude of the frequency modulation can be varied, so that the modulation may be either less than or greater than the expected line width of the NQR absorption signal. Modifications can be made to the rest of the oscillator to detect either the fundamental or the first harmonic of the modulation frequency. However, a modulation depth considerably greater than the linewidth has been most often used, and the spectrometer will be described in the form suitable for detecting the first harmonic of the modulation frequency, with an indication where appropriate of the modifications necessary for detection at the modulation frequency. These

modifications are easily made.

Figure 3.1 (page 118) is a schematic outline of the origin and development of the NQR signal in the spectrometer. The audio-frequency signal, originating as described in section 2.4, is passed, together with radio-frequency and noise at all frequencies, through an RF rejection filter which attenuates the RF component of the signal, to the pre-amplifier. The pre-amplifier is housed in the same unit as the oscillator, and is combined with an AF selection filtering network. Its output consists of AF signal, AF noise over a considerable range of frequencies and phase relationships, and a small residual amount of RF. This output now goes to the narrow-band amplifier, which is sharply peaked at the frequency of the signal. The output from this stage includes mainly AF signal and AF noise at the same frequency. The next unit, the phase-sensitive detector, amplifies the AF, selects that part of the AF which has a particular phase relationship to a reference AF signal supplied to it (chosen so that it is mainly AF arising from the signal which is selected), and converts this AF to a DC signal suitable for driving a potentiometric recorder. This whole process is summarised in figure 3.1.

Figure 3.2 (page 119) is a block diagram of the complete main spectrometer system. All units supplied direct from the mains (double-outlined in figure 3.2) are separately fused. The units are either standard equipment which has been purchased,

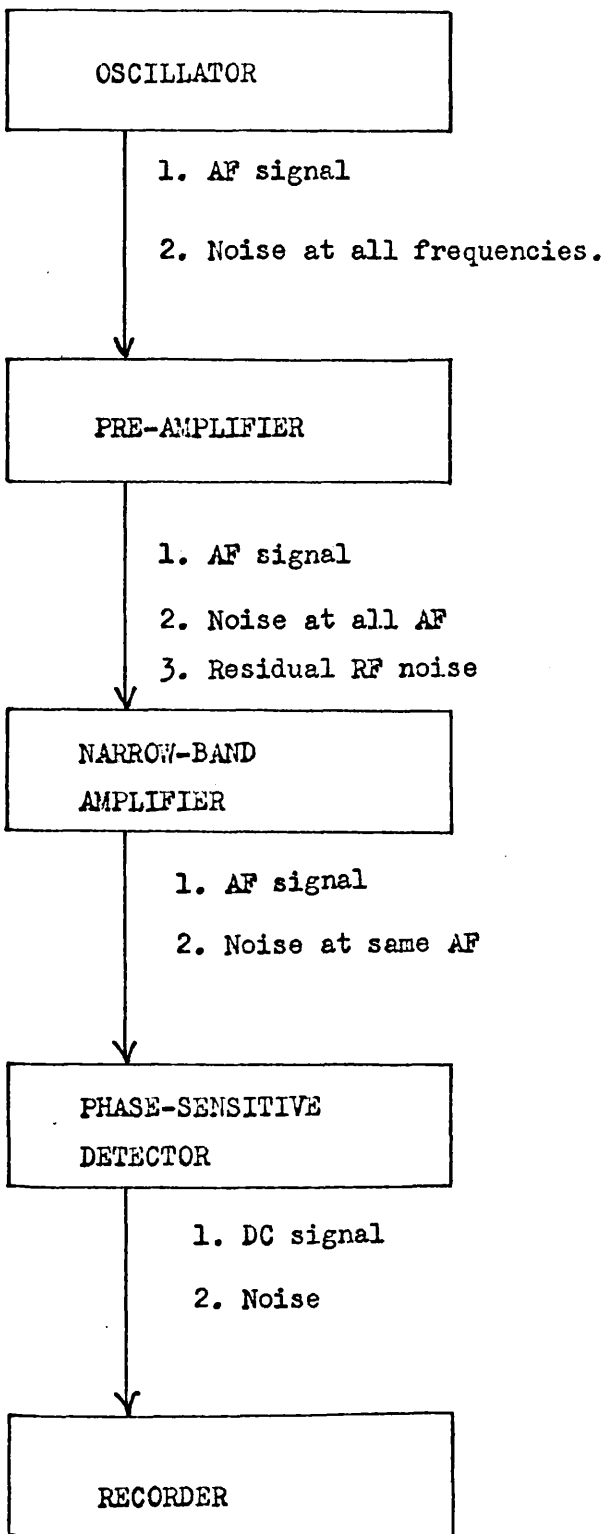


Figure 3.1. Path of an NQR signal through the spectrometer

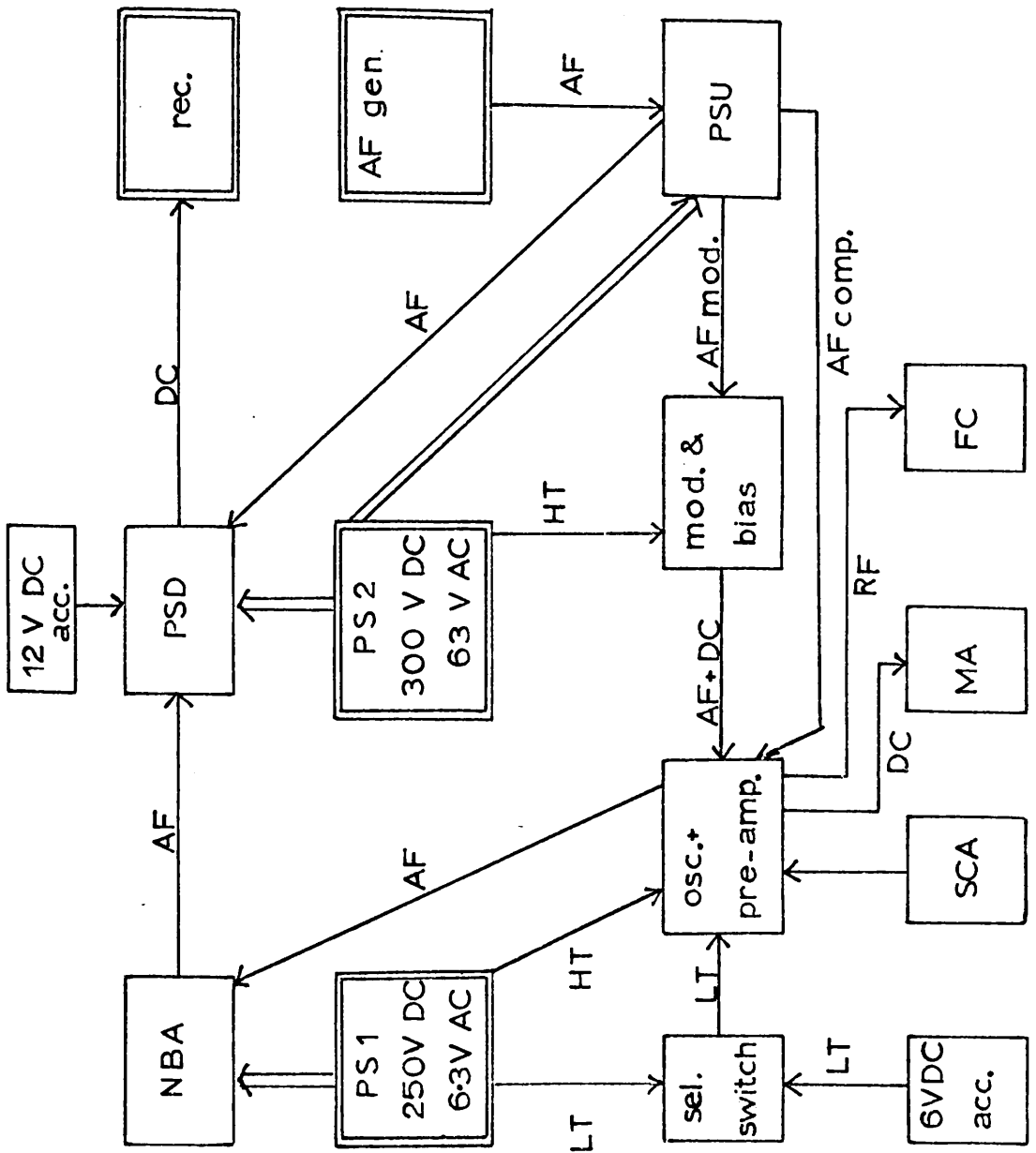


Figure 3.2. Block diagram of main spectrometer system.

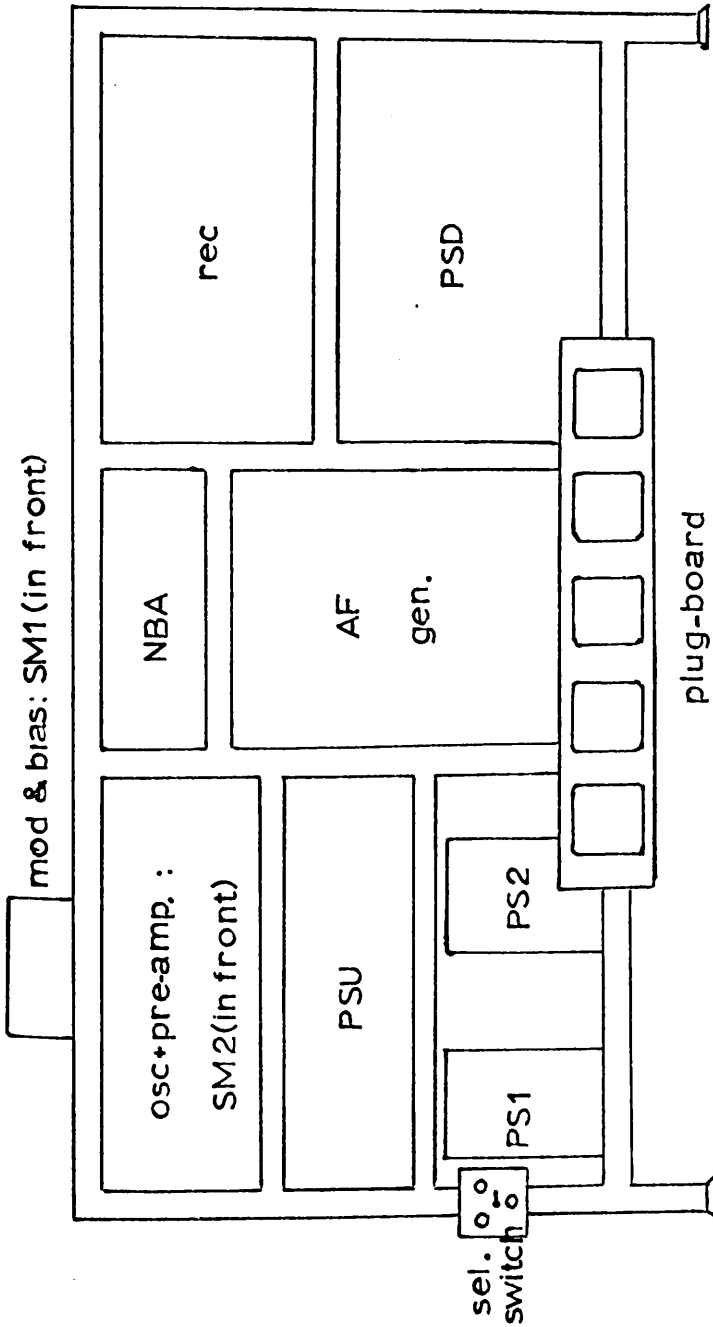


Figure 3.3. Front elevation of the main spectrometer

Key to figures 3.2 and 3.3: block diagram and front elevation
of main spectrometer

In figure 3.2, double outlining of a unit indicates that it is supplied directly from the mains. A double-line arrow represents the supply of both HT and heaters.

Abbreviations used

AC	alternating current	pre-amp.	pre-amplifier
acc.	accumulator	PS 1	power supply 1
AF	audio-frequency	PS 2	power supply 2
AF gen.	audio-frequency generator	PSD	phase-sensitive detector
comp.	compensation	PSU	phase-shift unit
DC	direct current	rec.	recorder
FC	frequency counter	RF	radio-frequency
HT	high tension	SCA	sample coil assembly
LT	low tension	sel.	selector
MA	microammeter	SM 1	sweep motor 1
mod.	modulation	SM 2	sweep motor 2
NBA	narrow-band amplifier	V	volts
osc.	oscillator		

or special units which have been designed and constructed for the spectrometer system. The following sections deal with them in greater detail.

Figure 3.3 (page 120) indicates the constructional layout of the spectrometer. The units are mounted on a Handy Angle rack which is separately earthed, and connections between the units are made where possible with co-axial cable to minimise pickup. Provision is made in the construction for the carrying out of low-temperature investigations (see next section). Details of the individual sections of the spectrometer are now considered in turn.

3.3 The sample coil assembly: low-temperature work

Figure 3.4 (page 123) is a diagram of the sample coil assembly. Experience showed that a single-layer coil gave greatest oscillator sensitivity, higher oscillation coherence and flatter RF response. The coil was made by winding SWG 22 copper wire on to a 1" diameter glass sample tube, which was cut to a length suitable for the coil in question. The coil was cemented to the sample tube with ICI 'Tensol' cement, so that coil and sample tube form one inseparable unit. The coil is mounted on the long axis of a cylindrical copper screening box $2\frac{1}{2}$ " in diameter, sealed permanently at one end, and closing at the other end with a copper lid (figure 3.4). This ensures that the coil is completely shielded from stray RF. The earthed side of the coil is soldered

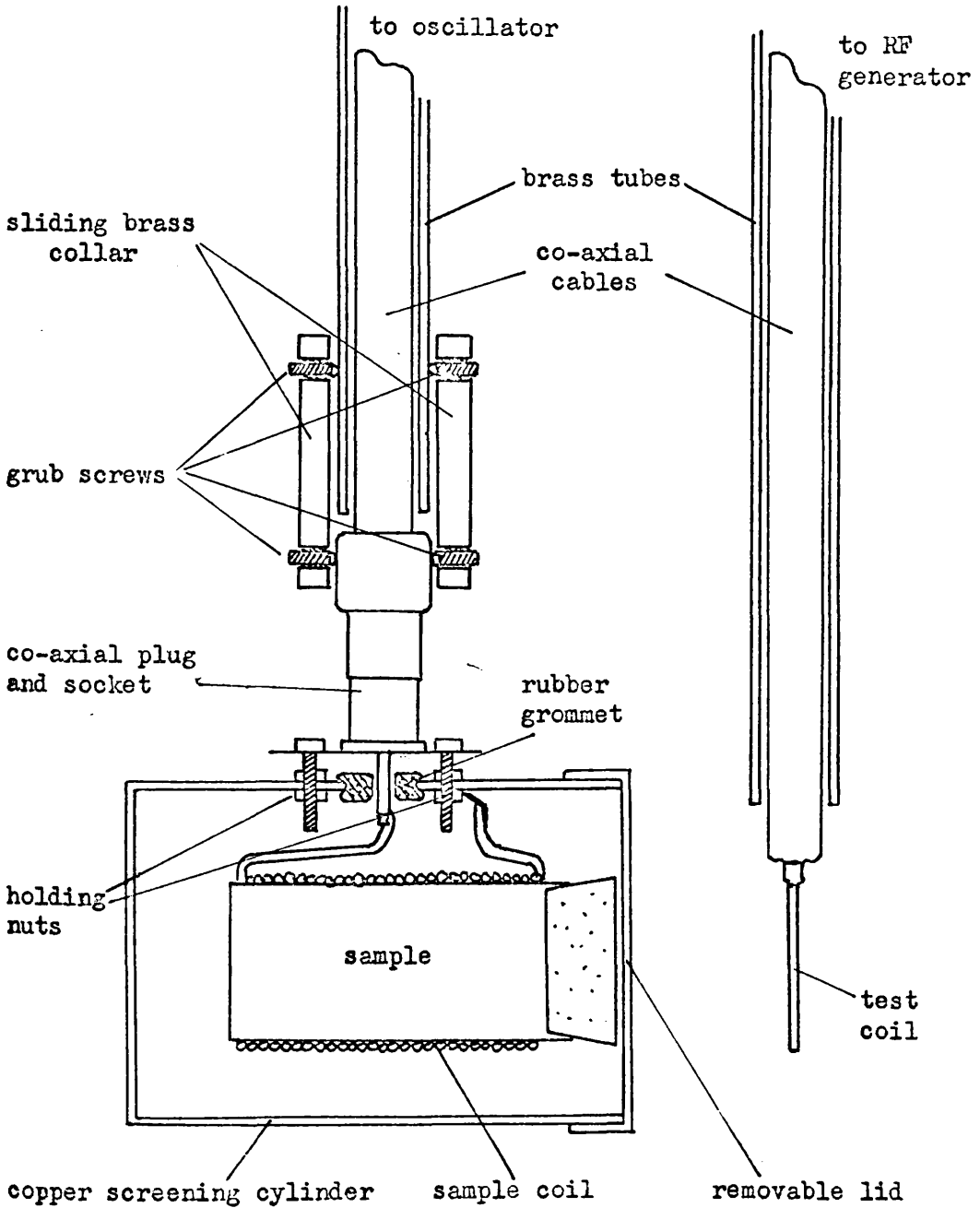


Figure 3.4. Sample coil assembly and RF test coil.

directly to the inside wall of the screening box, and the other end goes by a co-axial cable which passes through a 10" long $\frac{1}{4}$ " o.d. brass tube to socket 1 of the oscillator (see section 3.4). Apart from pickup of stray RF by the sample coil acting as an aerial, which is largely eliminated by the screening described above, it was found that a fruitful source of extra noise at this stage lay in movement of the whole coil assembly. This assembly had therefore to be as rigid as possible, while yet allowing the sample to be situated at the end of the brass rod so that it could be immersed in liquid nitrogen for low-temperature work. These requirements are difficult to reconcile. Eventually a solution was found by securing the two Belling-Lee plugs at either end of the brass rod to the rod by means of sliding collars fitted with grub screws (see figure 3.4 for the arrangement at the sample coil end; the same arrangement is repeated at the oscillator housing end). The rod itself is supported by a clamp screwed to a metal column, which is attached rigidly to the frame of the spectrometer for that purpose.

This arrangement allows the sample coil to be immersed in say liquid nitrogen contained in a Dewar flask which sits behind the power supplies (figure 3.3), and which can be raised on a lab-jack so that the sample can be immersed sufficiently slowly. Access to this part of the apparatus is from the left-hand side (figure 3.3).

3.4 The oscillator-preamplifier unit

These two stages are mounted in the same unit in order to try to eliminate pickup before the critical first amplification stage. Figure 3.5 (pages 126 - 128) shows the circuit details of this unit. The circuit is essentially a Robinson²² marginal oscillator, incorporating the modifications to the tank circuit suggested by Dutcher and Scott¹⁰, with the additional modifications of the inclusion of the pre-amplifier and an AF selection network in the same unit. The Robinson oscillator is used because of its remarkable freedom from microphonics²² and its high sensitivity, comparable to that of the Pound and Knight²⁰ oscillator.

It is not possible to use the normal 6.3 V AC heater supply from the power supply when the oscillator is in operation, since the 50 c/s hum picked up and amplified is much greater in amplitude than the 150 c/s or 300 c/s signal at the output: this 50 c/s pickup is partly eliminated by the narrow-band amplifier, but it does lead to considerably increased oscillator noise. Consequently, the heater supply to the oscillator comes from a large 6.3 V accumulator. In addition, it was found that after being switched on, the oscillator took some time to reach sufficiently stable operating conditions, and for the sake of reproducibility of control settings and performance it is better to keep the oscillator running continuously. This is managed by

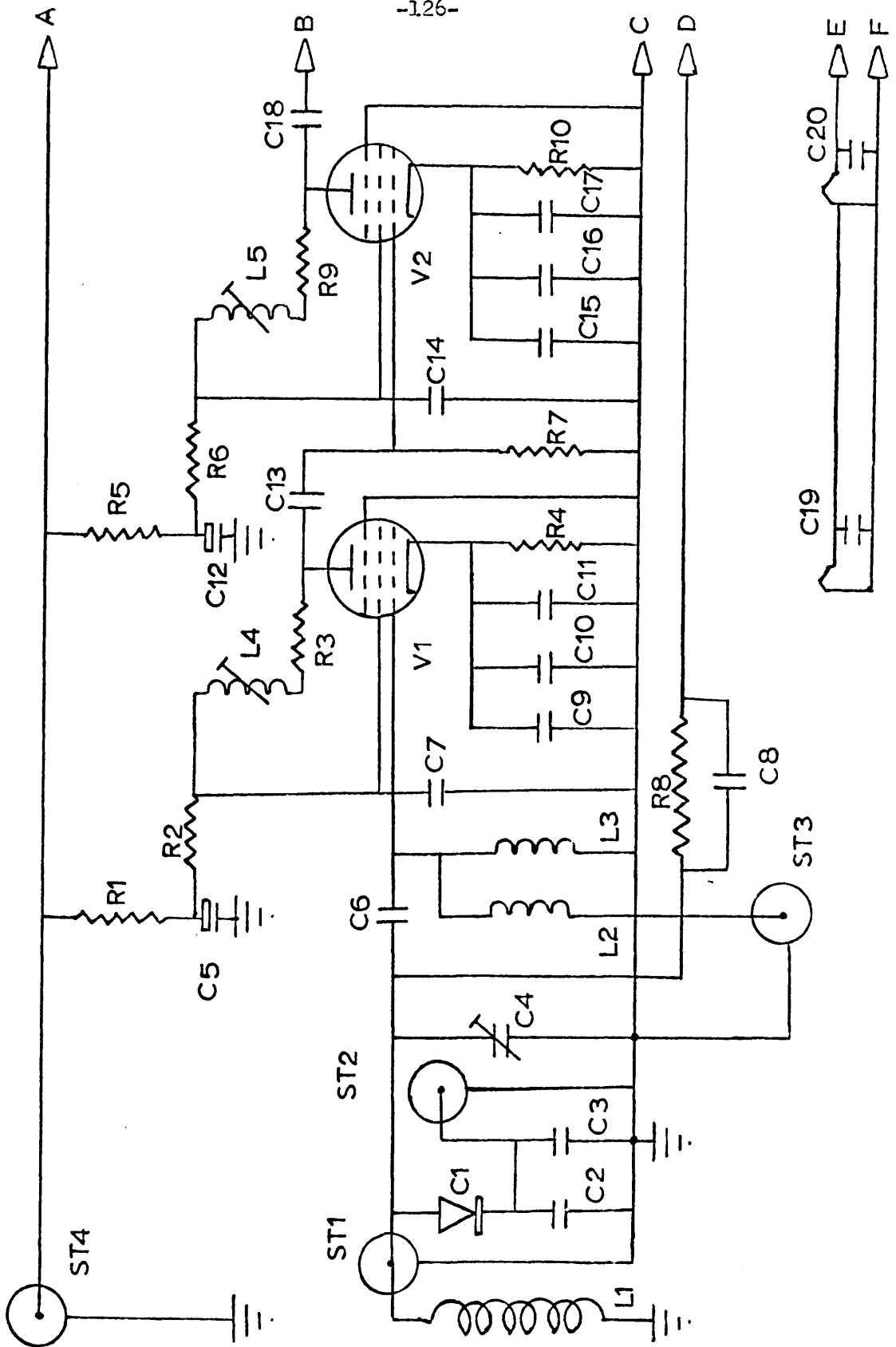


Figure 3.5a. Oscillator-detector.

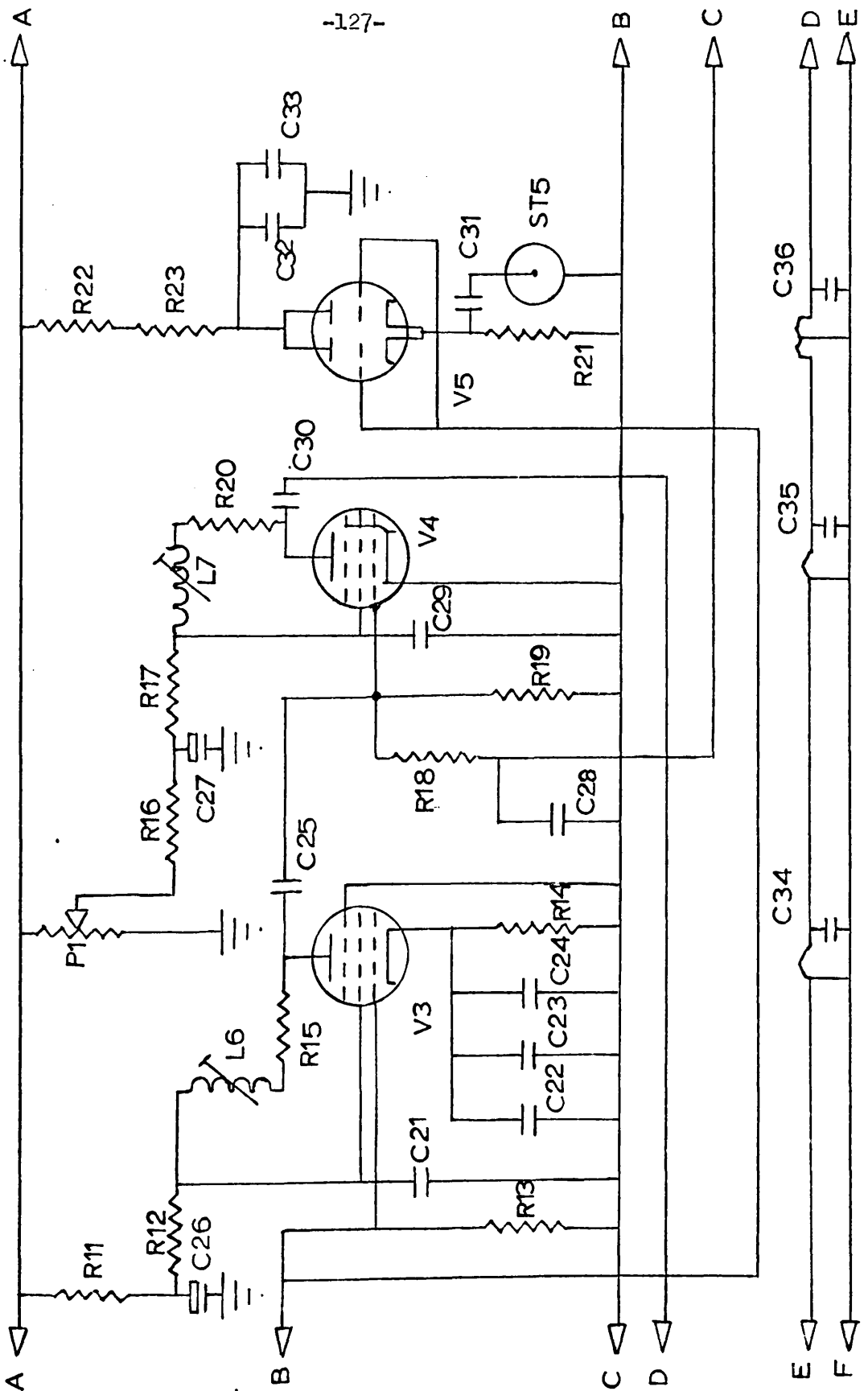


Figure 3.5b. Oscillator-detector.

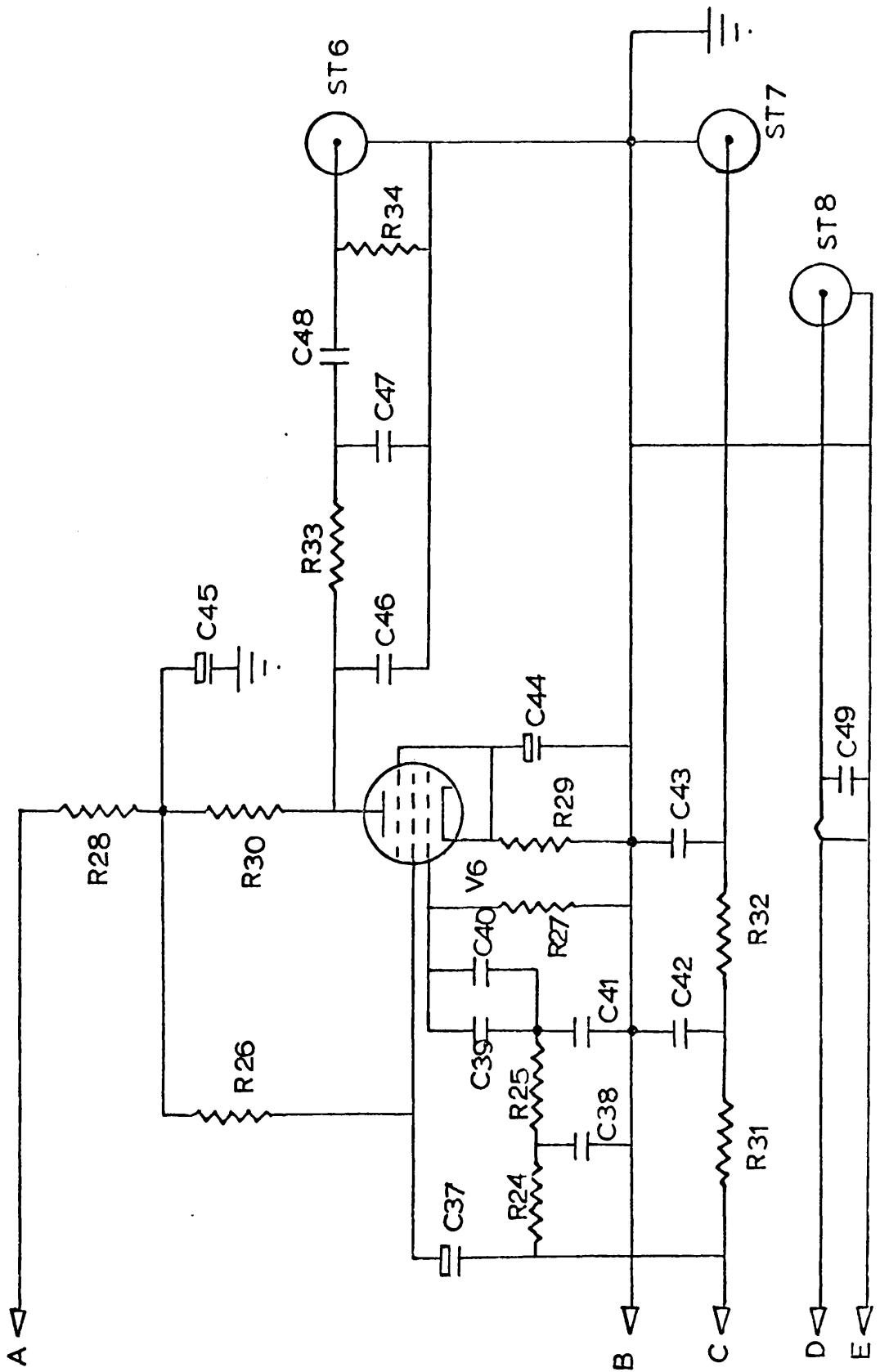


Figure 3.5c. Oscillator-detector.

Key to figure 3.5: oscillator-detector

Capacitors

All capacitances in μF unless otherwise indicated.

C1 Hughes diode HC 7005	C24 0.02	C37 0.25
C2 39 pF	C25 33pF	C38 100 pF
C3 39 pF	C26 32	C39 0.02
C4 variable up to 384 pF	C27 32	C40 0.02
C5 32	C15 0.01	C28 100 pF
C6 100 pF	C16 0.02	C29 0.005
C7 0.005	C17 0.02	C30 47pF
C8 5 pF	C18 470 pF	C31 470 pF
C9 0.01	C19 0.01	C32 0.02
C10 0.02	C20 0.01	C33 0.02
C11 0.02	C21 0.005	C34 0.01
C12 32	C22 0.01	C35 0.01
C13 470 pF	C23 0.02	C36 0.01
C14 0.005		

Inductors

All inductances in μH unless otherwise indicated.

L1 Sample coil.	L3 10 mH	L5 2	L7 6
L2 50	L4 2	L6 4	

Potentiometer and resistors

All resistances in Ω .

P1 100K: RF amplitude	R1 2.2K	R2 2.2K	R3 560
-----------------------	---------	---------	--------

Key to figure 3.5 (cont.)

Resistors (cont.)

R4 82	R12 2.2K	R20 330	R28 2.2K
R5 2.2K	R13 10K	R21 82	R29 680
R6 2.2K	R14 82	R22 4.7K	R30 33K
R7 10K	R15 1K	R23 4.7K	R31 47K
R8 1M	R16 6.8K	R24 47K	R32 100K
R9 560	R17 4.7K	R25 47K	R33 10K
R10 82	R18 47K	R26 150K	R34 1M
R11 2.2K	R19 10K	R27 1M	

Sockets

ST1 Sample coil.	ST5 RF output
ST2 Modulation and bias input.	ST6 AF output
ST3 Compensation input.	ST7 Microammeter output
ST4 HT +250 V.	ST8 Heaters 6.3 V

Valves

V1 6X4	V3 6X4	V5 6X4
V2 6X4	V4 6X4	V6 6X4

switching the oscillator heater supply over to the 6.3 V AC supply overnight or when the spectrometer is otherwise not in use, an arrangement which frees the 6.3 V accumulator for re-charging.

The processes of frequency modulation and the production of the signal are described in section 2.4 above. The frequency modulation is secured by applying the sinusoidal modulation voltage to a Hughes diode, HC 7005, back-biased for use as a voltage-variable capacitor. The modulation signal introduces amplitude modulation in the RF of the oscillator, and this amplitude modulation is of the same frequency and phase as any amplitude modulation caused by NQR absorption in the sample coil, provided that the modulation used is less than the line width of the signal. In that case, it is therefore detected by succeeding stages and displayed on the recorder: while the DC level due to this spurious amplitude modulation can be backed off at this stage, it is generally better to avoid introducing it at all, and thus avoid any risk of overloading the amplification stages following the oscillator. This is accomplished by introducing into the tank circuit an AF signal of the same frequency and effective amplitude as, but 180° out of phase with, the modulation signal on the Hughes diode: this is the compensation signal, introduced through L2 (figure 3.5a). Like the modulation signal, the compensation signal is supplied from the phase-shift unit

(section 3.6), which must maintain high stability in these AF signals over long periods. Obviously the compensation signal is necessary only when the modulation depth is less than the signal line width; when it is greater, the spurious amplitude modulation, being at the same frequency as the modulation signal, is not detected.

The frequency sweep may be carried out in two ways: by varying the DC bias on the Hughes diode (see section 3.5), or by rotating capacitor C4. The very slow rotation necessary to attain a reasonable sweep rate (not more than about 10 Kc/s/min for ^{14}N NQR resonances) is attained by coupling the capacitor shaft to a Sangamo motor unit S.7., 1 rev. per 12 hours. The alternative method of sweeping the frequency, described in the next section, produces an even slower frequency sweep.

In figure 3.5, valve V1 is the oscillator valve, and valves V2 and V3 are essentially RF amplifiers. V4 is the limiter valve, which controls the positive feedback through R8 and C8 to the tank circuit. The amount of feedback is controlled by potentiometer P1 (which is marked "amplitude" on the chassis). As is general with marginal oscillators, greatest sensitivity is obtained when P1 is adjusted so as to control the feedback to give a very low RF level. It was found by experiment that the best RF level was that corresponding to a reading on the microammeter of between 2 and 5 μA . Pre-adjustment of chokes

L4, L5, L6, and L7 is necessary to give a fairly flat RF level over the range of frequencies to be covered: this oscillator can be made to give a fairly flat response between about 1 Mc/s and 10 Mc/s. V5 is a double-triode cathode follower which allows one to take a part of the signal on the grid of V3 for monitoring on the radio-receiver, oscilloscope, or frequency counter (section 3.10): this latter is the only accurate way of determining the frequency of the oscillator, for example when a signal is detected. V6 and the associated resistive-capacitive network are the pre-amplifier valve and the audio-frequency selection filter respectively. Before the signal reaches this stage, most though not all of the RF has gone to earth through the small capacitance C28 (100 pF). As described in section 3.2, the signal now goes to the narrow-band amplifier via socket 6.

The microammeter is connected across socket 7 so that its reading is related to the RF level in the tank circuit. This is because V4 is unbiased, and runs grid current owing to the RF, which leads to a (negative) DC level on the lower side of R18. This DC level is registered on the microammeter. It is blocked before it reaches V6 by capacitors C39 and C40.

3.5 The modulation and bias unit

The circuit diagram of this unit is shown in figure 3.6 (page 134). The unit is entirely concerned with delivering the correct AF and DC bias level to the Hughes diode in the oscillator. It

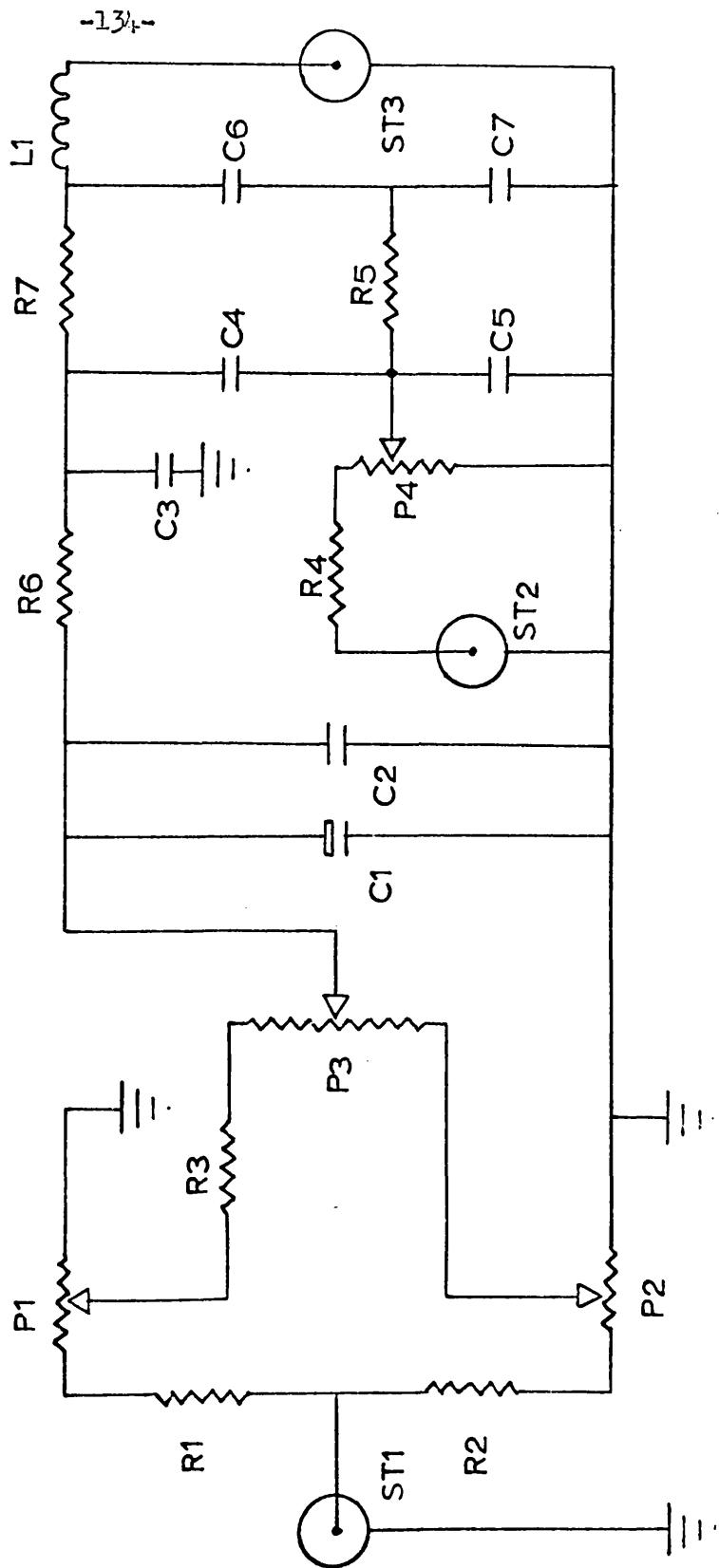


Figure 3.6. Modulation and bias unit.

Key to figure 3.6: modulation and bias unit

Capacitors

All capacitances in μF .

C1 32	C3 0.001	C5 0.001	C7 0.001
C2 0.0047	C4 1.0	C6 0.001	

Inductor

L1 2.5 mH

Potentiometers and resistors

All resistances in Ω .

P1 500K pre-set	P4 200K	R2 1M	R5 10K
P2 500K pre-set	R1 1M	R3 100K	R6 100K
P3 100K ten-turn helipot	R4 680K	R7 100K	

Sockets

ST1 HT +300V.	ST2 AF input	ST3 AF and DC output.
---------------	--------------	-----------------------

is designed especially to avoid pickup at this stage, even a very small amount of which drastically affects the oscillator noise level. The unit is mounted as close as possible to the oscillator (directly above it: figure 3.3) and its output is carried to socket 2 of the oscillator by as short as possible a piece of doubly screened co-axial cable. The high tension (300 V DC) comes in at socket 1 (figure 3.6) and is led via R1-P1-R3 and R2-P2 either end of P3, a 100K ten-turn Colvern helipot. P1 and P2 are preset potentiometers on the back of the unit, which are used to adjust the low and high potential ends respectively of P3, which is used to set the bias on the Hughes diode in the oscillator, if the frequency sweep method described in section 3.4 is employed. Another method of sweeping the oscillator frequency is available through this unit, for if potentiometer P3 is turned slowly, a slowly varying DC bias is delivered to the Hughes diode, with a consequent slow change in the oscillator frequency. Potentiometer P3 is turned by means of a Sangamo motor unit type S.7., 2 revs. per hour, with the drive taken through a 1:6 reduction gearing, giving a resultant rate at the potentiometer shaft of 1 rev. per 3 hours. The actual rate of voltage sweep can be determined by the settings of P1 and P2: test points from the ends of P3 are provided external to the chassis to enable these settings to be made more easily.

The AF modulation signal is taken in through socket 2,

and may be suitably attenuated by potentiometer P4, which is marked "modulation amplitude" on the chassis. The combined DC bias and superimposed AF modulation signal of the correct amplitude are delivered from socket 3 through the choke L1, which serves to isolate the unit from any back-RF from the oscillator. The modulation frequency for a marginal oscillator is arbitrarily chosen. The frequency used in this spectrometer has always been 150 c/s, but this can easily be changed if necessary.

3.6 The phase-shift unit

This unit supplies a modulation signal and compensation signal to the oscillator, and a reference signal to the phase-sensitive detector, all controllable in relative amplitudes and phases. The unit also supplies a calibration output, which is useful for various setting-up procedures, as a comparison with other AF signals, and in checking the AF stages of the spectrometer.

The total gain from the tank circuit to the recorder output is of the order of one to ten million. Thus, it is evident that the relative stability of the modulation, compensation and reference signals must be exceptionally high. Figure 3.7 (pages 138 and 139) shows the circuit employed, which is exactly that described by Dutcher⁹. The circuit has been found to maintain this high stability.

In figure 3.7, the input stage (V1) is a cathode coupled

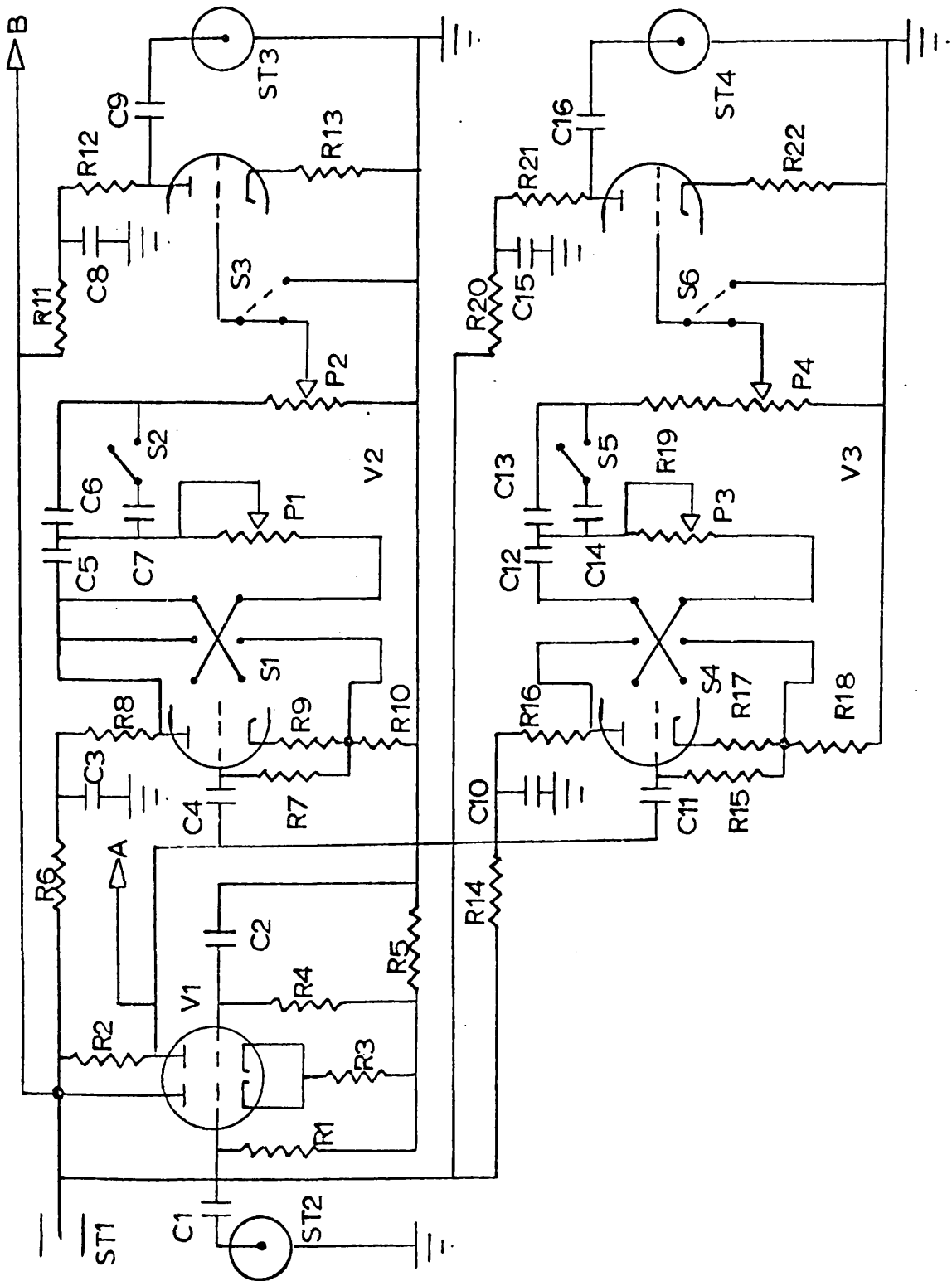


Figure 3.7a. Phase-shift unit.

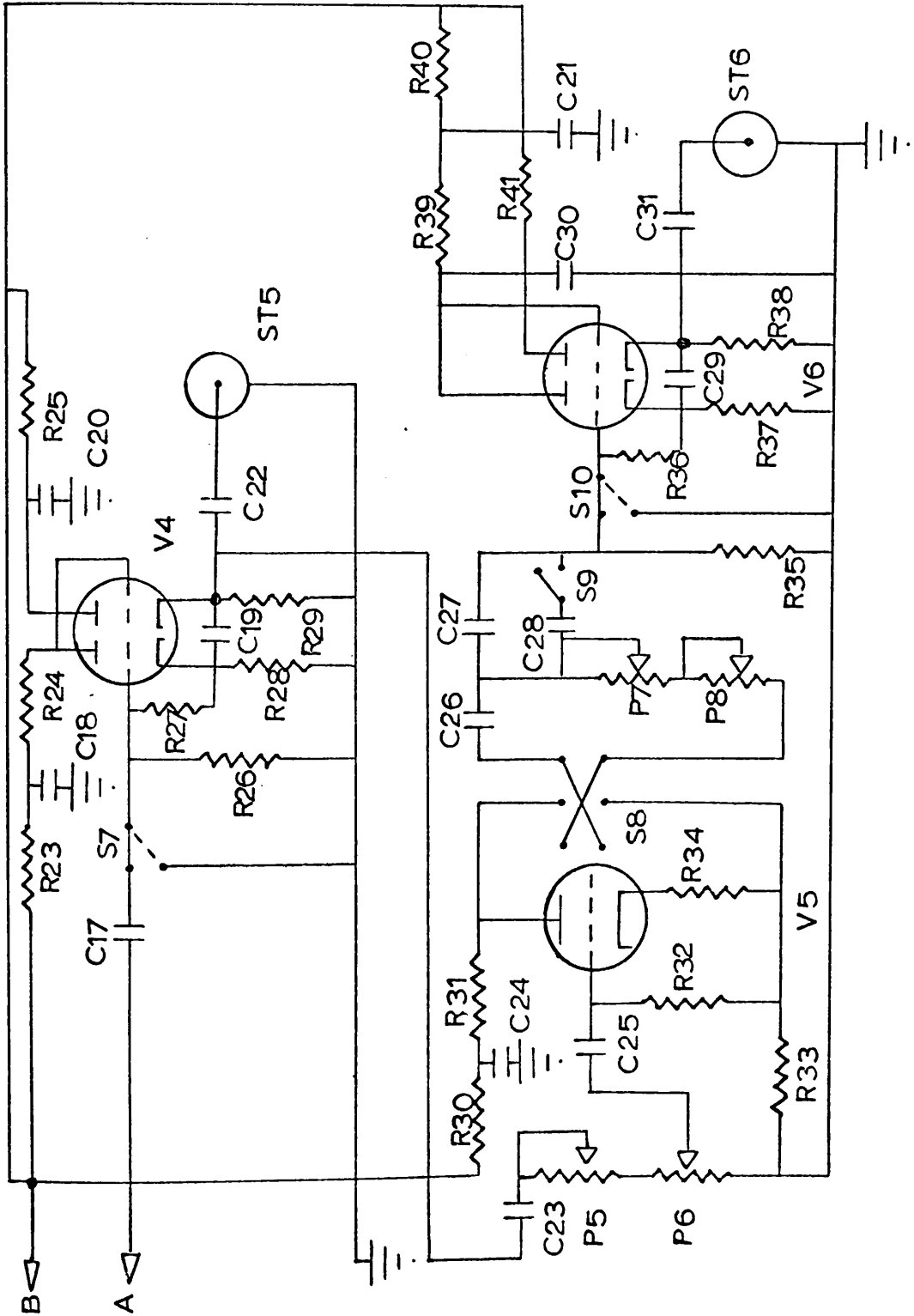


Figure 3.7b. Phase-shift unit.

Key to figure 3.7: phase-shift unit

Capacitors

All capacitances in μF .

C1 0.1	C9 0.1	C17 0.1	C25 0.1
C2 0.1	C10 20	C18 20	C26 0.03
C3 20	C11 0.1	C19 0.5	C27 0.0015
C4 0.1	C12 0.03	C20 20	C28 0.1
C5 0.03	C13 0.0015	C21 20	C29 0.5
C6 0.0015	C14 0.1	C22 0.5	C30 20
C7 0.1	C15 20	C23 0.1	C31 0.5
C8 20	C16 0.1	C24 20	

Potentiometers and resistors

All resistances in Ω .

P1 1M log: phase-shift			R10 12K
P2 1M: reference signal amplitude			R11 4.7K
P3 1M log: calibrate phase-shift			R12 47K
P4 100K: calibrate amplitude			R13 4.7K
P5 10K: compensate amplitude (fine)			R14 4.7K
P6 1M: compensate amplitude (coarse)			R15 470K
P7 1M log: compensate phase-shift (coarse)			R16 12K
P8 10K: compensate phase-shift (fine)			R17 3.3K
R1 470K	R4 470K	R7 470K	R18 12K
R2 10K	R5 4.7K	R8 12K	R19 1M
R3 470	R6 4.7K	R9 3.3K	R20 4.7K

Key to figure 3.7 (cont.)

Resistors (cont.)

R21 47K	R27 15K	R32 470K	R37 1K
R22 4.7K	R28 1K	R33 12K	R38 22K
R23 47K	R29 22K	R34 3.3K	R39 4.7K
R24 4.7K	R30 4.7K	R35 1M	R40 47K
R25 4.7K	R31 12K	R36 2.2M	R41 4.7K
R26 470K			

Switches

S1 Reference signal phase reverse	S6 Calibrate on-off
S2 Reference signal amplitude range	S7 Modulate on-off
S3 Reference signal on-off	S8 Compensate phase reverse
S4 Calibrate phase reverse	S9 Compensate amplitude range
S5 Calibrate amplitude range	S10 Compensate on-off

Sockets

ST1 HT +300V	ST4 Calibrate output
ST2 AF input	ST5 Modulate output
ST3 Reference signal output	ST6 Compensate output

Valves

V1 6SN7	V3 6SN7	V5	V6 6SN7
V2 6SN7	V4 6SN7		

amplifier which supplies three further stages from the anode of its second stage. The phase-sensitive detector reference channel (V2) and calibration channel (V3) are conventional phase-shift networks. The modulation channel (V4) is a negative feedback amplifier with a cathode follower output. No provision for gain or phase control is made in this channel, since the phase of the other signals can be adjusted relative to the modulation signal, and the amplitude is controlled at the modulation and bias unit described above. The compensation signal is derived from the output of the modulation channel, and then goes through an isolating amplifier (V5) to a phase shift network and then to a feedback amplifier stage (V6) like that used in the modulation channel.

The greatest instability between modulation and compensation signals comes from V5 and the phase shift circuitry between V5 and V6. Instability has been greatly reduced by use of 2 watt resistors throughout and of silver-mica capacitors where possible.

The key to figure 3.7 (pages 140 and 141) gives a description of the use of the numerous control components in the unit. All switches are mounted at the rear, and all potentiometers at the front, of the unit.

3.7 The narrow-band amplifier

The narrow-band amplifier is a highly selective amplifier

which amplifies only frequencies very near the selected frequency, so reducing the bandwidth of the noise as well as amplifying the resonance signal. A response curve showing this behaviour is given for a peaking frequency of 150 c/s in figure 3.8, (page 144) and figure 3.9 (page 145) gives the circuit of the unit. This circuit is modified from part of a circuit given by Mulay¹⁸.

When the spectrometer was first being built, a circuit for a narrow-band amplifier given by Wallace²⁷ was used. Apart from the difficulty of selecting and matching the two stagger-tuned twin-T networks required by that circuit, it was found that the half-width of the response curve was appreciably more than the 5 c/s claimed. The present circuit has been found satisfactory, with a very high gain at the response peak, using only one twin-T network.

The twin-T network, as shown in figure 3.9, is the essential feature of the narrow-band amplifier. The complete theory of twin-T networks is given by Tuttle²⁶, but their important property is their sharply peaked rejection of a null frequency, ν_0 (c/s) given by (r in ohms, c in farads)

$$\nu_0 = \sqrt{\pi/2\pi rc} \quad 3.7.1$$

where r and c are the resistance and capacitance respectively in each of the input and output arms, and the resistances r' and c' in the earthed arm are given by:

$$r' = r/2n \quad 3.7.2a$$

-114-

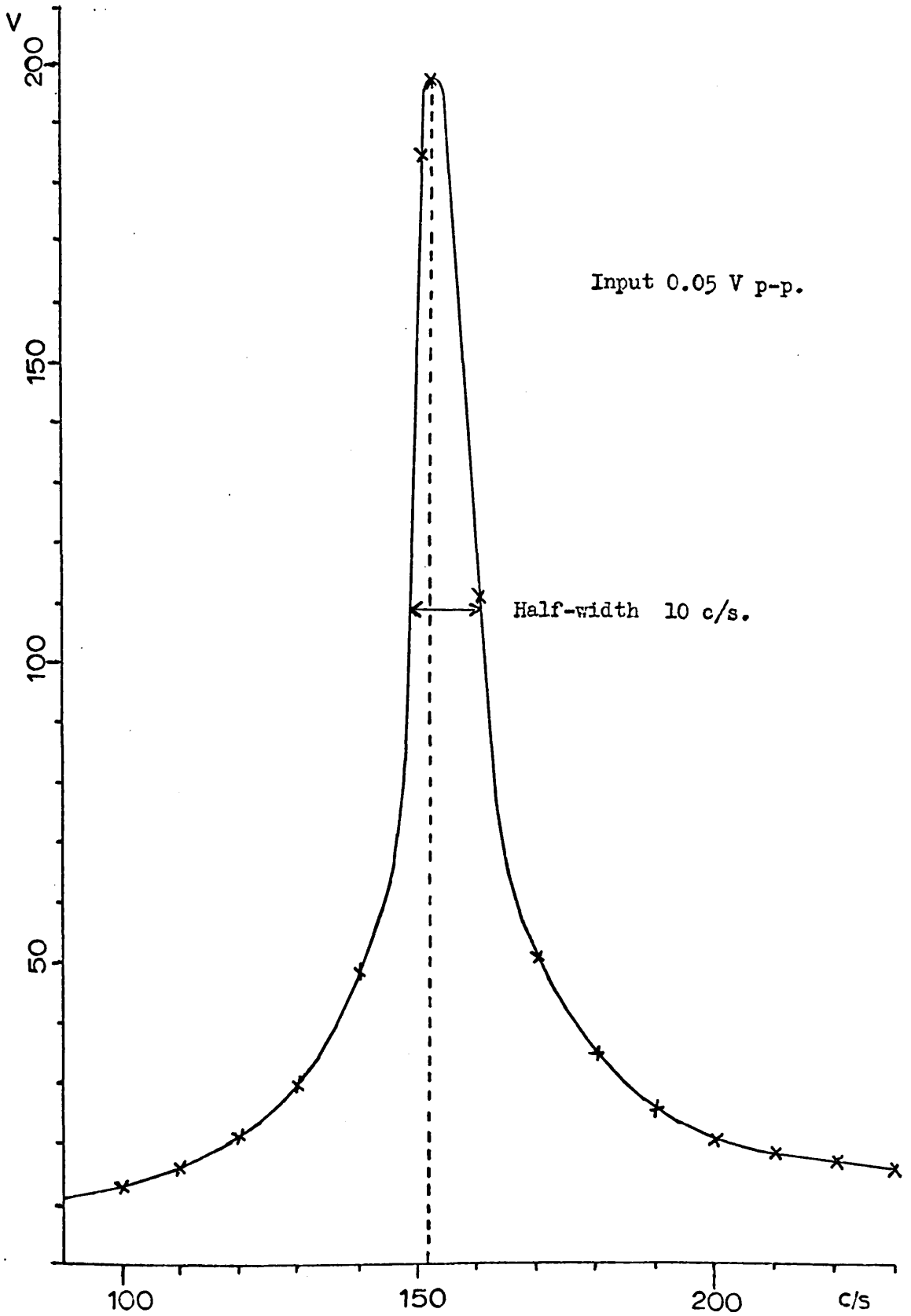


Figure 3.8. Narrow-band amplifier response.

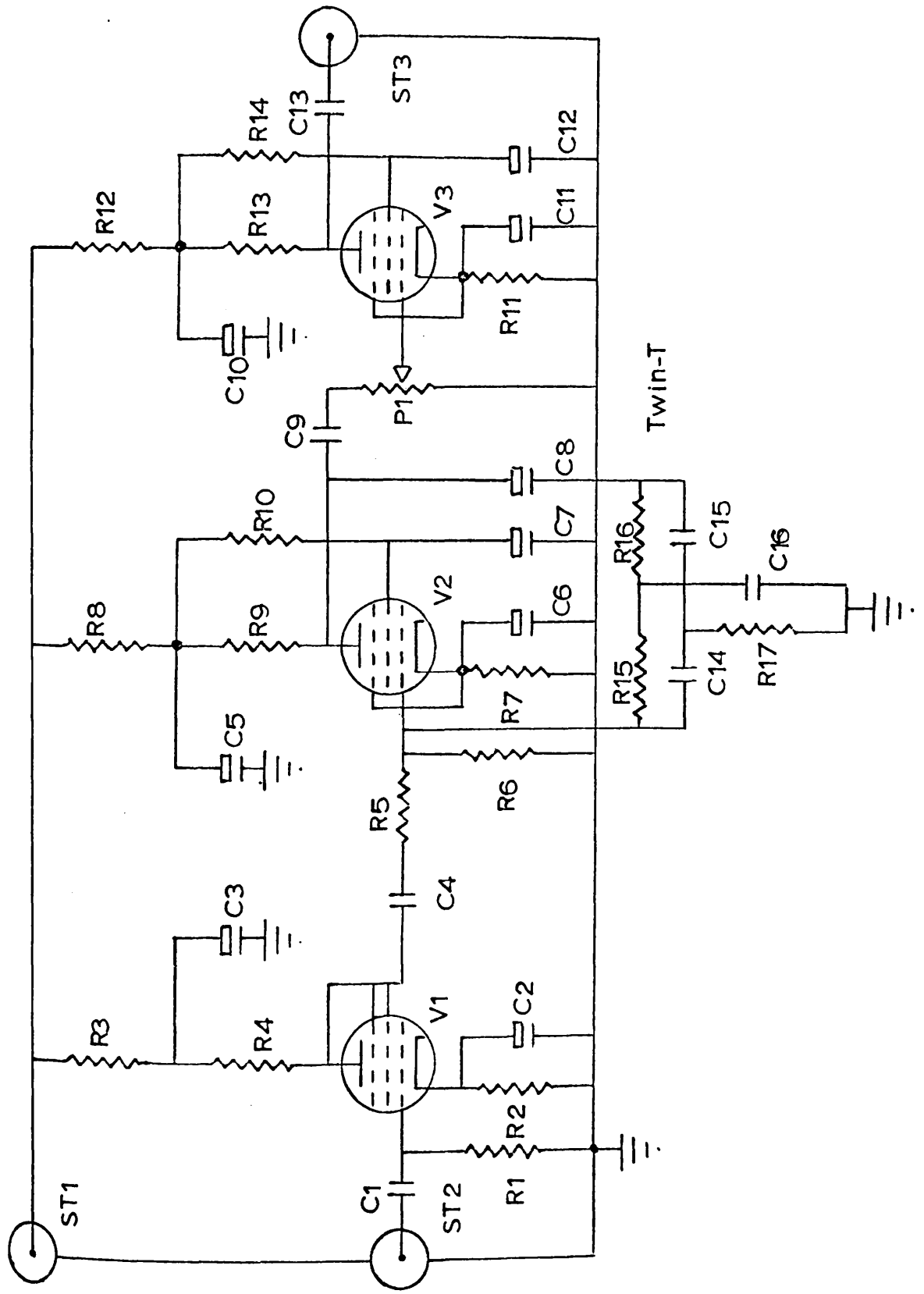


Figure 3.9. Narrow-band amplifier.

Key to figure 3.9: Narrow-band amplifier

Capacitors

All capacitances in μF unless otherwise indicated.

C1 0.002	C5 20	C9 0.002	C13 0.01
C2 2.0	C6 25	C10 20	C14 3600 pF
C3 20	C7 8.0	C11 4.0	C15 3600 pF
C4 0.001	C8 0.5	C12 0.5	C16 7200 pF

Potentiometer and resistors All resistances in Ω .

P1 1M: gain	R5 2.2M	R10 1.2M	R14 1.2M
R1 1M	R6 2.2M	R11 2.2K	R15 150K
R2 6.8K	R7 10K	R12 10K	R16 150K
R3 10K	R8 220K	R13 220K	R17 75K
R4 100K	R9 2.2K		

Sockets

ST1 HT +300 V	ST2 Input	ST3 Output
---------------	-----------	------------

Valves

V1 6SJ7	V2 6SJ7	V3 6SJ7
---------	---------	---------

and $c' = 2c/n$ 3.7.2b

where for most applications $n = 1$. The values used for a peak at 300 c/s are given in the key to figure 3.9 (page 146), and the values used for 150 c/s are $c = 2950$ pF, $r = 360K\Omega$ (nominal values; actual components have to be chosen to match and to give the sharpest peaking as close as possible to the desired frequency). For greater stability, wire-wound matched resistors and silver-mica capacitors are used in the construction of the twin-T units, which are made to be easily demountable from the narrow-band amplifier for change of detection frequency.

The circuit (figure 3.9) is essentially a three-stage pentode amplifier, with negative feedback through the twin-T network from the anode of V2 to the grid of V2, where therefore the selection of the correct frequency occurs. Potentiometer P1 controls the gain of the instrument. The circuit could hardly be simpler in design or operation, and has been found to be reliable in use.

3.8 The square-wave generator

The phase-sensitive detector reference signal from the phase-shift unit is not in fact fed directly to the phase-sensitive detector itself. It goes instead to the square-wave reference generator (circuit diagram figure 3.10, page 148). The square-wave generator is completely transistorised, and is mounted on the chassis of the phase-sensitive detector. It is not shown

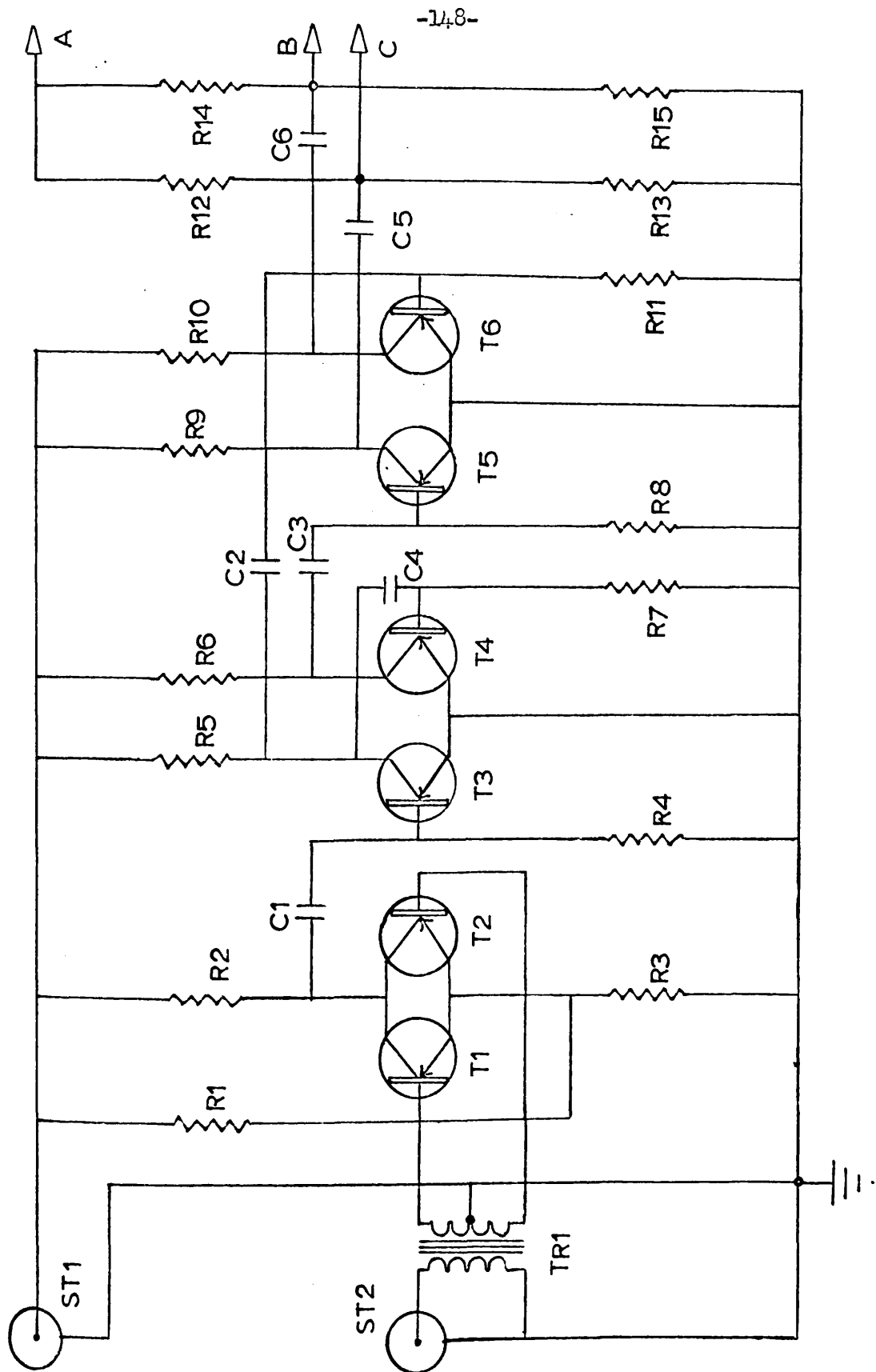


Figure 3.10 Square-wave generator.

Key to figure 3.10:square-wave generator

Capacitors

All capacitances in μF .

C1 16	C3 10	C5 1.0	C6 1.0
C2 10	C4 10		

Resistors

All resistances in Ω .

R1 10K	R5 2.2 K	R9 2.2K	R13 3.3M
R2 12K	R6 2.2K	R10 2.2K	R14 10M
R3 2.2K	R7 1.2K	R11 1K	R15 3.3M
R4 1.2K	R8 1K	R12 10M	

Sockets

ST1 -12V input	ST2 Reference signal input.
----------------	-----------------------------

Transistors

T1 OC72	T3 OC72	T5 OC72	T6 OC72
T2 OC72	T4 OC72		

Transformer

TR1 Midget mains transformer 1:1 centre-tapped.

separately from the latter in the block diagram of the spectrometer (figure 3.2). Transistors T1 and T2 in figure 3.10 together with the centre-tapped transformer TR 1 act as a frequency doubler for detection at the first harmonic of the modulation frequency. The circuit may be modified for detection at the modulation frequency by disconnecting the centre-tap to the secondary of TR1 and by disconnecting the input to the base of T2 and connecting this lead to earth. With these simple modifications, the unit gives a good square wave at the input frequency (i.e. at the modulation frequency). Resistances R12-R14 and R13-R15 are matched pairs to give suitable equal positive biases on the grids of valves V3 and V4 of the phase-sensitive detector (see figure 3.11: the points marked A, B, and C in this figure are connected to the points marked A, B, and C in figure 3.10). Capacitors C5 and C6 block the DC bias from the transistor circuit: resistors R12, R13, R14 and R15 are made large to minimise surges through these capacitors, with possible damage to the transistors, when the HT supply is switched on or off. This trouble was in fact experienced before the resistor values were increased.

The circuit of this unit is that described by Wallace²⁷, with some changes. The -12V negative bias for the transistors is derived from a 12-volt car accumulator battery.

3.9 The phase-sensitive detector

The circuit diagram of this part of the spectrometer system

is given in figure 3.11: the design is exactly that used by Dean⁸. The incoming signal, attenuated at the ten-position potential divider S1 to a level which gives no overloading of following stages, is amplified by a two-stage triode amplifier V1 (see figure 3.11, page 152), and is converted to a DC level by the phase-sensitive detector network proper (V2, V3, and V4). This floating DC output is taken through a double cathode follower (V5), controlled by an opposite-ganged dual potentiometer P1. The time constant of the instrument is controlled by the five-position switch S2, and P1 acts as a zero control for the output.

3.10 Auxiliary units

The following pieces of equipment are auxiliary in that they were bought as standard supplies from manufacturers, and not specially built for the spectrometer:

1. An Advance Components Ltd. radio-frequency generator type E model 2. This provides a standard known radio-frequency (which can be checked on the frequency counter for exact readings) of adjustable amplitude. Its output is used to check the radio-frequency stages of the spectrometer.

For this purpose, a one-turn coil to act as an aerial is mounted beside the sample coil, and is supported by a brass tube running parallel to, and similar to, the brass tube which supports the sample coil (section 3.3; see also figure 3.3). This aerial can be connected to the radio-frequency signal generator, and

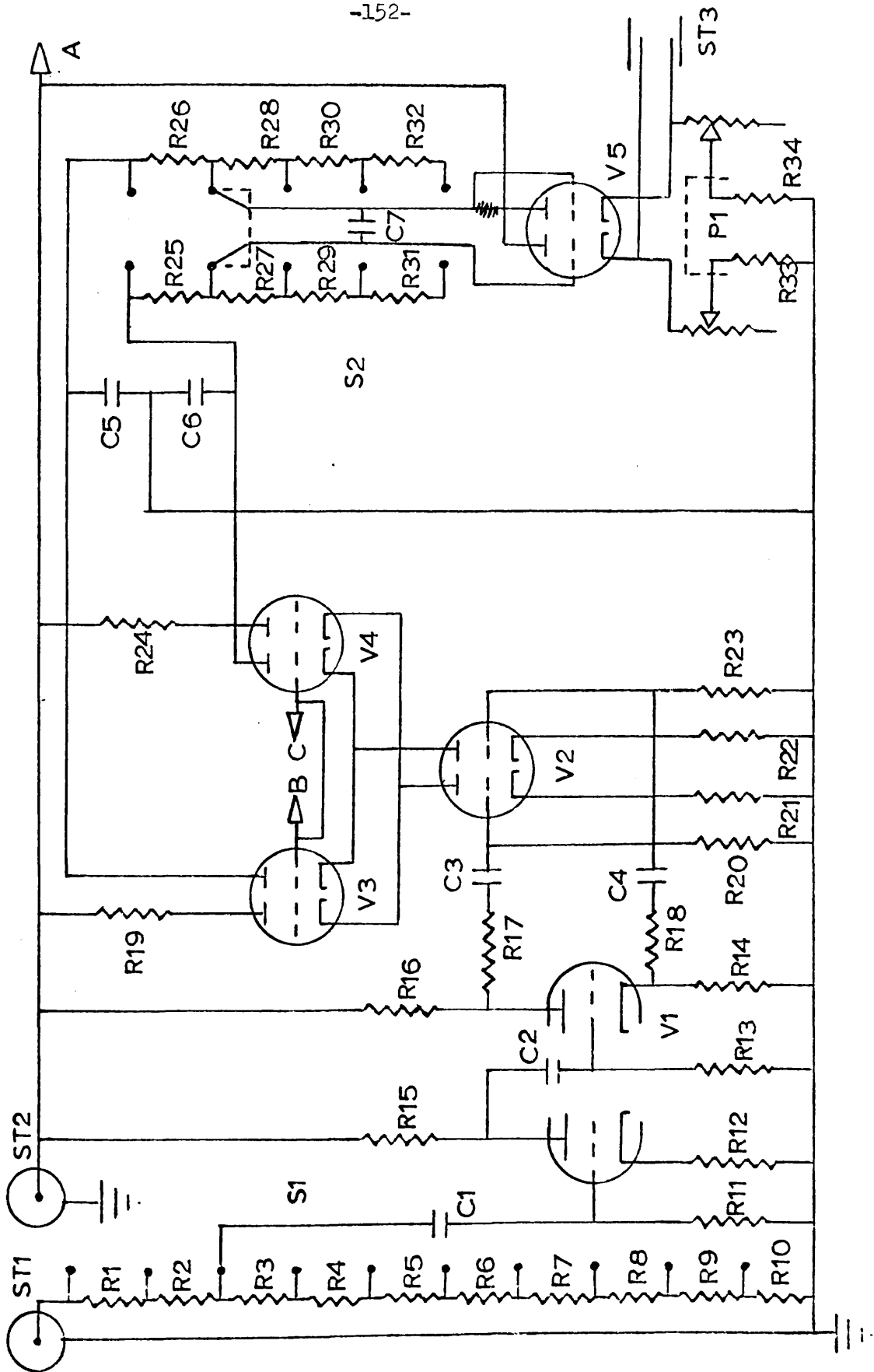


Figure 3.11. Phase-sensitive detector.

Key to figure 3.11: phase-sensitive detector

Capacitors

All capacitances in μ F.

C1 0.1	C3 0.1	C5 1.0	C7 10
C2 0.1	C4 0.1	C6 1.0	

Potentiometer and resistors All resistances in Ω .

F1 25K-25K opposite-ganged dual	R17 22K	R26 220K	
R1 220K	R9 0.47K	R18 22K	R27 470K
R2 100K	R10 0.47K	R19 400K 1%	R28 470K
R3 47K	R11 220K	R20 100K	R29 1M
R4 22K	R12 33K	R21 1.5K 1%	R30 1M
R5 10K	R13 220K	R22 1.5K 1%	R31 2.2M
R6 4.7K	R14 6.8K	R23 100K	R32 2.2M
R7 2.2K	R15 47K	R24 400K 1%	R33 15K 2W
R8 1.0K	R16 6.8K	R25 220K	R34 15K 2W

Sockets

ST1 Input	ST2 HT +300V	ST3 Output
-----------	--------------	------------

Valves

V1 12AU7	V3 12AX7	V4 12AX7	V5 12AU7
V2 12AX7			

Switches

S1 Ten-position attenuator

S2 Time constant, five-position

the arrangement can be used to give an indication of spectrometer sensitivity, and to provide marker peaks of known frequency during a frequency sweep of the oscillator, since when the oscillator frequency coincides with the radio-frequency signal generator frequency, energy is exchanged between the two and a signal produced in the spectrometer: this signal is displayed on the recorder.

2. An Advance Components Ltd. AF signal generator type 81A. This supplies the input to the phase-shift unit (section 3.6).
3. Two International Electronics Ltd. power supplies, type DSM 2, one supplying 250 V DC and 6.3 V AC, and the other 300 V DC and 6.3 V AC. Apart from the oscillator heater supply when the oscillator is in operation (section 3.4) and the square-wave generator low tension supply (section 3.8), these units between them supply HT and heaters for all the units of the spectrometer. They are shown in the block diagram (figure 3.3)
4. A Bausch and Lomb laboratory recorder V.O.M.-5, used with floating input provision (compare section 3.9).
5. A Marconi Frequency Counter Meter Type TF 1345/2, which is used to measure the frequency of the oscillator either directly, using the output from socket 5 (figure 3.5; section 3.4), or by measurement of the frequency of the RF signal generator markers.
6. An Eddystone H.F. Communications receiver model 940, which is used for general monitoring of radio-frequency events, especially modulation and sweep rate.

7. A Telequipment oscilloscope type D33R, which is used in setting-up the modulation signal amplitude, and the compensation signal with correct amplitude and phase when that signal is being used. It is also used for general monitoring of the signals at the various AF stages of the spectrometer when necessary.

3.11 Operation of the spectrometer

The following procedure is recommended for operation of the spectrometer:-

1. Set the oscillator frequency by adjusting C4 on the oscillator. If the first method of frequency sweep is to be used, the bias on the diode should be about 10 V. If the frequency is to be swept by varying the bias, first set the limits of its voltage sweep (section 3.5). The diode can safely take a bias of up to 50 V.
2. Set the modulation level, if necessary by using the oscilloscope. If the modulation depth is to be less than the line width, the peak-to-peak amplitude of the modulation signal should be less than 0.1 V. If it is to be greater, then the modulation amplitude should be greater, but not more than 0.5 V. Lower modulation depths are obtained for the same voltage swing by increasing the bias on the diode.
3. Where necessary set the compensation signal. This is best done by looking at the output from the pre-amplifier on the oscilloscope and adjusting the amplitude and phase of the compensation

signal to minimise the output at the modulation frequency.

4. Set the phase shift of the reference signal. This has to be done by trial and error to give the strongest displayed signal on the recorder, but initially the reference signal should be set at the same phase as the modulation signal, and of the correct amplitude to give a symmetrical square-wave from the square-wave generator: this latter setting is critical.

5. Set the narrow-band amplifier gain, phase-sensitive detector input attenuation and time constant, and recorder gain to suit the nature of the signal. The best settings of these controls have to be found empirically, but this is a fairly easy process.

The settings of the other controls present no difficulty. The sweep motor should be switched on a minute or two before the recorder motor is started, to give the oscillator time to become stable after the sweep is begun.

3.12 Testing spectrometer performance

As described in section 3.10(1), some indication of the spectrometer sensitivity can be obtained by examining the response to a signal from the RF signal generator. An RF signal of 2 μ V from the generator can be made to give a signal on the recorder with a signal-to-noise ratio of 10:1. A more important test is to search for a known ^{14}N NQR signal, and for this purpose the ^{14}N NQR signal in hexamethylenetetramine, first reported by Watkins and Pound²⁶ at 3.3062 Mc/s at 26.6° C,

was chosen because of the reported high intensity of this signal.

Such a signal, obtained at room temperature with hexamethylenetetramine as sample, is shown in figure 3.12 (page 158). The signal-to-noise ratio must be in excess of 10:1, which compares well with other reported sensitivities. However, the performance of the spectrometer was not reliable: adjustment was found to be too difficult in the first place, and very difficult to repeat; and the spectrometer seemed too sensitive to extraneous interference. Although the signal in section 3.12 is intense, indicating that this resonance at least can be well displayed, detecting the signal called for the oscillator to be working at the limits of its stability. Such a condition is of course unsatisfactory, and depends too much on factors which are hardly, if at all, controllable. Because of the apparent advantages of the super-regenerative oscillator (section 2.3), it was decided to build one in an attempt to find a more reliable experimental method.

3.13. The super-regenerative oscillator

The final form of the circuit diagram is shown in figure 3.13 (page 159). The starting-point for the design was that of Weber and Todd²⁹, but the present instrument is so greatly modified, including in particular the quenching circuit due to Tong²⁵, that it is essentially a different and new design.

The sample coil is wound on to the glass sample tube as

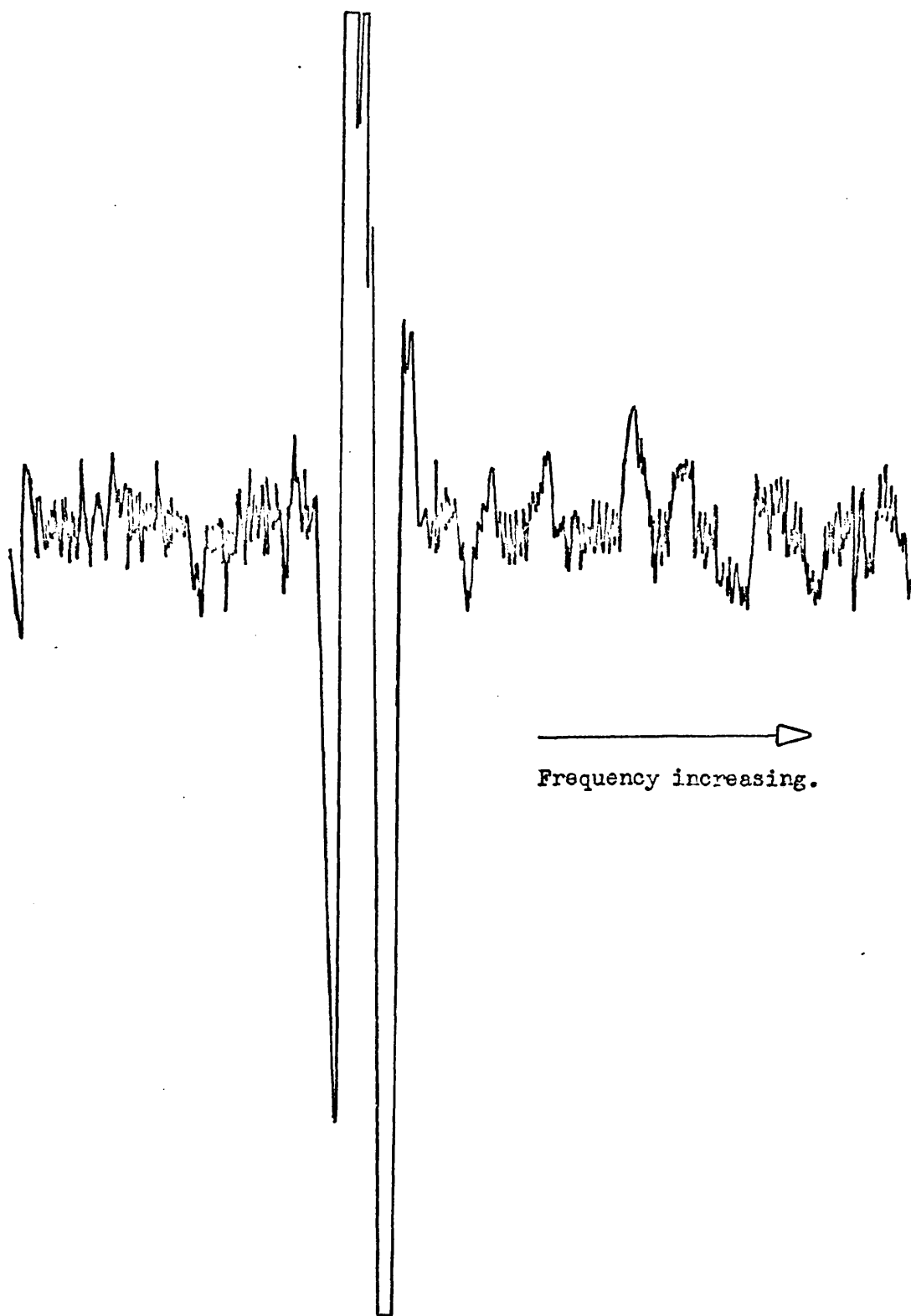


Figure 3.12. NQR signal from hexamethylenetetramine.

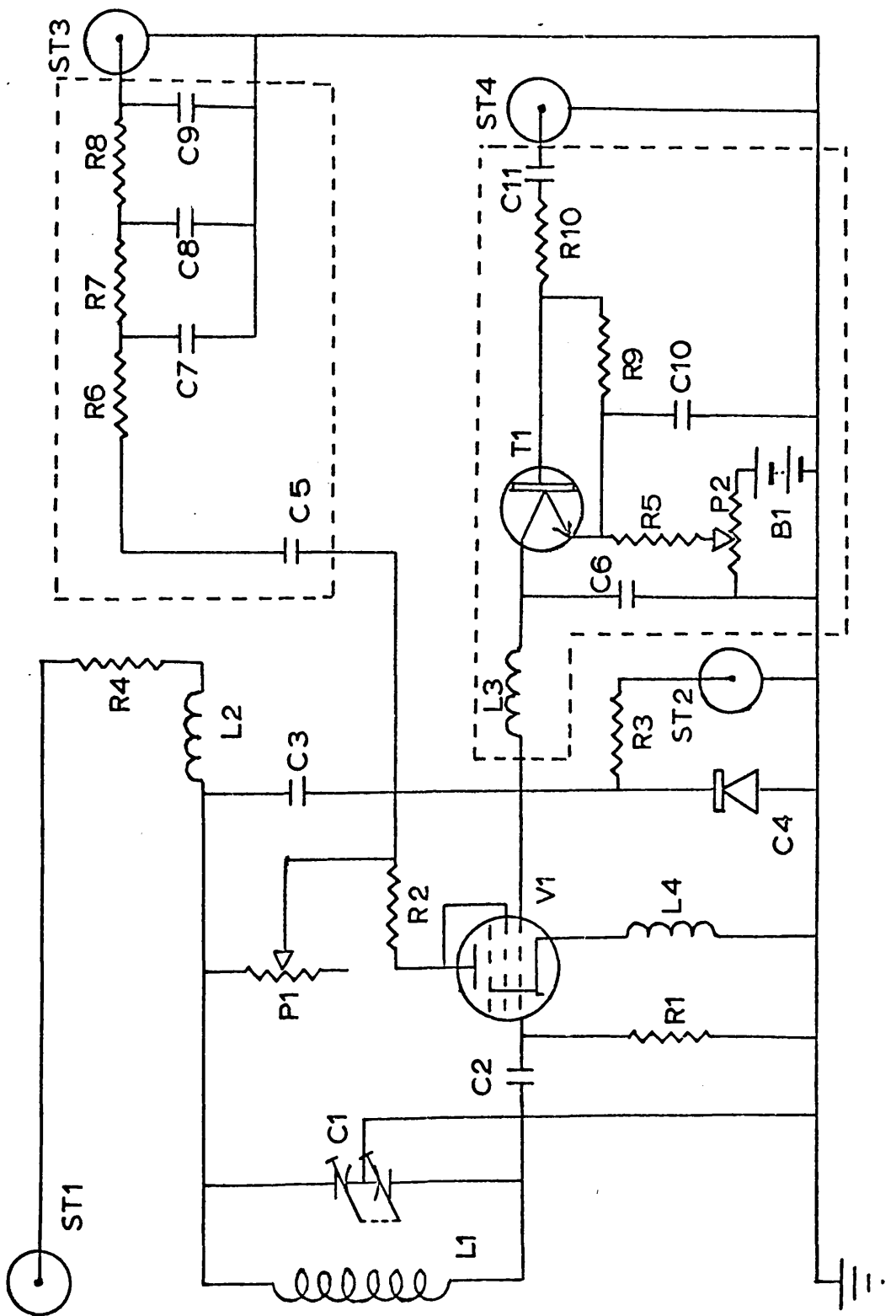


Figure 3.13. The super-regenerative oscillator.

Key to figure 3.13: Super-regenerative oscillator

Battery

B1 12V car accumulator

Capacitors

All capacitances in μF unless otherwise stated.

C1 double-gang 10-50 pF	C5 39 pF	C9 2200 pF
C2 200 pF	C6 0.01	C10 2200 pF
C3 Hughes diode HC 7001	C7 2000 pF	C11 2200 pF
C4 0.5	C8 0.22	

Inductors

Inductances are in μH unless otherwise stated.

L1 Sample coil	L3 22	L4 10
L2 10 mH		

Potentiometers and resistors

All resistances are in Ω .

P1 25 K 10-turn helipot	R3 1 M	R7 42 K
P2 25 K 10-turn helipot	R4 3.3 K	R8 42 K
R1 150 K	R5 5.6 K	R9 1.2 M
R2 10 K	R6 42K	R10 3.3 K

Transistor

T1 BFY 57

Valve

V1 6AM6

Sockets

ST1 HT + 250V	ST3 output	ST4 quench input
ST2 modulation and bias input.		

described in section 3.3, and is connected permanently to a two-pin screw-on plug. The socket into which this plug fits is bolted to the end of a $\frac{1}{2}$ " o.d. brass tube with a right-angle bend. The other end of the brass tube is bolted to the oscillator chassis. In this way the sample coil is held away from and below the chassis for low-temperature work. A screened two-core cable runs from the plug at the end of the brass rod, through the brass rod, and directly into the oscillator, where the leads from the coil are soldered to tags on a perspex mount. The whole construction is intended to secure rigidity of the sample coil and as few plug-socket connections as possible. Different sample coils, to cover different frequency ranges, are mounted separately on plugs so that the coils are easily interchangeable.

In figure 3.13, the main tuning of the oscillator is governed by the dual-ganged capacitor C1. At one stage in the development of the instrument, the frequency of the oscillator was swept by driving this capacitor by means of a small electric motor, but this method was at length abandoned for two reasons. Small mechanical discontinuities in the gear-train of the motor, and the difficulty of attaining bend-free coupling between the motor shaft and the capacitor shaft with consequent mechanical strain on the capacitor, combined to produce extra noise in the tank circuit. In addition, it was found that the frequency dependence of the optimum quench amplitude and RF amplitude

settings was more marked with this method of frequency sweep, compared to the method of slowly varying the DC bias on the Hughes diode C₄. The explanation of this second effect is probably that the RF amplitude variation with frequency is greater when C₁ is varied than when C₄ is varied.

The method which was finally used, varying the DC level at C₄, also has the advantages that the sweep motor drives a potentiometer in the modulation and bias unit, and is therefore not mechanically coupled to the oscillator chassis; and that any small fluctuations in the DC level should be smoothed out by the modulation unit circuit.

Resistance R₂, which lowers the maximum possible HT at the anode of V₁, and inductance L₄, which puts a small cathode load to the oscillator valve, are both intended to damp to some extent the RF oscillations. This was found to be necessary because the oscillator is otherwise inclined to squeg (self-quench) at some RF frequencies. L₄ in addition eliminates some of the variation with frequency of the RF amplitude.

The oscillator valve, a pentode, was originally used as such, because of the theoretically better performance of a pentode compared to a triode. The quenching signal was then applied to the second grid: however the quenching circuit, shown in figure 3.13, was found to give better control of coherence when the valve was used as a triode (early circuits were

plagued by a tendency to discontinuous jumps from a coherent to a highly incoherent state).

In the quenching circuit, which is due to Tong²⁵, transistor T1 is used as a switch. Potentiometer P2, which supplies part of the negative voltage of the battery to the emitter of the transistor, is essentially a "coherence" control. The quench waveform used was simply a 10 Kc/s sine wave from an AF signal generator: however variations of the amplitude of this sine wave, and of the bias on the transistor emitter, permitted a degree of control of t_{OFF} (section 2.3). This circuit is mounted separately from the RF side, which is completely shielded. The output filter is also separately mounted.

3.14 Auxiliary equipment

When originally built, the oscillator was intended for oscilloscope display of suitable nuclear quadrupole lines where possible. Although this aspect of the work was not carried very far, a circuit was built and tested which was found to act very satisfactorily in amplifying a sawtooth repetitive sweep from the x-output of the oscilloscope and applying it, by way of a cathode follower, to the voltage-variable capacitor C4 (figure 3.13). Figure 3.14 gives the circuit diagram for this unit (page 164), which is built into the same chassis as the oscillator.

For recorder display, the DC bias for the frequency-sweep

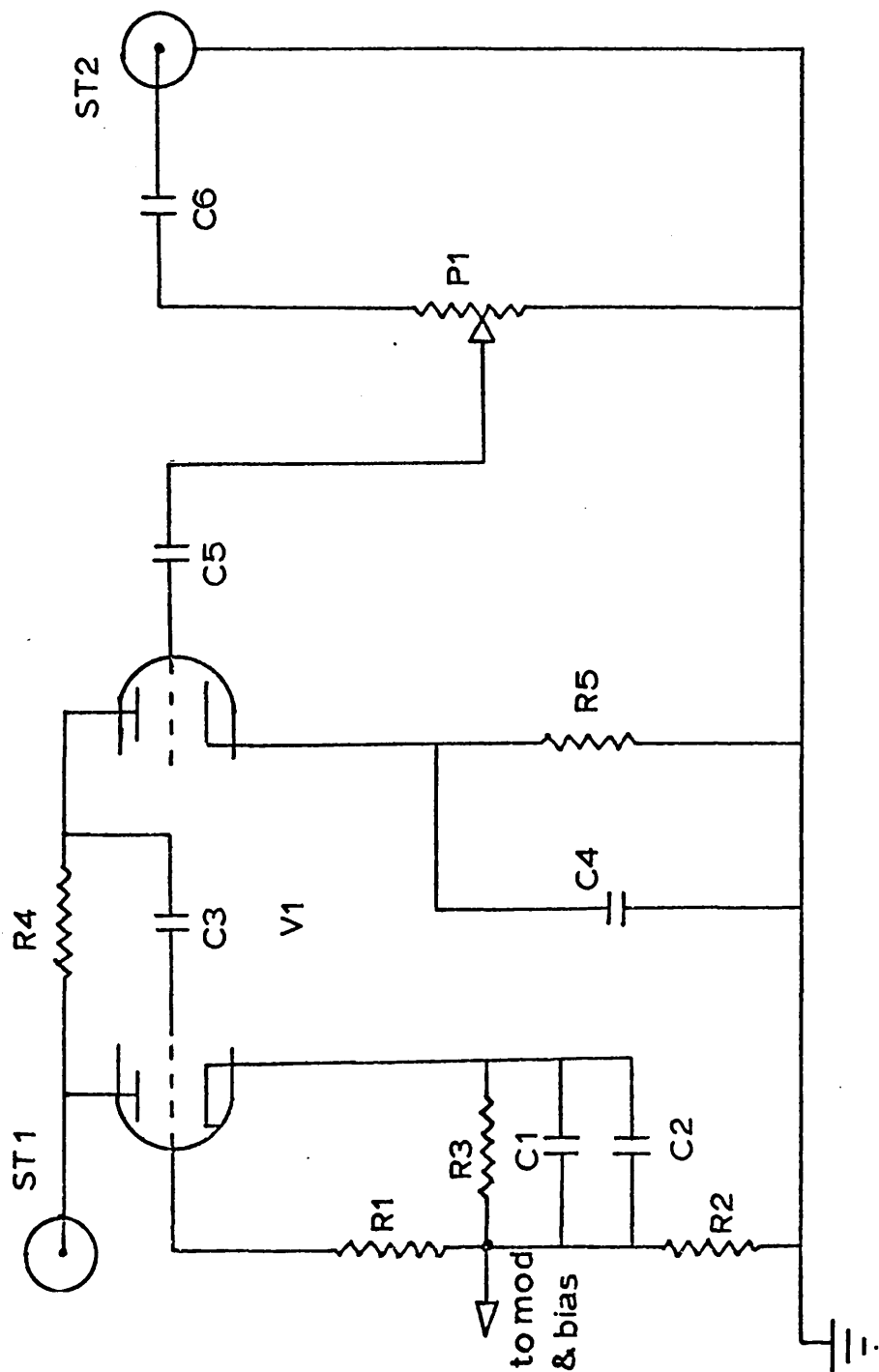


Figure 3.14. Amplifier and cathode follower for repetitive sweep.

Key to figure 3.14: amplifier and cathode follower for repetitive sweep

Capacitors

All capacitances are in μF .

C1 125	C3 0.5	C5 0.5
C2 125	C4 250	C6 0.5

Potentiometer and resistors

All resistances are in Ω .

P1 5M	R2 100K	R4 150K
R1 1M	R3 10K	R5 3.3K

Valve

V1 12AT7

Sockets

ST1 HT + 250V	ST2 sawtooth input
---------------	--------------------

method discussed above was derived from a modulation and bias unit like that shown in figure 3.6, except that the values of R3 and P3 of figure 3.6 were modified to provide suitable DC levels for the different Hughes diode employed here, and that R1, R2, P1 and P2 in that figure were dispensed with for the sake of simplicity, while one end of P3 was connected to earth. It is worth noting that with readily available values for the ten-turn helical potentiometer (up to 50K), R3 and P3 would carry a considerable current, and care needs to be taken to avoid excessive load on these components. The modulation signal, at 310 c/s, derived ultimately from another signal generator, is mixed with the DC level in this unit and led to the Hughes diode, as in the marginal oscillator.

In the work with the super-regenerative oscillator, a Brookdeal lock-in amplifier and phase-sensitive detector system was used instead of the units described in sections 3.7, 3.8 and 3.9. The phase-shift unit (section 3.6) was still used, but merely as an amplifier and divider to supply the modulation, and the reference for the lock-in detector.

3.15 Conclusions

As was true for the marginal oscillator, the sensitivity of the super-regenerative oscillator can be tested by passing a small test signal, from an RF signal generator, through a near the sample coil of the oscillator. This procedure, described

in full in section 3.10 (1), gave a very strong signal indeed for a $5\ \mu\text{V}$ signal through the test coil. In spite of the large number of sideband responses, the signal-to-noise ratio was high: around 50:1. This is a relatively much stronger signal than could be obtained from the marginal oscillator. The signal from hexamethylenetetramine, showing the characteristic alternate inversion of an NQR signal from a super-regenerative oscillator, was also observed. However, the setting-up of the system was still a rather uncertain procedure, with the best control settings changing very much with changing frequency, and it is felt that the instrument would be difficult to use in a search for an unknown resonance.

Experiences with NQR spectrometers over three years have been disappointing. With all the many modifications tried, using both the marginal oscillator and several types of super-regenerative oscillator, a number of conclusions emerge.

1. Attention to lay-out and wiring principles for the RF side is particularly important in attempts to detect ^{14}N signals. A modification of the wiring between sample coil and the rest of the tank circuit can produce a tenfold improvement in spectrometer sensitivity.

2. Oscillators which have given good results with ^{35}Cl NQR do not necessarily give good results for ^{14}N on a simple change of their operating frequency and of operating parameters

such as quench frequency.

3. In spite of the theoretically simpler operation of a marginal oscillator, it seems that future work on ^{14}N NQR spectroscopy should concentrate on the development of the super-regenerative oscillator, which is capable of greater sensitivity, and which by the nature of its operation reduces the nuisance of over-critical setting of operating conditions. It is clear that the simple type of super-regenerative oscillator system described here will not do as it stands. If the drawbacks of multiple response and variable sensitivity could be overcome at the radio-frequencies needed for the study of ^{14}N NQR, there is a possibility of NQR becoming a feasible almost-routine technique, as NMR and ESR are now. Systems of sideband suppression, automatic gain stabilisation, and automatic, reasonably reliable, frequency measurement are needed. Tong²⁵ has described such a set of techniques to be applied to ^{35}Cl NQR studies, and his methods and circuits may be adaptable to ^{14}N NQR. Unfortunately the author became aware of Tong's work only near the end of the experimental work described in this thesis, and time did not permit a serious attempt at using these new results for ^{14}N NQR. Some of the more obvious changes which suggested themselves were included, and results seem to show that these changes were at least in the right direction.

1. A. Abragam, "The Principles of Nuclear Magnetism", Oxford University Press, Oxford, 1961.
2. D.J. Barnes, J. Sci. Instr., 1963, 40, 507.
3. S. Britz and S. Hacobian, Austr. J. Chem., 1967, 20, 2047.
4. P.A. Casabella, Dissertation Abstr., 1959, 20, 1397.
5. P.A. Casabella and P.J. Bray, J. Chem. Phys., 1958, 29, 1105.
6. T.P. Das and E.L. Hahn, "Nuclear Quadrupole Resonance Spectroscopy", Solid State Physics, supp. 1 (eds. Seitz and Turnbull), Academic Press, 1958.
7. C. Dean, Thesis, Harvard, 1952; Phys. Rev., 1954, 96, 1053.
8. C. Dean, Rev. Sci. Instr., 1960, 31, 934.
9. C.H. Dutcher, jr., M.Sc. thesis, University of Florida, 1961.
10. C.H. Dutcher, jr., and T.A. Scott, Rev. Sci. Instr., 1961, 32, 457.
11. A.R. Edmonds, "Angular Momentum in Quantum Mechanics", Princeton University Press, Princeton, N.J., 1957.
12. S. Fallieros and R.A. Ferrell, Phys. Rev., 1959, 116, 660.
13. A.I. Kitaigorodski and K.V. Mirskaya, Kristallografiya, 1965, 10, 162.
14. S. Kojima, M. Minematsu and M. Tanaka, J. Chem. Phys., 1959, 31, 271.
15. H. Kruger, Z. Physik, 1951, 129, 401; 1951, 130, 371.
16. J.M. Lehn and M. Franck-Neumann, J. Chem. Phys., 1965, 43, 1421.

17. M. Minematsu, J. Phys. Soc. Japan, 1959, 14, 1030.
18. L.N. Mulay, "An Improved NMR Apparatus and Study of Sandwich Compounds, Etc.", Harvard University, 1957.
19. G.E. Pake, "Nuclear Magnetic Resonance", Solid State Physics, (eds. Seitz and Turnbull), 1956, 2, 24, Academic Press, 1956.
20. R.V. Pound and W.D.Knight, Rev. Sci. Instr., 1950, 21, 219.
21. A. Roberts, Rev. Sci. Instr., 1947, 18, 845.
22. F.N.H. Robinson, J. Sci. Instr., 1959, 36, 481.
23. L.I. Schiff, "Quantum Mechanics", McGraw-Hill Book Co. Inc., New York, 1955.
24. C.P. Slichter, "Principles of Magnetic Resonance", Harper & Row, New York, 1963.
25. D.A. Tong, Ph.D. Thesis, Leeds, 1965.
26. W.N. Tuttle, Proc. Inst. Radio Engineers, 1940, 23.
27. R. Wallace, Ph.D. Thesis, Glasgow, 1964.
28. G.D. Watkins and R.V. Pound, Phys. Rev., 1952, 85, 1062.
29. K.E. Weber and J.E. Todd, Rev. Sci. Instr., 1962, 33, 390.
30. J.R. Whitehead, "Super-regenerative Receivers", Cambridge University Press, Cambridge, 1950.

In Part B, nuclear quadrupole resonance (NQR) spectroscopy is introduced, and quadrupole resonance is treated theoretically, with special reference to the ^{14}N nucleus. A description is given of the two main types of instrument used to detect NQR: the marginal oscillator and the super-regenerative oscillator. Modulation is discussed.

Two complete spectrometer systems for detection of ^{14}N NQR have been designed and constructed, and details of these systems are given. The first system uses a marginal oscillator; the second uses a super-regenerative oscillator which is externally quenched.

PART C

CHEMICAL APPLICATIONS OF NUCLEAR QUADRUPOLE RESONANCE

1.1 Introduction

It has been shown in Part B (section 1.3) that a nucleus for which $I = 1$ has three pure NQR transition frequencies, given by (equation 1.3.6 of Part B):

$$\begin{aligned} \nu_1 &= (3 + \eta) eQq/4 \\ \nu_2 &= (3 - \eta) eQq/4 \\ \nu_3 &= \eta eQq/2 \end{aligned} \quad 1.1.1$$

These frequencies ν_i depend on a nuclear quantity Q , which for one nucleus is invariant from one situation to another, and two independent parameters q and η , which are related to the charge distribution around the nucleus. As explained in Part B, section 1.2, q and η are defined by:

$$\begin{aligned} q &= V_{ZZ} \\ \eta &= (V_{XX} - V_{YY})/V_{ZZ} \end{aligned} \quad 1.1.2$$

where X , Y , and Z represent the principal axes of the field-gradient tensor V_{AB} : this tensor will be represented with respect to a set of axes, x , y , z , defined later, as $V_{\alpha\beta}$.

At the outset, the contributions to $V_{\alpha\beta}$ may be divided into two groups:

- (a) intramolecular contributions
- and (b) intermolecular contributions.

It will be convenient to consider separately, modifications to

the contributions from each of these groups from

(c) temperature-dependent effects.

1.2 Intramolecular contributions: introduction

Intramolecular contributions are dominant in the gas phase: the arguments of this chapter, along with a consideration of the temperature-dependent effects described in chapter 2 should account for observed nuclear quadrupole coupling constants obtained from microwave spectroscopy.

The origin of the system to which the field gradient tensor $V_{\alpha\beta}$ is to be referred is taken to be the ^{14}N nucleus under discussion: to maintain generality, and to avoid confusion with chemical symbols, this nucleus will be represented by A, and the nuclei of other atoms in the molecule by B,C... . The orientation of the axes is most conveniently defined with respect to these nuclei. In compounds of interest in this thesis, nitrogen (A) has no more than three bonds. If all three bonds are directed to the same second atom B (i.e. $\text{A}\equiv\text{B}$), the z axis is defined in the direction AB: it is not usually necessary to define the x and y axes. If two bonds are directed to one atom B and the third to C ($\text{B}=\text{A}-\text{C}$) the z axis is defined in the direction AB as before, and the plane BAC is defined as the yz plane (BAC cannot be collinear). If all three bonds are directed to three different atoms ($\text{B}-\text{A}-\overset{\text{C}}{\text{D}}$), then again the AB direction is made the z axis, and the plane BAC is

defined as the yz plane (A, B, C and D cannot be coplanar).

The field gradient tensor $V_{\alpha\beta}$ due solely to intramolecular effects is given by:

$$V_{\alpha\beta} = \int \psi_t^* \bar{V}_{\alpha\beta t} \psi_t d\tau \quad 1.2.1$$

where ψ_t is a function describing the total charge distribution in the isolated molecule. $\bar{V}_{\alpha\beta t}$ is the operator:

$$\bar{V}_{\alpha\beta t} = \sum_i q_i \frac{3\alpha_i\beta_i - r_i^2\delta_{\alpha\beta}}{r_i^5} \quad 1.2.2$$

where the sum is over all the charges in the molecule except nucleus A, and the charge q_i has Cartesian co-ordinates $\alpha_i, \beta_i \dots$

This notation is used throughout Part C. $\delta_{\alpha\beta}$ is written for $\delta_{\alpha_i\beta_i}$, and $r_i^2 = x_i^2 + y_i^2 + z_i^2$.

To ascertain ψ_t for molecules of any size is well known to be impossibly difficult, and a number of approximations must be made, the more important of which in the initial analysis will be noted explicitly. Some of the approximations will be allowed to stand; others will be modified, for the sake of convenience in later sections. This procedure is itself obviously not rigorous.

In the Born-Oppenheimer approximation, the nuclei are treated separately and are considered to be fixed: the part of ψ_t describing the nuclei is evaluated separately. Thus equation 1.2.1 becomes:

$$V_{\alpha\beta} = \int \psi_e^* \bar{V}_{\alpha\beta} \psi_e d\tau + e \sum_{k=1}^K Z_k \left[\frac{3\alpha_k\beta_k - r_k^2\delta_{\alpha\beta}}{r_k^5} \right] \quad 1.2.3$$

The sum is over the K nuclei other than nucleus A. $\bar{V}_{\alpha\beta}$ now refers to the electrons only, and e is the magnitude of the electronic charge. ψ_e is the function describing the electron distribution, and further approximations concern only this function.

The most suitable perfectly general function ψ_e is a sum of Slater's determinants:^{146,198,201}

$$\psi_e = (N!)^{-\frac{1}{2}} \sum c(k,1,\dots,v) \det \{ \varphi_k(1) \varphi_1(2) \dots \varphi_v(n) \} \quad 1.2.4$$

where, for example, $\varphi_k(1)$ is the kth function for electron 1, and the sum is over all chosen configurations, the number of which may be large (section 1.7). In practice, the function given by equation 1.2.4 is too complex to evaluate for any but very simple systems. The usual simplification is the rather drastic, although to some extent theoretically justifiable⁴⁰, one of taking only one determinant in the sum of equation 1.2.4. This amounts to ignoring configuration interaction. Electron correlation effects are notoriously neglected in simple molecular-orbital (MO) descriptions⁴⁷, for example. Compensation can, however, be attempted later (section 1.7) in other ways, for instance by using correlated wave functions^{145,194}. Adopting this simplification, of using only one Slater determinant, gives for the integral of equation 1.2.3:

$$\int \psi_e^* \bar{V}_{\alpha\beta} \psi_e d\tau = \sum_{i=1}^n \int \varphi_i^* (q_{\alpha\beta})_i \varphi_i d\tau = \bar{V}_{\alpha\beta e} \quad 1.2.5$$

$$\text{where } (q_{\alpha\beta})_i = -e \left[\frac{3\alpha_i \beta_i - \delta_{\alpha\beta} r_i^2}{r_i^5} \right] \quad 1.2.6$$

the sum is over the n electrons, and the φ_i are one-electron molecular orbitals, which are taken as usual to be orthogonal. They are not in general the $\varphi_k(1)...$ of equation 1.2.4.

In writing expressions for the φ_i , the third approximation, the LCAO approximation, can be used:

$$\varphi_i = \sum_{j=1;J}^{m_i} c_{ij} \chi_j(J) \quad 1.2.7$$

where $\chi_j(J)$ is an atomic orbital centred on nucleus J , one of the molecule's $K+1$ nuclei. If, as is usual, the φ_i of equation 1.2.7 are the space-parts of the molecular orbitals, a fourth approximation is implied: spin-spin and spin-orbit interactions are neglected. Then the n electrons, in a molecule of $^1\Sigma$ ground state, can be arranged in coupled-spin pairs, occupying the $v = n/2$ molecular levels of lowest energy (but see section 1.7).

Before using equation 1.2.7 in equation 1.2.5, it is helpful to consider the forms the φ_i might take. Experience from both MO calculations^{47,151,185}, and from chemical and spectroscopic properties, indicate that only very rarely are all orbitals on all $K+1$ nuclei important in describing the molecular orbitals. The fifth approximation is to divide the φ_i into orbitals centred mostly on one nucleus (one-centre) and those centred on some group of nuclei (multicentre).

If one-centre orbitals on nucleus J are denoted by $\varphi_i^{(1)}(J)$:

$$\varphi_i^{(1)}(J) = \sum_j c_{ij} \chi_j(J) \quad (J \text{ constant}) \quad 1.2.8$$

Some of the $\varphi_i^{(1)}$ may in fact be adequately represented by an unchanged, or little-changed, atomic orbital $\chi_j(J)$. If multi-centre φ_i are indicated by $\varphi_i^{(m)}$, equation 1.2.5 becomes, since the φ_i are now two-electron* functions:

$$\begin{aligned} v_{\alpha\beta e} &= 2 \sum_{i=1}^{v_1} \int \varphi_i^{(1)*}(J) (q_{\alpha\beta})_i \varphi_i^{(1)}(J) d\tau + 2 \sum_{i=v_1+1}^v \int \varphi_i^{(m)*}(q_{\alpha\beta})_i \varphi_i^{(m)} d\tau \\ &= q_{\alpha\beta}^{(1)} + q_{\alpha\beta}^{(m)} \quad \text{say,} \end{aligned} \quad 1.2.9$$

where v_1 is the number of one-centre orbitals, and v as before is the total number of molecular orbitals. Substituting for $\varphi_i^{(1)}(J)$, using equation 1.2.8, in the first term of equation 1.2.9, gives for $q_{\alpha\beta}^{(1)}$:

$$\begin{aligned} q_{\alpha\beta}^{(1)} &= 2 \sum_{i=1}^{v_1} \left[\sum_{j=1}^{m_i} c_{ij}^2 \int \chi_j^*(J) (q_{\alpha\beta})_i \chi_j(J) d\tau \right. \\ &\quad \left. + 2 \sum_{j \neq k}^{m_i} c_{ij} c_{ik} \int \chi_j^*(J) (q_{\alpha\beta})_i \chi_k(J) d\tau \right] \end{aligned} \quad 1.2.10$$

where J is constant.

Using expression 1.2.7 for $q_{\alpha\beta}^{(m)}$ gives, similarly:

$$\begin{aligned} q_{\alpha\beta}^{(m)} &= 2 \sum_{i=v_1+1}^v \left[\sum_{j=1}^{m_i} c_{ij}^2 \int \chi_j^*(J) (q_{\alpha\beta})_i \chi_j(J) d\tau \right. \\ &\quad \left. + 2 \sum_{j \neq k}^{m_i} c_{ij} c_{ik} \int \chi_j^*(J) (q_{\alpha\beta})_i \chi_k(J') d\tau \right] \end{aligned} \quad 1.2.11$$

where $J \neq J'$.

* (i.e. there are 2 electrons with the same orbital φ_i)

The operator $(q_{\alpha\beta})_i$ is, like the co-ordinate system, centred on A. The matrix elements in equation 1.2.10 are of two types: one-centre ($J \equiv A$) and symmetrical two-centre ($J \neq A$). The m_i terms of the first sum in the square brackets of equation 1.2.11 are exactly like the terms of equation 1.2.10: like them, they may be one-centre or two-centre. The $m_i(m_i-1)$ terms of the second sum are unsymmetrical two-centre ($J \equiv A \neq J'$, or $J \neq A \equiv J'$), or three-centre ($J \neq A \neq J'$).

1.3 Application to nitrogen-containing compounds

Equations 1.2.9, 1.2.10 and 1.2.11 can now be applied to the particular case of a nitrogen-containing molecule. The various integrals defined above derive from various types of orbitals, and it is useful in evaluating these integrals, and in finding the c_{ij} , to list here a classification scheme for the φ_i . The full classification to be used is:

1. One-centre orbitals:
 - (a) those little changed from an atomic orbital $\chi_j(J)$
 - (i) those centred on A
 - (ii) those not centred on A
 - (b) those consisting of combinations of atomic orbitals $\chi_j(J)$
 - (i) those centred on A
 - (ii) those not centred on A
2. Multicentre orbitals:
 - (a) those one of whose centres is A

(b) those none of whose centres is A.

It has been extensively demonstrated that orbitals in class 1(a) are those corresponding to the closed-shell atomic orbitals underlying the valence orbitals, for first row elements the 1s orbital. This sixth approximation is particularly good for first-row elements, with whose compounds this Part is mainly concerned. If the 1s atomic orbital on nucleus J is represented by $\chi_{1s}(J)$ then orbitals of type 1(a) contribute, from equation 1.2.10:

$$q_{\alpha\beta}^{1s} = 2 \int \chi_{1s}(A) q_{\alpha\beta} \chi_{1s}(A) d\tau + 2 \sum_{J \neq A} \int \chi_{1s}(J) q_{\alpha\beta} \chi_{1s}(J) d\tau \quad 1.3.1$$

if from now onwards it is assumed that the atomic orbitals are real (see section 1.8), to the tensor $V_{\alpha\beta e}$. For clarity, the electronic suffix i may now be dropped, and $q_{\alpha\beta}$ be taken to refer to the electrons in the orbital on which it operates only.

Orbitals of types 1(b) and 2 may best be considered together, since type 1(b) orbitals may be regarded as hybridised orbitals which do not overlap with orbitals on other atoms. For nitrogen, and for all first-row elements, only the 2s and 2p atomic orbitals are important in the formation of hybrids: this assumption constitutes the seventh approximation.

If the only restrictions on the hybridised atomic orbitals are the very general ones of orthogonality and normalisation,

a quite general set of fourteen, not linearly independent, simultaneous equations in thirteen unknowns may be written, using the co-ordinate system conventions given earlier. Details of the solving of these equations need not be given here. The results obtained by the author were:

$$\begin{aligned} h_1(A) &= a_1s + a_6p_z \\ h_2(A) &= a_2s - (a_1a_2/a_6)p_z + (a_5/a_6)p_y \\ h_3(A) &= a_3s - (a_1a_3/a_6)p_z - (a_2a_3/a_5a_6)p_y + (a_4/a_5)p_x \\ h_4(A) &= a_4s - (a_1a_4/a_6)p_z - (a_2a_4/a_5a_6)p_y - (a_3/a_5)p_x \end{aligned} \quad 1.3.2$$

The h_j are the hybrid orbitals on A. The hybrid orbitals on B,C..., other first-row elements are formally identical with a corresponding choice of co-ordinate system, and the convention that the coefficients a_j are replaced by $b_j, c_j \dots$. For convenience, $\chi_{2s}(A)$ and $\chi_{2p}(A)$ etc. are written s and p , etc. a_1, a_2 and a_3 may be chosen freely so far as the mathematics is concerned; as will be shown, physical considerations often indicate the best choice for them. The other a_j are dependent on the first three as follows:

$$\begin{aligned} a_4 &= (1 - a_1^2 - a_2^2 - a_3^2)^{\frac{1}{2}} \\ a_5 &= (1 - a_1^2 - a_2^2)^{\frac{1}{2}} \\ a_6 &= (1 - a_1^2)^{\frac{1}{2}} \end{aligned} \quad 1.3.3$$

If a_1, a_2 and a_3 are all nonzero, equations 1.3.2 describe sp^3 hybridisation. If $a_3 = 0$, the hybridisation is $sp_y p_z$, and if in addition $a_2 = 0$, the hybridisation is sp_z . If

$a_1 = a_2 = a_3 = 0$, there is no hybridisation, and it is likely^{47,198} that this situation never occurs.

The multicentre orbitals, on A and B and perhaps on centres E, F ... in addition, can now be dealt with. In accordance with the fourth approximation, page 177, only the orbital of lowest energy in each set is considered. Like all the orbitals in its set, φ_1 has the form:

$$\varphi_1(\text{ABE}...) = \alpha_1\varphi_1(\text{A}) + \beta_1\varphi_1(\text{B}) + \epsilon_1\varphi_1(\text{E}) + \dots \quad (m_1 \text{ centres}) \quad 1.3.4$$

where $\varphi_1(\text{ABE}...)$ involves at least h_1 on A and one orbital on B.

There are two other possible multicentre orbitals with one centre on A:

$$\varphi_2(\text{ACF}...) = \alpha_2\varphi_2(\text{A}) + \gamma_2\varphi_2(\text{C}) + \zeta_2\varphi_2(\text{F}) + \dots \quad (m_2 \text{ centres}) \quad 1.3.5$$

$$\varphi_3(\text{ADG}...) = \alpha_3\varphi_3(\text{A}) + \delta_3\varphi_3(\text{D}) + \eta_3\varphi_3(\text{G}) + \dots \quad (m_3 \text{ centres}) \quad 1.3.6$$

as well as a number of molecular orbitals with no centre on A.

These last, $\varphi_j(\text{JJ}'...)$ say, have the form:

$$\varphi_j(\text{JJ}'...) = \sum_{J \neq A}'' \kappa_j \varphi_j(J) \quad (m_j \text{ centres}) \quad 1.3.7$$

where the double-primed summation is restricted to those κ_j not used for $\varphi_1(\text{ABE}...)$, $\varphi_2(\text{ACF}...)$ or $\varphi_3(\text{ADG}...)$.

There is, finally, the orbital $h_4(\text{A})$ (equation 1.3.2) which by convention is not used in molecular bonding orbitals.

Combining the contributions from the multicentre orbitals (equations 1.3.4, 1.3.5, 1.3.6, 1.3.7) gives for $q_{\alpha\beta}^{(m)}$, using equations 1.2.9 and 1.2.11:

$$\begin{aligned}
 \frac{1}{2}q_{\alpha\beta}^{(m)} &= \alpha_1^2 (\varphi_1(A) | q_{\alpha\beta} | \varphi_1(A)) + \beta_1^2 (\varphi_1(B) | q_{\alpha\beta} | \varphi_1(B)) + \dots \\
 &\quad (m_1 \text{ diagonal terms}) \\
 &+ 2\alpha_1\beta_1 (\varphi_1(A) | q_{\alpha\beta} | \varphi_1(B)) + 2\alpha_1\varepsilon_1 (\varphi_1(A) | q_{\alpha\beta} | \varphi_1(E)) + \dots \\
 &\quad (\frac{1}{2}m_1(m_1-1) \text{ cross terms}) \\
 &+ (\text{similar terms from } \varphi_2 \text{ and } \varphi_3) \\
 &+ \sum_{j; j \neq A}'' \kappa_j^2 (\varphi_j(J) | q_{\alpha\beta} | \varphi_j(J)) \\
 &+ \sum_{j,k; j \neq j' \neq A}'' \kappa_j \kappa_k (\varphi_j(J) | q_{\alpha\beta} | \varphi_k(J'))
 \end{aligned} \tag{1.3.8}$$

where now a type of bra-ket notation is adopted for the integrals.

The contribution from $h_4(A)$ is the one-centre integral:

$$q_{\alpha\beta}^{(1)h} = 2(h_4 | q_{\alpha\beta} | h_4) \tag{1.3.9}$$

Finally, there may be one-centre hybrid orbitals on nuclei other than A. Their contribution $q_{\alpha\beta}^{(1)h'}$ to the field gradient at A is:

$$q_{\alpha\beta}^{(1)h'} = 2 \sum_{j \neq A}^{j=1,2,3} (h_j(J) | q_{\alpha\beta} | h_j(J)) \tag{1.3.10}$$

The orbital components $\varphi_j(A)$ are by convention the $h_j(A)$ of equation 1.3.2. The orbital components $\varphi_j(J)$, $J \neq A$, may also be described by sets of equations like equations 1.3.2, provided a suitable choice of axes is made, and provided J is a first-row nucleus. This leaves undecided the choices of b_j , c_j ... in such equations.

All the results of sections 1.2 and 1.3 may now be combined.

Then:

equation 1.3.11

$$\begin{aligned}
 & V_{\alpha\beta} = e \sum_{k=1}^K z_k \left[\frac{3\alpha_k \beta_k - r_k^2 \delta_{\alpha\beta}}{r_k^5} \right] \quad \text{from nuclei (eqn. 1.2.3)} \\
 \text{I:} & \\
 \text{II:} & + 2(\chi_{1s}(A) | q_{\alpha\beta} | \chi_{1s}(A)) \quad \text{unchanged orbital on A (1ai; 1.3.1)} \\
 \text{III:} & + 2 \sum_{J \neq A} (\chi_{1s}(J) | q_{\alpha\beta} | \chi_{1s}(J)) \quad \text{unchanged orbitals not on A (1aii; 1.3.1)} \\
 \text{IV:} & + 2(h_4(A) | q_{\alpha\beta} | h_4(A)) \quad \text{one-centre orbital on A (1bi; 1.3.9)} \\
 \text{V:} & + 2 \sum_{J \neq A}^{j=1,3,2} (h_j(J) | q_{\alpha\beta} | h_j(J)) \quad \text{one-centre orbitals not on A (1bii; 1.3.10)} \\
 \text{VI:} & + 2 \sum_{j=1}^3 \alpha_j^2 (h_j(A) | q_{\alpha\beta} | h_j(A)) \quad \text{diagonal terms, } \phi_1(ABE\dots) \text{ etc. (2a; 1.3.8)} \\
 \text{VII:} & + 2 \sum'_{j; J \neq A} \kappa_j^2 (h_j(J) | q_{\alpha\beta} | h_j(J)) \quad \text{diagonal terms, including those from } \phi_1(ABE\dots) \text{ etc., which do not involve A (2a, 2b; 1.3.8)} \\
 \text{VIII:} & + 4\alpha_1 [\beta_1 (h_1(B) | q_{\alpha\beta} | h_1(A)) + \epsilon_1 (h_1(E) | q_{\alpha\beta} | h_1(A)) + \dots] \quad \begin{array}{l} (m_1 - 1 \text{ terms}) \\ \text{off-diagonal terms involving A, from } \phi_1(ABE\dots) \end{array} \quad (2a; 1.3.8) \\
 \text{IX:} & + 4\alpha_2 [\gamma_2 (h_2(C) | q_{\alpha\beta} | h_2(A)) + \zeta_2 (h_2(F) | q_{\alpha\beta} | h_2(A)) + \dots] \quad \begin{array}{l} (m_2 - 1 \text{ terms}) \\ \text{off-diagonal terms involving A, from } \phi_2(ACF\dots) \end{array} \quad (2a; 1.3.8) \\
 \text{X:} & + 4\alpha_3 [\delta_3 (h_3(D) | q_{\alpha\beta} | h_3(A)) + \eta_3 (h_3(G) | q_{\alpha\beta} | h_3(A)) + \dots] \quad \begin{array}{l} (m_3 - 1 \text{ terms}) \\ \text{off-diagonal terms involving A, from } \phi_3(ADG\dots) \end{array} \quad (2a; 1.3.8) \\
 \text{XI:} & + \sum'_{j; J \neq J', \neq A} \kappa_j \kappa_{j'} (h_j(J) | q_{\alpha\beta} | h_{j'}(J')) \quad \begin{array}{l} \text{off-diagonal terms from orbitals with no centre on A} \\ (2a, 2b; 1.3.3) \end{array}
 \end{aligned}$$

Equation 1.3.11 is in fact a form of equation 1.2.3, with some of the terms written out explicitly. In terms VII and XI of equation 1.3.11, the primed summation implies exclusion of the α_j only, and the two-centre integrals, both from molecular orbitals with one centre on A, and from those with no centre on A, have been combined; they are separated in equation 1.3.8. Exactly analogous remarks apply to the three-centre integrals of term XI.

If it is supposed that the co-ordinates α_k of the nuclei are known, there remain four general problems before the right-hand side of equation 1.3.11 can be evaluated. These concern:

- (i) finding the best values for the "atomic" coefficients k_j , as in equation 1.3.2. The use of these coefficients is implied by the use of the $h_j(A)$ in equation 1.3.11, and by the remarks about the $\phi_j(J)$ made on page 183.
- (ii) finding the best values for the "molecular" coefficients κ_j .
- (iii) choosing suitable atomic wave functions $\chi_j(J)$ for equations 1.3.11 and 1.3.2.
- (iv) evaluating the integrals of equation 1.3.11.

Before these are dealt with in turn, the possibilities of simplifying equation 1.3.11 will be considered.

1.4 Simplification of the more general equation

The most widely-used modification of equation 1.3.11 is

due basically to Townes and Dailey^{234,235} with some adaptations and further interpretations.^{58,65}

This modification first takes all three-centre integrals (term XI) and all off-diagonal two-centre integrals (terms VIII, IX and X) to be zero. The diagonal two-centre integrals (terms III, V and VII), together with the nuclear term I, are taken to be zero. This is because term I is opposite in sign, and about equal in magnitude, to the sum of terms III, V and VII. If $\chi_{1s}(A)$ is a one-term spherically symmetric Slater atomic orbital, term II is zero too.

This rather drastic pruning leaves only terms IV and VI of equation 1.3.11. These two terms are identical in form. If it is assumed that χ_{2s} , like χ_{1s} , is spherically symmetric, then equation 1.3.2 and the remaining terms of equation 1.3.11, give:

$$\begin{aligned} \frac{1}{2}V_{\alpha\beta} = & (p_z | q_{\alpha\beta} | p_z) (\alpha_1^2 a_6^2 + (a_1^2/a_6^2) \sum_{j=2}^4 \alpha_j^2 a_j^2) \\ & + (p_y | q_{\alpha\beta} | p_y) (\alpha_2^2 a_5^2 + (a_2^2/a_5^2 a_6^2) \sum_{j=3}^4 \alpha_j^2 a_j^2) \\ & + (p_x | q_{\alpha\beta} | p_x) (\alpha_3^2 a_4^2/a_5^2 + \alpha_4^2 a_3^2/a_5^2) \end{aligned} \quad 1.4.1$$

If Slater-type p_α functions are used, it can be shown that, for conditions of symmetry often encountered or assumed, all off-diagonal matrix elements of $q_{\alpha\beta}$ are zero. Furthermore, for these functions,

$$(p_\alpha | q_{\alpha\alpha} | p_\alpha) = -\frac{1}{2}(p_\beta | q_{\alpha\alpha} | p_\beta) \quad \alpha \neq \beta \quad 1.4.2$$

Thus, if the α_j and a_j are known, q and η (equation 1.1.2) can be calculated, since now the tensor is diagonalised, and $A = \alpha$. The problems of putting a value on the nuclear quadrupole moment Q , and of choosing good atomic wave-functions p_α , are avoided, and the error in assuming χ_{1s} and χ_{2s} to be spherically symmetric (section 1.7) is to some extent corrected, by defining $q_{at} = (p_\alpha | q_{\alpha\alpha} | p_\alpha)$, and by calculating not the absolute values of $eQV_{\alpha\alpha}$, but the ratios $eQV_{\alpha\alpha}/eqq_{at}$. The parameter eqq_{at} is interpreted as the coupling constant per electron in the free atom. For ^{14}N , with an approximately spherically symmetric ground state, this quantity is of course hypothetical. The value used is around 10 Mc/s.

Used in conjunction with assumptions, some more reasonable than others, about bonding in the molecule, the theory of Townes and Dailey has been very widely used to interpret NQR data for halogen-containing molecules, and to a lesser extent and rather less successfully, for nitrogen-containing molecules^{e.g. 2, 121, 148, 202}. The main difficulties in using the Townes and Dailey treatment are the same as the difficulties which will be met in the more extended arguments given later: one, or perhaps two, experimental figures arise from a much larger number of parameters, the κ_j and k_j of section 1.3 expressed in various ways, which must be evaluated by some means independent of nuclear quadrupole interactions; and a good choice of

atomic and molecular wave functions is crucial.

These considerable difficulties have hitherto impeded the widespread application of NQR results to structural and other chemical problems. It must be considered whether a reasonably accurate, perhaps semi-empirical, approach to the interpretation of NQR is possible, which would correspond perhaps to the use of NMR in general organic chemistry. The general problems listed at the end of section 1.3 will now be considered.

1.5 The "atomic" coefficients

The choice of the coefficients a_j is the well-known problem of determining the hybridisation of an atom in a molecule. Equation 1.3.2 is a general form for four hybrid orbitals: in its derivation, the conditions of orthogonality, normality and "complete use" of the component orbitals were assumed to hold. Although orthogonality may not be strictly necessary³⁸ recent analyses, of considerable complexity and subtlety,^{4,34,59} of the concept of hybridisation have seemed to show that many of the simple ideas are quite adequate for all normal chemical purposes in describing a bond. In particular, a recent study of the N_2 molecule²¹⁶, using density difference functions, has attempted to determine "a more general definition of hybridisation in a molecule". The results of the various molecular orbital treatments give good support for the concept of hybridisation, and confirm that the physical assumptions implied

by the use of equations like 1.3.2 are reasonably good.

The simplest way of measuring hybridisation is when the parameters a_j and a_k , for example, for the hybrid orbitals h_j and h_k (on nucleus A) can be related to the molecular angle $JAK \equiv \vartheta_{jk}$, where h_j is used for the bonding to J and h_k for the bonding to K. Then,

$$\cos \vartheta_{jk} = -a_j a_k / [(1 - a_j^2)(1 - a_k^2)]^{1/2} \quad (j, k = 1 \dots 4) \quad 1.5.1$$

Similar equations, of course, apply to angles centred on the nuclei B, C ... subject to the conventions already used. An element like carbon, which uses all its valence electrons in bonding orbitals, i.e. no lone pairs, is at the vertex of six such angles, five of which are geometrically independent. Physically, of course, no more than three of the angles can be arbitrarily fixed, since sp^3 hybridisation allows only three independent variables (equation 1.3.2). If three of the molecular angles can be measured, then equations of the form of equation 1.5.1 can be solved to give these three independent variables.

An atom like nitrogen, nucleus A, has normally one lone pair, and so is at the vertex of three, mutually independent, angles. If these three angles can be measured, then again equations 1.5.1 will determine the a_j . A group VI atom, oxygen for example, generally forms two bonds and is at the vertex of only one angle, so that only one of the variables is eliminated and this method cannot be used. For the halogens, which as a rule

form but one bond, there is no measurable interorbital angle, and again the geometrical method has no application.

Even for group IV and group V elements, this method of determining the hybridisation parameters depends on the validity of equation 1.5.1, and the equation holds only if for instance the bonding orbital between A and J, say, is directed along the line AJ. This simple picture may not be adequate for two principal, and related, reasons. First, the bonding of A, J and K may best be described not by two bonds A-J and A-K, but by nonlocalised orbitals embracing all three centres, it being necessary to allow significant interaction between J and K. Gordy⁸⁰ describes a situation like this, where the NQR results for H_2S indicate a hybridisation value for S very different from that indicated from the bond angle and equation 1.5.1. Gordy suggests an explanation in terms of nonlocalised orbitals on all three atoms: he supposes that the two "bonds" in a postulated system $S=H_2$ have different ionic characters, so that his description is not equivalent to the localised orbital description,⁴⁷ and the hybridisation values predicted are lower. Also, the difficulty with the physical interpretation implied by equation 1.5.1 is removed. However, a description like this is plausible only in the fragment $-AH_2$, since only the H - H approach is close enough to allow much interaction. Furthermore, the results for H_2S can also be explained by admitting some

d-character in the hybrid orbitals, when equation 1.5.1 would not hold, and for a number of reasons this explanation seems preferable. If this explanation is adopted, the difficulty may not extend to compounds of first-row elements, for which hybridisation involving d-orbitals is less likely.

The second possible bar to the use of equation 1.5.1 concerns the existence of "bent" or "banana" bonds. These are supposed to exist simply when the direction of the hybrid orbitals (as determined for example by some of the methods described later in this section) is away from the internuclear axis. Attempts at exact description of hybridisation have seemed to indicate that the existence of bent bonds must be admitted, although recent very detailed calculations,⁶³ based on slightly different assumptions suggest that the bending is not necessarily as large as was thought. In any case, the geometrical method certainly gives a good indication of hybridisation in most situations. A recent examination of the possibilities in group function calculations of describing the bonding in N_2 by banana bonds, or by conventional π -bonds, has favoured the latter: the two descriptions are not equivalent here because some allowance is made for correlation effects.⁴⁷

A theoretically attractive method of deciding hybridisation parameters lies in the use of NMR, especially of $^{15}N-H$, $^{13}C-H$ and $^{15}N-^{13}C$ coupling constants. Nuclear spin-spin interactions

through the electrons have been proposed to proceed by three different mechanisms¹⁷⁹: (1) the Fermi contact interaction (2) the electron-nuclear dipole-dipole interaction and (3) the nuclear spin - electron orbital interaction. As described, for example, in Part A of this thesis, original calculations^{183,184} and extensions of them^{111,116,169} have established that the coupling of protons with other nuclei derives chiefly from the contact term (1). If this is true, the coupling constant between A and B should be proportional to the contributions to the bond s-character from the atomic orbitals on A and B.

For a two-centre bond, $\phi_1(AB)$ has the form (equation 1.3.4)

$$\phi_1(AB) = \alpha_1 \phi_1(A) + \beta_1 \phi_1(B) \quad 1.5.2$$

In the general case, $\phi_1(A)$ and $\phi_1(B)$ are the hybrids $h_1(A)$ and $h_1(B)$ (equation 1.3.2). If B is hydrogen, $\phi_1(B)$ is the hydrogen 1s orbital. In the notation of sections 1.2 and 1.3, the s-characters from A and B are $a_1^2 \alpha_1^2$ and $b_1^2 \beta_1^2$ respectively.

In this analysis then, one would expect a linear relationship of the form

$$a_1^2 \alpha_1^2 b_1^2 \beta_1^2 = j' J_{AB} + k' \quad 1.5.3$$

where j' and k' are constants for a given pair of nuclei AB, and J_{AB} is the coupling constant between them. The constant k' may not be zero because of residual coupling, for instance from mechanisms (2) or (3): however it might be expected to be small compared to J_{AB} . The parameters α_1 and β_1 determine

the "ionic character" (section 1.6) of the bond between A and B, and this may be obtainable from other sources (next section).

But it is not a bad approximation to suppose that α_1 and β_1 will be nearly constant for a particular pair of nuclei AB, and this assumption has experimental support¹⁶³. Even though α_1 and β_1 , being determined by electronegativity which is in turn dependent on hybridisation,²¹¹ do vary to a certain extent, the product $\alpha_1^2 \beta_1^2$ can be shown^{163b} to vary much less. Then the product $\alpha_1^2 \beta_1^2$ may be assimilated in the constants j' and k' , and equation 1.5.3 can be simplified to:

$$a_1^2 b_1^2 = jJ + k \quad 1.5.4$$

This interpretation has been extensively applied to $^{13}\text{C-H}$ coupling constants,^{113,163,206} for which $j = 2.00 \times 10^{-13}$ sec. and $k = 0$. For the pair $^{15}\text{N-H}$, good results have been obtained with $j = 4.3 \times 10^{-3}$ sec. and $k = -6 \times 10^{-2}$, and a rough correlation for the pair²⁰ $^{13}\text{C-}^{15}\text{N}$ has been made, with $j = 8 \times 10^{-3}$ sec. and $k = 0$.

Apart from the approximation described above regarding α_1 and β_1 , many other assumptions are made in this type of analysis.⁷⁵ The assumptions of the predominance of the contact term, of the justifiability of representing all excited states by a mean, constant excitation energy^{6,156} (compare part A, section 2.2: the derivation of equation 1.5.3 here depends on this), of the presence of perfect pairing, and for some authors^{75,163}

the neglect of overlap, all limit the accuracy of the method. Nevertheless, Muller¹⁶² feels that it provides the best experimental method of determining hybridisation, and its practical success, in view of all the assumptions, is surprisingly good. The method breaks down for some compounds, e.g. diphenylketimine, owing apparently to a larger nuclear-spin electron-orbital effect. This explanation is supported,^{20,135} and a warning when the method may not be applicable is given, by the fact that in compounds which do not fit linear relationships like equation 1.5.4, ¹⁵N has a large downfield chemical shift, suggesting that deviations are associated with low-lying excited states (and hence the greater importance of spin-orbital coupling).

This method has been developed into a number^{122,155,163b} of subsidiary methods, which may sometimes be useful in estimating hybridisation. Thus, Muller and Pritchard¹⁶³ suggest the equation

$$r(\text{C-H}) = 1.1597 - 2.09 \times 10^{-3} a_1^2 \quad 1.5.5$$

applicable to substituted methanes CH_3X , relating the C-H bond distance in Å to a_1^2 ; this equation depends on an analysis of ¹³C-H coupling constants, and is at its least accurate for methane itself. Also for compounds of the type CH_3X , they suggest a relationship

$$J_{\text{C-H}} = 22.6E_X + 40.1r(\text{C-X}) + 5.5 \quad (\text{c/s}) \quad 1.5.6$$

where E_X is the electronegativity of X and $r(\text{C-X})$ the bond

length in Å. This relationship could again be applied to a determination of carbon hybridisation. Both equations 1.5.5 and 1.5.6 would of course be of practical use only if the appropriate ^{13}C -H coupling constants were not known. Equation 1.5.6, indeed, involving as it does E_X which is often not known, especially for groups, is of more practical use⁶⁷ in determining E_X .

Various other relationships involving hybridisation have been proposed. Dependences of bond lengths, electronegativity differences²⁵¹ and ^{14}N chemical shifts^{90,94} have for example all been suggested, but the methods are often qualitative, and all seem less capable of giving reasonably reliable values⁴ than the two main procedures described. The other approaches therefore need not be discussed here.

1.6 The "molecular" coefficients

The separation of the "molecular" coefficients μ_j from the "atomic" coefficients k_j discussed in section 1.5 is in one sense artificial. An ab initio molecular orbital calculation would give only the c_{ij} , as in equation 1.2.7. The c_{ij} correspond in general to products $\mu_j k_j$, and cannot, in such a calculation, be readily analysed into the μ_j and the k_j separately; nor indeed would such an analysis be necessary. An account of the theory involved in the evaluation of field gradient tensors from the MO standpoint is given by Cotton and Harris,⁴⁶ who

however make what amount to the Townes and Dailey approximations in the treatment of the sum of matrix elements in an equation like equation 1.3.11 of this thesis, and do not consider in any detail the evaluation of the c_{ij} . Similarly, Malli and Fraga¹⁵² give expressions for field gradients which depend on knowing analytic Hartree-Fock functions for the molecule. And as has already been pointed out, most light molecules and all other molecules are inaccessible to such methods, or at least the labour called for is prohibitive.

Approximate molecular wave functions have, however, been published for a number of nitrogen-containing molecules, in particular for pyridine and related compounds^{e.g. 194,241} and and for molecules containing the $-C\equiv N$ fragment.^{e.g. 25,161} Attempts, however, to use already-published self-consistent field molecular orbitals directly, in the calculation of nuclear quadrupole coupling constants in, for example, nitrogen,¹⁹⁰ nitric oxide,³⁷ the CN radical,¹⁸² deuterium cyanide⁵⁸ and monodeuterated ammonia¹²⁰ (this last for both ^{14}N and 2D quadrupole coupling constants) have had only limited success. The explanation for this lack of success lies no doubt in the fact that the molecular wave functions used were derived by controlling the variable parameters in the wave function to give the best agreement with empirical energies and sometimes bond distances. These physical properties of the molecule are sensitive to the

form of the wave function at relatively large distances from the nucleus, and insensitive to the form of the wave function close to the nucleus; this is not necessarily the form of the dependence of the field gradient at the nucleus. Thus wave functions derived so as to work well for energies may easily not give good results for nuclear quadrupole coupling constants.

In any case a readily usable procedure for interpreting NQR results cannot depend on an SCF-MO approach, which is too difficult. Recent work by Peters¹⁷¹ and Bykov³⁰ has confirmed what was earlier an assumption: that the results of a more rigorous SCF-MO calculation may often be approximated by an application of the two principles of bond ionic character and electronegativity.

Ionic character can easily be defined for a two-centre bond, and thus a two-centre orbital, only. The generality of section 1.3 therefore suffers a further curtailment. However, an extension to multicentre orbitals of the arguments presented later can readily enough be imagined, and it may be that such an extension would give useful results. Nevertheless, such success for multicentre bonds has not been widely demonstrated, as it has for two-centre bonds, and the rest of this section is restricted to two-centre orbitals.

In the notation of section 1.3, such an orbital, centred on atoms A and B, would be (equation 1.3.4)

$$\varphi_1(AB) = \alpha_1\varphi_1(A) + \beta_1\varphi_1(B) \quad 1.6.1$$

Ionic character originated logically from the valence bond (VB) method. In the present MO treatment, ionic character i can similarly be represented :

$$i_{AB} = \beta_1^2 - \alpha_1^2 \quad 1.6.2$$

This definition is unsatisfactory, because of difficulties in connection with overlap populations: electrons apparently associated with neither A nor B, but with "the space between them". If then the overlap integral,

$$S_{AB} = \int \varphi_1(A)\varphi_1(B)d \quad 1.6.3$$

for this purpose is taken to be zero, then if $\varphi_1(AB)$ is normalised,

$$i_{AB} = 1 - 2\alpha_1^2 = 2\beta_1^2 - 1 \quad 1.6.4$$

Notice that $i > 0$ if A has a lower orbital population, for the bond AB, than B.

Thus if i_{AB} is known, α_1^2 and β_1^2 , and by extension, all the α_j^2 , can be found. The most fruitful way of evaluating i_{AB} is through the concept of electronegativity. The actual form of the relationship between i_{AB} and on the electronegativities X_A and X_B of A and B naturally depends on the definitions of X_A and X_B . Pauling's original verbal definition of electronegativity¹⁷⁰ was "the power of an atom to attract electrons to itself". Mulliken's quantification of this was to put

$$X_K = (I_K + E_K)/2 \quad 1.6.5$$

where I_K and E_K are the ground-state first ionisation potential and electronegativity of the atom K. This equation will be of interest later, as will Wilmshurst's²⁵⁴ empirical equation, relating Mulliken's electronegativities to the ionic character:

$$i_{AB} = |(X_A - X_B)| / (X_A + X_B) \quad 1.6.6$$

It is also of interest that this equation was derived from a study of nuclear quadrupole coupling constants in halogens.

Following the pioneer work of Pauling and of Mulliken, very varied definitions of electronegativity have been proposed, depending for example on effective charge,³³ covalent radii,⁶⁴ nuclear magnetic resonance coupling constants¹³⁶ (see also Part A), and many others which are correlated and compared by, for example, Allred and Hensley.⁸ More recently, several workers have suggested that electronegativity depends on the environment of the atom in the molecule. Pritchard and Sumner^{180,211} for instance introduced variable electronegativity in connection with MO descriptions of molecules. The original verbal definition of electronegativity given by Pauling (see above) suggests that electronegativity be identified with some potential function, i.e. a derivative of energy with respect to some suitable physical parameter. Thus Iozkowski and Margrave¹⁰⁶ defined electronegativity as the derivative of ionisation energy with respect to charge. This type of definition immediately suggests that the potentials on both electrons in a bond orbital should be

equalised. This principle, of electronegativity equalisation, is important. It is however subject to serious limitations which are discussed later.

A definition of electronegativity in terms of a potential function presupposes a suitable expression for the energy of the electron, or equivalently of the orbital, which is to be used in the formation of the bond (orbital). Such an expression should contain experimentally available parameters. It may be based on spectroscopic terms and transition energies, as in the system described by Klopman.¹²⁷ Expressions based directly on spectroscopic values, however, are complicated both in theory and in practice, and they depend explicitly on quantities difficult to evaluate, such as shielding factors. Also, Klopman's treatment does not clearly identify electronegativity as a property of the orbital and not of the atom. This identification is made consistently in the series of papers^{11,96,97,249,250} by Jaffé, Whitehead and collaborators, and for this reason chiefly, the last treatment of electronegativity is the most satisfactory available, and is to be preferred.

The original treatment^{96,97} has been changed slightly in presentation and formalism for the purposes of this thesis; but the account given here, apart from the last part, which is new, is essentially the same as that given by the original authors.

It has been found that the energy $E(n)$ of an orbital can

be adequately described by:

$$E(n) = K + \dot{a}n + \frac{1}{2}\dot{b}n^2 \quad 1.6.7$$

where n is the occupation number of the orbital and K , \dot{a} and \dot{b} are constants for that orbital: the dots on \dot{a} and \dot{b} are intended to emphasise that these are not the k_j of previous sections. In accordance with the suggestion made above that electronegativity can be identified with a potential, the electronegativity, $X(n)$ is defined:

$$-X(n) = \frac{\partial E}{\partial n} = \dot{a} + \dot{b}n \quad 1.6.8$$

It is pointed out⁹⁶ that such a definition assumes that (i) the occupation number n can assume any value, including fractional values, between 0 and 2, (ii) the function 1.6.7 is indeed continuous and differentiable. With these assumptions, equation 1.6.8 shows that electronegativity is a linear function of the occupation number. The parameters \dot{a} and \dot{b} may be deduced from the ionisation potential I , and the electron affinity E , of the valence state orbital. For, adopting the convention that I and E are negative if the process, removal or acceptance of an electron respectively, to which they refer is exothermic, and vice-versa:

$$\begin{aligned} I &= E(0) - E(1) \\ -E &= E(1) - E(2) \end{aligned} \quad 1.6.9$$

Then from equation 1.6.7:

$$\begin{aligned} -I &= \dot{a} + \frac{1}{2}\dot{b} \\ +E &= (2\dot{a} + 2\dot{b}) - (\dot{a} + \frac{1}{2}\dot{b}) = \dot{a} + \frac{3}{2}\dot{b} \end{aligned} \quad 1.6.10$$

whence

$$\begin{aligned} \bar{a} &= -\frac{1}{2}(E + 3I) \\ b &= I + E \end{aligned} \quad 1.6.11$$

and so

$$-X(n) = -\frac{1}{2}(E - 3I) + (I + E)n \quad 1.6.12$$

When two atomic orbitals form a molecular orbital, the principle of electronegativity equalisation described above requires that the occupation numbers of the orbitals change so as to equalise the electronegativities of the corresponding orbitals of atoms A and B. Using subscripts to indicate parameters relating to A and B:

$$-\frac{1}{2}(E_A - 3I_A) + (I_A + E_A)n_A = -\frac{1}{2}(E_B - 3I_B) + (I_B + E_B)n_B \quad 1.6.13$$

Ionic character is readily defined¹¹ in terms of n_A :

$$i_{AB} = 1 - n_A \quad 1.6.14$$

It is also true that:

$$n_A + n_B = 2 \quad 1.6.15$$

Combining equations 1.6.13, 1.6.14 and 1.6.15 gives

$$i_{AB} = (E_A + I_A - E_B + I_B)/2(E_A + E_B + I_A + I_B) \quad 1.6.16$$

A close similarity between this equation and the purely empirical one put forward by Wilmshurst (equation 1.6.6) can easily be demonstrated.¹¹ However, an examination of equation 1.6.8, identifying X_{atomic} with $X(1)$, shows that equation 1.6.16 does not describe any simple relationship between ionic character and electronegativity difference.

The principle of electronegativity difference has been

questioned by Pritchard.¹⁸¹ His conclusions suggest that, instead of the condition for strict electronegativity equalisation,

$$X_A - X_B = 0 \quad 1.6.17$$

there should be substituted an equation of the form

$$X_A - X_B = p(X_A(1) - X_B(1)) \quad 1.6.18$$

which leads to a modified version of equation 1.6.16:

$$i_{AB} = -(1-p)(A^+ - B^+)/2(A^+ + B^+) \quad 1.6.19$$

where now $A^+ = I_A \pm E_A$

and $B^+ = I_B \pm E_B \quad 1.6.20$

in general $K^+ = I_K \pm E_K$

Pritchard's results for an isolated C-N π -bond amount to a value for p of 0.2, which as can be seen from equation 1.6.19, will lead to a reduction by 20% of the ionic character from $p=0$, not as stated by Tong²³³ to an increase of 10%. However values of p , which depends on the atoms, type of bond, hybridisation and on all the electrons in the rest of the molecule, are too difficult to calculate for every case. Until tables of values for p can be obtained, it may be best to assume $p=0$ in equation 1.6.19. It appears from Pritchard's calculations that usually $0 < p < 1$ (in fact p is probably often less than 0.5) and the variations in the value of p in compounds of first-row elements may not be large. It can be said therefore that the ionic characters calculated by putting $p = 0$, i.e. as in equation 1.6.16, will be too large, but fairly consistently so.

The ionic character, then, can be calculated in terms of the ionisation potentials and electron affinities of the appropriate orbitals. For a particular principal quantum number in a particular atom A, I_A and E_A depend mainly on (i) the hybridisation, and occupation numbers, of the orbitals other than that for which I and E are to be determined, and (ii) the hybridisation of the orbital to which I and E apply. Factor (i) can be concisely referred to as the "other-electron distribution", and factor (ii) as the "Hybridisation". As is usual with such problems, this analysis at once implies that factors (i) and (ii) can indeed be treated separately, and that there is no interaction term between the two; such a separation need not be correct.

For the orbital h_j of atom A (equation 1.3.2), then, I_{Aj} and E_{Aj} , and therefore A_j^+ and A_j^- , depend on the other-electron distribution. The question of how best to describe this dependence has been taken up in a slightly different form by Whitehead, Baird and Kaplansky.²⁴⁹ They found that I and E for an orbital having a particular hybridisation could be well approximated by a three-term power series, up to the quadratic, in n_T , where n_T is the total number of electrons in the valence orbitals other than the valence orbital for which I and E were defined; in some elements n_T did not include the electrons of assumed lone pairs. This dependence is on the total occupation number

only of the other valence orbitals, and not on the distribution of the electrons among these orbitals. Whitehead et al. emphasise that this simplification holds only if these other orbitals have the same hybridisation as each other. Since the effective shieldings by s electrons and by p electrons are different, this will not do if a range of hybridisation in the other orbitals, and probably too different hybridisations for some or all of them, are to be admitted. In view of the findings of Whitehead et al., it seems reasonable to guess that in the more general case, a satisfactory description of I and E might be made by similar three-term power series in n_s and n_p separately, with n_s and n_p defined by

$$\begin{aligned} n_s &= \sum_{i \neq j} n_i a_i^2 \quad i = 1 \dots 4 \\ n_p &= \sum_{i \neq j} n_i (1 - a_i^2) \quad i = 1 \dots 4 \end{aligned} \quad 1.6.21$$

where n_i is the gross occupation number of orbital h_i , and the other symbols have their usual meanings. Thus the dependence of A_j^+ on the other-electron distribution can be written:

$$A_j^+ = K_A^+ + b_{A1}^+ n_{Asj} + b_{A2}^+ n_{Asj}^2 + c_{A1}^+ n_{Apj} + c_{A2}^+ n_{Apj}^2 \quad 1.6.22$$

The A_j^+ depend also on the hybridisation, that is on the value of a_j^2 , which for convenience may be written s_{Aj} . There is of course a large number of possibilities for this dependence. Whitehead et al.²⁴⁹ allow to a very restricted extent for the effect of hybridisation by listing the values of their parameters, which

describe a dependence on n_T , for a few selected values of hybridisation. Such a table implies that the parameters are all functions of s_{Aj} , although of course Whitehead et al. do not attempt to give such functions. If the dependence of each parameter of equation 1.6.22 is, correspondingly, assumed to have the form of an m -term polynomial in s_{Aj} , then it would become necessary to find $5m$ subsidiary parameters, probably not fewer than 15. The objection to this is that such a relationship would be cumbersome to apply, although it would give an accurate description of the dependence of A_j^+ on s_{Aj} , n_{Asj} and n_{Apj} . The necessary parameters could, however, be determined by a method exactly like that described later, and the complete dependence of A_j^+ would be, dropping the subscripts A and j for clarity:

$$\begin{aligned}
 A^+ = & \sum_{i=0}^m \bar{K}_i^+ s^i + n_s \sum_{i=0}^m b_{1i}^+ s^i + n_s^2 \sum_{i=0}^m b_{2i}^+ s^i + n_p \sum_{i=0}^m c_{1i}^+ s^i \\
 & + n_p^2 \sum_{i=0}^m c_{i2}^+ s^i
 \end{aligned} \tag{1.6.23}$$

It is worth considering whether a less complicated, although it may be less exact, equation than 1.6.23 could be found. The obvious alternative to making the coefficients of n and n^2 themselves functions of s is to add to the other-electron dependence given by equation 1.6.22 a separate dependence on s of A_j^+ . Thus,

$$A^{\pm} = K^{\pm} + \sum_{i=1}^{n-1} a_i^{\pm} s^i + b_1^{\pm} n_s + b_2^{\pm} n_s^2 + c_1^{\pm} n_p + c_2^{\pm} n_p^2 \quad 1.6.24$$

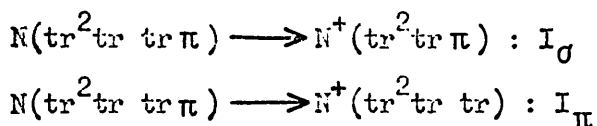
A similar investigation,¹¹ not however considering the effect of n_s and n_p , has found that a sum such as that in equation 1.6.24 may usefully be limited to the term in s^2 . Then equation 1.6.24 becomes

$$A^{\pm} = K^{\pm} + a_1^{\pm} s + a_2^{\pm} s^2 + b_1^{\pm} n_s + b_2^{\pm} n_s^2 + c_1^{\pm} n_p + c_2^{\pm} n_p^2 \quad 1.6.25$$

This equation has seven parameters, compared to the 5m (perhaps 15) of equation 1.6.22, for each of A^+ and A^- . This gain in simplicity however will as usual mean a loss in accuracy.

Parameters for equations 1.6.23 or 1.6.25 have not been published, nor have parameters for I or E in a form easily adaptable to the general types of equation 1.6.23 and 1.6.25. The evaluation of the parameters, for each atom, is approached through an evaluation of I and E for a number of configurations of the atom and its ions, whose orbitals have differing values of s , n_s and n_p . Now I and E can be measured directly only for the orbital of highest energy in the ground state of the neutral atom A, and in the ground state of some of its ions (say $A(-)$, $A(+)$, $A(2+)$ and $A(3+)$ where all these ions exist: often they do not). Recourse must be had therefore to valence-state configurations, which are either excited atomic configurations or hypothetical atomic configurations in which the electrons remain in hybrid orbitals which they may have occupied in

the molecule, and are not allowed to rearrange. For simplicity, intermediate hybridisations need not be considered, and calculation need be done only for digonal (di), trigonal (tr) and tetrahedral (te) hybrids. The means of calculating I_A and E_A for a variety of orbitals is best shown by an example: the calculation of I_A for a likely valence state of nitrogen, $N(tr^2 tr \pi)$. I_N in this case, as often in other cases, may refer to the removal of an electron from either one of two different orbitals, the tr or the π . The two cases are represented:



It is easily seen that

$$I_v = I_g + P^+ - P^0 \quad 1.6.26$$

where I_v is the ionisation potential (I_σ or I_π) of $N(tr^2 tr \pi)$, I_g is the ground state ionisation potential of nitrogen, P^+ is the promotion energy of $N^+(tr^2 tr \pi)$ or of $N^+(tr^2 tr)$ respectively above the ground state of the N^+ ion, and P^0 is the promotion energy of the configuration $N(tr^2 tr \pi)$ above the ground state of the N atom. The required promotion energies are given by Hinze and Jaffé⁹⁶ for this example, as is the first ionisation potential of nitrogen. The process can be extended in principle to all valence state configurations, containing at least one unpaired electron, of neutral N, and of N^- , N^+ , N^{2+} and N^{3+} , using the electronegativity or first, second or

third ionisation potential as appropriate, and with P^+ and P^0 now referring to the valence state promotion energies of the dipositive and positive, tripositive and dipositive ... ions respectively.

The calculation of valence state electron affinities of orbitals can be done in a similar way, using equations of the form of equation 1.6.27, which refers to the first such electron affinity, and serves as an example:

$$E_v = E_g + P^0 - P^{\bullet -} \quad 1.6.27$$

with the terms defined analogously to those in equation 1.6.26.

It is to be noted that the electron affinity of an unoccupied orbital is equal in magnitude, but opposite in sign, according to the convention set out before equation 1.6.9, to the ionisation potential of the same orbital in the same configuration, but when the occupation number is one. This halves the number of calculations needed to describe all orbitals in all configurations of the atom.

Some of the required promotion energies are given by Hinze and Jaffe,⁹⁶ but unfortunately many of the promotion energies needed for a full account of the atoms and ions Be^- , B , B^- , C^+ , C , N^{2+} , N^+ , O^{3+} , O^{2+} , O^- , F^{3+} and F are not given. Some of the missing promotion energies must have been used in calculations described by these authors then⁹⁶ and later¹¹,^{97,249} and are therefore presumably available though unquoted;

a few of the gaps can be filled by working back from their published results or from other papers.

The results of the process described above, for some configurations of nitrogen, are shown in Table 1.6.1 (page 211), where the values of s , n_s and n_p are also shown; the subscripts refer to the values of s , n_s and n_p are also shown; the subscripts The information needed for a similar table for the ions of nitrogen is not given by Hinze and Jaffé, but some of the information has been gathered from a large number of measurements, mainly spectroscopic, published elsewhere. This additional information is irregularly distributed, but along with the values given in table 1.6.1 it may be used partly to analyse a dependence of the type given by equations 1.6.23 or 1.6.25

Although Table 1.6.1 gives eleven states, since for N always $n_p = 4 - n_s$, all seven parameters K , a_1 , a_2 , b_1 , b_2 , c_1 and c_2 for each of A^+ and A^- cannot be determined uniquely, although relationships between them can. The parameters for a reduced form of equation 1.6.25:

$$A^{\pm} = K_R^{\pm} + a_1^{\pm} s + \frac{a_2^{\pm}}{2} s^2 + b_{1R}^{\pm} n_s + b_{2R}^{\pm} n_s^2 \quad 1.6.28$$

this representing all the information to be extracted from Table 1.6.1, were calculated using a least-squares curve-fitting procedure. The results are shown in Table 1.6.2 (page 211).

Notice that the parameters a^{\pm} in Table 1.6.2 are those for the full equation 1.6.25. The full set of parameters

TABLE 1.6.1: SOME VALENCE STATES OF N, AND CORRESPONDING PARAMETERS

State and orbital rfd. to	I(eV)	E(eV)	s	n _s	n _p
N(s ² _{ppp})	13.94	-0.84	0	2	2
N(sp ² _{pp})	26.92	-14.05	1	0	4
N(sp ² _{pp})	14.42	-2.54	0	1	3
N(di ² _{diππ})	23.91	-7.45	0.5	1	3
N(di ² _{diππ})	14.18	-1.66	0	1.5	2.5
N(di ² _{diππ})	22.10	-6.84	0.50	0.5	3.5
N(di ² _{diππ})	14.11	-2.14	0	1	3
N(tr ² _{trtrπ})	20.60	-5.14	0.33	1	3
N(tr ² _{trtrπ})	14.12	-1.78	0	1.33	2.67
N(tr ² _{trtrπ})	19.72	-4.92	0.33	0.67	3.33
N(te ² _{tetete})	18.93	-4.15	0.25	1	3

The values of I and E are taken from Hinze and Jaffé.⁹⁶

TABLE 1.6.2: PARAMETERS FOR NITROGEN (eV)

K _R ⁺	+19.78	K _R ⁻	+ 4.29
b _{1R} ⁺	- 8.16	b _{1R} ⁻	+13.16
b _{2R} ⁺	+ 2.06	b _{2R} ⁻	- 3.29
a ₁ ⁺	+ 9.63	a ₁ ⁻	+35.77
a ₂ ⁺	-16.87	a ₂ ⁻	+ 0.79

could be similarly calculated if the necessary promotion energies were available. Three points are worth making about Table 1.6.2. First, the parameters given reproduce the values of Table 1.6.1 with a mean deviation of about 7.5%. For comparison, Whitehead et al.²⁴⁹ give parameters obtained by fitting only three variables to not more than six points, and in itself this mathematically simpler task must give greater accuracy, which reproduce observed values with a mean deviation of about 2.9%. Thus the loss in accuracy in adopting a simpler equation like 1.6.25 seems to be not unreasonable, especially since equation 1.6.25 in use would give much more flexibility than the procedure of Whitehead et al. Second, it will be seen that $a_1^- \gg a_2^-$, which means that I-E is almost linearly proportional to the s character of the hybrid orbital. This observation has been frequently confirmed previously,^{96,100,127,249} and makes a useful approximation. Similar calculations which were made on other atoms confirm that the relationship $b_{1R}^+ / b_{2R}^+ \doteq -4$ seen in Table 1.6.2 holds generally for first-row elements, as does the observation that the $b^+ - b^-$ pair are opposite in sign. Physically, these observations mean that the shielding of the nuclear charge is greatest when $n_s = 2$, which is a reasonable conclusion, since then the s orbital occupancy is as high as possible. Third, a partial extension of the calculations to include positive ions of nitrogen, using information from other sources, suggests that $b_2^+ \doteq c_2^+$,

and that b_1^+ and c_1^+ are usually of the same order of magnitude. If the assumptions of Whitehead et al.²⁴⁹ are correct, then the situation when all the other orbitals have equal hybridisation is the limiting case in which n_s and n_p may be combined into n_T .

The parameters of equation 1.6.25, then, could be calculated for every atom of interest and tabulated. The best procedure then for the calculation of the ionic character for all the bonds of a molecule is a self-consistency procedure in the occupation numbers of the atomic orbitals, assuming initially one electron per atomic bonding orbital for every atom in the molecule, and two electrons in every non-bonding orbital (but see Chapter 2). Then A^+ and B^+ can be found for two bonded atoms (equation 1.6.25); i_{AB} from equation 1.6.19; $n_A(B)$ from equation 1.6.14 and $n_B(A)$ from equation 1.6.15. This new value of $n_A(B)$ can then be used to calculate A^+ for the orbital of A which forms a bond between A and C, and the same procedure yields a value of $n_A(C)$. All the bonds of A can be dealt with in turn, and the procedure of "rotating on A" continued until the values of $n_A(B)$, $n_A(C)$... are self-consistent. The final value of $n_A(B)$ determines $n_B(A)$, and this value can be kept fixed while rotating on B. The cycle is repeated for all the atoms of the molecule. This procedure, although not strictly self-consistent, because of the limitation of such

parameters as $n_B(A)$ once $n_A(B)$ is fixed, has the advantage that values of the $n_A(K)$ can be obtained which are not greatly in error compared to the better values obtained by the full self-consistent group-orbital electronegativity method described by Whitehead *et al.*²⁴⁹; thus useful values of the $n_A(K)$ can be got by rotating on atom A only. The method is essentially that described by Gallais, Voigt and Labarre,⁷⁸ who give more details. The whole procedure can be carried out by hand calculation.

Methods similar to those described above have been applied with considerable success to NQR frequencies in chlorine,²⁵⁰ by Whitehead and Jaffé, and variants of the idea of group orbital electronegativities have been used in the interpretation of NMR frequencies⁵⁴ and Taft polar substituent constants.⁶¹ Huheey uses a form of the theory of Whitehead and co-workers, in which he develops a definition^{100,102,103} of electronegativity which, like the electronegativity described here, is variable; however Huheey assumes that the electronegativities of all the orbitals are equal - electronegativity is therefore essentially an atomic property again - and that all orbitals are equally hybridised (however he gives no indication that he is aware of these two assumptions). Even in this very curtailed form, the notion of variable electronegativity has remarkable success in correlating polar substituent constants¹⁰¹ and NMR coupling constants.⁹⁹

1.7 Choice of explicit atomic orbitals

For the sake of simplicity, many of the decisions which properly belong to this section have already been made, by implication or at best without justification, in sections 1.2 and 1.3. Some of the approximations made in these previous sections can now be rationalised to some extent. Even when these approximations were made, equation 1.3.11 was derived; that equation is a weighted sum of matrix elements of $1s$ atomic orbitals on all nuclei, and of hybrid orbitals $h_j(J)$ on all nuclei. The hybrid orbitals (equation 1.3.2) are functions of the $2s$ and $2p$ orbitals on all nuclei. Thus the best choice of $1s$, $2s$ and $2p$ atomic orbitals, on at least first-row nuclei, needs to be considered in this section. As has been said earlier, it will be easiest to consider the form of the atomic orbitals when a number of simplifying assumptions are made, and then to consider the changes which follow when some of these assumptions are discarded or modified. Apart from the approximations mentioned in sections 1.2 and 1.3, which relate mainly to the simplification of the molecular orbitals, two simplifications particularly concerned with atomic orbitals are made at this point: it is assumed that the potential field with which the electrons interact is independent of (i) time and (ii) the angular co-ordinates of the electron. A physical interpretation of these two assumptions is that each electron moves in an

average spherically symmetric potential field; this is of course the familiar Hartree self-consistent field.

The choice of the explicit atomic orbitals to be used, even with the foregoing simplifications, is a complex question.^{62,208} Most ab initio calculations usually employ functions recognisable as atomic orbitals, of one of the forms given below, but in accurate calculations, the functions are complicated, and molecular as much as atomic considerations dictate their choice. If a small basis set of atomic orbitals is used, an ab initio calculation usually produces poorer agreement with empirical values than does a semi-empirical calculation. Extending the basis set of course leads to greater difficulties in computation, and to greater difficulty of interpretation in simple chemical terms, although often improving the fit of calculated to observed physical quantities. All of this suggests that the most fruitful approach to the choice of atomic orbitals might be to allow physical considerations to influence the choice.

The best description of an atomic orbital (AO) in a many-electron atom is a single function, involving all the co-ordinates of all the electrons and of the nucleus. But the ^{Stern}~~Stern~~-Oppenheimer approximation referred to in section 1.2 makes it sufficient to refer all space co-ordinates of the electrons to the nucleus as origin; and using the Hartree self-consistent field approximation, as modified by Fock to take account of

exchange, yields the well-known Hartree-Fock self-consistent field functions (HFFs). These functions are in general sums of antisymmetrised products of one-electron wave functions, and only for closed-shell atoms, or atoms with one electron over, or fewer than, a closed shell, is a one-term function a good description of the AOs. When available, the many-term HFF for an atom could be used in reasonably simple calculations, at the cost of some labour and computer time. In general, however, it is easier to seek analytical expressions of the HFF. The factors in the antisymmetrised products are the AOs with which this section deals. In general, they consist in turn of a product:

$$\psi_{\text{HFF}} = N' \cdot R(r) \Theta(\vartheta) \Phi(\phi) S(s) T(t) \quad 1.7.1$$

where N' is a normalising factor, independent of the three space co-ordinates r, ϑ and ϕ (these are ordinary spherical co-ordinates), the spin co-ordinate s (for one electron, $s = \pm \frac{1}{2}$) and time, t ; and the other factors in the product are each dependent on one only of the five chosen independent variables. The most general HFF is a function of t , and it is for such time-dependent functions that many of the well-known properties of HFFs, especially the inclusion of one normalised determinant for each term of a single configuration, can be most readily derived. However, it has been shown^{19,208} that localised (i.e. time-independent) functions are as mathematically

satisfactory as the more general HFs. This is also more convenient physically, and indeed it has been implicit in the preceding sections that the stationary atomic functions could be used. If assumptions of the perfect-pairing type are used, and this is reconsidered later, then $S(s)$ has the same form in the space co-ordinates for either value of s . Thus $S(s)$ and $T(t)$ can be absorbed into the normalising factor, and now

$$\psi_{r\vartheta\varphi} = N.R(r)\Theta(\vartheta)\Phi(\varphi) \quad 1.7.2$$

Since the Hartree-Fock approximation assumes that the potential in which each electron finds itself is spherically symmetric, the parts of $\psi_{r\vartheta\varphi}$ which are dependent on ϑ and φ must simply be the spherical harmonics, or linear combinations of them, for the same l , since they are all degenerate:

$$\Theta(\vartheta)\Phi(\varphi) = \sum_{m=-l}^{+l} a_m^l Y_m^l(\vartheta, \varphi) \quad 1.7.3$$

where a_m^l is a mixing coefficient. The expansion of equation 1.7.3 is discussed in the following section.

The difficulty, of course, lies in the analytical expression of the r -dependent part. The best expression would have the form:

$$R(r) = \sum_i a_i p_i(r) \exp(-b_i r^{x_i}) \quad 1.7.4$$

where a_i is a constant (but not a normalisation constant: all normalisation constants are by convention here included in N),

$p_i(r)$ is a polynomial in r or a variable directly proportional to r , and the exponential contains two adjustable parameters b_i and x_i . For example, in the hydrogen-like functions, one term only is used in the sum; $a_i = 1$; $x_i = 1$; $b_i = Z/n$, where Z is the central charge and n the principal quantum number; and

$p_i(r)$ is closely related to the associated Laguerre polynomials

$$L_{n+1}^{2l+1} :$$

$$p_i(r) = \rho L_{n+1}^{2l+1}(\rho) \quad 1.7.5$$

$$\text{where } \rho = \frac{2Z}{n} \cdot r \quad 1.7.6$$

when r is measured, as throughout this thesis, in Bohr radii.

For reproducing HFFs analytically, however, more than one term is often used in the sum of equation 1.7.4, with a simpler form of $p_i(r)$. Typically

$$p_i(r) = r^{n^*-1} \quad 1.7.7$$

where n^* is now a so-called "effective" quantum number. If in equation 1.7.4, $p_i(r)$ is given by equation 1.7.7, and $x_i=2$, the expansion is Gaussian. If $x_i=1$, the function is of the form first proposed by Slater.²¹³ These two values of x_i are the only two which have been used to any extent.^{53,208} In either case, b_i of equation 1.7.4 is defined very similarly to the definition given above:

$$\begin{aligned} b_i &= Z^*/n^* \quad \text{or} \\ b_i &= Z^*/n \end{aligned} \quad 1.7.8$$

where Z^* is an "effective" nuclear charge.

The Gaussian expansion ($x_i = 2$) has been investigated by a large number of workers. e.g. 71,143,186,187,188,230 The advantage of this expansion is that the mathematics¹⁹³ of evaluating matrix elements of a Gaussian function is simpler for most operators of physical interest. The disadvantage is that more terms are needed in the sum of equation 1.7.4 to give a satisfactory description of the HFF. A fairly extensive examination of the possibilities of Gaussian functions was made by Reeves and co-workers^{186,187,188} who have also presented⁷¹ closed formulae for the evaluation of Gaussian matrix elements. They consider various methods for finding b_i for each of a number of terms in a Gaussian expansion, and succeed to some extent for some purposes. Whatever the potentialities of Gaussian functions might be — and their mathematical simplicity is certainly attractive — the uncertainties of evaluating the increased number of parameters, the difficulty of allowing for correlation effects, and the shortage of published studies compared to Slater orbitals, make the latter the better choice at the moment for most studies of atomic or molecular properties: they are probably to be preferred simply because of the amount of information available for them.

The simple formula proposed by Slater²¹³ was one term of the sum of equation 1.7.4. Thus:

$$R(r) = r^{n^*-1} \exp(-z^*r/n^*) \quad 1.7.9$$

where now z^* is written for Z^* , and it was for this simplified form of equation 1.7.4 that Slater proposed "tentative rules" for finding z^* and n^* which are still widely used. Slater's main criterion for fixing his rules was the closest possible approximation of the energy given by a Slater function to the true energy (energy-minimisation) while avoiding complexity in the rules. It is interesting that the values of z^* found by Slater semi-empirically have recently been given some purely theoretical support.⁹² Modifications of the Slater rules, often using more than one exponential,^{98,146} and new, though of course similar, sets of rules have been proposed. Clementi and Raimondi,⁴¹ for example, reported z^* for atomic number z up to 36, for a single exponential. Energy minimisation for an atom stresses the matching of the analytical wave function to the HFF near the nucleus, in that region where the electronic function has most effect on energy. More recently, Burns²⁷ has given tables which can be used to find σ (where $z^* = z - \sigma$) for both single-exponential Slater functions (equation 1.7.9) and hydrogen-like wave functions (equations 1.7.5-6), in which the matched quantity is not energy but the expectation value (moment) of the wave function. This puts more emphasis on good reproduction of the outer parts of the HFF.²¹⁴ The distinction between matching the outer and matching the inner part of a wave function becomes important when orthogonalised Slater wave functions are used (see below).

The difference is less important when single-exponential Slater functions, or hydrogen-like functions, are used.

Many other recipes for finding z^* have been proposed, using for instance covalent radii,¹⁸ or electron resonance.^{e.g. 70}

There is one point remaining with regard to Slater orbitals. For some purposes, especially connected with the mathematical expansions of functions, it is assumed that all atomic orbitals on one centre are orthogonal. However the Slater 1s and 2s orbitals, as given by equations 1.7.2 and 1.7.9, would not be orthogonal in that simple form. A modified 2s function χ_{2s}^{or} can readily be constructed, orthogonal to χ_{1s} :

$$\chi_{2s}^{\text{or}} = (\chi_{2s} - S\chi_{1s})/(1 - S^2)^{\frac{1}{2}}$$

1.7.10

where $S = \int \chi_{1s}^* \chi_{2s} d\tau$

It must now be considered whether the Slater orbitals, of whatever form, can be modified to take account of the fact that assumptions (i) and (ii), page 215, are inexact physically. Assumption (i) was that the potential field which the electrons are in is time-independent. The corrections to the simplest type of wave function to allow for the errors inherent in this assumption are of course the much-studied electron correlation modifications to the wave function.

An excellent though now somewhat out-of-date review of correlation is given by Löwdin,^{14,5} and more recent reviews^{e.g. 19,42} are also rather elementary. It is not proposed to reiterate the

details of correlation corrections here, and only these aspects of correlation which are relevant to this section are discussed.

The main difficulty in treating electron correlation is the usual one of the complexity of the problem. Solutions which are mathematically tractable do not as a rule give very accurate results physically, while physical exactness can be attained only at the price of mathematical complications which are often overwhelming. Ultimately, physical exactness is more important, and some mathematical difficulties have to be accepted. Nevertheless it seems likely that in the interpretation of NQR, there is room for improvement in physical accuracy without making the consequent mathematics impossibly difficult.

Ideally, one should use a correlated wave function, but this is a quite unattainable ideal at present. The "atoms-in-molecules" approach, which has considerable appeal to a chemist, would allow instead the use of linear combinations of correlated atomic functions, e.g. ¹⁰ and this approach has already been implied by the use of LCAO (section 1.2). But LCAO necessarily cannot include many molecular types of correlation whose importance has recently been demonstrated.⁹¹ The separation principle for σ - π molecular systems has also been shown⁵ not to hold always, so that such peculiarly molecular effects as "vertical" and "in-out" correlation should be considered. However, the type of correction to be made is so uncertain that at present

any attempt to include such effects may even decrease the accuracy of the wave function.^{44, 46} It is therefore difficult to do more than acknowledge the probable importance of these influences.

The main way to date of treating correlation in many-electron atomic systems depends on the superposition of configurations (configuration interaction). If a set of N ordered one-electron indices $k_1 < k_2 < \dots < k_N$ is called an ordered configuration K , and if Ψ_K is an associated Slater determinant:

$$\Psi_K(x_1, x_2, \dots, x_N) = (N!)^{-\frac{1}{2}} \det\{\psi_{k_1}, \psi_{k_2}, \dots, \psi_{k_N}\} \quad 1.7.11$$

where the x_j are the electron co-ordinates, in general including spin, then the basis of configuration interaction is that the correlated wave function may be described by a linear combination of the Ψ_K :

$$\Psi = \sum_K c_K \Psi_K \quad 1.7.12$$

The c_K can be determined in the usual way by the use of the variation principle, and solving the secular equation. If one term only is taken in equation 1.7.12, the result is the conventional Hartree-Fock scheme. For helium, taking one determinant only leads⁴⁵ to a correlation error, the difference between the exact eigenvalue of the Hamiltonian and its expectation value for the function being considered, of about 26.30 kcal/mole. To get higher accuracy, more terms are needed, but results show that if the angular dependence of the basis orbitals of

the Ψ_K is expressed in terms of spherical harmonics, convergence is often slow. For example, a computationally staggering 37 configurations are needed¹⁹ to reduce the correlation error for Be to just 1 kcal/mole.

If the wave function Ψ has a symmetry property represented by a projection operator O_p , then equation 1.7.12 may be modified to:

$$\Psi = \sum_K c_K O_p \Psi_K \quad 1.7.13$$

The basis set Ψ_K may now be reduced to the symmetry-adapted set, consisting of these Ψ_K whose symmetry under O_p is equivalent to the elements of symmetry of Ψ . This formalism has the advantage also that it leads to a certain type of splitting of the secular equation, and greater flexibility in the basis set is possible.

If only the leading term in the sum of equation 1.7.13 is used, then a generalisation of the Hartree-Fock model can be made, which allows for some correlation effects by using different functions for each set of electron co-ordinates, as opposed to the conventional spin-pairing procedure. This is concisely referred to as "different orbitals for different spins" and the method is therefore in this sense a special case of the symmetry-operator basis expansion method. The correlation error for helium by this method is¹⁴⁵ about 16 kcal/mole,

which is at least better than the correlation energy arising from the use of one unmodified determinant. The computational difficulties, however, are still considerable.

A system for allowing for correlation which has recently received much attention is the cluster expansion method. Starting usually from the HFF for the atom,²¹⁰ although versions have been proposed which start from analytical Slater and other functions,⁴⁴ deviations from the HFF are calculated which are due to the perturbations from binary encounters in the Hartree-Fock field of the other electrons. Further deviations, from three-body, etc., interactions can then be considered, but it is usually assumed that two-electron correlation is very much more important than the higher effects. While this assumption is certainly mathematically convenient, for the treatment even of binary interactions is very complicated, it is not certain that it is justified. Although the higher terms seem to be small individually, their greater number, if the total number of the electrons is not small, may easily make their total influence appreciable.

All of the foregoing so-called "expansion" methods depend for their utility on the choice of the basis orbitals of the Ψ_K . Any of the types of analytical function described earlier in this section may be, and have been, used. However, the basis set used should be mathematically complete in the sense

that an arbitrary normalisable one-electron function should be expressible in that basis. Thus, if hydrogen-like functions are used, the continuum must be included. Other functions, however, which are variations of the hydrogen-like functions, may be used. The basis set need not have a ready physical interpretation (cf. Gaussian bases) but it is sometimes convenient to express the total correlated wave function in terms of the Löwdin¹⁴⁷ "natural spin orbitals". If a truncated basis set is used, then scaling the wave function is important, and leads to considerable reductions in the correlation error. Scaling is achieved, for example in a function like the sum in equation 1.7.12, by multiplying the function by a scaling factor $\eta^{3N/2}$, where N is defined by equation 1.7.11, and η is adjustable so that the virial theorem is obeyed. Iterative alternate solving for the c_K , then for η , leads to a correctly scaled wave function.

The main method of treating correlation which does not depend on the use of expansions in basis sets of uncorrelated one-electron functions is perhaps also the most obvious: that of using correlated wave functions, i.e. functions which include the interelectronic distances r_{ij} explicitly. Two types of correlated wave functions have been used. The first type has proved practical only for two-electron systems, for which excellent results have been obtained. The classic example is the expansion found by Hylleraas for the 1^1S ground state of the

He atom; Hylleraas¹⁰⁵ used power series in (r_1+r_2) , (r_2-r_1) and r_{12} . The second type is capable of much more general application. It consists in multiplying the wave function by a correlation factor $g(r_{12}, r_{13}, r_{23} \dots)$ which is a function of all the interelectronic distances. This can be extended to the multiplication of a wave function already modified to some extent to take account of correlation. Thus a function of the form of equation 1.7.12, or of equation 1.7.13, may both be multiplied by g :

$$\Psi = g \sum_K c_K \Psi_K \quad 1.7.14$$

$$\Psi = g \sum_K c_K^0 \Psi_K \quad 1.7.15$$

Even if only the leading determinant in either of the sums in these two equations is taken, the correlation error is markedly reduced as compared to its value for the corresponding approximations of taking only one term in the sum of equation 1.7.12 or of equation 1.7.13. For helium, the one-term approximation gives a correlation error of about 2.3 kcal/mole and 1.16 kcal/mole for equations 1.7.14 and 1.7.15 respectively. This improvement is all the more remarkable because the correlation factor used to achieve it had the astonishingly simple form:

$$g(r_{12}) = 1 + \alpha_{12} r_{12} \quad 1.7.16$$

where α_{12} is an adjustable parameter. In the many-electron case, an extension of equation 1.7.16:

$$g_{ij} \equiv g(r_{ij})_{i,j} = 1 + \sum_{i < j} \alpha_{ij} r_{ij} \quad 1.7.17$$

has given considerable reductions in correlation errors.

The figures quoted above show that the method of correlation factors, especially when combined with other methods, is potentially a very powerful one. Even when it is used alone, the improvement of the wave function is significant. It will be seen that the correlation factor is at its most effective when used on the lead term of a symmetry-adapted basis set determinant. However, even a single Slater determinant is much refined by multiplication by a g_{ij} of the form given by 1.7.17. As usual, a balance has to be struck between accuracy and convenience, and it does seem that the use of g_{ij} multiplying a single determinant is a very fair compromise. It is of course very far from being the best available method, in the sense of the most accurate; but it does lead to a reduction in the correlation error which is well worthwhile, considering the simplicity of the procedure.

Numerous other methods for taking account of correlation have been proposed, including notably Bohm-Pines' plasma model¹⁷⁶ and the self-consistency scheme of Brueckner.^{23,24} It is however not necessary to discuss them here.

The last major modification to the simple atomic orbital

is of particular importance to the theory of NQR. Assumption (ii), page 215, was that the potential field with which the electrons interact was independent of the electronic angular co-ordinates, i.e. spherically symmetric. In fact, there are time-dependent variations from spherical symmetry due to the other electrons, and the allowances already discussed for electron correlation are necessary partly because of these deviations. Apart from this, there are deviations from a spherically symmetric field because (a) the nucleus itself, being neither a point charge nor a charged sphere, has a quadrupole moment which distorts the orbitals of those electrons which would otherwise have been described by a spherically symmetric orbital (the "core" electrons) and this distorted orbital therefore alters the quadrupole interaction; (b) this distortion can also be caused by the electrons which could never be described by a spherically symmetric orbital (the "valence" electrons: the $2p_x$, $2p_y$ or $2p_z$, or the hybrid orbitals in first-row elements), or (c) by extra-atomic charges. This whole set of distortions and interactions is now referred to as the "Sternheimer effect", although originally Sternheimer^{218,219,220} dealt only with effects of types (a) and (b) in a free atom.

The part played by the core electrons in NQR may be looked on in two ways. The quadrupolar nucleus, with moment Q , may induce in the core electrons a quadrupole moment ΔQ , by which

Q is modified. The modified "apparent" quadrupole moment Q' , with which the field gradient at the nucleus then interacts, is therefore given by:

$$Q' = Q + \Delta Q \quad 1.7.18$$

This is the description used by Sternheimer in his earlier papers. Alternatively, the distorted core may be considered to add a contribution to the field gradient at the nucleus, with which the unmodified Q then interacts. The two descriptions have been shown^{57,226} to be equivalent, and the latter will be used here.

As shown in detail in equation 1.3.11, $V_{\alpha\beta}$ is a sum of contributions from various sources:

$$V_{\alpha\beta} = \sum_i V_i \quad 1.7.19$$

where here the V_i represent contributions from sources including, to anticipate chapter 2, those outside the molecule. The very extensive studies of this problem have demonstrated that the effect of the core polarisation is an addition ΔV_i to each of the V_i , which can be well represented by the very simple relationship:

$$\Delta V_i = -\gamma_i V_i \quad 1.7.20$$

The sign in equation 1.7.20 is chosen because of the convention that if the core polarisation opposes the other contributions (shielding) then γ_i is positive, and vice-versa. Thus the

corrected value of $V_{\alpha\beta}$ would be:

$$V_{\alpha\beta} = \sum_i V_i (1 - \gamma_i) \quad 1.7.21$$

The quantities γ_i , the quadrupole shielding factors, are very dependent on the source of the contribution V_i , and in particular on the distance of the charge or charges producing V_i from the nucleus, and on the wave function used to describe them if they are electrons.

The methods used up till about 1961 to calculate γ_i and related quantities have been thoroughly reviewed by Dalgarno.⁵⁵ There are at present four important theoretical ways of estimating the γ_i . Three of these essentially look on the problem as one of perturbation with a Hamiltonian of the type $r^2(3 \cos^2\theta - 1)$. The basic methods of solution are, first, to solve numerically the first-order perturbation equation (done especially by Sternheimer and collaborators^{76,221,223,225,227}) This method, and the related Thomas-Fermi model, which is not now used, were historically first to be used. The second method is to treat the first-order equation by a variational procedure of minimising the second-order energy, thus obtaining perturbed wave functions which can be used to calculate γ_i (Das et al.,^{26,57,253} Burns²⁸, Wikner²⁹ and Ingalls¹⁰⁹). This method tends to underestimate γ_i for the nuclei of heavy atoms, for which the first method is better. Both methods,

however, ignore coupling between electron orbitals, and the third method (Dalgarno,^{55,56} Kaneko¹¹⁴ and Allen⁷) use a fully-coupled approximation.

The most recently developed, and in some respects the most promising, method is the unrestricted Hartree-Fock (UHF) method,¹³⁴ developed especially by Watson and Freeman.^{245,246,247,248} This method leads to values of the γ_i consistently greater than the corresponding values from other methods,²⁴⁸ probably because the inner shells are allowed to react to the greater distortion of the outer shells. Like the other methods, the UHF method is more successful with positive, especially unipositive, ions than with negative ions, though even here there has been limited progress.^{65,246} The most serious problem in the UHF approach is that the wave functions for the distorted closed shells no longer have 1S character, so that the single-determinant wave functions are no longer eigenfunctions of L^2 or of S^2 . The effects of this breakdown of correct symmetry are uncertain.

The conclusions reached, by whatever method, on the dependences of the γ_i are similar. The polarisation of the core can be analysed into two parts: radial excitations, from one principal quantum number shell to another; and angular excitations, within the same principal quantum number. The contributions to the γ_i from these two types of excitation can be

estimated separately. It is found that the angular contribution is usually relatively small and shielding ($\gamma_i > 0$), while the radial contribution may be very large indeed (see below) and is generally antishielding ($\gamma_i < 0$). The angular contribution is only slightly, and the radial part very strongly, dependent on the wave function used as a starting point; this can easily be understood by inspection of the kind of analytical wave functions used, e.g. equations 1.7.2-4. The inclusion of exchange terms is important for the calculation of the γ_i for the ground state of ions, although²²³ not so important for excited states. This has been demonstrated, for instance, by comparisons^{28,224} of results from Hartree and from Hartree-Fock wave functions, the latter giving the lowest γ_i . The UHF method takes best account of exchange terms, which the first method mentioned above neglects completely, and which the second method allows for only partially.

The UHF method, by definition, omits correlation effects between electrons. The inclusion of correlation effects is known⁸⁹ to be important for evaluations using two-electron operators, but not one-electron operators like $(q_{\alpha\beta})_i$ (equation 1.2.6). On the one hand, therefore, although it is doubtful what the effect of neglecting electron correlation in wave functions is for NQR, it is on the other hand not certain that antishielding factors calculated by the UHF method for

uncorrelated wave functions are meaningful when used with correlated wave functions. In this connection, it seems not always to be appreciated that the better a description of the true state of things a wave function is, then as a rule the smaller in magnitude will be the γ_i derived using it (compare the results from Hartree and from Hartree-Fock wave functions), and that for a wave function incorporating all multipole and distorting effects, correlation, and all other influences, all the γ_i would be zero. Thus, if γ_i from the UHF method are used with correlated wave functions, it might naïvely be expected that these γ_i would be too great in magnitude.

As well as the distorting tendencies (a), (b) and (c) listed on page 230, there are other such tendencies which may contribute to the field gradient at the nucleus. These include second-order quadrupole effects,^{221,223} dipole effects^{e.g.222} and relativistic effects,²⁴⁶ all of which are less important than the effects already outlined, either because the terms are intrinsically small, or because they often cancel.

Apart from the dependence of the γ_i on the wave functions used to describe both core and valence electrons, they are very dependent for any type of wave function on the distance R from the nucleus of the charge or charges making the contribution V_i (equation 1.7.19). In general, if R is much less than the atomic radius, $(1-\gamma_i) \div 1$, and it may not be serious to ignore

the correction. If R has about the value of the atomic radius, and this applies to valence electrons, the value of γ_i varies considerably. For a free atom in which only the valence electron interactions are considered, γ_i , in these circumstances represented conventionally by R or R_q (the latter will be used to avoid confusing with R above), is usually positive and has a value of ~ 0.1 . If R is very much greater than the atomic radius, γ_i is conventionally represented by γ_∞ , and is typically large and negative. It may be remarked that γ_∞ is also the appropriate factor²⁸ for multiplication of these effects mentioned in the preceding paragraph which arise from charges well outside the core.

The modified field gradient $V_{\alpha\beta}$ of equation 1.7.21 may therefore be crudely approximated by:

$$V_{\alpha\beta} = V_{\text{val}}(1 - R_q') + V_{\text{ext}}(1 - \gamma_\infty') \quad 1.7.22$$

where the sum of equation 1.7.21 has been split into two terms.

V_{val} represents the sum of all the contributions from the "valence" electrons, i.e. terms ~~III~~, IV, VI, VIII, IX and X of equation 1.3.11, and V_{ext} represents the sum of all contributions from charges wholly external to the core of A, i.e. all the other terms of equation 1.3.11 except II, whose contribution is effectively included by making these corrections. R_q' and γ_∞' are correction factors which may be approximately equal to R_q and γ_∞ as defined previously; however, they are averaged factors

standing for a range of exact correction factors whose values may vary between wide limits. The validity of this is very uncertain, particularly for R_Q which refers to values of R for which γ_1 is changing most quickly, but no better simple method is at present available. These considerations also call into question the Townes-Dailey device (section 1.4) of defining a q_{at} , which assumes that R'_Q is very nearly equal to R_Q . V_{ext} is usually much smaller than V_{val} , and when the latter is non-zero, the former is usually disregarded, but this may be unjustified if γ_∞ is very large, as it is for heavy ions. The implications of this for the temperature dependence of NQR are indicated in chapter 2.

Luckily for the interpretation of the NQR of ^{14}N , the corrections necessary are generally smaller, and often much smaller, than those for other atoms. Also, the core radius of the nitrogen atom is quite small, so that the approximation $\gamma'_\infty \doteq \gamma_\infty$ is better than it sometimes is. For nitrogen, $R_Q \doteq 0$ (the ground state of the nitrogen atom is spherically symmetric; however the probable valence states of nitrogen are very different from the ground state), and for γ_∞ , recent UHF calculations¹³⁴ give $\gamma_\infty(N^{5+}) = 0.0996$ and $\gamma_\infty(N^{3+}) = 0.351$.

1.8 Evaluation of the integrals

Equation 1.3.11 calls for the evaluation of the following types of one-electron integral:

- (i) $(\psi_A | q_{\alpha\beta} | \psi_A)$ 1-centre, terms II, IV and VI;
- (ii) $(\psi_B | q_{\alpha\beta} | \psi_B)$ symmetrical 2-centre, terms III, V and VII;
- (iii) $(\psi_B | q_{\alpha\beta} | \psi_A)$ unsymmetrical 2-centre, terms VIII, IX and X; and
- (iv) $(\psi_B | q_{\alpha\beta} | \psi_C)$ 3-centre, term XI.

If correlated wave functions are used, corresponding two-electron integrals may be needed. The subscripts denote the nucleus on which the operator or orbital is centred. B and C in this section simply mean nuclei other than A.

If the ψ_K are orbitals based on a Gaussian set, fairly simple closed formulae can be given.¹⁹³ Following the conclusions of the previous section, however, the use of Gaussian orbitals will not be developed here, and only the evaluation of matrix elements in a Slater basis will be considered. The most commonly used form of the Slater-type orbitals $\psi_{n|m}$ is:

$$\psi_{n|m} = N_{n|m} R_n Y_m^l \quad 1.8.1$$

In this form, $\psi_{n|m}$ is an eigenfunction of \mathcal{H} , M and H_z . R is the radial part, and Y_m^l is a spherical harmonic in ϑ and φ whose definition is taken here in the form:

$$Y_m^l = \left\{ \frac{(2l)!}{(l-m)!} (1-x^2)^{|m|/2} \right\}^{1/2} \frac{1}{l!} \times \left(\frac{d^{l+|m|}}{dx^{l+|m|}} \right) (x^2-1)^l e^{im\varphi} \quad 1.8.2$$

where $x = \cos \vartheta$

and e in this equation only is the exponential base.

The orbitals used in the preceding sections, however, are the

standing-wave solutions, which are linear combinations of the

ψ_{nlm} . The relationships are:

$$\psi(1s) = \psi_{100} \quad 1.8.3a$$

$$\psi(2s) = \psi_{200} \quad 1.8.3b$$

$$\psi(2p_x) = \frac{1}{\sqrt{2}}(\psi_{211} + \psi_{21-1}) \quad 1.8.3c$$

$$\psi(2p_y) = \frac{1}{\sqrt{2}i}(\psi_{211} - \psi_{21-1}) \quad 1.8.3d$$

$$\psi(2p_z) = \psi_{210} \quad 1.8.3e$$

etc.

In consequence, the angular parts of the standing-wave solutions are corresponding linear combinations of the Y_m^l . The angular parts for the most important wave functions for the first-row elements become:

$$\Theta(\vartheta)\Phi(\varphi)(1s) = \Theta(\vartheta)\Phi(\varphi)(2s) = 1 \quad 1.8.4a$$

$$\Theta(\vartheta)\Phi(\varphi)(2p_x) = \sin\vartheta\cos\varphi \quad 1.8.4b$$

$$\Theta(\vartheta)\Phi(\varphi)(2p_y) = \sin\vartheta\sin\varphi \quad 1.8.4c$$

$$\Theta(\vartheta)\Phi(\varphi)(2p_z) = \cos\vartheta \quad 1.8.4d$$

Thus the angular part for $2p_\alpha$ is simply α/r , where $\alpha \equiv x, y$ or z .

The radial part of the Slater wave functions is still given by equation 1.7.9:

$$R_n = r^{n-1} \exp(-\zeta r/n) \quad 1.8.5$$

where now ζ is used for the effective nuclear charge, and n is exactly the principal quantum number.

The description of the functions is completed by listing the values of N :

$$N(1s) = (\zeta^3/\pi)^{\frac{1}{2}} \quad 1.8.6a$$

$$N(2s) = (\zeta^5/96\pi)^{\frac{1}{2}} \quad 1.8.6b$$

$$N(2p_x) = N(2p_y) = N(2p_z) = (\zeta^5/32\pi)^{\frac{1}{2}} \quad 1.8.6c$$

Extensions of equations 1.8.4-6 for other orbitals are of course readily available in standard texts^{198,211} if they should be necessary.

The integration of the angular parts is readily enough carried out using the following standard integrals:

$$\int \cos^m x \sin x \, dx = -(\cos^{m+1} x)/(m+1) \quad 1.8.7$$

$$\int \cos x \sin^n x \, dx = (\sin^{n+1} x)/(n+1) \quad 1.8.8$$

$$\int \cos^m x \sin^n x \, dx = \frac{\cos^{m-1} x \sin^{n+1} x}{m+n} + \frac{m-1}{m+n} \int \cos^{m-2} x \sin^n x \, dx \quad 1.8.9$$

$$\int \cos^m x \sin^n x \, dx = \frac{\sin^{n-1} x \cos^{m+1} x}{m+n} + \frac{n-1}{m+n} \int \cos^m x \sin^{n-2} x \, dx \quad 1.8.10$$

The values of the definite integrals over $0-\pi$ and $0-2\pi$ are needed separately for many of the expansions of multicentre integrals, and for convenience they are set out in Table 1.8.1, page 241, for the most commonly occurring functions.

The radial integrals are simply evaluated by using:

$$\int_0^\infty x^n \exp(-ax) \, dx = n! / a^{n+1} \quad (n \text{ a positive integer; } a > 0) \quad 1.8.11$$

For noninteger n , analytical closed-form functions are available²⁰⁹ but since Slater functions with noninteger n have not been used in section 1.7, the evaluation need not be discussed here. As already indicated in section 1.7, the radial part is that

TABLE 1.8.1: VALUES OF $\int_0^a f(x)dx$ FOR ANGULAR FUNCTIONS

$f(x)$	$a = \pi$	$a = 2\pi$
1	π	2π
$\sin x$	2	0
$\cos x$	0	0
$\sin^2 x$	$\pi/2$	π
$\cos x \sin x$	0	0
$\cos^2 x$	$\pi/2$	π
$\sin^3 x$	$4/3$	0
$\cos x \sin^2 x$	0	0
$\cos^2 x \sin x$	$2/3$	0
$\cos^3 x$	0	0
$\sin^4 x$	$3\pi/8$	$3\pi/4$
$\cos x \sin^3 x$	0	0
$\cos^2 x \sin^2 x$	$1/8$	$\pi/4$
$\cos^3 x \sin x$	0	0
$\cos^4 x$	$3\pi/8$	$3\pi/4$
$\sin^5 x$	$16/15$	0
$\cos x \sin^4 x$	0	0
$\cos^2 x \sin^3 x$	$4/15$	0
$\cos^3 x \sin^2 x$	0	0
$\cos^4 x \sin x$	$2/5$	0
$\cos^5 x$	0	0

part of the atomic wave function whose analytic form presents most difficulty.²²⁸ The radial integral

$$\int f^*(r) \cdot (r^{-3}) \cdot f(r) r^2 dr = \langle 1/r^3 \rangle \quad 1.8.12$$

where $\langle 1/r^3 \rangle$ is as usual the average value of $1/r^3$ for the electron in that orbital. The quantity $\langle 1/r^3 \rangle$ is one which is found in many spectroscopic contexts apart from N_2R , and it is sometimes possible to find empirical or semi-empirical values for it.^{104,128} If these values are used, then of course the N of equation 1.8.6 need to be modified so as not to include the radial normalisation factor twice over. If Slater-type orbitals are used, reference to Table 1.8.1 and evaluation of equation 1.8.11 show that, if only orbitals with $n=1$ or 2 are used, the only non-zero one-centre matrix elements for first-row elements are:

$$(p_\alpha | q_{\alpha\alpha} | p_\alpha) = -e \cdot \zeta^3 / 30 = d_1 \quad 1.8.13a$$

$$(p_\alpha | q_{\beta\beta} | p_\alpha) = +e \cdot \zeta^3 / 60 = d_2 \quad 1.8.13b$$

$$(p_\alpha | q_{\alpha\beta} | p_\beta) = +e \cdot \zeta^3 / 40 = s \quad 1.8.13c$$

In view of the facts that the one-centre matrix elements, connecting orbitals on A only, are larger than the multicentre matrix elements considered later, and that the Townes-Dailey theory virtually considers only such matrix elements, it is of some interest to examine the implications of equations 1.8.13 for matrix elements diagonal in A. In particular, the off-diagonal tensor components, given by 1.8.13c, may be written:

$$V_{xy}(A) = -(\alpha_3 - \alpha_4)(a_2 a_3 a_4 / a_5^2 a_6^2)s \quad 1.8.14a$$

$$V_{yz}(A) = +[(a_1^2 + a_2^2 - 1)(\alpha_2 - \alpha_4) + a_3^2(\alpha_3 - \alpha_4)] \\ \times (a_1 a_2 / a_5 a_6^2)s \quad 1.8.14b$$

$$V_{zx}(A) = -(\alpha_3 - \alpha_4)(a_1 a_3 a_4 / a_5 a_6^2)s \quad 1.8.14c$$

in the notation of previous sections. Equations 1.8.14 show that, if one-centre contributions alone to the tensor $V_{\alpha\beta}$ are considered, then the off-diagonal components are zero, and the molecular axes xyz are parallel to (but not necessarily congruent with) the principle axes XYZ, if $a_3 = a_2 = a_1 = 0$ (no hybridisation) or if $a_3 = a_2 = 0$ (sp_z hybridisation); but if only $a_3 = 0$ (sp^2 hybridisation) then only if $\alpha_2 = \alpha_4$. The first two conditions are those encountered, or assumed, most often in halogen compounds. When the hybridisation is sp^2 , then the condition $\alpha_2 = \alpha_4$ is essentially the familiar one that the two hybrid bonds directed away from the z axis must have equal ionic characters.

It is also of interest that, if the xyz and XYZ axes are congruent, the condition for cylindrical or higher symmetry ($\eta = 0$) can be shown to be:

$$\alpha_2(1 - a_1^2 - a_2^2)^2 + \alpha_3[a_2^2 a_3^2 - a_4^2(1 - a_1^2)] \\ + \alpha_4[a_2^2 a_4^2 - a_3^2(1 - a_1^2)] = 0 \quad 1.8.15$$

Equation 1.8.15, in the special conditions just listed, is of course simplified; and many of the conclusions of the Townes and Dailey analysis turn up as special cases of the boundary

conditions for equations 1.8.14 and 1.8.15 taken together.

In the general case, determination of the direction of the principal axes is difficult. However, in the interpretation of results, great simplification is sometimes made possible by symmetry considerations. Thus, any n -fold rotation or rotation-reflection axis ($n > 2$) means that $\eta = 0$. In addition, $q = 0$ if two or more rotation axes, ^{3-fold} twofold or higher, exist, as in cubic or tetrahedral symmetry. Only two twofold rotation axes, or a reflection plane containing one twofold axis, define the principal axes.

The evaluation of two-centre matrix elements is more difficult. The simple overlap terms, which are needed for some purposes connected with the interpretation of NQR, have been thoroughly tabulated,²² particularly by Mulliken et al.¹⁶⁴ No comparable tabulation exists for the matrix elements of $q_{\alpha\beta}$, and except in a few favourable cases¹⁵⁷ analytical closed expressions have not been found.³⁶

In general, matrix elements of the pattern $(B|A|B)$ are evaluated most conveniently by expanding the operator centred on A about a new origin centred on B. For the purposes of such an expansion, it is more convenient to revert to the ψ_{211} and ψ_{21-1} wave functions than to use the p_{α} forms. Matrix elements evaluated in this way can of course be easily reconverted to matrix elements for the p_{α} form of the wave function

by use of equation 1.8.3. The method of expansion is described, and has been developed in detail, by Pitzer et al.¹⁷⁷ The operator is expanded in terms of spherical harmonics about B, and the resulting infinite sum of integrals is evaluated by integration separately in three ranges 0 to R- ϵ , R- ϵ to R+ ϵ , and R+ ϵ to ∞ (R is the internuclear distance AB). ϵ is then put equal to zero and the integrals in the three ranges added. Wallace,²⁴³ who simplifies this very tedious procedure to some extent by introducing Wigner 3-j symbols into the evaluation, as suggested by Edmonds,⁶⁹ gives explicit formulae for the matrix elements $(\psi_B | q_{zzA} | \psi_B)$ - page 162 of reference 243.

Two-centre matrix elements of the pattern (A|A|B) are more difficult to evaluate than two-centre matrix elements of the other type. Expansion of the function on B about A gives a doubly infinite sum of one-centre matrix elements, which can be expressed, as described by Barnett and Coulson^{13,14} in terms of "Z functions". These are defined by:

$$Z_{m,n,l+\frac{1}{2}}(\kappa, \tau) = \int_{t=0}^{\infty} \exp(-\kappa t) \cdot \zeta_{m,n}(l, t; \tau) t^{l+\frac{1}{2}} dt \quad 1.8.16$$

where l, m and n are integral parameters, $\kappa = \zeta_A / \zeta_B$ and the ζ_K refer to the radial part of the orbital centred on K and have the same meaning as in equation 1.8.13; $t = \zeta_B r_A$ with r_A the distance from A; $\tau = \zeta_B R$, and the functions $\zeta_{m,n}(l, t; \tau)$ are defined¹³ when $m=0$ as a product of two standard Bessel functions of purely imaginary argument, and as a weighted sum

of such products when $n \neq 0$. The evaluation of the Z functions is fully described by Barnett and Coulson. Again using Wigner 3-j symbols, Wallace²⁴³ gives a number of explicit expansions in terms of Z functions for some unsymmetrical two-centre matrix elements (there are errors in Wallace's tabulation). For noninteger n, methods are available²⁰⁹ for expressing two-centre overlap and Coulomb integrals, which could be extended to the evaluation of matrix elements of $q_{\alpha\beta}$. Again, however, this need not be discussed here. Simpler closed expressions which apply to linear molecules only are given for both types of two-centre integral by McLean and Yoshimine.¹⁵⁷

The value of three-centre integrals is so small as not to justify the labour of computing them, except in a few special situations, the most important of which are multicentre molecular orbitals, which generally imply conjugation and have already been excluded, and linear molecules, in certain of which three-centre integrals may have slightly higher values, although still very small compared to those of the one- and two-centre integrals. Closed expressions for three-centre integrals in a linear molecule are again given by McLean and Yoshimine.¹⁵⁷

If a correlation factor $g(r_{ij})$, as described in section 1.7, is included in the wave function, then as well as the preceding types of matrix element, integrals of the form:

$$\int_0^\infty dr_1 dr_2 r_1^{n_1-1} r_2^{n_2-2} \exp(-\zeta_1 r_1 - \zeta_2 r_2) g(r_{12}) \quad 1.8.17$$

will need to be evaluated. Here, the subscripts 1 and 2 refer to the two electrons and all other symbols have their previous meaning. The evaluation of such integrals has been discussed in a very general way by Karl,¹¹⁵ and for more limited circumstances, and consequently with simpler closed expressions, by many authors, such as Roberts,¹⁹² whose treatment would be adequate for any ordinary purpose connected with the interpretation of NQR.

2.1 Introduction

The existence of intermolecular effects is demonstrated by the difference between the nuclear quadrupole coupling constant in the gaseous state and that in the solid state: the first is obtained usually from microwave spectroscopy and the second from pure NQR. The difference depends on the compound being studied; usually eQq for the solid is lower than in the gas. For nitrogen-containing compounds, the solid at 77°K has, typically, a value of eQq some 10% to 20% lower than the value in the gas (see Appendix C1).

Intermolecular contributions to the field gradient are therefore smaller than intramolecular contributions, and the difficulty of estimating them is greater than even the difficulty of estimating intramolecular effects. Such success as has been attained in the study of intermolecular contributions has been more qualitative than quantitative. However, an outline of current methods of making these estimations is given in this chapter.

Three ways might be distinguished in which the quadrupole coupling constant in the solid state could be altered from its value in the gas state by the influence of other molecules. There is the direct effect of charge distributions in nearby

molecules, as modified by the electrons of the molecule under consideration. This is dealt with in section 2.2. There is the indirect effect of the change in the actual molecular wave functions because of the Van der Waals interactions between molecules, discussed in section 2.3. Finally, chemical bonds, and especially hydrogen bonds, may exist in the solid and not in the gas: the changes due to this new bonding are relatively large, and it might be said that the molecules in the solid are different from those in the gas. This forms the theme of section 2.4.

In compounds of nitrogen, as in most other compounds, the value of the quadrupole coupling constant is found to be very temperature-dependent. The temperature coefficients found for nitrogen-containing compounds vary over a wider range than those found, for example, for chlorine, but usually the temperature coefficient is negative, and its magnitude is from 10^{-5} to 10^{-3} Mc/sec/degree. Sections 2.5 and 2.6 deal with this subject.

There are many other observable effects of the crystal structure on the quadrupole resonance spectra.⁵⁸ Most importantly, treatments analogous to the Bloch equations for NMR¹⁴⁹ exist for spin-echo and other transient-effect experiments⁵⁸ and for broadening not associated with thermal motion.^{3,58,77} These topics are however peripheral to the main object of Part C,

and are not considered further.

2.2 Direct intermolecular effects

In the gas, thermal motion averages to zero (or nearly to zero) the effects of charges on molecules other than that containing nucleus A, but in the solid, thermal motions are much more restricted and there are residual effects from these charges on the electric field gradient tensor at the nucleus.

Suppose the molecule in which a particular nitrogen nucleus A is situated is surrounded by other molecules, labelled 1 ... i ... m. Consider first the contribution of one molecule, thought of simply as a charge distribution, to the tensor $V_{\alpha\beta}$. The potential, V_i , from a charge distribution described by a function $\rho_i(\underline{r})$, located near a point \underline{r}_i , where r_i is large compared to molecular dimensions, is given by:

$$V_i = \int [\rho_i(\underline{r}) / (r - r_i)] d\tau \quad 2.2.1$$

Equation 2.2.1, if expanded using the binomial theorem (the procedure is of course like that used in chapter 1 of Part B), becomes:

$$V_i = \int \rho / r_i d\tau + \int (\rho \underline{r} \cdot \underline{u}_{ri} / r_i^2) d\tau + \int [\rho (3(\underline{r} \cdot \underline{u}_{ri})^2 - r^2) / 2r_i^3] d\tau + \dots \quad 2.2.2$$

where \underline{u}_{ri} is the unit vector \underline{r}_i / r_i .

The first term in equation 2.2.2 is a monopole term, the second a dipole term, the third a quadrupole term, and so on. The 2^n -pole moment can be defined by its general component $2^n \rho \alpha_1 \dots \alpha_n$:

$$2^n p_{\alpha_1 \dots \alpha_n} = \int \rho \left(\prod_{i=1}^n \alpha_i \right) d\tau \quad 2.2.3$$

Thus the contribution to V_i of the 2^n -pole term has the form $2^n p/r_i^{n+1}$ (the exact form depends actually on the exact definitions adopted for the p : equation 2.2.3 is only a common form).

Therefore, if the $\alpha\beta$ component of the contribution of the 2^n -pole term of the i th molecule is represented by ${}^n V_{\alpha\beta i}$, then ${}^n V_{\alpha\beta i}$ has the space-dependent part:

$$\frac{(n+1)(n+3)\alpha\beta - (n+1)r_i^2 \delta_{\alpha\beta}}{r_i^{n+5}} \quad 2.2.4$$

Equations like equation 1.2.6 represent the special case of expressions like 2.2.4 when $n = 0$.

The total contribution to $V_{\alpha\beta}$ from m external charge distributions would therefore be:

$$V_{\alpha\beta} = \sum_{j=1}^n \sum_{i=1}^m j V_{\alpha\beta i} \quad 2.2.5$$

However, the Sternheimer effect for molecules has to be taken into account. It has been shown²⁸ that the modification of $V_{\alpha\beta}$ due to monopole, dipole ... effects can be described by multiplying by the same factor $(1-\gamma_M)$. Finally, then,

$$V_{\alpha\beta} = (1 - \gamma_M) \sum_{j=1}^n \sum_{i=1}^m j V_{\alpha\beta i} \quad 2.2.6$$

γ_M is analogous to γ_∞ for the atom. The value of γ_M has not been widely studied^{58,65,226} but rough semi-empirical

considerations⁵⁵ suggest that for most covalent molecules, $0 < \gamma_M < 1$ (for example for Li_2 , γ_M has been calculated²²⁶ to be 0.24), and so the effect of the correction factor in equation 2.2.6 is probably to reduce the magnitude of the contributions $j_{V_{\alpha\beta i}}$.

It can be seen from expression 2.2.4 that $j_{V_{\alpha\beta i}}$ has the dimensions of $r_i^{-(j+3)}$, so that the magnitude of $j_{V_{\alpha\beta i}}$ falls off quite quickly as j increases, and in practice terms for $j \geq 3$ are very rarely considered. Furthermore, for a neutral molecule, the "monopole moment" (i.e. charge) given by equation 2.2.3 is obviously zero, and so, in consequence, is $0_{V_{\alpha\beta i}}$. If the molecule has no dipole moment, $1_{V_{\alpha\beta i}}$ is also zero, and so on. Finally, even if $0_{V_{\alpha\beta i}}$ or $1_{V_{\alpha\beta i}}$ are not zero, in many molecular crystals, the terms in the summation of the $V_{\alpha\beta i}$, i.e. the summation over the molecules, are roughly equal in magnitude but opposite in sign,⁷⁷ and the result of the summation over all the molecules is much smaller in magnitude than is any one term.

The conclusion is, therefore, that, unless most of the following conditions are met:—

- (i) $\gamma_M \gg 0$,
- (ii) intermolecular distances are about equal to intramolecular distances,
- (iii) the molecules are charged (this includes ionic crystals,

where the "molecules" are ions),

(iv) the molecules have a large dipole or higher multipole moment,

(v) one particular molecule is at a site of very low crystalline symmetry (this does sometimes occur because for example of strains in the crystal⁷⁷),

then direct effects may to a very good approximation be neglected.

In crystals of organic nitrogen-containing compounds, it is likely that none of these conditions, except (ii), and occasionally (iii) or (iv), is usually operative. With these few exceptions, then, the approximation applies to the compounds considered in this thesis.

2.3 Indirect intermolecular effects

Apart from the direct effect discussed in the preceding section, neighbouring molecules can also affect the field gradient tensor indirectly. The energy of cohesion of molecules in a molecular crystal is made up from (i) direct Coulomb interactions between charge distributions on the molecules, (ii) contributions from polarisation and dispersion forces between the molecules, (iii) possible hydrogen bonding, and (iv) sometimes true "chemical" bonds. Any or all of these influences may affect the molecular wave function, and so alter from their values in the gas phase either or both of the "atomic" and "molecular" coefficients dealt with in sections

1.5 and 1.6 respectively. Effects (i) and (ii) are considered in this section, and effects (iii) and (iv) in the next one: to some extent this division is arbitrary, and effects (i) to (iv) simply represent increasing electronic perturbation from the state in the isolated molecule.

Fundamentally, the electronic wave function for a molecule in a crystal is different from the wave function for the isolated molecule because additional potential terms, arising from the presence of the other molecules, have to be included in the Schrödinger equation. Any attempt to estimate the new wave function by incorporating these new terms is likely to succeed only for very simple crystals indeed, and those at very low temperatures: the solid phases of He and Ne are examples. For molecules of practical interest, an approach more likely to be fruitful is to take the isolated-molecule wave function (itself inexact) and to try to estimate the perturbations which are induced on that by the other molecules. This involves a knowledge of the dependences of the lattice energy on the crystal and other environmental parameters.

There are two theoretical problems in the treatment of intermolecular forces in a crystal: the determination of the forces, and hence energy, between two otherwise isolated molecules; and the statistical-mechanical generalisation of the results to an assembly of molecules in a crystal. Both problems,

and especially the first, are unsolved, and a general theory of intermolecular forces seems unlikely in the foreseeable future.

If for the present discussion other thermodynamic effects such as the effect of entropy are neglected, it can be said that the wave function of a molecule in a crystal is such as to minimise potential energy. If it is assumed that the isolated-molecule wave function does this for the isolated molecule, the perturbation arises from the minimisation of solid-state energy. Binary intermolecular interaction forces are generally classified²¹ as short-range and long-range forces.

Short-range forces are overwhelmingly repulsive, governed mainly by the Pauli exclusion principle, although also having contributions from simple interelectronic repulsion terms. The associated energy, E_S , can be shown by quantum-mechanical calculations to have the form:

$$E_S = F(r, \vartheta, \varphi) \exp(-Ar) \quad 2.3.1$$

where r, ϑ , and φ are the co-ordinates of one molecule with respect to axes fixed in the other, $F(r, \vartheta, \varphi)$ is a polynomial in r, ϑ and φ ; if r is small, other terms describing the orientation of the second molecule are of course necessary. In favourable cases, ϑ and φ are not necessary in the description; this is sometimes true because of thermal motion. E_S increases rapidly with decreasing r and is numerically the same as,

although opposite in sign to, the energy which would in incomplete orbitals have led to chemical combination. Intermediate-range forces, or "long short-range" forces²¹, such as charge exchange, are sometimes considered, but there is little evidence of their importance.

The long-range binary forces are predominantly attractive. They are conventionally divided into dipole-dipole, dipole-induced-dipole, and dispersion forces. For all of these forces, also, the molecular orientation is almost certainly important, unless the molecule has high symmetry intrinsically or because of thermal motion, but in practice most work has concentrated on the elucidation of the dependence on simple separation. The long-range energy of interaction between two molecules 1 and 2 a distance r apart, and with dipole moments and polarisabilities μ_1, μ_2 and α_1, α_2 respectively, is:

$$E_L = -\frac{1}{r^6} \left[\frac{2\mu_1^2 \mu_2^2}{3kT} + \mu_1^2 \alpha_2 + \mu_2^2 \alpha_1 + \frac{3}{2} h \alpha_1 \alpha_2 \frac{v_1 v_2}{v_1 + v_2} \right] \quad 2.3.2$$

The first term in the brackets represents the dipole-dipole interaction. It is the average attractive energy of two dipoles, and it is therefore temperature-dependent; the use of the Boltzmann distribution in the evaluation of this term accounts for the presence of the Boltzmann constant k . It is assumed that there are no net charges on any of the molecules, that

is that there are no ions. If ions are present, there is of course a Coulombic attraction term proportional to r^{-1} , and this is much the most important term; the existence of such an overwhelmingly important term makes the interpretation of NQR results in ionic crystals much easier than it is in molecular crystals.^{43,77,125} The dipole-dipole term is in fact the leading term in the expansion of the multipole interaction energy (compare equation 2.2.2): higher multipole interaction terms depend on higher inverse powers of r and are therefore smaller, although they may need to be considered for some purposes.¹⁵⁸

The second and third terms in brackets in equation 2.3.2 are dipole-induced-dipole terms. They are generally small, unless the dipole polarisability α is very large. As for the dipole-dipole terms, higher multipole terms exist, but they are very small indeed.

The fourth term in brackets in equation 2.3.2 represents London (dispersion) forces, which, it seems likely, are most important for crystals of most organic compounds, especially those containing π systems.¹⁷⁸ In this term, ν_1 and ν_2 represent the characteristic frequency of the charge distribution. Especially in non-polar molecules, the London term is usually the largest of the terms in equation 2.3.2. This, together with the facts that London forces are additive pairwise to a reasonable

approximation, and for simple molecules at least are little dependent on orientation, has led to most work being done on the assumption of the dominance of dispersion forces in molecular crystals, and within its obvious limitations, this has been developed and modified considerably.⁹

By combining equations 2.3.1 and 2.3.2, the lattice energy E for an unmixed crystal at constant temperature can be written:

$$E = -Ar^{-6} + Br^{-n} \quad 2.3.3$$

where A replaces the term in brackets in equation 2.3.2, and Br^{-n} has been used instead of the form of equation 2.3.1 for E_s ; although the latter is more accurate, it is mathematically less convenient. Values of n which have been used range from 9 to 12 (Lennard-Jones potential). The difficulties in using an expression such as 2.3.3 in an attempt to evaluate the change in molecular electronic wave functions are enormous.

The principal ones are:

- (i) μ , α and v all depend in an uncertain way on the wave function;
- (ii) even if these dependences were known, an iterative minimisation of E , with respect to r and the three interconnected variables μ , α and v is probably necessary: the iteration may not be convergent, and it is mathematically formidable;
- (iii) even if (i) and (ii) were overcome, equation 2.3.3, or even equations 2.2.1 and 2.2.2 together, are of uncertain

accuracy: only leading terms in expansions are taken, and the expansions themselves may not be justified.⁹

In face of these difficulties, most workers have interpreted effects of the type discussed here only qualitatively.⁵⁸ Thus, if E in equation 2.3.3 is to be minimised, then, given the intermolecular separation, A should be maximised. From equation 2.3.2, this means that μ , α and v should be maximised also, and changes in the wave function which tend to increase μ , α or v should be favoured. Unfortunately, the increase of all three parameters is usually not consistent. Examples are known⁵⁸ where the change in NQR coupling constants of halogens can be accounted for by an increase in μ . However, μ for nitrogen-containing compounds does not usually depend simply on the ionic character of a bond between nitrogen and another element: in such a situation, increased ionic character would tend to increase q in many molecules. The dependence of α on the wave function is very complex⁵⁵ and usually α is strongly anisotropic, so generalised statements are even more difficult to make than for the effect of changes in μ . It is very roughly true, however, that π -systems have higher α s than have σ -systems. The value of v increases as the extension of the wave function, as measured for instance by $\langle r^2 \rangle$, decreases, but no detailed study of its variation for molecules exists. Thus the variation of α and v can be accompanied by very complicated changes

in hybridisation.

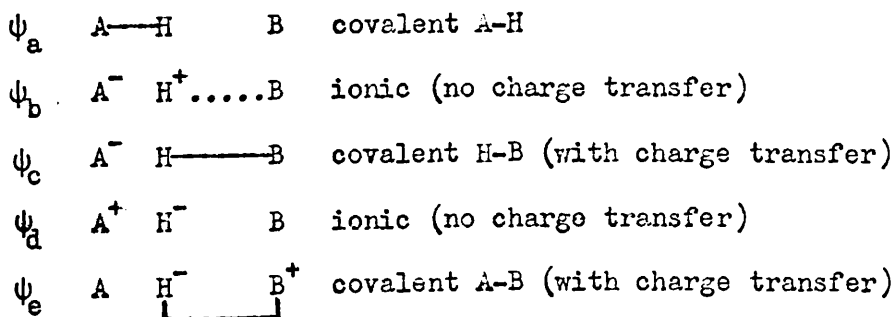
2.4 Intermolecular bonding

If hydrogen bonding is included in the phrase "intermolecular bonding", it is likely that intermolecular bonding effects make the most significant contributions to the change in nuclear quadrupole parameters in passing from the gas to the solid phase. The most successful explanations of such changes have depended on intermolecular bonding in the crystal; however the great difficulty of making arguments based on indirect effects should be remembered. Thus, intermolecular bonding has been invoked with considerable success⁵⁸ to explain the NQR frequencies of the solid halogens. In nitrogen NQR, the decrease of 12.6% in eQq in going from gas to solid in NH_3 was accounted for by O'Konski and Flautt¹⁶⁸ by supposing an increase in ionic character on the formation of hydrogen bonds, for example, and the interpretation of the observed eQq for BrCN and ICN by Watkins and Pound²⁴⁴ in terms of intermolecular bonding is a classic example of this approach.

An estimate of the effect of hydrogen bonding depends on having a theory of the hydrogen bond, and there is no general agreement on such a theory.¹⁷⁵ The three most popular accounts, which are obviously not mutually exclusive, are the electrostatic model, the VB description, and the MO description, in order of decreasing popularity. The electrostatic model attributes

the energy of the bond H...B in A-H...B to the electrostatic attraction between the positive hydrogen and the resultant negative charge distribution, including the lone-pair distribution, on B. The latter can be determined from the non-bonding orbital as given by equations like equation 1.3.2. Either the charges can be placed to give the correct dipole moment,¹³⁹ or the hybridised non-bonding orbital can be replaced by a point charge at its centroid,¹⁹⁹ and the energy calculated. There are special difficulties in using the electrostatic picture of the hydrogen bond to predict quantitatively the change in NQR frequencies from those in the isolated molecule: the argument back from simple physical quantities like dipole moment directly to associated quantum mechanical features like the wave function is notoriously full of pitfalls.

The VB description depends usually on the five canonical structures shown below at most:



The coefficients of mixing a ... e corresponding to the wave function labels given as subscripts above can be estimated semi-empirically, as by Coulson and Danielsson,⁴⁸ or by an attempt

at a more rigorous variational calculation.^{48,237} Unfortunately, the values of $a \dots e$ are very strongly dependent on uncertain parameters, and estimates of them made rest on a number of assumptions which are difficult to justify quantitatively. Thus Coulson and Danielsson⁴⁸ assume that the ionic character does not change when the H-bond forms, in direct contradiction to the experimental findings of for example O'Konski and Flautt,¹⁶⁸ and that the A-H distance is constant, which agrees poorly with other experimental evidence.¹⁷⁵ The less empirical procedures give values of $a \dots e$ which do not depend on unattractive physical assumptions, but which do depend on mathematical assumptions made to increase the tractability of complicated integrals; and again the coefficients depend strongly on parameters whose value is uncertain, e.g. in ice I, for $r_{O-H} = 1.00 \text{ \AA}$, $c^2 \doteq 0.11$, whereas for $r_{O-H} = 1.07 \text{ \AA}$, $c^2 \doteq 0.22$. Nevertheless, if reliable values could be found, the contribution of the H-bond to the components of $V_{\alpha\beta}$ could be found very simply indeed.

Like the VB picture, the MO description would essentially be used to calculate afresh the contribution of the electrons involved in the H-bond to the $V_{\alpha\beta}$, rather than to attempt to find changes from the value in the isolated molecule. The MO description of the H-bond has received surprisingly little attention, considering the attractions of simplicity which it has.

The treatment given by Pimentel¹⁷⁴ can be generalised to give three orbitals from the three component atomic orbitals (since the H-bond involves four electrons, more than the bonding orbital must be considered). The three hydrogen-bond orbitals are:

$$\begin{aligned} \text{(bonding)} \quad \psi_1 &= \lambda_1 [(h_A + b_1 h_B) + a_1 s] \\ \text{(nonbonding)} \quad \psi_2 &= \lambda_2 [b_2 h_A - h_B] \\ \text{(antibonding)} \quad \psi_3 &= \lambda_3 [(h_A + b_3 h_B) - a_3 s] \end{aligned} \quad 2.4.1$$

where λ_1 , λ_2 and λ_3 are normalising constants, s is the $1s$ orbital of hydrogen, and h_A and h_B are appropriate orbitals, of the general form given by equations 1.3.2, on A and B.

The coefficients a_1 , a_3 , b_1 , b_2 and b_3 could be determined semiempirically from a knowledge of the physical characteristics of the bond, or from electronegativity considerations like those outlined in section 1.6. The detailed estimation of the coefficients of a generalised MO description of a H-bond does not seem to have been made, although this would be very interesting and useful in its application to NQR.

The situation then is that, although the electrostatic model of the hydrogen bond is most often used, the quantum mechanical descriptions, either VB or MO, offer the best hope for at least a semi-quantitative account of the effect of hydrogen-bond formation on NQR frequencies.

The largest changes between gas and solid occur when

new chemical bonds are formed in the solid. Although such a phenomenon is often of great chemical interest, there is little that is new from the point of view of calculating the NQR frequencies in the solid. A different molecule exists, and the obvious procedure is to try to calculate the components $V_{\alpha\beta}$ at the quadrupolar site for the new molecule, using the methods, extended or modified as necessary, discussed in chapter 1. The description by Watkins and Pound²⁴⁴ of the solid-state NQR of ICN and BrCN in this way, using VB language, is well-known⁵⁸ and need not be repeated here; it is a good example of this for the Townes and Dailey theory.

2.5 Temperature dependence: introduction

As stated in section 2.1, the temperature dependence $\left(\frac{\partial\nu}{\partial T}\right)$ of most NQR lines is negative. But in addition, the dependence of NQR frequency on temperature is often interrupted by one or more discontinuities. These may be due to phase changes, which usually cause sudden sharp shifts in the resonance frequency; or to the onset of hindered rotation, which is characterised by the gradual broadening and disappearance of the resonance lines. In the second situation, the resonance can sometimes be detected at a higher temperature and at a much lower frequency. The temperature dependence is generally markedly different in different phases.

The second type of discontinuity is discussed in the

next section.

Most measurements of temperature dependence are made at constant pressure. Apart from the effect of temperature on the vibrational-rotational crystal motions, and through them on the field gradient at the nitrogen nucleus, there are effects due to volume changes. The twin dependence on volume and temperature may be expressed in a complete differential:

$$dv = \left(\frac{\partial v}{\partial T}\right)_V dT + \left(\frac{\partial v}{\partial V}\right)_T dV \quad 2.5.1$$

$$\text{so that } \left(\frac{\partial v}{\partial T}\right)_P = \left(\frac{\partial v}{\partial T}\right)_V + \left(\frac{\partial v}{\partial V}\right)_T \left(\frac{\partial V}{\partial T}\right)_P \quad 2.5.2$$

$$\text{or } \left(\frac{\partial v}{\partial T}\right)_P = \left(\frac{\partial v}{\partial T}\right)_V + \alpha V_0 \left(\frac{\partial v}{\partial V}\right)_T \quad 2.5.3$$

where α is the volume coefficient of expansion. The first term on the right of equation 2.5.3 is the temperature dependence discussed in section 2.6. The second term describes the volume-dependent frequency change. The two effects can be separated by making measurements of the pressure dependence of the resonance frequency, at constant temperature. Then,

$$dv = \left(\frac{\partial v}{\partial V}\right)_T dV \quad 2.5.4$$

$$\therefore \left(\frac{\partial v}{\partial P}\right)_T = \left(\frac{\partial v}{\partial V}\right)_T \left(\frac{\partial V}{\partial P}\right)_T = -\beta V_0 \left(\frac{\partial v}{\partial V}\right)_T \quad 2.5.5$$

where β is the compressibility. From a knowledge of α and β ,

$\left(\frac{\partial v}{\partial T}\right)_V$ in equation 2.5.3 can be found.

The a priori calculation of $\left(\frac{\partial v}{\partial V}\right)_T$ involves a knowledge of the temperature and volume dependences of the effects

discussed in sections 2.3 and 2.4. Kushida et al.¹³³ suggest the decomposition of the term:

$$\left(\frac{\partial v}{\partial V}\right)_T = \left(\frac{\partial v}{\partial q}\right)_T \cdot \frac{dq}{dV} + \left(\frac{\partial v}{\partial \eta}\right)_T \cdot \frac{d\eta}{dV} + N(T) \quad 2.5.6$$

where $N(T)$ is a sum of temperature-dependent vibration-effect terms. They postulate two limiting cases. In a perfect ionic lattice, q would be proportional to r^{-3} , where r is the inter-ionic distance. Then, if

$$V \propto r^3 \quad 2.5.7$$

$$\text{and} \quad q \propto r^{-3} \quad 2.5.8$$

$$\text{then} \quad q \propto V^{-1} \quad \text{i.e.} \quad \frac{dq}{dV} < 0 \quad 2.5.9$$

while $\frac{d\eta}{dV} = 0$. In a molecular crystal, except at high pressures, the volume variations of q and η depend on intermolecular effects, and little progress seems feasible in the theoretical calculation of their influences. However since v in a solid is usually less than v in a gas, it is a reasonable guess that $\left(\frac{\partial v}{\partial V}\right)_T > 0$. This qualitative argument suggests that $\left(\frac{\partial v}{\partial V}\right)_T$ is negative when the field gradient is largely due to surrounding ions, and positive in molecular crystals.

A considerable range of relative importance in the two terms of equation 2.5.3 has been observed.⁵⁸ This relative importance depends of course on the value of α as well as on the values of $\left(\frac{\partial v}{\partial T}\right)_V$ and $\left(\frac{\partial v}{\partial V}\right)_T$. The latter term has been dealt with briefly, and the calculation of the former, the "direct"

term, will now be considered.

2.6 The direct temperature dependence

The theoretical treatment of the direct temperature effect was first set out by Bayer,¹⁷ extended by Kushida,¹³² and somewhat modified by Skripov.²¹² Since no temperature-dependence measurements or calculations were done for this thesis, and since the theory is very well-known, it will be summarised here very briefly. A fuller account is given for instance by Das and Hahn.⁵⁸

The simplest case, when $\eta=0$ and only torsional vibrations are important, is considered. This amounts to the oscillation of the principal axes of the $V_{\alpha\beta}$ tensor about their equilibrium positions. For oscillations about the principal axes X, Y and Z fixed in the molecule (these are the same principal axes as are used in chapter 1), new tensor components for space-fixed axes X'Y'Z' may be written:

$$\begin{aligned}
 V_{X'X'} &= (1 - \theta_Y^2 - \theta_Z^2)V_{XX} + \theta_Z^2 V_{YY} + \theta_Y^2 V_{ZZ} \\
 V_{Y'Y'} &= \theta_Z^2 V_{XX} + (1 - \theta_X^2 - \theta_Y^2)V_{YY} + \theta_X^2 V_{ZZ} \\
 V_{Z'Z'} &= \theta_Y^2 V_{XX} + \theta_X^2 V_{YY} + (1 - \theta_X^2 - \theta_Y^2)V_{ZZ} \\
 V_{X'Y'} &= \theta_Z V_{XX} + (\theta_X \theta_Y - \theta_Z)V_{YY} - \theta_X \theta_Y V_{ZZ} \\
 V_{Y'Z'} &= -\theta_Y \theta_Z V_{XX} + \theta_X V_{YY} + (\theta_Y \theta_Z - \theta_X)V_{ZZ} \\
 V_{Z'X'} &= (\theta_Z \theta_X - \theta_Y)V_{XX} - \theta_Z \theta_X V_{YY} + \theta_Y V_{ZZ}
 \end{aligned}
 \tag{2.6.1}$$

where θ_K is the small displacement about axis K, and only terms up to and including θ_K^2 have been retained. Since the

torsional frequencies are high compared to the NQR frequencies, the values of θ_K and θ_K^2 in equation 2.6.1 can be replaced by averages. Now

$$\langle \theta_X \rangle = \langle \theta_Y \rangle = \langle \theta_Z \rangle = 0 \quad 2.6.2$$

so that X'Y'Z' is also the principal axes system. The values of θ_K^2 can be approximated by replacing the three torsional motions by quantum-mechanical oscillators, so that

$$A_K \omega_K^2 \langle \theta_K^2 \rangle = \hbar \omega_K \left[\frac{1}{2} + \frac{1}{\exp(\hbar \omega_K / kT) - 1} \right] \quad 2.6.3$$

where A_K and ω_K are, respectively, the moment of inertia and the torsional frequency about the axis K.

From equations 2.6.3 and 2.6.2 in 2.6.1, the new components of V_{AB} can be found, and hence the new values of q and η , which can be substituted in an equation like equation 1.1.1, to give a new value of v . Finally, differentiation with respect to T gives the direct temperature-dependence coefficient

$\left(\frac{\partial v}{\partial T} \right)_V$. Such a process, if $\eta' \ll 1$, gives for $I=1$ (i.e. nitrogen)

$$\frac{1}{v_0} \left(\frac{\partial v}{\partial T} \right)_V = \frac{-\hbar^2}{2kT^2} \left[\frac{E_X}{A_X(1 - E_X)^2} + \frac{E_Y}{A_Y(1 - E_Y)^2} \right] \quad 2.6.4$$

$$\text{where} \quad E_K = \exp(\hbar \omega_K / kT) \quad 2.6.5$$

and v_0 is the frequency of the stationary molecule.

It might be pointed out here parenthetically that the treatment just outlined assumes that the temperature variation is entirely due to variation in the Boltzmann occupation of the torsional levels, which affects V_{val} , equation 1.7.21,

whereas V_{ext} in that equation is supposed to be relatively independent of temperature. As a rule this is probably right, but if γ_{∞} is large, the variation of V_{ext} may also need to be allowed for.

Often for nitrogen, η is large, and equation 2.6.4 must be extended accordingly. An important point about equation 2.6.4 is that it makes $\left(\frac{\partial v}{\partial T}\right)_V$ negative. Referring back to equation 2.5.3 and to the conclusions come to in section 2.5 regarding $\left(\frac{\partial v}{\partial V}\right)_T$, it appears, since $\left(\frac{\partial v}{\partial T}\right)_P$ is usually negative, the temperature-dependent term given by equation 2.6.4, the direct term, must usually be larger than $\left(\frac{\partial v}{\partial V}\right)_T$, the volume term. However, as the temperature decreases, the direct term decreases much more quickly than the volume term, and sometimes the latter may become dominant in equation 2.5.3. In that case, there is a temperature, often in the range $150^{\circ} - 250^{\circ}$ K, at which $\left(\frac{\partial v}{\partial T}\right)_P$ is zero; above this temperature it is negative and the direct term is dominant. This theoretically predicted behaviour has been quite satisfactorily demonstrated^{15,58,189} in several compounds.

It was assumed in the derivation of equation 2.6.4 that the torsional frequencies ω_K were high compared to the resonance frequency. This is generally true, but in certain compounds at low temperatures the ω_K may be less than ν : the "stationary" value ν_0 is close to the value observed. At high temperatures,

the rapid torsional motions cause an alteration in the resonance frequency, and an equation describing this frequency ν_T can readily be written down from equations 2.6.1; equation 2.6.4 was derived from such an equation. As has been shown, in general $\nu_T < \nu_0$. Then at intermediate temperatures, the resonance is "smeared out" between ν_0 and ν_T , and is often so broadened as to be unobservable. This is the simple explanation for the discontinuities which were referred to at the beginning of section 2.5 as being due to the onset of hindered rotation.

3.1 Introduction

Although most of the individual methods, discussed in chapter 1 of this Part, of putting values on the various parameters from which the electric field gradient tensor can be determined from an equation like equation 1.3.11, are described elsewhere, some of these methods, and particularly the method of calculating the "molecular" coefficients χ_j as described in section 1.6, have been modified or extended by the author. Also, it seems that the combination of methods described in sections 1.4 to 1.8 has not been applied to the calculation of field-gradient terms at nitrogen nuclei, starting the calculations from other molecular quantities. It seemed worthwhile to attempt to apply these methods in a few cases of interest. The main theoretical difficulty is that most of the parameters discussed in sections 1.4 to 1.8 could be determined in a number of different ways, and it is difficult to decide on first principles which is to be preferred. The calculations of which the results are given in this chapter are preliminary trials, undertaken to see if the methods show enough promise to warrant a more detailed examination than is given in chapter 1.

Although the methods of chapter 1 are much less difficult .

mathematically than the calculation of $V_{\alpha\beta}$ from a correct Hartree-Fock wave function, the calculations which have to be done are nevertheless quite formidable, and only a few simple molecules have been studied, with the help of simplifying assumptions.

3.2 The molecular calculations

A simplified version of the methods of chapter 1 was applied to the molecules shown in the second column of Table 3.2.2. No attempt was made to estimate the effects of the solid state, or of temperature, on the frequencies. The molecules were deliberately chosen to avoid so far as possible complications of unknown structure and bonding: for example the series XCN, although of great interest for the theoretical calculation of NQR parameters, have uncertain amounts of double-bond character in the X-C bond.

The required interatomic distances and interbond angles were taken from "Interatomic Distances" and Supplement.¹¹⁰ The nitrogen hybridisation coefficients a_i in compounds 1 and 2, and the corresponding coefficients for carbon in compound 2, were estimated using bond angles in equation 1.5.1. The adjacent ^{13}C - ^{15}N coupling constants for compounds 3, 5 and 6 are unfortunately not available, and the ^{13}C - ^{15}N coupling constant for compound 4 is anomalous,²⁰ so the generally good values of j and k cannot be used in equation 1.5.4. Accordingly,

the nitrogen and carbon hybridisation in compounds 3 to 6 was taken to be sp_z with two equivalent bonds, although this is unsatisfactory and probably wrong^{165,166} (see section 3.3).

The "molecular" coefficients were calculated as indicated at the end of section 1.6 (page 213). The iteration procedure was carried out for all the atoms of the molecule, using the obvious simplifications from molecular symmetry when possible, except for compound 2, for which only the carbon parameters were adjusted; this fixes the nitrogen parameters. The simplified equation 1.6.25 was used for nitrogen. The coefficients of that equation can be estimated by using the relationships suggested on pages 212 and 213: $b_2^+ \doteq c_2^+$ and $b_1^+ \doteq c_1^+$; the latter is the less reliable. These lead to:

$$\begin{aligned} b_2^+ &= b_{2R}^+/2 \\ K_R^+ &= K^+ + 4b_1^+ + 16b_2^+ \end{aligned} \quad 3.2.1$$

These equations, and the values given in Table 1.6.2 on page 211, leave only the problem of separating K and b_1 . The K values were estimated from the values of I and E for N^{4+} , for which $n_s = n_p = 0$, with the assumption of no hybridisation. This is certainly inexact, but enough atomic parameters for greater accuracy were not available. The method of Whitehead et al.²⁴⁹ was used for carbon; these authors do not give parameters for sp hybridised carbon, and these had to be calculated. The final orbital occupation numbers n_s and n_p , equation 1.6.21,

were used to calculate ζ (see later).

The choice of the atomic orbital is probably the most difficult and the most crucial choice. A Sternheimer correction was applied by multiplying terms I, ~~II~~^{III}, V and ~~VI~~ of equation 1.3.11 by 0.9, see page 236, and no attempt was made to use correlated wave functions.

The choice of a method for finding the effective charge ζ is very important because of the ζ^3 dependence of $V_{\alpha\beta}$: equation 1.8.13. Some idea of the usefulness of different systems may be gained from Table 3.2.1. Column 2 of that Table shows

TABLE 3.2.1 COMPARISON OF VALUES OF ζ (SEE TEXT)

Column	1	2	3	4	5	6
	¹⁴ N	-10	4.4	3.3	3.9	5
	³⁵ Cl	109.7	8.4	5.2	6.1	14

the value of $(eQq)_{at}$ in Mc/s which is most often used in the Townes-Dailey analysis for ¹⁴N and ³⁵Cl. Column 3 gives the value of ζ , as calculated from equation 1.8.13 for ¹⁴N and a corresponding equation for ³⁵Cl, using for ¹⁴N $Q = 1.47 \times 10^{-28} e$ e.s.u. cm² and for ³⁵Cl $Q = -7.97 \times 10^{-26} e$ e.s.u. cm². The fourth, fifth and sixth columns give for comparison the values

of ζ which would be calculated by the rules of Burns,²⁷ Slater²¹³ and Barnes and Smith¹² respectively. The last is included because these values come from a consideration of quadrupole hyperfine structure in atomic spectra, with interpolations. Sternheimer corrections are not made in Table 3.2.1 since the Townes and Dailey treatment essentially ignores them. However, the estimation of atomic effects should include spin-dependent effects, which can reasonably be neglected in most molecules. For this and other reasons, Table 3.2.1 is more illustrative than quantitative. As can be seen, the values of Burns, which are intended to reproduce the outer parts of the wave function, are lowest, and those of Barnes and Smith highest: they would appear to be too high. From considerations of this kind, it was decided to use Slater rules for a single-exponential function, as well as a modified set of rules which were devised for the purpose, not only of course from a consideration of Table 3.2.1 although they happen to give "good" values for comparison in that Table. The new rules were based on a consideration only of elements up to and including Cl, and could certainly not be extended to heavier elements without the modifications suggested in section 3.3. The screening parameter σ ($\zeta = Z - \sigma$) is calculated by dividing the electrons into groups as in the unmodified Slater rules, and allowing a contribution to σ of 0.4 from each electron in the same group as the electron under consideration

(Slater 0.35), 0.6 for each electron in the next group in towards the nucleus (Slater 0.85), and 1.0 for each electron further in (Slater 1.0). Physically, this means naively that, since the shielding of the lower-lying electrons is being given less weight, and conversely, more allowance is being made for penetration of outer electrons, and the wave function for these electrons, nearer the nucleus, is being enhanced. For the purposes of trial only, those modified values were used as well as the unmodified Slater values, and the results are shown in Table 3.2.2. In both cases, the values of ζ were adjusted for the variation in n_s and n_p calculated. This amounts to the correction suggested by Townes and Schawlow,²³⁶ who give values for ϵ , where eQq is to be multiplied by $(1+\epsilon)$ for each stage of ionisation. As a rough check, application of the Slater rules to the first ionisation of N gives a correction equivalent to $\epsilon = 0.30$ and, for Cl, $\epsilon = 0.18$. The modified rules give 0.31 and 0.12 respectively. The corresponding figures given by Townes and Schawlow are 0.3 and 0.15. The correction for ionisation was, obviously, not applied.

One-centre and symmetrical two-centre integrals (see the classification scheme on page 238) were calculated as described in full and as suggested, respectively, in section 1.8. Unsymmetrical two-centre integrals were not however evaluated as discussed in section 1.8, although that method is almost

certainly the most accurate. The evaluation of the Z functions is long and difficult; instead the integrals $(\psi_B | q_{zzA} | \psi_A)$ were approximated by the expression:

$$(\psi_B | q_{zzA} | \psi_A) = \frac{1}{2} S_{AB} (2 - |S_{AB}|) [(\psi_B | q_{zzA} | \psi_B) + (\psi_A | q_{zzA} | \psi_A)] \quad 3.2.2$$

where $S_{AB} = (\psi_A | \psi_B)$

and $|S_{AB}|$ is the magnitude of S_{AB} , for which the tabulated values of Mulliken et al.¹⁶⁴ were used. The evaluation of the matrix elements in square brackets has just been dealt with. Equation 3.2.2 is simply an extension, to matrix elements of q_{zz} , of the approximation given by Cusachs and Cusachs⁵³ for matrix elements of \mathcal{H} . So far as the author knows, it has not previously been applied in this way, although Cotton and Harris suggest a similar extension⁴⁶ of Mulliken's earlier and less accurate approximation, without saying how effective it is in use, or whether they have used it. But equation 3.2.2 did give apparently reasonable values, and is much easier to use than the full analytical evaluation.

The results of the foregoing are given in columns 3 and 4 of Table 3.2.2 on page 278. Columns 5 and 6 give observed values of eQq , taken from Appendix C1, where references can be found.

3.3 Discussion and conclusions

Most of the experimental papers reporting the values quoted in Table 3.2.2 give some discussion of the results, all

TABLE 3.2.2: RESULTS OF TRIAL CALCULATIONS

No.	Cpd.	$ (\text{eqq})_z $ (calc) ^a	$ (\text{eqq})_z $ (calc) ^b	$\text{eqq}(\text{obs})^c$	$\text{eqq}(\text{obs})^d$
1	NH ₃	2.6	3.1	3.1607	-4.0924
2	N(CH ₃) ₃	4.0	5.0	5.1939	-5.47
3	HCN	3.1	3.9	4.0183	-4.58
4	H ₃ CCN	2.9	3.7	3.7378 ^e	-4.214
5	Cl ₃ CCN	3.8	4.7	-	-4.7
6	F ₃ CCN	4.7	5.6	4.0521	-

Notes

- a Given in Mc/s to the nearest 0.1 Mc/s. Calculated using Slater rules.
- b Given in Mc/s to the nearest 0.1 Mc/s. Calculated using modified Slater rules.
- c In Mc/s for the solid at 77° K.
- d In Mc/s for the gas (from microwave spectroscopy).
- e Mean for two frequencies for two crystalline forms.

in terms of the Townes-Dailey description, applied rather quantitatively. The lower coupling constant of CH_3CN compared to that of HCN is explained by hyperconjugation, which is supposed to be decreasingly important in the series CH_3CN , CCl_3CN , CF_3CN . Whether or not some such effect is important, it can be seen from the Table that some at least of the difference can be accounted for by changes in the atomic orbital populations. However, as remarked in section 3.2, the assumption of constant hybridisation in the series 3 - 6 is a poor one, and no doubt there are changes in hybridisation: this would affect all the molecular parameters.

In addition, Kern and Karplus¹²¹ have calculated $(eqq)_{zz}$ for N in HCN using 2-exponential basis orbitals (except for H, for which they used one exponential) to describe the Hartree-Fock functions for the molecule. The result of their calculation was -1.66 Mc/s . Similarly, Kern¹²⁰ used a number of published exact wave functions for NH_3 , which gave results ranging from -2.6 to -6.4 Mc/s . Considering the difficulty and rigour of these calculations, these results are disappointing. The large errors probably flow from small errors in choosing the orbital exponents ζ , as discussed in section 3.2. This is probably further demonstrated by the value of -9.5 Mc/s . obtained earlier for HCN by Bassompierre.¹⁶ Of course the values in the fourth column of Table 3.2.2 were obtained from rather arbitrarily

adjusted values of ζ ; column 3 shows how much worse the results from simple Slater exponents are.

Since solid-state effects were ignored, the values should perhaps be compared to the gas-phase values in column 6. Apart from the value for Cl_3CCN , which is, fortuitously of course, exactly right, and the value for F_3CCN for which no comparison can be made, all of the values are too low. This agrees with the suggestion made earlier that perhaps ζ needs to be quite high in NQR theoretical calculations. However, the trend and the order of magnitude are more or less correctly predicted.

The molecules in Table 3.2.2 were selected to avoid serious complications in describing the bonding; they are of two chemical types only; and the results may not be typical even for these types. Nevertheless, it does seem that semi-empirical calculation gives as good results, for nitrogen at least, as more rigorous calculations, with much less effort. The main problem is the evaluation of ζ ; it is possible that investigation like Burns's²⁷ but with the aim of reproducing NQR results, and using different shielding for s and p electrons, would give quite good prediction of NQR frequencies with much less labour than an ab initio MO calculation.

Note The following tables are intended to list every observation published of a nuclear quadrupole coupling constant for ^{14}N , by whatever experimental method. The literature has been searched up to the end of December 1967, but the lists may not be complete because, apart from the possibility of overlooking a paper, issues of some less common foreign journals for the end of 1967 had been neither received nor abstracted in the abstracting journals by February 1968, when the tables were finally produced. Values of doubtful accuracy, or with very large quoted errors (over 100%) have been omitted unless the compound is of particular interest. No list purporting to approach comprehensiveness has been published for several years.

Column 1 gives the reference number (see appendix C2). Where more than one report has been made of the same experimental quantity, only that seeming to be the most accurate or reliable has been included.

Column 2 gives the compound, formula, and experimental method. If no indication of the last is given, it is to be taken to be pure NQR. MW is used to abbreviate microwave spectroscopy: if only coupling constants along the principal inertial axes are given, these are quoted in this column in the order χ_{aa} , χ_{bb} unless otherwise indicated; always of course

$\chi_{cc} = -(\chi_{aa} + \chi_{bb})$. NMR and ESR have their usual meanings.

Extra information is sometimes included: t.d. is short for temperature dependence, and all temperatures are in °K.

In the columns giving results, if no error is given, the error is ± 1 in the last quoted figure. The symbol \pm with no figure following it is used to show that the error is not stated, but is greater than ± 1 in the last place. Figures in brackets are interpolations.

TABLE 1: ALIPHATIC AMINES

		T, °K	eQq, Mc/s	$\eta, \%$
167	methylamine, CH_3NH_2 . MW	-	-3.6 ± 0.3	
141	d-methylamine, CD_3ND_2 . MW. 2.35 ± 0.05 , 2.12 ± 0.05	-		
1	ethylenediamine, $\text{H}_2\text{N}(\text{CH}_2)_2\text{NH}_2$ t.d. 77-280	77	3.9965	31.3
85	hexanediamine, $\text{H}_2\text{N}(\text{CH}_2)_6\text{NH}_2$.	77	4.03	35
150	cyanamide, H_2NCN . MW. $3.05 \pm 1.85 \pm$			
239	piperazine, $\text{HN}(\text{C}_2\text{H}_4)_2\text{NH}$ t.d. 255-346. at 300, $\omega_1 = 3.0161$, $\omega_2 = 3.6035$, $\frac{d\omega_1}{dT} = 20 \text{ c/s/}^\circ\text{K}$, $\frac{d\omega_2}{dT} = 381 \text{ c/s/}^\circ\text{K}$.	300 (77)	4.4131 4.47	26.6 (31)

TABLE 1 (CONTINUED)

		T, °K	eQq, Mc/s	$\eta, \%$
88	triethylenediamine, $N:(C_2H_4)_3:N$	77	4.9247	0
153	trimethylamine, $(CH_3)_3N$. MW.	-	-5.47	0
168	"	77	5.1939 \pm 0.0001	0
244	hexamethylenetetramine, $(CH_2)_6N_4$	299.6	4.4083 \pm 0.0001	0
		273	4.4265 \pm 0.0001	0
		199	4.4747 \pm 0.0001	0
		77	4.5435 \pm 0.0001	0

TABLE 2: AROMATIC AMINES

130	p-chloroaniline, p-Cl.C ₆ H ₄ NH ₂	77	4.117	24.3
130	p-bromoaniline, p-Br.C ₆ H ₄ NH ₂	77	4.135	23.1
130	p-phenylenediamine, p-NH ₂ .C ₆ H ₄ NH ₂ . Other transns. (^a very weak): 2.690 ^a , 2.694 ^a , 3.2109, 3.2129	77	3.91 \pm 0.001	26.4
85	2-aminopyridine, 2-NH ₂ .C ₅ H ₄ N (<u>probably</u> the N underlined)	77	3.745	3.5

TABLE 3: "AMINES": N IN CONJUGATED SYSTEMS




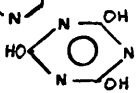
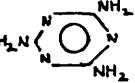
		T, °K	eQq, Mc/s	η ,%
217	pyridine, C_5H_5N . MW -4.88 ± 0.04 , 1.43 ± 0.03	-		
85	"	77	4.572	37.4
		77	4.591	39.3
		77	4.574	41.5
		77	4.601	40.3
		mean 77	4.5845	39.6
85	γ -picoline, $4-CH_3 \cdot C_5H_4N$	190	4.3736	33.68
		77	4.4140	34.24
197	pyridazine, 	77	5.18892 \pm	8.53 \pm
68	" MW. -4.64 , 1.38	-		
197	pyrimidine, 	77	4.43621 \pm	38.6
197	pyrazine, 	77	4.85783 \pm	53.6
252	cyanuric acid, 	77	?	>14
	Lines at 2.7915 & 2.7829 due not to $\eta \neq 0$, but diff. sites.			
252	melamine, 	77	?	>14
	Line at 2.5865 - ring N?			
129	cyanuric chloride, $(CNCl)_3$	77	4.083	1.7

TABLE 4: AMIDES AND RELATED COMPOUNDS

		T, °K	eQq , Mc/s	η ,%
131	formamide, HCONH_2 MW. $1.9 \pm 1.7 \pm$	-		
87	"	77	2.274	37.8
130	urea, NH_2CONH_2	77	3.507	32.3
86	" Lines at 2.3260, 2.8741 (at 199). t.d. 0.174 & 0.325 kc/deg. resp.	(77	3.507	32.3)
252	d-urea, $\text{CO}(\text{ND}_2)_2$. One line at 2.9140	77		
191	carbonyl fluoride, NH_2COF . MW	-	-4.05	16.5

TABLE 5: UNCONJUGATED CYANIDES (NITRILES)

238	hydrogen cyanide, HCN . MW	-	-4.58 ± 0.05	0
166	"	195	3.8904 ± 0.0003	0
		77	4.0183 ± 0.0003	0
238	cyanogen fluoride, FCN . MW	-	-2.67 ± 0.05	0
238	cyanogen chloride, ClCN . MW	-	-3.63 ± 0.1	0
31	" nothing seen at 199	77	3.219 ± 0.001	1.57
238	cyanogen bromide, BrCN . MW	-	-3.83 ± 0.08	0
244	"	297.2	3.2851 ± 0.0002	0.14
	(calculated assuming $\eta \neq 0$ when	273	3.2979 ± 0.0002	0
	two lines seen)	199	3.3249 ± 0.0002	0.32

TABLE 5 (CONTINUED)

		T, °K	ϵ'' , Mc/s	η , %
244	cyanogen bromide, BrCN (cont.) (calculated assuming $\eta \neq 0$)	77	3.3541 ± 0.0002	0.56
238	cyanogen iodide, ICN. MW	-	-3.80 ± 0.1	0
244	" (calcd. using reptd. frequencies). No reson- ance seen at 77, 2.52-2.57	299.8 273 199 (77	3.3899 ± 0.0002 3.3935 ± 0.0002 3.4016 ± 0.0002 3.411	0.14 0 0 0)
119	methyl cyanide (acetonitrile), CH ₃ CN. MW	-	-4.214 ± 0.016	0
166	" α form: slow cooling β form: fast cooling	77 77	3.7380 ± 0.0003 3.7375 ± 0.0003	0.46 0.82
242	monochloroacetonitrile, ClCH ₂ CN. MW			
85	"	77	3.8943	14.1
231	trifluoroacetonitrile, F ₃ CCN. MW	-	$-4.7 \pm$	
165	trichloroacetonitrile, Cl ₃ CCN.	77	4.0521 ± 0.0003	0.53 ± 0.02
137	propionitrile (ethyl cyanide) CH ₃ CH ₂ CN MW. $-3.3 \pm$	-		
32	"	77	3.7756 ± 0.0003	2.08 ± 0.01
85	isobutyronitrile, (CH ₃) ₂ CHCN one line at 2.880	77		

TABLE 5 (CONTINUED)

	T, °K	eQq, Mc/s	$\eta, \%$
84 n-butyronitrile, $\text{CH}_3(\text{CH}_2)_2\text{CN}$ one line seen, no freq. given			
32 malononitrile, CNCH_2CN	77	3.9216 ± 0.0003	7.57 ± 0.01
229 t.d. 140 to 298			
173 sulphur dicyanide, $\text{S}(\text{CN})_2$. MW $-1.51 \pm 0.30 \pm$	-		
205 silyl cyanide, H_3SiCN . MW	-	-4.7 ± 0.5	0
240 germyl cyanide, H_3GeCN . MW	-	-5.0 ± 0.1	0
150 cyanamide, NH_2CN . MW $-3.30 \pm$, $2.86 \pm$			

TABLE 6: CONJUGATED CYANIDES (see also Table 3)

88 cyanogen, $(\text{CN})_2$	77	4.269	2.2
45 acrylonitrile, $\text{CH}_2=\text{CHCN}$. MW	-	-4.21 ± 0.04	0
238 cyanoacetylene, $\text{CH} \equiv \text{CCN}$. MW	-	-4.28 ± 0.05	0
204 methylcyanoacetylene, $\text{CH}_3\text{C} \equiv \text{CCN}$. MW	-	-4.4 ± 0.5	0
165 benzonitrile, $\text{C}_6\text{H}_5\text{CN}$	77	3.8854 ± 0.0003	10.73 ± 0.02
165 picolinonitrile, 2-CN. $\text{C}_5\text{H}_4\text{N}$	77	3.9583 ± 0.0003	7.16 ± 0.02
165 isonicotinonitrile, 4-CN. $\text{C}_5\text{H}_4\text{N}$	77	3.8951 ± 0.0003	1.44 ± 0.02

TABLE 7: COMPOUNDS RELATED TO CYANIDES

		T, °K	$e\eta q$, Mc/s	η ,%
119	methyl isocyanide, CH_3NC . MW	-	0.483 ± 0.017	0
207	isocyanic acid, $\text{HN}:\text{C}:\text{O}$. MW	-	2.00 ± 0.05	0
52	methyl isocyanate, $\text{CH}_3\text{N}:\text{C}:\text{O}$. MW	-	$2.3 \pm$	0
108	methoxy thiocyanate, CH_3SCN	198	3.4786	46.29
		77	3.5154	47.32
108	ethyl thiocyanate, $\text{CH}_3\text{CH}_2\text{SCN}$	77	3.5903	47.35
108	ethylene thiocyanate, $(\text{CH}_2\text{SCN})_2$	299	3.5005	47.24
		198	3.5240	47.06
		77	3.5448	46.71
107	potassium thiocyanate, KSCN	77	2.4314 ± 0.0002	2.81 ± 0.02
107	potassium selenocyanate, KSeCN	77	2.8449 ± 0.0002	4.97 ± 0.02
207	isothiocyanic acid, $\text{HN}:\text{C}:\text{S}$. MW	-	1.2 ± 0.2	0

TABLE 8: OTHER ORGANIC COMPOUNDS

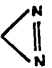



172	diazirine,  MW 1.0,	-		
	$\chi_{cc} - \chi_{bb} = 6.2 \pm 0.3$			
60	oxazole,  MW -3.99, 1.58	-		
60	isoxazole,  MW	-		
	$\chi_{aa}, \chi_{bb}, \chi_{cc}$ all < 1 .			
51	1,2,5-oxadiazole,  MW -0.69 \pm 0.09, -0.46 \pm 0.13	-		

TABLE 8 (CONTINUED)


		T, °K	eQq, Mc/s	$\eta, \%$
66	1,2,5-thiadiazole 	-		
	MW 1.0, $\chi_{cc}-\chi_{bb}=5.2 \pm 0.3$			
232	ethyleneimine, $\text{CH}_3\text{CH:NH}$.	-		
	MW 0.69, 2.17			
93	N-methyl ethyleneimine, $\text{CH}_3\text{CH:NCH}_3$. MW 3.35 ± 0.02 , 0.63 ± 0.02	-		
196	N-methyl methyleneimine, $\text{CH}_2\text{:NCH}_3$. MW $1.9 \pm 0.3, 3.2 \pm 0.2$	-		
203	diazomethane, CH_2N_2 . MW	-		
140	formaldoxime, $\text{H}_2\text{C:NOH}$ (d-form, $\chi=3.1$)	-	$3.0(=\chi_{aa}?)$	$\neq 0$
95	nitroethylene, $\text{CH}_2\text{:CHNO}_2$. MW $-0.883 \pm 0.049, +0.014 \pm 0.024$			

TABLE 9: INORGANIC COMPOUNDS

144	nitrogen, N_2 . MW (finds eQ)	-		
200	" line shapes, t.d. 1.5-34.5 (assuming $\eta=0$)	4.2	4.6497	0
159	nitrogen in β -quinol clathrate	<5	~ 3.6	0?
79	ammonia, NH_3 . MW	-	-4.0924 ± 0.0015	0

TABLE 9 (CONTINUED)

		T, °K	ν_{eq} , Mc/s	δ
138	ammonia, NH_3 . (cont.)	77	3.1607	0
138	NHD_2 - NDH_2 for various D/H ratios.			
138	d-ammonia, ND_3	77	3.2307	0
118	" MW	-	-4.10	0
35	ammonium dihydrogen phosphate, $(\text{NH}_4)_2\text{HPO}_4$ NMR	291	0.0246	0
35	d-ammonium dihydrogen phosphate, $(\text{ND}_4)_2\text{DPO}_4$ NMR	291	0.0273	0
73	hydrazoic acid, HN_3 . MW	α -	4.85 ± 0.10	0
	$\text{HN} \begin{smallmatrix} \text{N} \\ \alpha \end{smallmatrix} \begin{smallmatrix} \text{N} \\ \beta \end{smallmatrix} \begin{smallmatrix} \text{N} \\ \gamma \end{smallmatrix}$	β -	-1.35 ± 0.10	0
		γ -	0.7	
72	potassium azide, KN_3 NMR	α -	1.028 ± 0.03	3 ± 2
	$\text{KN} \begin{smallmatrix} \text{N} \\ \alpha \end{smallmatrix} \begin{smallmatrix} \text{N} \\ \beta \end{smallmatrix} \text{N}$	β -	1.79 ± 0.03	4 ± 2
117	hydrazine, H_2NNH_2 . MW	-	-4.09?	?
2	" 2 XTL posns.	77	4.819	78.6
		77	4.821	82.8
195	nitrous oxide, N_2O . MW	α -	-0.792 ± 0.005	0
	$\text{N} \begin{smallmatrix} \text{N} \\ \alpha \end{smallmatrix} \begin{smallmatrix} \text{O} \\ \beta \end{smallmatrix}$	β -	-0.238 ± 0.005	0
255	nitric oxide, NO . MW	-	-2	0?
74	nitrogen dioxide, NO_2 . MW	-		
	$0.90 \pm 0.12, -3.42 \pm 0.12$			

TABLE 9 (CONTINUED)

		T, °K	eQq, Mc/s	,%
50	<u>trans</u> -nitrous acid, HONO. MW	-		
	1.91±0.12, -5.39±0.30			
50	d- <u>trans</u> -nitrous acid, DONO. MW	-		
	1.68±0.12, -5.17±0.30			
160	nitric acid, HONO ₂ . MW	-		
	0.93±0.05, -0.82±0.05			
160	d-nitric acid, DONO ₂ . MW	-		
	0.82±0.05, -0.62±0.05			
81	sodium nitrate, NaNO ₃ . NMR	-	0.745	0
83	nitrosyl fluoride, NOF. MW	-		
	1.7±0.1, -5.0±0.1			
82	nitrosyl chloride, NOCl. MW	-		
	1.0±0.4, -4.8±0.2			
82	nitrosyl bromide, NOBr. MW	-		
	⁷⁹ Br 0.4±0.3, -4.4±0.3			
	⁸¹ Br 0.6±0.5, -4.4±0.3			
124	thionitrosyl fluoride, NSF. MW	-	-1.66±0.05	-5.86±0.05
123	thionitrosyl trifluoride, NSF ₃ . MW	-	+1.19±0.05	0
215	nitryl fluoride, NO ₂ F. MW	-		
	0.7±, 1.5±			
39	nitryl chloride, NO ₂ Cl. MW	-	small	small

TABLE 9 (CONTINUED)

		T, °K	eQq, Mc/s	,%
142	difluoramine, F ₂ NH. MW	-	-8.9±0.4	44
49	nitrogen trifluoride, NF ₃ . MW	-	-7.09	0
154	"	0	7.0681±0.0007	0.112±0.002

1. Y. Abe, J. Phys. Soc. Japan, 1963, 18, 1804.
2. Y. Abe, Y. Kamishina and S. Kojima, J. Phys. Soc. Japan, 1966, 21, 2083.
3. A. Abragam and K. Kambe, Phys. Rev., 1953, 91, 894.
4. R. Alden, J. Kraut and T.G. Traylor, J. Phys. Chem., 1967, 71, 2379.
5. M.H. Alexander, J. Chem. Phys., 1967, 46, 1953.
6. S. Alexander, J. Chem. Phys., 1961, 34, 106.
7. L.C. Allen, Phys. Rev., 1960, 118, 167.
8. A.L. Allred and A.L. Hensley, J. Inorg. Nuclear Chem., 1961, 17, 43.
9. A.T. Amos and J.I. Musher, Chem. Phys. Letters, 1967, 1, 149.
10. T. Arai, J. Chem. Phys., 1957, 26, 435.
11. F. Bailly, J. phys. (Paris), 1966, 27, 335.
12. R.G. Barnes and W.V. Smith, Phys. Rev., 1954, 93, 95.
13. M.P. Barnett and C.A. Coulson, Phil. Trans. Roy. Soc. (London), A1951, 221.
14. M.P. Barnett and C.A. Coulson, "Quantum Mechanical Methods in Valence Theory", U.S. Office of Naval Research, 1951.
15. B.L. Barton, J. Chem. Phys., 1967, 46, 1553.
16. A. Bassompierre, J. chim. phys., 1954, 51, 614.
17. H. Bayer, Z. Physik, 1951, 130, 227.
18. B. Beagley, Chem. Communications, 1966, 388.

19. R.S. Berry, J. Chem. Education, 1966, 43, 283.
20. G. Binsch, J.B. Lambert, B.W. Roberts and J.D. Roberts,
J. Amer. Chem. Soc., 1964, 86, 5564.
21. S. Bratoz, Colloque Nat., Centre Nat. Rech. Sci., 1965, 29.
22. D.A. Brown and N.J. Fitzpatrick, J. Chem. Phys., 1967,
46, 2005.
23. K.A. Brueckner, Phys. Rev., 1954, 96, 508.
24. K.A. Brueckner, C.A. Levinson and H.M. Mahmoud, Phys.
Rev., 1954, 95, 217.
25. L. Burnelle, Theoret. Chim. Acta, 1964, 2, 177.
26. G. Burns, J. Chem. Phys., 1959, 31, 1253.
27. G. Burns, J. Chem. Phys., 1964, 41, 1521.
28. G. Burns, Phys. Rev., 1959, 115, 357.
29. G. Burns and E.G. Wikner, Phys. Rev., 1961, 121, 155.
30. G.V. Bykov, Zh. Fiz. Khim., 1967, 41, 743.
31. P.A. Casabella and P.J. Bray, J. Chem. Phys., 1958, 28, 1182.
32. P.A. Casabella and P.J. Bray, J. Chem. Phys., 1958, 29, 1105.
33. S. Chandra and S. Chandra, Tetrahedron, 1966, 22, 3403.
34. J. Chantelot and A. LaForgue, J. chim. phys., 1966, 63, 749.
35. T. Chiba, Bull. Chem. Soc. Japan, 1965, 38, 490.
36. R.E. Christoffersen and K. ruedenberg, J. Chem. Phys.,
1967, 47, 1855.
37. Chun-Chin Lia, J. Chem. Phys., 1960, 33, 878.
38. T.A. Claxton, Nature, 1965, 208, 891.

39. L. Clayton, Q. Williams and T.L. Weatherly, J. Chem. Phys., 1959, 30, 1328; err. 1959, 31, 554.
40. E. Clementi, J. Chem. Phys., 1967, 46, 3842.
41. E. Clementi and D.L. Raimondi, J. Chem. Phys., 1963, 38, 2686.
42. I. Cohen and T. Bustard, J. Chem. Education, 1966, 43, 187.
43. M.H. Cohen and F. Reif, "Nuclear Quadrupole Effects in NMR Studies of Solids", Solid State Phys., 1957, 5, 321 (eds. Seitz and Turnbull).
44. W.R. Conkie, J. Chem. Phys., 1965, 43, 3408.
45. C.C. Costain and B.P. Stoicheff. J. Chem. Phys., 1959, 30, 777.
46. F.A. Cotton and C.B. Harris, Proc. Nat. Acad. Sci. U.S.A., 1966, 56, 12.
47. C.A. Coulson, "Valence", Oxford University Press, Oxford, 1952.
48. C.A. Coulson and U. Danielsson, Arkiv Fysik, 1954, 8, 239,245.
49. M. Cowan and W. Gordy, Bull. Amer. Phys. Soc., 1960, 5, 241.
50. A.P. Cox and R.L. Kuczkowski, J. Amer. Chem. Soc., 1966, 88, 5071.
51. A.P. Cox and P.H. Saegberth, J. Chem. Phys., 1965, 43, 166.
52. R.F. Curl, V.M. Rao, K.V.L.N. Sastry and J.A. Hodgson, J. Chem. Phys., 1963, 39, 3335.
53. L.C. Cusachs and B.B. Cusachs, J. Phys. Chem., 1967, 71, 3977.
54. B.P. Dailey and H.N. Shoolery, J. Amer. Chem. Soc., 1955, 77, 3977.

55. A. Dalgarno, Adv. Phys., 1962, 11, 281.
56. A. Dalgarno, Proc. Roy. Soc. (London), 1959, A251, 282.
57. T.P. Das and R. Bersohn, Phys. Rev., 1956, 102, 733.
58. T.P. Das and E.L. Hahn, "Nuclear Quadrupole Resonance Spectroscopy", Solid State Phys., Supp. 1 (eds. Seitz and Turnbull), Academic Press, 1958.
59. E.R. Davidson, J. Chem. Phys., 1967, 46, 3320.
60. D.W. Davies and W.C. Mackrodt, Chem. Communications, 1967, 345.
61. M.A. Davis, J. Org. Chem., 1967, 32, 1161.
62. G. Del Re, Internat. J. Quantum Chem., 1967, 1, 293.
63. G. Del Re, U. Esposito and M. Carpentieri, Theoret. Chim. Acta, 1966, 6, 36.
64. G. Derflinger and O.E. Polansky, Theoret. Chim. Acta, 1963, 1, 316.
65. H.W. De Wijn, J. Chem. Phys., 1966, 44, 810.
66. V. Dobyns and L. Pierce, J. Amer. Chem. Soc., 1963, 85, 3553.
67. A.W. Douglas, J. Chem. Phys., 1966, 45, 3465.
68. H. Dreizler and H.D. Rudolph, Z. Naturforsch., 1967, A22, 531.
69. A.R. Edmonds, "Angular Momentum in Quantum Mechanics", Princeton University Press, Princeton, N.J., 1957.
70. H.R. Falle and R. Luckhurst, J. Mol. Spec., 1967, 22, 469.
71. R. Fletcher and C.M. Reeves, Computer J., 1963, 6, 287.
72. R.A. Forman, J. Chem. Phys., 1966, 45, 1118.
73. R.A. Forman and D.R. Lide, J. Chem. Phys., 1963, 39, 1133.

74. P.D. Foster, J.A. Hodgeson and R.F. Curl, J. Chem. Phys., 1966, 45, 3760.
75. K. Frei and H.J. Bernstein, J. Chem. Phys., 1963, 38, 1216.
76. H.M. Foley, R.M. Sternheimer and D. Tycko, Phys. Rev., 1954, 93, 734.
77. Y. Fukai, J. Phys. Soc. Japan, 1964, 19, 175.
78. F. Gallais, D. Voigt and J.F. Labarre, J. chim. phys., 1965, 62, 761.
79. J.P. Gordon, Phys. Rev., 1955, 99, 1253.
80. W. Gordy, in "Techniques of Organic Chemistry", Vol. IX: "Chemical Applications of Spectroscopy", Interscience, London, 1956.
81. M. Gourdji and L. Guibé, Compt. rend., 1965, 260, 1131.
82. A. Guarnieri and P.G. Favero, Nuovo Cimento, 1965, 39, 76.
83. A. Guarnieri, G. Zuliani and P.G. Favero, Nuovo Cimento, 1966, B45, 84.
84. L. Guibé, Acad. Roy. Belg., Classe Sci., Mém., 1961, 33, 333.
85. L. Guibé, Ann. Phys. (Paris), 1962, 7, 177.
86. L. Guibé, Compt. rend., 1960, 250, 1635.
87. L. Guibé and E.A.C. Lucken, Compt. rend. Acad. Sci. (Paris), Ser. A,B, 1966, 263B, 815.
88. P.J. Haigh and L. Guibé, Compt. rend., 1965, 261, 2328.
89. G.G. Hall, Rept. Prog. Phys., 1959, 22, 1.
90. P. Hampson and A. Mathias, Mol. Phys., 1966, 11, 541.

91. A.E. Hansen, Theoret. Chim. Acta, 1967, 7, 230.
92. K.H. Hansen, Theoret. Chim. Acta, 1966, 6, 268.
93. M.D. Harmany and M. Sancho, J. Chem. Phys., 1967, 47, 1911.
94. D.E. Herbison-Evans and R.E. Richards, Mol. Phys., 1964, 8, 19.
95. H.D. Hess, A. Bauder and Hs.H. Günthard, J. Mol. Spec., 1967, 22, 208.
96. J. Hinze and H.H. Jaffé, J. Amer. Chem. Soc., 1963, 85, 148.
97. J. Hinze, M.A. Whitehead and H.H. Jaffé, J. Amer. Chem. Soc., 1963, 85, 148.
98. J.O. Hirschfelder and A.C. Walls, Sci. Tech. Aerospace Rept., 1966, 4, 2183.
99. J.E. Huheey, J. Chem. Phys., 1966, 45, 405.
100. J.E. Huheey, J. Inorg. Nuclear Chem., 1965, 27, 2127.
101. J.E. Huheey, J. Org. Chem., 1966, 31, 2365.
102. J.E. Huheey, J. Phys. Chem., 1965, 69, 3284.
103. J.E. Huheey, J. Phys. Chem., 1966, 70, 2086.
104. C.M. Hurd and P. Coddin, J. Phys. Chem. Solids, 1967, 28, 523.
105. E.A. Hylleraas, Z. Phys., 1939, 54, 347.
106. R.P. Iczkowski and J.L. Margrave, J. Amer. Chem. Soc., 1961, 83, 3547.
107. R. Ikeda, D. Nakamura and M. Kubo, Bull. Chem. Soc. Japan, 1967, 40, 701.
108. R. Ikeda, D. Nakamura and M. Kubo, J. Phys. Chem., 1966, 70, 3626.

109. R. Ingalls, Phys. Rev., 1962, 128, 1155.
110. "Interatomic Distances", Chem. Soc. Special Publication No. 11, London, 1958; "Interatomic Distances Supplement", Chem. Soc. Special Publication No. 18, London, 1965.
111. C.J. Jameson and H.S. Gutowsky, J. Chem. Phys., 1964, 40, 1714.
112. C.K. Joergensen, S.M. Horner, W.E. Hatfield and S.Y. Tyree, Internat. J. Quantum Chem., 1967, 1, 191.
113. C. Juan and H.S. Gutowsky, J. Chem. Phys., 1962, 37, 2198.
114. S. Kaneko, J. Phys. Soc. Japan, 1959, 14, 1600.
115. J.H. Karl, J. Chem. Phys., 1967, 46, 4219.
116. M. Karplus and D.M. Grant, Proc. Nat. Acad. Sci. U.S.A., 1959, 45, 1269.
117. T. Kasuya, Sci. Papers Inst. Phys. Chem. Res. (Tokyo), 1962, 56, 1.
118. Y. Kato, J. Phys. Soc. Japan, 1961, 16, 122.
119. M.K. Kemp, J.M. Pochan and W.H. Flygare, J. Phys. Chem., 1967, 71, 765.
120. C.W. Kern, J. Chem. Phys., 1967, 46, 4543.
121. C.W. Kern and M. Karplus, J. Chem. Phys., 1965, 42, 1062.
122. P. Kitzinger and J.M. Lehn, Chem. Communications, 1967, 660.
123. W.H. Kirchoff and E.B. Wilson, J. Amer. Chem. Soc., 1962, 84, 334.
124. W.H. Kirchoff and E.B. Wilson, J. Amer. Chem. Soc., 1963, 85, 1276.

125. A.I. Kitaigorodskii and K.V. Mirskaya, Kristallografiya, 1965, 10, 162.
126. M. Klessinger, J. Chem. Phys., 1967, 46, 326; 1965, 43, S117.
127. G. Klopman, J. Chem. Phys., 1965, 43, S124.
128. E. Kochanski and G. Berthier, Colloq. Int. Centre. Nat. Rech. Sci., 1966, 164, 177.
129. S. Kojima and M. Minematsu, J. Phys. Soc. Japan, 1960, 15, 355.
130. S. Kojima, M. Minematsu and M. Tanaka, J. Chem. Phys., 1959, 31, 271.
131. R.J. Kurland and E.B. Wilson, J. Chem. Phys., 1957, 27, 585.
132. T. Kushida, J. Sci. Hiroshima Univ., 1955, A19, 327.
133. T. Kushida, G.B. Benedick and N. Bloembergen, Phys. Rev., 1956, 104, 1364.
134. J. Lahiri and A. Mukherji, Phys. Rev., 1966, 141, 428; 1967, 153, 386.
135. J.P. Lambert, B.W. Roberts, G. Binsch and J.D. Roberts, Sci. Tech. Aerospace Rept., 1965, 3, 876.
136. P. Laszlo and P. von R. Schleyer, J. Amer. Chem. Soc., 1963, 85, 2709.
137. V.W. Laurie, J. Chem. Phys., 1959, 31, 1500.
138. S.S. Lehrer and C.T. O'Konski, J. Chem. Phys., 1965, 43, 1941.
139. J. Lennard-Jones and J.A. Pople, Proc. Roy. Soc. (London), 1951, 205A, 155.
140. I.N. Levine, J. Mol. Spec., 1962, 8, 276.

141. D.R. Lide, J. Chem. Phys., 1957, 27, 343.
142. D.R. Lide, J. Chem. Phys., 1963, 38, 456.
143. T.K. Lim and M.A. Whitehead, J. Chem. Phys., 1966, 45, 4400.
144. C.C. Lin, Phys. Rev., 1960, 119, 1027.
145. P.-O. Löwdin, Adv. Chem. Phys., 2, 207, Interscience, New York, N.Y., 1960.
146. P.-O. Löwdin, Phys. Rev., 1953, 90, 120.
147. P.-O. Löwdin, Phys. Rev., 1955, 94, 1474, 1490, 1509.
148. E.A.C. Lucken, Trans. Farad. Soc., 1961, 57, 729.
149. F. Lurçat, J. Phys. Radium, 1958, 19, 713.
150. J. MacDonald and J.K. Tyler, private communication.
151. V. Magnasco and A. Operico, J. Chem. Phys., 1967, 47, 971.
152. G. Malli and S. Fraga, Theoret. Chim. Acta, 1966, 6, 54.
153. D.E. Mann and D.R. Lide, Bull. Amer. Phys. Soc, 1957, 2, 212.
154. G.A. Matzkanin, T.A. Scott and P.J. Haigh, J. Chem. Phys., 1965, 42, 1646.
155. W. McFarlane, J. Chem. Soc., A1967, 1660.
156. A.D. McLachlan, J. Chem. Phys., 1960, 32, 1263.
157. A.D. McLean and M. Yoshimine, J. Chem. Phys., 1967, 46, 1812.
158. A.J. van der Merwe, Z. Naturforsch., 1967, A22, 593.
159. H. Meyer and T.A. Scott, Phys. Chem. Solids, 1959, 11, 215.
160. D.J. Millen and J.R. Horton, J. Chem. Soc., 1960, 1523.
161. J.B. Moffat and R.J. Collens, Canad. J. Chem., 1967, 45, 655.
162. N. Muller, J. Chem. Phys., 1962, 36, 359.

163. N. Muller and D.E. Pritchard, J. Chem. Phys., 1959, 31, 768, 1472.
164. R.S. Mulliken, C.A. Rieke, D. Orloff and H. Orloff, J. Chem. Phys., 1949, 17, 1248.
165. H. Negita and P.J. Bray, J. Chem. Phys., 1960, 33, 1876.
166. H. Negita, P.A. Casabella and P.J. Bray, J. Chem. Phys., 1960, 32, 314.
167. T. Nishikawa, J. Phys. Soc. Japan, 1957, 12, 668.
168. C.T. O'Konski and T.J. Flautt, J. Chem. Phys., 1957, 27, 815.
169. D.E. O'Reilly, J. Chem. Phys., 1962, 36, 274.
170. L. Pauling, "The Nature of the Chemical Bond", 3rd. edn., Cornell University Press, Ithaca, N.Y., 1960.
171. D. Peters, J. Chem. Soc., A1966, 644, 656.
172. L. Pierce and S.V. Dobyms, J. Amer. Chem. Soc., 1962, 84, 2651.
173. L. Pierce, R. Nelson and C. Thomas, J. Chem. Phys., 1965, 43, 3423.
174. G.C. Pimentel, J. Chem. Phys., 1951, 19, 446.
175. G.C. Pimentel and A.L. McLellan, "The Hydrogen Bond", Freeman & Co., New York, N.Y., 1960.
176. D. Pines, Solid State Phys., 1955, 1, 368.
177. R.M. Pitzer, C.W. Kern and W.N. Lipscomb, J. Chem. Phys., 1962, 37, 267.
178. M. Pollack and R. Rein, J. Chem. Phys., 1967, 47, 2039, 2045.
179. J.A. Pople, W.G. Schneider and H.J. Bernstein, "High-Resolution

- Nuclear Magnetic Resonance", McGraw-Hill, New York, N.Y., 1959.
180. H.O. Pritchard and F.H. Sumner, Proc. Roy. Soc. (London), 1956, A235, 136.
181. H.P. Pritchard, J. Amer. Chem. Soc., 1963, 85, 1876.
182. K.F. Purcell, J. Chem. Phys., 1967, 47, 1198.
183. N.F. Ramsay, Phys. Rev., 1953, 91, 303.
184. N.F. Ramsay and E.M. Purcell, Phys. Rev., 1952, 85, 143.
185. B.J. Ransil and J.J. Sinai, J. Chem. Phys., 1967, 46, 4050.
186. C.M. Reeves, J. Chem. Phys., 1963, 39, 1.
187. C.M. Reeves and R. Fletcher, J. Chem. Phys., 1965, 42, 4073.
188. C.M. Reeves and M.C. Harrison, J. Chem. Phys., 1963, 39, 11.
189. C.B. Richardson, Dissertation Abstr., 1963, 23, 3942.
190. J.W. Richardson, J. Chem. Phys., 1961, 35, 1829.
191. J.S. Rigden and R.H. Jackson, J. Chem. Phys., 1966, 45, 3646.
192. P.J. Roberts, J. Chem. Phys., 1965, 43, 3547.
193. P.J. Roberts, Proc. Phys. Soc., 1966, 88, 625.
194. B.R. Russell, R.M. Hedges and W.R. Carper, Mol. Phys., 1967, 12, 283.
195. M. Sancho and M.D. Harmany, J. Chem. Phys., 1966, 45, 1812.
196. K.V.L.N. Sastry and R.F. Curl, J. Chem. Phys., 1964, 41, 77.
197. E. Schempp and P.J. Bray, J. Chem. Phys., 1967, 46, 1186.
198. L.I. Schiff, "Quantum Mechanics", McGraw-Hill Book Co. Inc., New York, N.Y., 1955.

199. W.G. Schneider, J. Chem. Phys., 1955, 23, 26.
200. T.A. Scott, J. Chem. Phys., 1962, 36, 1459.
201. E. Scrocco, Adv. Chem. Phys., 1963, 5, 519, Interscience,
New York, N.Y., 1963.
202. E. Scrocco, Ricerca Sci., 1960, 5, supp. no. 30, 61.
203. J. Sheridan, Adv. Mol. Spec. (ed. Mangini), 139, Pergamon
Press, London, 1962.
204. J. Sheridan and L.F. Thomas, Nature, 1954, 174, 798.
205. J. Sheridan and A.C. Turner, Proc. Chem. Soc., 1960, 21.
206. J.N. Shoolery, J. Chem. Phys., 1959, 31, 1427.
207. J.N. Shoolery, R.G. Shulman and D.M. Yort, J. Chem. Phys.,
1951, 19, 250.
208. J.N. Silverman and G.H. Brigman, Rev. Mod. Phys., 1967,
39, 228.
209. H.J. Silverstone, J. Chem. Phys., 1966, 45, 4337.
210. O. Sinanoglu, Proc. Nat. Acad. Sci. U.S.A., 1961, 47, 1217.
211. H.A. Skinner and H.O. Pritchard, Trans. Farad. Soc., 1953,
49, 1254.
212. F.I. Skripov, Fiz. Sbornik, L'vov. Univ., 1957, 3, 75.
213. J.C. Slater, Phys. Rev., 1930, 36, 51.
214. J.C. Slater, "Quantum Theory of Atomic Structure", Vol. I,
McGraw-Hill Book Co. Inc., New York, N.Y., 1960.
215. D.F. Smith and D.W. Magnuson, Phys. Rev., 1952, 87, 226A.
216. P.R. Smith and J.W. Richardson, J. Phys. Chem., 1967, 21, 924.

217. G.O. Sørensen, J. Mol. Spec., 1967, 22, 325.
218. R.M. Sternheimer, Phys. Rev., 1950, 80, 102.
219. R.M. Sternheimer, Phys. Rev., 1951, 84, 244.
220. R.M. Sternheimer, Phys. Rev., 1952, 86, 316.
221. R.M. Sternheimer, Phys. Rev., 1954, 95, 736.
222. R.M. Sternheimer, Phys. Rev., 1954, 96, 951.
223. R.M. Sternheimer, Phys. Rev., 1957, 105, 158.
224. R.M. Sternheimer, Phys. Rev., 1959, 115, 1198.
225. R.M. Sternheimer, Phys. Rev., 1963, 132, 1637.
226. R.M. Sternheimer and H.M. Foley, Phys. Rev., 1953, 92, 1460.
227. R.M. Sternheimer and H.M. Foley, Phys. Rev., 1956, 102, 731.
228. A. Sureau, Theoret. Chim. Acta, 1967, 8, 76.
229. A. Sussman and A. Alexander, Solid State Communications,
1967, 5, 259.
230. H. Taketa, S. Huzinga and K. Oohata, J. Phys. Soc. Japan,
1966, 21, 2306, 2313.
231. L.F. Thomas, J.C. Heeks and J. Sheridan, Z. Elektrochem.,
1957, 61, 935.
232. W.M. Tolles and W.D. Gwinn, J. Chem. Phys., 1965, 42, 2253.
233. D.A. Tong, Ph.D. Thesis, Leeds, 1963.
234. C.H. Townes and B.P. Dailey, J. Chem. Phys., 1949, 17, 782.
235. C.H. Townes and B.P. Dailey, J. Chem. Phys., 1952, 20, 35.
236. C.H. Townes and A.L. Schawlow, "Microwave Spectroscopy",
McGraw-Hill Book Co., London, 1955.

237. H. Trubomura, Bull. Chem. Soc. Japan, 1954, 27, 445.
238. J.K. Tyler and J. Sheridan, Trans. Farad. Soc., 1963, 59, 2661.
239. A. Tzalmona, Phys. Letters, 1966, 20, 478.
240. R. Varma and K.S. Bughton, J. Chem. Phys., 1967, 46, 1565.
241. A. Veillard and G. Berthier, Theoret. Chim. Acta, 1966, 4, 347.
242. K. Wada, Y. Kikuchi, C. Matsumara, K. Hisoto and Y. Monso,
Bull. Chem. Soc. Japan, 1961, 34, 337.
243. R. Wallace, Ph.D. Thesis, Glasgow, 1964.
244. G.D. Watkins and R.V. Pound, Phys. Rev., 1952, 85, 1062.
245. R.E. Watson and A.J. Freeman, Phys. Rev., 1963, 131, 250.
246. R.E. Watson and A.J. Freeman, Phys. Rev., 1963, 131, 2566.
247. R.E. Watson and A.J. Freeman, Phys. Rev., 1963, 132, 706.
248. R.E. Watson and A.J. Freeman, Phys. Rev., 1964, 135, A1209.
249. M.A. Whitehead, D.H. Baird and R.N. Kaplansky, Theoret.
Chim. Acta, 1965, 3, 135; err. 1966, 6, 190.
250. M.A. Whitehead and H.H. Jaffé, Theoret. Chim. Acta, 1963, 1, 209.
251. M.A. Whitehead and H.H. Jaffé, Trans. Farad. Soc., 1961,
57, 1854.
252. R.H. Widman, J. Chem. Phys., 1965, 43, 2922.
253. E.G. Wikner and T.P. Das, Phys. Rev., 1958, 109, 360.
254. J.K. Wilmshurst, J. Chem. Phys., 1959, 30, 561.
255. M. Yamazaki, M. Sakamoto, K. Hijikati and C.C. Lin, J. Chem.
Phys., 1961, 34, 1926.

In chapter 1, the factors which contribute to the electric field gradient tensor and so to the nuclear quadrupole resonance (NQR) frequencies in an isolated molecule are analysed. Methods of finding various molecular and atomic parameters which are needed for estimating the contributions of these factors are reviewed and discussed, and a few possible extensions or modifications of some of these methods are suggested. Mathematical techniques for evaluating the integrals which come out of these methods are also briefly reviewed. Chapter 2 contains a short discussion of intermolecular effects on the electric field gradient tensor.

In chapter 3, the results of the application of the methods described and suggested in chapter 1 to some simple molecules are given, with some further discussion of points of important detail. These results seem to be promising enough to justify a proper, more detailed, study of the possibilities of semi-empirical calculations of NQR frequencies.